

INCORPORATING DIGITAL DATA INTO RAPID  
GEOMORPHIC ASSESSMENTS

By

ABIGAIL PARNELL

Bachelor of Science in Biosystems & Agricultural

Engineering

Oklahoma State University

Stillwater, Oklahoma

2016

Submitted to the Faculty of the  
Graduate College of the  
Oklahoma State University  
in partial fulfillment of  
the requirements for  
the Degree of  
MASTER OF SCIENCE  
December, 2018

**INCORPORATING DIGITAL DATA INTO RAPID  
GEOMORPHIC ASSESSMENTS**

Thesis Approved:

Dr. Daniel Storm

---

Thesis Adviser

Dr. Garey Fox

---

Dr. Paul Weckler

---

Dr. Jason Vogel

---

## **ACKNOWLEDGEMENTS**

The experience of getting a Master of Science degree has taught me some valuable lessons and has been a kind of coming of age experience for me. I would not have been able to intern with NRCS through the Pathways Program without continuing my education. In addition, I was not considering getting a Masters until Dr. Garey Fox approached me. Dr. Fox was a professor in the Biosystems & Ag Engineering Department at the time and under whom I had done undergrad research for as well. I would also not have learned the same lessons in self-discipline and motivation if I had not followed through and finished this project. Completing this Masters has provided me with the opportunity to take on a large project by myself, compared to the prepared problems presented to me during my undergrad experience. This meant that I had to learn to not only problem solve, but also how to define the problem itself. A valuable experience to have before entering the workforce!

Dr. Fox deserves special recognition as one of the main influences and supporters of my work in the research field. I would not have been able to finish this degree without his input. The support and advice from Dr. Dan Storm was also invaluable. I appreciate how Dr. Storm took the time to understand and give feedback on my project, even in the midst of retiring. I would also like to thank Dr. Jason Vogel, Dr. Paul Weckler, and Dr. John Veenstra, who have all

helped serve on my committee, or sat in on meetings. And of course, this project never would have been possible without the Biosystems & Ag Engineering Department and the various funding sources required.

I would also like to thank all of the people who I interacted with and who provided me with support and information. This includes Jean Lemmon and Kim Shaw from the Blue Thumb organization, who patiently answered all my questions and helped me get the information that I needed to perform my validation site visits. A big thank you goes to Kay Frank, who welcomed me onto her property for one of the validation site visits, showed interest in the work that I was doing, and passionately cared about the well-being of our waterways. I'd also like to thank Lori Etheridge and Stephen Nechero who helped provide information about the LIDAR flight dates. And Dr. Jason Kelley who provided me with feedback early on in the project as well as provide me with access to a tool I considered using in the analysis of the LIDAR DEMs, which I ended up not having time to explore, but am happy to include as a reference.

I'd also like to thank all of my friends and mentors, both in the university and at home. I am so thankful for the help and friendship of Holly Enlow, who helped me settle in to grad-life and had answers for so many day-to-day questions. I'd also like to thank the BAE Graduate Student Association, who provided me with an on-campus community. I loved being able to share this experience with so many others who I could call friends. My family and my Church also were a huge support. There were so many times where their prayers

and encouragement blessed me! God has blessed me so richly in my opportunities and in my family! I am especially grateful to my parents, who held me accountable, encouraged me, and cheered me on to the finish line. I am happy that I had so many people who celebrated with me as I made it through the final stages of the process with me! I am thankful for Elsa, who would both yell at me to get back to work, and also make sure that I came home and take a break so I didn't burn out. I'm grateful for Sam, who sent encouraging text messages and celebrated with me at the conclusion. Rachel proved a good friend and mentor throughout the process! I was so happy to have someone to share with me in my worries and successes.

I hope that I have worked to the best of my ability and been a good example of not just a good student and researcher, but a faithful Christian. Unless the Lord builds the house! It has only been through His Mercy that I have made it this far! So out of everything that I have gained, I pray that out of all of it, God would be glorified!

Name: ABIGAIL PARNELL

Date of Degree: DECEMBER, 2018

Title of Study: INCORPORATING DIGITAL DATA INTO RAPID GEOMORPHIC ASSESSMENTS

Major Field: BIOSYSTEMS & AGRICULTURAL ENGINEERING

Abstract:

Channel widening and migration can lead to sediment pollution and can be indicative of an imbalanced stream system. Rapid Geomorphic Assessments (RGAs) are on-site methods used to rank stream reaches in terms of stability. RGAs are relatively easy and quick to perform. Subjective measurements and on-site estimates of reach-length parameters create uncertainty in the RGAs. The primary objective of this study was to develop digital RGA methods that integrate readily available data and resources. Digital methods were developed and compared to historical site assessments. Then, the methods were validated by comparing digital RGAs to on-site assessments on several different streams. The digital methods included several different resources, including LIDAR for streambank measurements, Web Soil Survey for bank material and vegetation metrics, and Google Earth to perform visual assessments needed for specific RGAs. Study areas for the validation included second to fourth order streams in Oklahoma in the Ozark Highlands, the Central Great Plains, and the Cross Timbers ecoregions. The resulting digital RGAs performed reasonably well, successfully ranking stream reaches in the same stability ranking as the on-site assessment 38% of the time for two commonly used RGAs: Bank Erosion Hazard Index (BEHI) and the Channel Stability Index (CSI). The digital CSI performed better in the development stage with an 83% success rate. The decrease in performance could be due to several compounding factors such as channel visibility and image availability on Google Earth. Specific metrics should continue to be measured on-site to improve the accuracy of the digital RGAs. For example, a difference of up to twenty points can be avoided if the primary bank material is identified on-site. This project has illustrated the possibility that digital data can be successfully incorporated into RGAs, where digital RGAs have several benefits including the reduced time to assess larger areas and no longer being dependent on land access.

## TABLE OF CONTENTS

| Chapter   | Page |
|---|------|
| I. STUDY BACKGROUND & LITERATURE REVIEW .....           | 1    |
| Rapid Geomorphic Assessments .....                      | 2    |
| Bank Erosion Hazard Index (BEHI) .....                  | 2    |
| Channel Stability Index (CSI) .....                     | 7    |
| Project Overview .....                                  | 10   |
| Literature Review .....                                 | 11   |
| Rapid Geomorphic Assessment Limitations .....           | 11   |
| Bank Erosion Hazard Index.....                          | 11   |
| Channel Stability Index.....                            | 15   |
| Improvements of Rapid Geomorphic Assessments.....       | 16   |
| Potential Data Sources for Digital RGAs.....            | 18   |
| Visual Assessments .....                                | 19   |
| Channel Bed/Bank Characterization .....                 | 20   |
| Stream/Cross Sectional Geometry .....                   | 21   |
| II. METHODS.....  | 33   |
| Reach Length Methods .....                              | 33   |
| Reach Determination.....                                | 33   |
| Visual Assessment Methods .....                         | 34   |
| Channel Bed/Bank Characterization .....                 | 38   |
| Determining Primary Bank Material & Stratification..... | 38   |
| Bank/Bed Protection.....                                | 41   |
| Root Depth and Root Density.....                        | 42   |

|   |     |
|---|-----|
| Stream/Channel Geometry Methods.....              | 44  |
| Methodology for Bankfull Depth Measurement.....   | 44  |
| Methodology for Measuring “Baseflow” Depth.....   | 56  |
| Methodology for Bank Measurements.....            | 57  |
| Development Stage .....                           | 58  |
| Study Area Description.....                       | 58  |
| Reach Determination.....                          | 59  |
| Historical Data Set.....                          | 59  |
| Notes on Methods .....                            | 62  |
| Validation Stage.....                             | 63  |
| Fully Digital Scores .....                        | 65  |
| III. RESULTS & DISCUSSION .....                   | 101 |
| Reach Length Methods.....                         | 101 |
| Channel Bed/Bank Characterization Methods .....   | 104 |
| Primary Bank Material & Stratification .....      | 104 |
| Bank/Bed Protection.....                          | 106 |
| Root Depth and Root Density.....                  | 108 |
| Stream/Channel Geometry Methods.....              | 110 |
| Methodology for Bankfull Depth Measurement.....   | 110 |
| Methodology for Measuring “Baseflow” Depth.....   | 119 |
| Methodology for Bank Measurements.....            | 121 |
| Validation .....                                  | 123 |
| Fully Digital Scores .....                        | 129 |
| The Coefficient of Success.....                   | 136 |
| Time: Digital vs. On-Site.....                    | 137 |
| Digital Method Accuracy .....                     | 139 |
| IV. SUMMARY, CONCLUSIONS, AND RECOMENDATIONS..... | 170 |
| Digital RGA Limitations .....                     | 170 |
| Data Gaps .....                                   | 171 |
| Data Resolution.....                              | 173 |



|   |     |
|---|-----|
| Digital RGA Recommendations .....                     | 174 |
| General Recommendations .....                         | 174 |
| Bankfull Recommendations .....                        | 177 |
| Digital RGA Benefits .....                            | 178 |
| Answering the Research Questions: .....               | 179 |
| Future Work .....                                     | 181 |
| Stage of Chanel Evolution .....                       | 181 |
| Bank Protection and Woody Cover .....                 | 182 |
| Bankfull Depth Determination .....                    | 183 |
| Other BEHI Metrics .....                              | 184 |
| Automating Digital Rapid Geomorphic Assessments ..... | 186 |
| Conclusion .....                                      | 187 |
| REFERENCES .....                                      | 188 |
| APPENDIX .....  | 194 |

## LIST OF TABLES

| Table  | Page |
|--|------|
| <p><i>Table 1: Bank Erosion Hazard Index (BEHI) metrics, scores, stability rankings and associated aggregate scores. Table modified from table 1 from Rosgen (2001).</i>.....</p>  | 29   |
| <p><i>Table 2: Adjustment factors and score adjustments used in this study. Modified from Rosgen (2001) and Rosgen (1996).</i>.....</p>  | 30   |
| <p><i>Table 3: Channel Stability Index (CSI) metrics, scores, stability rankings and aggregate scores (Heeren et al., 2012; Simon and Downs, 1995). L = left Bank, R = right bank.</i>.....</p>  | 31   |
| <p><i>Table 4: Soil classes used and associated ranges of size, <math>\tau_c</math>, <math>k_d</math>, and erodibility class. For this study, the representative diameters were used to determine erodibility class.</i>.....</p>  | 94   |
| <p><i>Table 5: Regional equations used to calculate bankfull depth, for both the development and validation stages of the project. D = bankfull depth, Lm = Meander Wavelength, Lb = Along-Channel Bed Length, B = Meander Belt Width, Rc = Radius of Curvature, W = Bankfull Width, K = Sinuosity, and DA = Drainage Area.</i>.....</p> | 95   |
| <p><i>Table 6: USGS Stream gages and station ID for the development stage of the project. Note that all stations consist of several cross sections from only one land owner except for, FM1-2, FM3-4, and WC2-3, which represent single cross sections per station and land owners that span several stations.</i>.....</p>              | 96   |
| <p><i>Table 7: Details on LIDAR data used in both the development and validation stages of the project. The stream orders for the Fourche Maline and Spring Creek were determined using USEPA (2017b) WATERS GeoViewer tool.</i>.....</p>  | 97   |
| <p><i>Table 8: USGS Stream gages and station ID used in the validation stage of the project. Note the time frame of monitoring, which had an impact on the methods used.</i>.....</p>  | 98   |

|   |            |
|---|------------|
| <i>Table 9: Summary of all required measurements/observations, the corresponding RGA metrics, and the sources used in this study. ....</i>  | <i>99</i>  |
| <i>Table 10: Impacts of data limitations in the digital RGAs.....</i>   | <i>100</i> |
| <i>Table 11: Digital RGA success rates using Google Earth compared to historical RGAs for all Channel Stability Index (CSI) metrics. The methods tested are described in the Reach Length section of the methods. ....</i>  | <i>154</i> |
| <i>Table 12: Digital RGA success rates for the Bed/Bank Characterization methods from Bank Erosion Hazard Index (BEHI) and the Channel Stability Index (CSI), for both the development and validation data.....</i>   | <i>155</i> |
| <i>Table 13: Development success rates for Bank Erosion Hazard Index (BEHI) using digital Bankfull methods as well as the fully digital BEHI applied to second and fourth order streams as well as the fully digital success rate.....</i>  | <i>156</i> |
| <i>Table 14: Development stage success rates for Bank Erosion Hazard Index (BEHI) using digital Bankfull methods from Williams (1986) applied to fourth order streams as well as the fully digital BEHI.....</i>  | <i>156</i> |
| <i>Table 15: Validation stage success rates for Bank Erosion Hazard Index (BEHI) using digital Bankfull methods that applied to all validation streams. ....</i>  | <i>157</i> |
| <i>Table 16: All statistics for how well each bankfull method was able to match the historical measurement of bankfull depth using the development data set. (S2, Coefficient of Success; RMSE, Root Mean Square Error).....</i>  | <i>158</i> |
| <i>Table 17: Success rate for all channel geometry measurements. Used the average measurement from both banks (bank height, face lengths, etc.), not critical banks. Also used over-all success rates. Only put methods from Williams that applied to both second and fourth order streams. Channel Stability Index (CSI), Bank Erosion Hazard Index (BEHI). ....</i> | <i>160</i> |
| <i>Table 18: Average point difference between the individual metrics obtained on-site vs. digital. The aggregate category is referring to the average difference in overall score. ....</i>   | <i>161</i> |
| <i>Table 19: All metric/metric combinations that failed in the development stage. LIDAR was used to obtain the bankfull depth, and the LIDAR+StreamGage method was used to obtain the baseflow depth.....</i>   | <i>162</i> |
| <i>Table 20: All metric/metric combinations that failed in the validation stage. The LIDAR method was used to obtain the bankfull depth, and the LIDAR+StreamGage method, where possible, was used to obtain the baseflow depth. If the LIDAR+StreamGage method was not possible, the StreamStats method was used. ....</i>   | <i>164</i> |

*Table 21: Percentage of Channel Stability Index (CSI) metrics that failed when assessed individually for a specific reach/station which also failed the fully digital RGA. Both the development and validation stage was included. For the digital scores, the LIDAR+StreamGage method was used where applicable, and the StreamStats method otherwise..... 165*

*Table 22: Percentage of Bank Erosion Hazard Index (BEHI) metrics that failed when assessed individually for a specific reach/station which also failed the fully digital RGA. Both the development and validation stage was included. The LIDAR bankfull height method was used for the digital methods..... 166*

*Table 23: Coefficient of Success for the Channel Stability Index (CSI). The LIDAR+StreamGage method was used to obtain the baseflow depth for the development stage. For the validation stage, both the LIDAR+StreamGage and the StreamStats method were used and tested..... 167*

*Table 24: Coefficient of Success for the Bank Erosion Hazard Index. The LIDAR Bankfull Height was the bankfull method used. .... 167*

*Table 25: Approximate time it took to perform the digital and On-Site Rapid Geomorphic Assessments for the validation stage..... 168*

*Table 26: Individual metric accuracy for both the development and validation data. Methods were evaluated similar to success rate, with a full point being assigned to reaches where the same score was obtained using the digital and on-site method. If at least one team got the same categorical assessment, then half a point was given. .... 169*

## LIST OF FIGURES

| Figure   | Page      |
|--|-----------|
| <i>Figure 1: The different erodibility factors considered in the Bank Erosion Hazard Index. Taken from figure 6-25 in Rosgen (1996). .....</i>   | <i>27</i> |
| <i>Figure 2: Compare the visible features between cross sections obtained using LIDAR (above) and Google Earth (below). .....</i>  | <i>28</i> |
| <i>Figure 3: An example of how a stream meander feature is analyzed using the measuring and drawing tool as well as the historical imagery in Google Earth. Google Earth cited the image as coming from the U. S. Department of Agriculture, Farm Service Agency. ....</i>   | <i>67</i> |
| <i>Figure 4: The Google Earth image on the top was taken in 2008, while the picture on the bottom was taken in 2010. The red line indicates the top of the bank in 2010 in both pictures. The blue arrow indicates the direction the channel is going to migrate towards. Google Earth cited the top image from the U. S. Department of Agriculture, Farm Service Agency, and the bottom image as DigitalGlobe.....</i>  | <i>68</i> |
| <i>Figure 5: Examples of obvious mass wasting as evidenced by large cracks in the top bank. Google Earth cited both images as coming from DigitalGlobe.....</i>  | <i>69</i> |
| <i>Figure 6: The stream is flowing from the bottom to the top of the image, so that the left bank is on the left side of the image. The blue line represents the reach length, the green line represents woody vegetation that does not make up 100% of the reach. The red line represents bank affected by mass wasting, which is evidenced by a fallen tree visible in a different image. The brown line represents deposition that does not make up 100% of the reach. Google Earth cited the image as coming from the U. S. Department of Agriculture, Farm Service Agency. ....</i> | <i>70</i> |
| <i>Figure 7: Example of Web Soil Survey map. Note how the stream, denoted by a W in the soil map, does not line up with the course of the stream in the background imagery. ....</i>   | <i>71</i> |

*Figure 8: Note the selected streambank that is denoted as water (W) in the soil map. In this case, in deciding between using the Sm or CIF soil types, the Sm soil type was selected based on its closer topographic proximity to the selected bank..... 72*

*Figure 9: Figure 8 from Hanson and Simon (2001), describing the erodibility classes as defined by the critical shear stress ( $\tau_c$ ) and the erodibility coefficient ( $k_d$ ). Developed for cohesive soils. .... 73*

*Figure 10: Example of Google Earth vegetation type identified as Vegetated-Grass. Location: WC3. Obtained using Google Earth. Imagery date: 7/26/2015. .... 74*

*Figure 11: Figure 1 from Williams (1986). Describes meander features and how to measure them..... 74*

*Figure 12: Meander measurements for a site in the Fort Cobb reservoir (left) and from Barren Fork (right). Notice that at a similar eye altitude (in bottom right corner of each picture) there is a significant difference in meandering. Google Earth cited the image on the right as coming from the U. S. Department of Agriculture, Farm Service Agency. .... 75*

*Figure 13: Clockwise from the top left corner: 1) NAIP imagery and the cross sections for Station D. 2) DEM. 3) DEM with NAIP overlaid at 50% transparency. 4) Google Earth image for comparison..... 75*

*Figure 14: LIDAR cross section from Fivemile, a second order stream, with estimated Bankfull height indicated at the first major change in slope. Cross section taken from the left bank to the right. .... 76*

*Figure 15: LIDAR cross section from Barren Fork, a fourth order stream, with estimated bankfull depth indicated at the first major change in slope. Cross section taken from the left bank to the right. .... 76*

*Figure 16: LIDAR cross section with two possible bankfull surfaces. Cross section taken from the left bank to the right. .... 77*

*Figure 17: An Example of how it was assumed LIDAR interacts with an actual channel. The different relevant measurements are identified. .... 77*

*Figure 18: Notice how there is a distinct line in the point bar in the Google Earth Image (taken in 3/20/2016), while the LIDAR cross section captured both this point bar (green line) as well as what appears to be an old, less active point bar (red line). Note the stream is flowing from the top right down, with the left and right banks noted on the image. .... 78*

*Figure 19: In this example, there were several depositional surfaces and no clear indication of where the top of the apparent point bar was. The light blue line was chosen to represent the bankfull stage as it most closely matched the estimated bankfull in Google Earth. .... 79*

*Figure 20: Note the terrace and secondary channel on the left, which can be confirmed in the Google Earth Image. The green line represents the bankfull depth, which also corresponded to the top of the left bank, and the red line indicates the top of the right bank..... 80*

*Figure 21: US Environmental Protection Agency Level III Ecoregions for Oklahoma (Woods et al., 2005). .... 81*

*Figure 22: Fivemile Creek in western Oklahoma (left) and the Fort Cobb Watershed (right) with site locations (Saenz et al., 2016). .... 81*

*Figure 23: Figure 1 from Heeren et al. (2012). Location of Ozark streams used in the study. Site A was on Spavinaw, and sites B-E were on Barren Fork. .... 82*

*Figure 24: Locations of the historical Stations and the USGS Stream gage used in this study. Image obtained from Google Earth, imagery date: 10/27/2017. .... 83*

*Figure 25: Locations of the historical Stations and the USGS Stream gages used in this study. Image obtained from Google Earth, imagery date: 3/13/2018. .... 84*

*Figure 26: Locations of the historical Stations and the USGS Stream gages used in this study. Image obtained from Google Earth, imagery date: 10/16/2016. .... 85*

*Figure 27: Locations of the historical Stations and the USGS Stream gages used in this study. Image obtained from Google Earth, imagery date: 7/26/2015. .... 86*

*Figure 28: Comparison between the original team adjusted scores and the averaged team score using the development data set (which later are referred to as the historical aggregate score). Note that the final reports for FM1-WC3 sites only reported the final team adjusted stability rank, so an appropriate score was assigned to these points. .... 87*

*Figure 29: Comparison between the original team adjusted scores and the averaged team score using the development data set (which later are referred to as the historical aggregate score). Note that the final reports for FM1-WC3 sites only reported the final team adjust..... 88*

*Figure 30: Validation sites and stream gage used for Feather Creek in the Central Great Plains Ecoregion. Imagery was obtained using Google Earth, eye altitude at 396 m, imagery date of 2/25/2014. .... 89*

*Figure 31: Validation site and stream gage used for Spring Creek in the Ozarks Ecoregion. The imagery was obtained using Google Earth, eye altitude at 24 km, imagery date of 10/27/2017. .... 90*

*Figure 32: Validation site and stream gage used for Sandy Creek in the Cross Timbers Ecoregion. Imagery was obtained using Google Earth, eye altitude at 27 km, and imagery date of 12/30/2016. .... 91*

*Figure 33: Validation site and stream gage for Black Fork. Imagery was obtained using Google Earth, with eye elevation at 19 km, and imagery date of 3/20/2016. .... 92*

*Figure 34: Validation site and stream gage for Fourche Maline. Imagery was obtained using Google Earth, with eye elevation at 189 m, and imagery date of 1/17/2018. .... 93*

*Figure 35: Boxplots of the root depth obtained digitally and the root depth obtained on-site using the development data set. .... 141*

*Figure 36: Comparison of bankfull height measured in LIDAR and on-site using the development data set. .... 141*

*Figure 37: Interaction plot for the Two-Way Analysis of Variance (ANOVA) with Bankfull Depth as the response variable and Method and Stream Order as the treatment variables LIDAR-H refers to the bankfull height measured in LIDAR, LIDAR-D represents the bankfull height measured in LIDAR plus the baseflow depth measured using the LIDAR+StreamGage method. .... 142*

*Figure 38: Interval plot comparison between baseflow depth measured on-site (historical), vs. various digital methods using the development data. .... 143*

*Figure 39: Validation Site\_Fourche Maline - Reach 1. Google Earth image taken 1/17/2018. The red line represents the original reach used in the digital assessment. The circle is highlighting where major slumping was apparent on-site. The green line represents where the on-site assessment was performed. 144*

*Figure 40: Google Earth images (various imagery dates) of all the validation reaches that failed the digital Channel Stability Index (CSI). Going clockwise starting in the top left corner: Fourche Maline, reach 1 & 2; Feather; Spring, reach 4; Sandy, reach 1. Note how these reaches are relatively straight. .... 145*

*Figure 41: Google Earth images (various imagery dates) of the validation reaches which had a successful digital Channel Stability Index (CSI). Going clockwise and starting from the top: Spring reach 2, Black Fork reach 2, and Sandy reach 5. Note the clear meander present. .... 146*



*Figure 42: Development Channel Stability Index (CSI) comparing the historical vs the fully digital scores, separated by stream order. Any points that fall inside the shaded box are counted as successful..... 147*

*Figure 43: Validation Channel Stability Index (CSI) comparing the on-site vs the fully digital scores, separated by stream order. Any points that fall inside the shaded box are counted as successful. A. Using only the StreamStats method for baseflow depth. B. Using the LIDAR+StreamGage method where data allowed. .... 148*

*Figure 44: Validation Bank Erosion Hazard Index (BEHI) comparing the on-site vs the fully digital scores, separated by stream order. Any points that fall inside the shaded box are counted as successful..... 149*

*Figure 45: Validation Bank Erosion Hazard Index (BEHI) comparing the on-site vs the fully digital scores, separated by stream order. Any points that fall inside the shaded box are counted as successful..... 149*

*Figure 46: The absolute difference in time between the Google Earth imagery used and the on-site assessment, plotted against the resulting percent difference between the digital Channel Stability Index (CSI) and on-site score. Both development and validation stage data was used. .... 150*

*Figure 47: The absolute difference in time between the LIDAR collection date used and the on-site assessment, plotted against the resulting percentage difference between the digital Bank Erosion Hazard Index (BEHI) and on-site score. Both development and validation stage data was used. .... 151*

*Figure 48: The absolute difference in time between the LIDAR collection date used and the on-site assessment, plotted against the resulting percent difference between the digital Channel Stability Index (CSI) and on-site score. Both development and validation stage data was used. .... 152*

*Figure 49: LIDAR resolution used vs. the resulting percent difference between the digital and on-site Channel Stability Index (CSI) on-site score. Both development and validation stage data was used. .... 152*

*Figure 50: LIDAR resolution used vs. the resulting percent difference between the digital and on-site Bank Erosion Hazard Index score. Both development and validation stage data was used..... 153*

*Figure 51: Comparison between the amount of time needed vs the number of validation reaches assessed for the on-site and digital methods..... 153*

## **CHAPTER I**

### **STUDY BACKGROUND & LITERATURE REVIEW**

Excessive streambank erosion, channel widening and migration is a problem a wide range of people have to deal with, from landowners to federal and nonfederal agencies. Sediment is considered one of the most prevalent stream pollutants in the United States (USEPA, 2017a). Channel widening and migration are indicative of an unbalanced and unstable stream system and can be a primary source of sediment in many stream systems (Simon and Klimetz, 2008; Mukundan et al., 2011; Mckinley et al., 2013). Oklahoma in particular has reported sediment yields exceeding median stable yields by 7,410% (Simon and Klimetz, 2008). Rapid Geomorphic Assessments (RGAs) are accepted methods to assess stream stability (Habberfield et al., 2014; Heeren et al., 2012; Johnson et al., 1999; Krymer, 2012; Mukundan et al., 2011; Simon and Klimetz, 2008). On-site measurements categorize small stream segments, which are used to assess stream reaches with similar morphology. With proper training, RGAs are relatively easy to perform. Additionally, each site assessment is completed in one to two hours, and requires minimal equipment. However, RGAs present several challenges. With a large study are, the number of RGA sites needed can be impractical. RGAs also have to be conducted on site, which requires access to

property. Even though most RGA metrics are easily quantified, several rely on subjective measurements, e.g. bankfull depth. These subjective measurements make it more important for evaluators to be specially trained. It also is recommended for the RGA Bank Erosion Hazard Index (BEHI) to have at least two people perform the assessments to reduce subjectivity (Bigam, 2016).

### **Rapid Geomorphic Assessments**

Numerous RGAs have been developed and are reported in the literature. These include traditional assessments applied across the United States, such as the Channel Stability Index (CSI) and the Bank Erosion Hazard Index (BEHI), as well as those developed for a specific location. For example, the Oklahoma Ozark Streambank Erosion Potential Index (OSEPI) developed by Heeren et al. (2012) or the Vermont Department of Environmental Conservation (VTDEC) Stream Geomorphic Assessment RGA method. Several include similar metrics such as evidence of aggradation, degradation, channel widening, or change in the planform of the stream (MOE, 2003; Simon and Downs, 1995; Simon and Klimetz, 2008; VTDEC, 2003).

### **Bank Erosion Hazard Index (BEHI)**

The BEHI was developed based on Rosgen (1996) using a bank erodibility hazard rating guide. The goal of BEHI was to capture the potential increase in sediment loads caused by streambank erosion, which in turn was likely caused by changes in hydrology and land use. Rosgen (1996) specifically focused on variables that affected detachment and flow stress in the erosion risk

assessment. The BEHI included four measurements, five metrics plus two adjustment factors, and six stability rankings ranging from very low to extreme. The development of the BEHI metrics and their corresponding risk rankings was based on streambank erosion field observations, primarily in the west-central part of the United States (Rosgen, 2001). A field data collection/rating sheet is given in Figure A - 1 and Figure A - 2 in the appendix.

The four BEHI measurements required include bank height, bank face length, bankfull height, and root depth on the bank. These measurements were all performed on the critical bank, the bank that was the most at risk of erosion and failure (i.e., outside of the meander bend). Bank height was measured from the surface of the water to the top of the existing bank, and bankfull height was measured from the surface of the water to the top of the active floodplain. The bank height and bankfull height were used to assess the bank height ratio, the first BEHI metric. The closer this ratio was to one, the lower the risk rating. The rationale behind this metric was that the higher the bank was above the bankfull height, the higher the risk of the lower bank eroding and eventually causing mass wasting (Figure 1).

The following method for field identification of bankfull stage, or depth, was recommended (Leopold, 1995). The first step was to consider all existing data, including regional curves and gages when available. Regional data helps provide an idea of where the bankfull stage could be. Once in the field, a cross section representing a similar stream reach should be chosen. The bankfull stage

was then identified using indicators, the key indicator being the depositional surface of the active floodplain (Leopold, 1995). The supplemental indicators included the presence of depositional features, a break in the bank slope, and the lower limit of perennial vegetation on the bank. A change in vegetation from annuals to perennials could be used to help indicate where there is frequent enough scour to prohibit perennial growth (WSDNR, 2011). Another secondary indicator was a change in sediment size, which indicated a change in water energy (WSDNR, 2011).

Identifying bankfull stage on-site required training as well as experience and could be complicated by several factors. The floodplains of steep streams can be intermittent if not nonexistent, disturbed sites can exhibit false bankfull indicators, and bankfull depth tends to be underestimated on streams that lack any perennial vegetation (Leopold, 1995). Due to these difficulties in identifying bankfull, it is recommended to take multiple measurements along a stream to check consistency. It is also recommended that multiple people measure the same cross section, to help reduce subjectivity. Rosgen also recommends that the bankfull stage and the BEHI rankings be combined with at least three years of historical erosion data (Heeren et al., 2012; Rosgen, 2001). In the cases where floodplains are non-existent, the other indicators are allowable but are not recommended to stand on their own (Leopold, 1995).

The root depth, rooting density, and surface protection represented mechanisms to protect the streambank from erosion. The root depth estimated

the percent roots in the vertical bank and was measured from the base of the plant, typically at the top of the bank, to the approximate depth to the majority of the roots. Root density was estimated based on the visual assessment of the visible bank root systems, and was estimated as the percentage of the bank covered by roots. The root density should be dependent on the root depth metric (Bigham, 2016; Sass and Keane, 2012). The amount of surface protection refers to the amount of the streambank surface protected from water flow by plant roots, downed logs, and rocks. The surface protection should not be lower than the root density percentage, since it is a factor of bank protection. The higher the root depth, root density and surface protection, the higher the bank protection and the lower the risk of streambank instability (Figure 1).

The bankface length was the distance between the top of the bank to the surface of the water following the slope of the bank. The goal of measuring the bankface length was to determine the bank angle, which was calculated using bank height and bankface length. However, other tools can be used to measure the bank angle directly. There were two different BEHI ratings for the bank angle, one for all angles less than or equal to 90 degrees and the second for all angles greater than 90 degrees. The larger the bank angle the higher the erosion risk rating since steeper banks were more likely to be at risk of mass failure (Figure 1).

Once the five BEHI metrics were assessed, the individual metric scores were summed, which can range from 7.25 to 50 (Table 1). Before the scores

were placed in its hazard classification, the BEHI included two score adjustments (Table 2). The first adjustment was based on bank material. The bank material can adjust the score drastically, from changes to hazard classification for bedrock channels to no change for silt/clay materials (Rosgen, 1996). The lowest risk of streambank erosion occurred if the streambank was composed of bedrock, which adjusted the stream reach to the lowest hazard classification. Erodible bank materials, such as sand, adjusted the score by adding points, thus indicating the stream reach was at greater risk. The second adjustment was for the presence of stratification of the streambank, which added five to ten points depending on the number and location of layers. Stratification can introduce instabilities to the bank via seepage through more conductive and more easily eroded layers (Wilson et al., 2006).

According to the USDA Forest Service, the bankfull flow was the discharge that defined and maintained the current channel geometry (Leopold, 1995). Bankfull flow had a typical return period of 1.5 to 2 years and was the most active period of sediment transport and channel formation (Leopold, 1995). Rosgen (1996) defined bankfull discharge and depth as “consistent morphological indices which can be related to the formation, maintenance, and dimensions of the channel as it existed under the modern climatic regime”. The USDA Forest Service developed a video guide on the identification of bankfull stage, and described bankfull stage as being the flow at the point right before flooding (Leopold, 1995). Therefore, the bankfull stage was located at the point of transition from stream channel to floodplain (Leopold, 1995).

### Channel Stability Index (CSI)

The Channel Stability Index (CSI) was developed by Simon and Downs (1995) to assess instability specifically around in-stream structures. Simon and Klimetz (2008) provided an example of how the method can be used to rank reaches in terms of instability. A stable stream reach was defined as a system that was balanced in terms of hydraulic energy and sediment transport. Excess sediment deposition was one indicator used to identify an unstable stream that does not have enough hydraulic energy to transport sediment. The second indicator of an imbalanced stream was the presence of incision, channel widening and/or mass wasting (Simon and Klimetz, 2008). These erosion processes were indicative of more hydraulic energy than what was being used for sediment transport.

While the BEHI focused on weighing visible factors that affect the streambank in terms of erosion, the CSI attempted to classify the stream in terms of its stage of channel evolution, using the six stages of channel evolution (Simon and Hupp, 1986). The rationale behind the six-stage process is that an unstable stream transitions from a stable stream in equilibrium to a degrading stream caused by some disturbance in the hydraulic regime, and from there eventually stabilize again.

The goal of the CSI was to use the state of a channel reach to assess the stability and to identify the location of most likely future instability (Simon and Klimetz, 2008). The nine metrics used in the CSI included primary bed material,



bed/bank protection, degree of incision, degree of constriction, streambank erosion, streambank instability, established riparian woody-vegetative cover (sometimes referred to as percent woody cover in this study), occurrence of bank accretion, and the stage of the channel evolution model. The preliminary data collection included the bank height, bankface length, river stage at base flow, and the estimated width of channel at study site and upstream. In addition, the average diameter of streambed sediment was recorded. Most of the metrics had a maximum score of four points, which was intended to help reduce subjectivity (Simon and Klimetz, 2008). The streambank erosion metric had the ability to score as high as six points, since there could be evidence of both fluvial and mass wasting on both banks (Heeren et al., 2012). The CSI had three stability rankings, ranging from stable to highly unstable, with a higher final score indicating a more unstable reach.

Simon and Downs (1995) provided a helpful reference for the justification for some of the variables. Streambed material was included for an indication of potential erodibility. Bed/bank protection accounted for the combination of the streambed and streambank and the presence or absence of protection. The degree of channel constriction was calculated by dividing the channel width of the study cross section by the width of the channel downstream. This indicated whether or not the flow was constricted, causing an increase in velocity, which increased the risk of erosion. The streambank erosion metric added the mechanisms of erosion that were currently evident including both fluvial erosion and mass wasting. The percent woody cover was used as an indicator of the

channel roughness, with little to no cover being associated with low flow resistance and therefore higher erosion risks. More vegetative cover and established woody vegetation indicated an established and stable stream. The stage of the channel evolution model assigned the lowest score to the first stage, which was the stable stage where sediment or erosion was not expected. The highest score was assigned to the fourth stage as it included both channel widening and channel downgrading processes at the same time. In other words, it was the stage with the most active erosion.

The degree of incision was calculated by first taking the sum of the baseflow depth and the bank height. The baseflow depth was then divided by the sum. The smaller the ratio, the higher the degree of incision. The more incised the channel the higher the score. Streambank instability referred to the percent of the bank failing via mass wasting with higher scores assigned to reaches with evidence of both erosion processes. The occurrence of bank accretion referred to the evidence of fluvial deposition. Lower scores were given to reaches with higher percentages of deposition. The rationale was since there was not enough energy to transport sediment, i.e. deposition, then there was also not enough energy to severely erode the bank/bed. The score and ranking system for the CSI used in this study is summarized in Table 3. The evaluation forms this study used can be seen in Figure A - 3 and Figure A - 4 in the appendix.

## **Project Overview**

The goal of an RGA is to provide a tool that is easily used to pinpoint stream reaches in need of restoration and to prioritize sites for stabilization. There are ways to potentially improve the use of RGAs by reducing the amount of time in the field, improve the accuracy by reducing the dependency on subjective measurements, and minimize cost by utilizing readily available data. Utilizing data that has already been collected, including regional relationships, could also enhance the quality of the results, especially when identifying bankfull parameters that are dependent on the observer and their experience.

The objective of this study was to develop a methodology using readily-available digital data to conduct an RGA with a similar accuracy to using data collected on-site. In order to do this, RGA stability rankings using available digital data were compared to historic RGA rankings obtained using data collected onsite. The methods developed in this research may provide alternatives to improve the RGA by reducing the need for landowner access, expensive and time-consuming analysis of large watersheds, and reliance on subjective measurements.

In order to develop these methods, several research questions were addressed:

1. How sensitive are RGAs to the use of data measured off-site?
2. Are there metrics that must be measured on site, i.e. there is no digital data?

3. Is there an applicable stream size for these integrated methods?
4. How sensitive are digital RGAs to data resolution?
5. Are digital RGAs affected by different data collection times being used in the same assessment?

If the integrated methods can utilize available off-site data, then on-site measurements of RGA parameters could become more of a confirmation and focus on critical metrics.

### **Literature Review**

RGAs have been used for a number of applications in a range of areas. This includes instream structures (Johnson et al., 1999; Simon and Downs, 1995), evaluating erosion hazards (Rosgen, 1996; VTDEC, 2003), the creation of erosion prediction curves (Sass and Keane, 2012), linking sediment to streambank instability (Mukundan et al., 2011; Simon and Klimetz, 2008), assessment of performance of streambank stability restoration (Krymer, 2012), and others.

### **Rapid Geomorphic Assessment Limitations**

#### ***Bank Erosion Hazard Index***

One of the more controversial metrics used in the BEHI is the bankfull height. Bankfull indicators can be hard to identify, and it takes training and experience to recognize them. Part of the difficulty lies in the definition of bankfull, which was supposed to represent the current stable hydrologic regime. If the hydrology was nonstationary then bankfull changes with time as well

(Heeren et al., 2012; Simon et al., 2007; VTDEC, 2003). A dynamic bankfull defeats the purpose of the BEHI, which was to identify and rank reaches in terms of their stability. If the bankfull was an untrustworthy indicator of the current hydrologic regime, then this led to more errors in the assessment. The form of the channel, which was what the BEHI was characterizing, was not constant, and changed based on the physical processes (Simon et al., 2007).

Part of the difficulty with bankfull identification, but also the BEHI in general, was that it relies on the assessor's judgement. Variance in the scores can lead to as much as a three category difference in stability ranking for the same reach on the same day between different assessors (Bigham, 2016). The score could change based on each assessor's level of experience and knowledge, and whatever bias they brought into an assessment. One method to reduce variability was to conduct the assessment in teams of at least two people (Bigham, 2016).

The BEHI also included variables that were difficult to quantify, such as root density. Root density was hard to measure physically, but in the case of the BEHI, it was estimated visually. The assessor had to approximate the amount of root density based on the visible roots from the bank and the amount of vegetation on the bank. The visible roots on the bank may not provide an accurate picture of the amount of protection and strength that the root system may be adding to the streambank. Root density was also included in the surface

protection metric (Bigham, 2016; Rosgen, 2014), effectively counting it twice, thus creating a bias.

The BEHI has gone by other names, including the assessment of Streambank Erosion Potential in Rosgen (1996). If used as designed, the BEHI was merely a small part in a much larger hierarchical analysis of a stream, which included at least three years of erosion data for calibration (Heeren et al., 2012; Rosgen, 2001). It was not entirely clear how to characterize the primary bank material. In the original context, it was identified using a pebble count as described in Level II – Channel Materials (p. 5-25) of Rosgen (1996). Simon et al. (2007) criticizes this method, as it did not differentiate between the bed and bank materials, which may be significantly different.

Primary bank material in this study was identified on-site by visual inspection, though a texture-by-feel approach could have also been used (Bigham, 2016). In addition, while it was not the most sensitive metric, it contributed to the uncertainty of the analysis (Bigham, 2016). Part of the uncertainty was because the methodology was unclear, and because of the difficulty in visually estimating bank material sizes and proportions. Some of the historical RGAs used in this study did not include either of the BEHI adjustments, possibly because of the lack of clear methodology.

Along with pebble counts to identify channel materials, the BEHI used Near Bank Stress (NBS) estimates to predict erosion (Rosgen, 1996, 2001). However, the relationship between BEHI and NBS was not consistent for

differing ecological regions or stream types (Harmel et al., 1999). Rosgen reported both the BEHI and the NBS to be significant indicators of erosion ( $p=0.0001$ ) (Rosgen, 1996, 2001), while Harmel et al. (1999) did not find a significant relationship. They did observe an increase in erosion with an increase in the BEHI risk ranking, but the variability was so high that there was no significant difference ( $\alpha=0.05$ ) between the different categories (Harmel et al., 1999). Rosgen (2001) hypothesized that the difference was at least in part due to the extreme flows used in Harmel et al. (1999). For a RGA, the BEHI was not ideal, given the recommended three years of additional observations. However, without the three years of data, the BEHI relies on metrics whose measurement can be subjective.

Another major criticism of the BEHI, as well as other RGAs, was they were inadequate tools for predicting erosion by themselves. Simon et al. (2007) makes this criticism of the BEHI and the use of the Rosgen classification as the primary design tool in streambank erosion modeling. First, when trying to analyze the erosive effects of anthropogenic forces, the time and spatial scales of the RGAs have to match that of the disturbances. Simon et al. (2007) noted that these disturbances can cause channel evolution at rates that would normally only be seen at relatively large time scales, i.e. moving from geologic time to time periods ranging from 50 to 100 years. The BEHI provided only a “snapshot” in time of the stream and does not have a mechanism to predict erosion rates (Simon et al., 2007). Using the BEHI-NBS method to predict future erosion relies on the assumption that future erosion will occur similarly to the past (Bigham, 2016).

While this method may adequately model past erosion (Sass and Keane, 2012), future erosion predictions will likely have much higher uncertainty. Sass and Keane (2012) also highlighted how the metric scores are subjectively weighted, as they had to adjust for lower root densities than was experienced in the development of the BEHI.

### *Channel Stability Index*

The CSI has a temporal reference by incorporating an assessment of the stage of channel evolution model. However, the stage of channel evolution had been noted as a difficult metric to assess in the historical reports. While the CSI may add a temporal aspect, it still had its limitations for assessment in streambank restoration. CSI assessed only the stability of a reach, when it could be necessary to consider multiple aspects besides stability for stream restoration (Habberfield et al., 2014). Habberfield et al. (2014) also pointed out the difficulty in relying on the CSI alone, given the scale of assessment. The CSI is done at a reach scale, but biotic factors can change at smaller scales, which may not be sufficiently captured by the CSI in stable sites (Habberfield et al., 2014). While the CSI could successfully rank streams in terms of quality, it did not adequately capture the idea of dynamic stability, as there were unstable reaches that were still considered good habitat (Habberfield et al., 2014).

Habberfield et al. (2014) noted the inability of the CSI to differentiate between more stable reaches in terms of habitat quality. Heeren et al. (2012) noted problems differentiating between more reaches that are unstable. One



possible reason discussed by Heeren et al. (2012) was the inclusion of metrics that were difficult to assess, as well as not including some measure of cohesion. Heeren et al. (2012) also noted how each metric was equally weighted, which implies either one of two things. Either the source of instability is constant between reaches, or the contribution of each metric to stability is equal. Assuming the former to be true, this means that assessments across different regions could be incomparable, as their sources of instability change (Heeren et al., 2012).

The assumptions made concerning time limit the use of CSI in predicting future erosion. Heeren et al. (2012) assumed that the RGA, performed in 2010, represented the streambank stability from 2003 to 2008. The RGAs in 2010 may not be representative of conditions after the date they were collected. The CSI was also considered inadequate for modeling streambank erosion, since the current CSI score does not necessarily reflect future conditions, though there was a correlation between lateral bank retreat and percent instability and the percent woody cover (Heeren et al., 2012).

### Improvements of Rapid Geomorphic Assessments

The problems and limitations of RGAs have been recognized (Bigham, 2016; Habberfield et al., 2014; Harmel et al., 1999; Heeren et al., 2012; Simon et al., 2007). Regarding the BEHI, several recommendations have been proposed. Removing the bank height/bankfull height ratio has been tested (Newton and Drenten, 2015). The results indicated that RGAs that do not rely on the bankfull

metric produce similar stability rankings to the normal BEHI (Newton and Drenten, 2015). Additionally, Newton and Drenten (2015) added a pre-questionnaire to identify reaches with a BEHI ranking of moderate or higher. The pre-questionnaire was designed to save time, so only the reaches at higher risk were fully assessed. Newton and Drenten (2015) pre-screening included the identification of broad patterns, for example, whether or not 50% or more of the bank in question exhibited significant undercutting.

Sass and Keane (2012) proposed combining the root depth ratio and the root density into one metric, which they called woody vegetation present. The metric had two possible scores, either 8.5 for no woody vegetation or 2.5 for woody vegetation present. This adjustment was made due to the consistency of root density in the study area and calibrated the BEHI model for more accurate usage in the study area.

Modifications have been made to the CSI as well. Heeren et al. (2012) created an ecoregional RGA for the Ozark Ecoregion in Oklahoma, which simplified the RGA by removing metrics that were homogeneous across reaches. New and modified metrics were also included to better reflect the ecoregion-specific features. The resulting RGA, the Oklahoma Ozark Streambank Erosion Potential Index (OSEPI), had a higher correlation to recent streambank erosion compared to the CSI. Note that the OSEPI was likely not applicable outside of the region where it was developed and tested. While ecoregional RGAs are

promising, they require an initial assessment and testing to identify uniform metrics and other key bank features.

Phase II analysis in the VTDEC (2003) assessed similar metrics to the CSI. Both RGAs included an evaluation of the level of incision and presence of channel aggradation. While the CSI described the amount of woody cover for the reach, the VTDEC (2003) did not include vegetative analysis in its RGA. Vegetative cover was a significant predictor of erosion (Heeren et al., 2012; Sass and Keane, 2012). It was also shown that the addition of more quantitative woody cover metrics could benefit geomorphic assessments, especially when concerned with the riparian area (Keeton et al., 2017). Keeton et al. (2017) reported that forest structural metrics such as the basal area and dead tree density were positively correlated with VTDEC (2003) RGAs and suggested that the metrics could be assessed either on-site or by using LIDAR. This could imply that adding more quantitative measurements of woody cover to the CSI could be beneficial.

### **Potential Data Sources for Digital RGAs**

The goal of this research was to use readily available digital data and resources to perform RGAs. There were no current studies identified with this specific goal. There were, however, other studies using similar methods. For example, Faux et al. (2009) used LIDAR to measure bank height, face length, bankfull height and width, as well as the top width of the base flow channel. Many

other studies highlighted the potential of using LIDAR to cover larger areas more consistently and quicker than on-site techniques.

### Visual Assessments

One of the most accessible ways to assess reach length metrics off-site was Google Earth (Fisher et al., 2012). The useful capabilities for the research included its historical imagery and its measurement tools. The historical imagery was especially promising for this study given the need to compare data collected in previous years. There are typically two images available each year: one near the beginning of the year and one close to the end.

It should be noted that there were several different sources for the Google Earth imagery including DigitalGlobe and the U. S. Department of Agriculture, Farm Service Agency. For this project, if Google Earth provided a reference to the image source, it was noted in the figure caption.

Google Earth does have some limitations, which could affect its performance in digital RGAs. For example, cloud cover could obscure the view of the study stream. Other visual obstacles include the presence of deep shadows in steep landscapes, or dense vegetation (Atha, 2014; Fisher et al., 2012). There was also little published about Google Earth's data processing, but there was some obvious blending of several different resources. This leads to images that were not usable due to obvious distortion around seams (Fisher et al., 2012). There was also no guarantee of high-resolution imagery or complete data coverage for the area of interest, which Fisher et al. (2012) acknowledges and

Boardman (2016) experienced in his example study area. Since Google Earth used a wide range of sources, the resolution was not always consistent. The coverage was also not consistent across time, which could also seriously limit its use in contemporary studies (Boardman, 2016; Fisher et al., 2012). However, if Google Earth continues to keep up-to-date in terms of both extent and quality, then it could be a very helpful tool for performing RGAs. The potential for Google Earth was especially noted for the CSI which is more dependent on visual assessments than the BEHI.

#### Channel Bed/Bank Characterization

Several metrics depend on soil properties; for example, the primary bank material. USDA (2017) Web Soil Survey provides a large spatial coverage on soil characteristics, including soil types and horizons as well as typical plant associations and characteristic vegetation. The benefits of using Web Soil Survey included the fact that it is free and covers all of the U.S. Issues may arise, however, due to the low data resolution.

A plant species database that reports root density was currently not available. The original plan was to use procedures by Pollen and Simon (2005) to model the effect of vegetation on streambank stability. The Pollen and Simon (2005) method was based on field and laboratory studies reporting measured root density. Woody riparian species have an average of 75 to 250 roots crossing the shear plane with diameters ranging from 0 to 10 mm, while grasses modeled after switchgrass had 200 to 1000 roots crossing the shear plane with diameters

ranging from 0 to 5 mm (Simon and Collison, 2002; Pollen et al., 2004). Using these findings, however, lead to a root density ranging from 0 to 2% for woody species and 0 to 3% for grasses. This was based on using the Root-Area-Ratio (RAR), or the proportion of the soil sample covered by roots (CIRIA, 1990), and the soil sample was assumed to be 1 m<sup>2</sup>. In this case, the area covered by roots was determined by multiplying the area of the cross section of a root times the number of roots, and the average root depths for specific ecoregions were determined using the method described for metric 2. Another problem with using RAR was that it represented the cross-sectional area in relation to the shear plane, while the BEHI was required the area of the bank face covered by roots.

#### Stream/Cross Sectional Geometry

Both the BEHI and the CSI utilized stream characteristic metrics, such as face length and bank height, which were estimated using a variety of sources, including aerial images and LIDAR. Another potential resource considered was Google Earth, since it has the ability to generate cross sections by drawing a path and displaying an elevation profile.

The current research was not the first to utilize Google Earth to study geomorphology. It has already been recognized as a useful source in larger study areas and has been used to assess changes in coastal shorelines (Royo et al., 2016), measure landslides and channel widths (Fisher et al., 2012), study contemporary erosion by identifying the presence or absence of depositional or erosional features (Boardman, 2016), and in the identification of in-stream woody

debris (Atha, 2014). Fisher et al. (2012) reported that Google Earth was more accurate than LANDSAT at measuring channel widths and could be used to approximate landslide surface areas at smaller resolutions than previous tools.

Unfortunately, Google Earth's elevation profiles were not deemed suitable for this study's purposes. The profiles generated by Google Earth did not appear to be at a high enough resolution to accurately identify streambank features (Figure 2). The source of Google Earth elevation data was not available, which made it difficult to ascertain when and how these data were collected. While Google Earth was not a viable tool to assess the streambank geometry, the measuring tool was accurate enough for the measurement of reach length features. Obviously, LIDAR represented the most technologically advanced method and could provide the most accurate measurements of bank features. Given the inherent difficulty in determining bankfull height, the potential of LIDAR to detect one of the primary indicators, namely the floodplain, was promising.

Several sources provide free LIDAR data at high resolution (1 to 2 m) and others for a fee. USGS (2018a) Earth Explorer provided a variety of products including raw point cloud data. A point cloud contains data defined by a coordinate system. USDA (2018b) Geospatial Data Gateway, on the other hand, provided finished products such as Digital Elevation Models (DEMs) at horizontal resolutions as high as 1 m. Typically, LIDAR data have been collected by a variety of different companies with a variety of purposes. A resulting drawback is that the data available is not always consistent in quality or

completeness, in both the data itself as well as the metadata. For the current study, raw LIDAR data sets were available from USGS EarthExplorer, but only for the Fort Cobb study sites. USDA (2018b) Geospatial Data Gateway had processed image files for both the Great Plains and the Ozark ecoregions. There are benefits to using either raw LIDAR data or processed image files. A benefit to using processed image files is that the data has already been processed into a usable DEM. Raw LIDAR data clouds can be processed in ArcGIS, and resources are available that show how to create a DEM (e.g., Sumerling, 2011).

Logistics in using LIDAR could limit its use in the RGA. While LIDAR can provide an accurate snapshot of the stream, there is no guarantee that there will be data available for every study area, or that the data available will be relevant in terms of time. Another potential inhibitor to the use of LIDAR data are the software requirements to analyze these data, e.g. ESRI ArcGIS, and knowledge on how to use it. While ArcGIS is not free, some comparable software packages are available to the public, e.g. GRASS GIS. If the user is unfamiliar with LIDAR or ArcGIS, this can make the digital RGA process longer and more complicated than it was originally intended to be.

Faux et al. (2009) method for measuring bankfull height was dependent on finding the hydraulic plateau. This was done by calculating then plotting the hydraulic depth versus the flow elevation, with the maximum stage representing the bankfull. Where there were multiple terraces, the lowest elevation terrace was used to represent the active floodplain. This method produced comparable



results to on-site measurements (Faux et al., 2009). There were, however, several cases where the method underestimated bankfull, and Faux et al. (2009) suspected that more information would be needed in order to correctly identify bankfull.

One of the hurdles to the usage of LIDAR in stream applications was their ineffectiveness in penetrating water surfaces (Faux et al., 2009; McKean et al., 2009; Soar et al., 2017). There were bathymetric capable LIDAR and tools that were capable of bank measurements (McKean et al., 2009), as well as methods to integrate bathymetry into DEMs to create a continuous surface (Merwade et al., 2008). However, in terms of availability, there were no bathymetric data sets available for streams in Oklahoma at this time (NOAA, 2018). As bathymetric LIDAR data becomes more readily available, incorporating it into digital RGAs may be a practical alternative.

Another example of tools that could potentially be useful are the development of extraction tools for LIDAR point clouds or Digital Elevation Models (DEMs). There are several examples of this, including software packages easily installed into ArcMap. These include toolboxes made by individuals, for example, Riparian Detection and Riparian DEM toolboxes, which used DEMs to create rasters that delineate streambanks and channels (Kelley, 2017). Soar et al. (2017) also referenced several different toolboxes, including FluvialCorridor (Roux et al., 2015), RESonate (Williams et al., 2013), and IDRAIM (Rinaldi et al., 2015). There are benefits to using toolboxes already made, including the fact that

they are usually easy to install and use, and there may be published documents or public forums for any questions you may have. With the continued development of LIDAR and toolboxes such as those mentioned, Soar et al. (2017) felt that future applications could potentially be capable of assessing basin-wide streambank stability.

Another aspect of the stream geometry required by RGAs is stream flow data. For example, the CSI requires water depth during approximate baseflow conditions to estimate the degree of incision. Baseflow was typically assumed to be the depth of the water at the time that the RGA is performed. The BEHI has no direct stream flow requirements, but Manning's equation can be used to determine the flow depth at different flows, including the bankfull depth at the assumed 2-year return interval (Leopold, 1995).

The next potential resource that was considered was USGS (2018c) StreamStats. StreamStats provides several parameters required by Manning's equation, including the channel slope and the approximate flow at the point of interest. The channel 10-85 slope, referred to as CSL10\_85fm in StreamStats, was calculated using a 10 m resolution National Elevation Dataset (NED). The slope was calculated between two points: one 10% and one 85% of the length between the stream gage and its longest flow path.

Also significant for this research was the statistics provided by StreamStats on peak flood and intervals. The drainage area was also calculated, which was helpful for some of the regional equations used to calculate bankfull

depth. StreamStats provided estimates of the magnitude and frequency of peak flows on both gaged and ungaged streams. Estimates for ungaged streams were based on multiple-linear regression equations developed from gaged streams. The equations related peak streamflow to one or more basin characteristics (Lewis, 2010). StreamStats calculated both a peak flow and a controlled peak flood, which was referring to the difference between the natural peak flood and the peak flood with the presence of any flood control structures. The farther a structure is upstream, the less effect it has on the peak flow at the point of interest. In this study, the controlled peak flood was used in order to account for any flood control structures present.

Stream gages were another source for determining some of the streamflow statistics. Simple stream routing can be used to estimate streamflow at the point of interest when the gage is located upstream or downstream of the site. Most of the streams used in this study had stream gage data available.

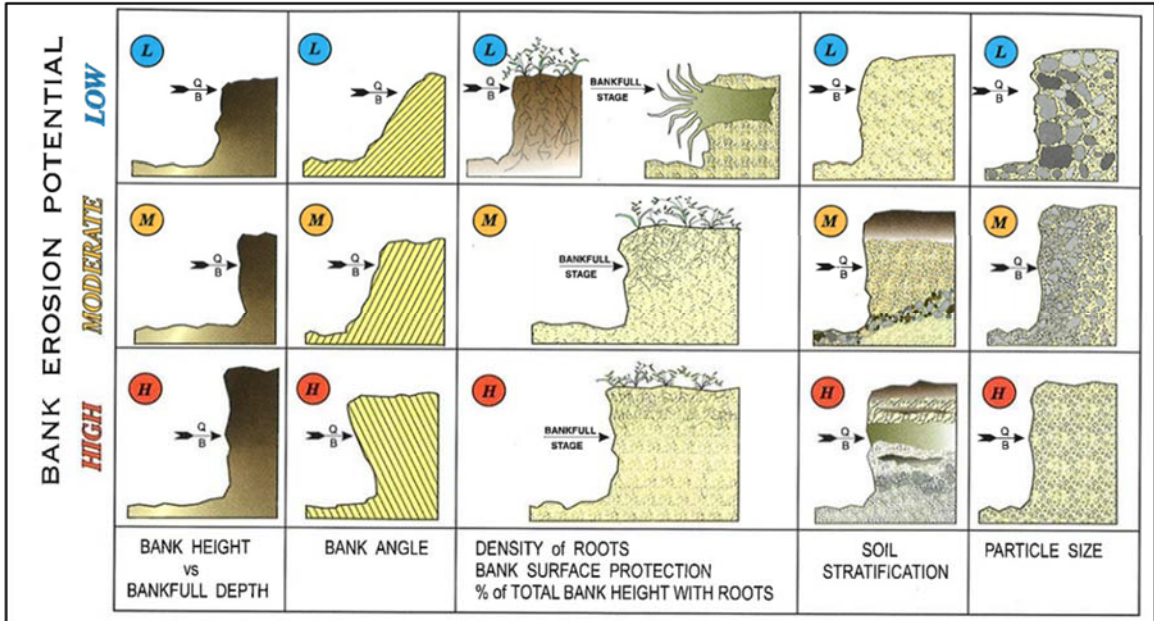


Figure 1: The different erodibility factors considered in the Bank Erosion Hazard Index. Taken from figure 6-25 in Rosgen (1996).

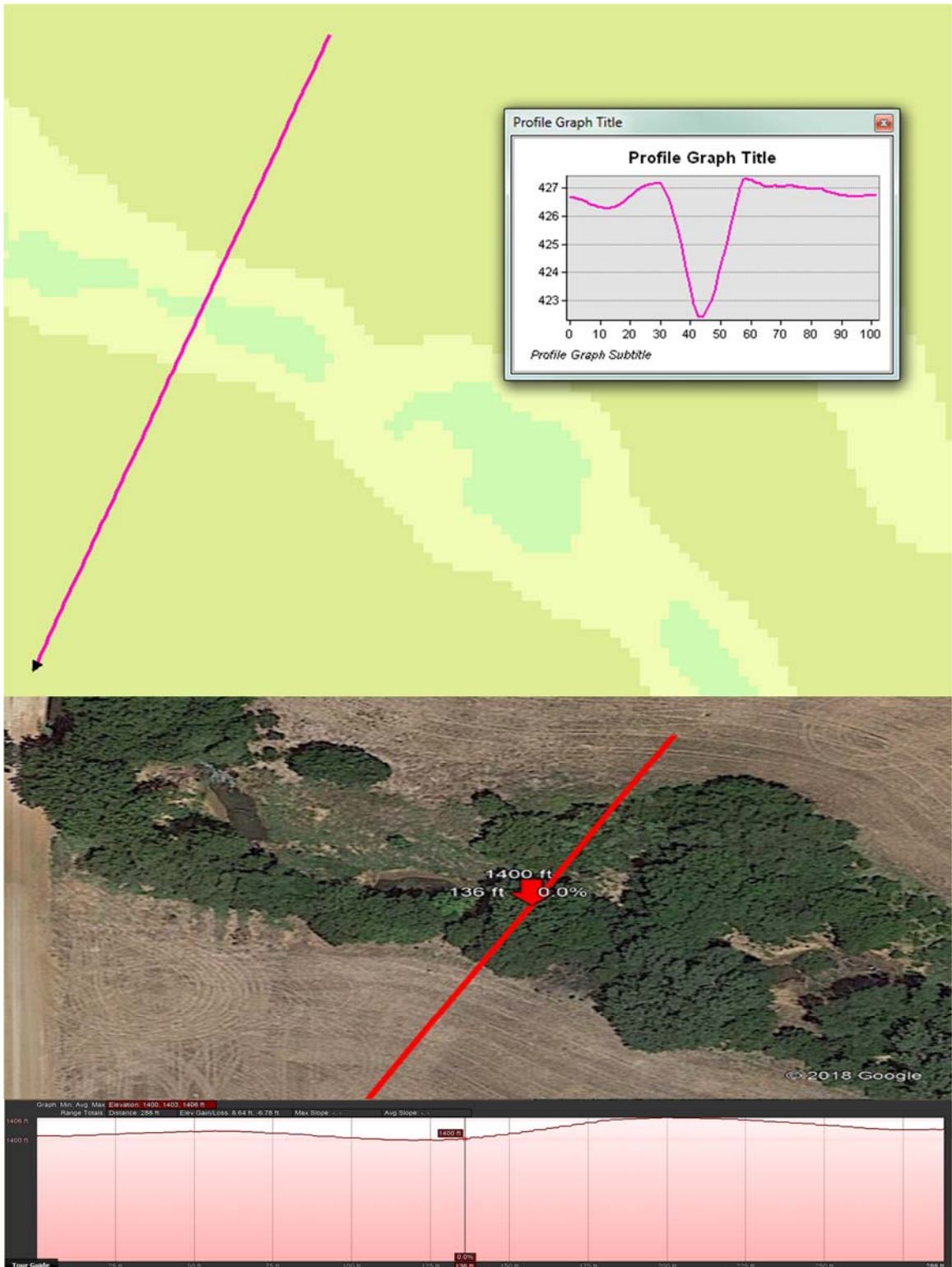


Figure 2: Compare the visible features between cross sections obtained using LIDAR (above) and Google Earth (below).

Table 1: Bank Erosion Hazard Index (BEHI) metrics, scores, stability rankings and associated aggregate scores. Table modified from table 1 from Rosgen (2001).

| Bank Erosion Hazard Index | Metric Number                   |                               |                     |                           |  | Aggregate Score   | Stability Rankings |
|---------------------------|---------------------------------|-------------------------------|---------------------|---------------------------|--|-------------------|--------------------|
|                           | 1                               | 2                             | 3                   | 4                         | 6  |                   |                    |
|                           | Bank Height/<br>Bankfull Height | Root Depth/Bank<br>Height (%) | Root<br>Density (%) | Surface<br>Protection (%) | Bank Height/Face<br>Length (Bank<br>Angle) |                   |                    |
| Value                     | 1.0-1.1                         | 90-100                        | 80-100              | 80-100                    | 0.0-0.34 (0-20°)                           | X ≤ 7.25          | Very Low           |
| Score                     | 1.45                            | 1.45                          | 1.45                | 1.45                      | 1.45                                       |                   |                    |
| Value                     | 1.11-1.19                       | 50-89                         | 55-79               | 55-79                     | 0.35-0.86 (21-60°)                         | 7.25 < X ≤ 14.75  | Low                |
| Score                     | 2.95                            | 2.95                          | 2.95                | 2.95                      | 2.95                                       |                   |                    |
| Value                     | 1.2-1.5                         | 30-49                         | 30-54               | 30-54                     | 0.87-0.985 (61-80°)                        | 14.76 < X ≤ 24.75 | Moderate           |
| Score                     | 4.95                            | 4.95                          | 4.95                | 4.95                      | 4.95                                       |                   |                    |
| Value                     | 1.6-2.0                         | 15-29                         | 15-29               | 15-29                     | 0.985-1.0 (81-90°)                         | 24.75 < X ≤ 34.75 | High               |
| Score                     | 6.95                            | 6.95                          | 6.95                | 6.95                      | 6.95                                       |                   |                    |
| Value                     | 2.1-2.8                         | 5-14                          | 5-14                | 10-14                     | 0.87-0.99 (91-119°)                        | 34.75 < X ≤ 42.5  | Very High          |
| Score                     | 8.5                             | 8.5                           | 8.5                 | 8.5                       | 8.5  |                   |                    |
| Value                     | >2.8                            | <5.0                          | <5.0                | <10.0                     | <0.87 (>119°)                              | 42.5 < X ≤ 50     | Extreme            |

Table 2: Adjustment factors and score adjustments used in this study. Modified from Rosgen (2001) and Rosgen (1996).

| Adjustment Factor     |                 | Score Adjustment |
|-----------------------|-----------------|------------------|
| Primary Bank Material | Clay            | -20              |
|                       | Cobble          | -10              |
|                       | Silt            | +0               |
|                       | Boulder         | +0               |
|                       | Bedrock         | +0               |
|                       | Gravel          | +5               |
|                       | Sand            | +10              |
| Stratification        | No Layers       | +0               |
|                       | Two Layers      | +5               |
|                       | Multiple Layers | +10              |

Table 3: Channel Stability Index (CSI) metrics, scores, stability rankings and aggregate scores (Heeren et al., 2012; Simon and Downs, 1995). L = left Bank, R = right bank.

| CSI   | Metric Number        |  |                        |                            |                                    |                            |       |                                      |        |                                  |        | Aggregate Score & Stability |                                       |
|-------|----------------------|--|------------------------|----------------------------|------------------------------------|----------------------------|-------|--------------------------------------|--------|----------------------------------|--------|-----------------------------|---------------------------------------|
|       | 1                    | 2  | 3                      | 4                          | 5                                  | 6                          |       | 7                                    |        | 8                                |        |                             | 9                                     |
|       | Primary Bed Material | Bed/Bank Protection                      | Degree of Incision (%) | Degree of Constriction (%) | Stream bank Erosion                | Streambank Instability (%) |       | Established Riparian Woody Cover (%) |        | Occurrence of Bank Accretion (%) |        |                             | Channel Evolution Model               |
|       |                      |  |                        |                            |                                    | L                          | R     | L                                    | R      | L                                | R      |                             |                                       |
| Value | Bedrock              | Bed & Banks both protected               | 76-100                 | 76-100                     | None (Both)                        | 0-10                       | 0-10  | 76-100                               | 76-100 | 76-100                           | 76-100 | One                         | X≤10<br><i>Stable</i>                 |
| Score | 0                    | 0  | 0                      | 0                          | 0                                  | 0                          | 0     | 0                                    | 0      | 0                                | 0      | 0                           |                                       |
| Value | Boulder/Cobble       | No Bed Protection & Both banks Protected | 51-75                  | 51-75                      | Fluvial (One)                      | 11-25                      | 11-25 | 51-75                                | 51-75  | 51-75                            | 51-75  | Two                         |                                       |
| Score | 1                    | 1  | 1                      | 1                          | 1                                  | 0.5                        | 0.5   | 0.5                                  | 0.5    | 0.5                              | 0.5    | 1                           |                                       |
| Value | Gravel               | Bed protected & No Bank Protection       | 26-50                  | 26-50                      | Fluvial (Both), Mass Wasting (One) | 26-50                      | 26-50 | 26-50                                | 26-50  | 26-50                            | 26-50  | Six or Three                | 10<X<20<br><i>Moderately Unstable</i> |
| Score | 2                    | 2  | 2                      | 2                          | 2                                  | 1                          | 1     | 1                                    | 1      | 1                                | 1      | 1.5 - 2                     |                                       |



Table 3 continued.

| CSI   | Metric Number        |                                    |                        |                            |  |                             |        |                                      |       |                                  |       | Aggregate Score & Stability |                                 |
|-------|----------------------|------------------------------------|------------------------|----------------------------|--|-----------------------------|--------|--------------------------------------|-------|----------------------------------|-------|-----------------------------|---------------------------------|
|       | 1                    | 2                                  | 3                      | 4                          | 5  | 6                           |        | 7                                    |       | 8                                |       |                             | 9                               |
|       | Primary Bed Material | Bed/Bank Protection                | Degree of Incision (%) | Degree of Constriction (%) | Stream bank Erosion                          | Stream bank Instability (%) |        | Established Riparian Woody Cover (%) |       | Occurrence of Bank Accretion (%) |       |                             | Channel Evolution Model         |
|       |                      |                                    |                        |                            |  | L                           | R      | L                                    | R     | L                                | R     |                             |                                 |
| Value | Sand                 | Bed protected & One Bank Protected | 11-25                  | 11-25                      | Fluvial (One), Mass Wasting (One)            | 51-75                       | 51-75  | 11-25                                | 11-25 | 11-25                            | 11-25 | Five                        | <i>X≥20<br/>Highly Unstable</i> |
| Score | 3                    | 3                                  | 3                      | 3                          | 3  | 1.5                         | 1.5    | 1.5                                  | 1.5   | 1.5                              | 1.5   | 3                           |                                 |
| Value | Silt/Clay            | No bed or bank protection          | 0-10                   | 0-10                       | Combination of Mass Wasting & Fluvial (Both) | 76-100                      | 76-100 | 0-10                                 | 0-10  | 0-10                             | 0-10  | Four                        |                                 |
| Score | 4                    | 4                                  | 4                      | 4                          | 4 - 6  | 2                           | 2      | 2                                    | 2     | 2                                | 2     | 4                           |                                 |

## CHAPTER II

### METHODS

#### **Reach Length Methods**

Reach length metrics assessed with Google Earth included: bank protection (Metric 2), degree of constriction (Metric 4), streambank erosion (Metric 5), streambank instability (Metric 6), percent woody cover (Metric 7), occurrence of bank accretion (Metric 8), and the stage of channel evolution (Metric 9). Table 3 summarizes the CSI metric numbers and names. The tools used in Google Earth can be seen in Figure 3.

#### Reach Determination

Reaches were delineated using the following information. Portions of stream were broken into roughly homogeneous sections based on the shape and vegetation. Google Earth was used to determine the shape of the channel, and any major changes in vegetation. USDA (2017) Web Soil Survey provided additional information, such as the presence of bedrock, which was significant for critical bank determination.

Another important characteristic that was identified was the critical bank. The critical bank represents the bank which is considered most at risk for

streambank erosion. This feature was significant for this study since several of the RGA metrics are assessed using the critical bank alone. In general, Google Earth was used to identify the critical bank, which was often the bank opposite of a point bar. For streams lacking obvious point bars, the critical bank was identified as the taller bank as measured using LIDAR.

### Visual Assessment Methods

The degree of constriction (CSI Metric 4) requires the width of the channel to be measured at two places: once at the representative cross section and once at a place approximately a quarter of a meander upstream, measuring the width at bankfull (Heeren et al., 2012). The bankfull widths were estimated in Google Earth for each cross section, relying on the obvious transitions from sandy material to vegetation or annual vegetation to woody vegetation. Estimating the width was more difficult if trees obscured the stream edge. In those cases, the width was assumed to fall somewhere slightly inside the tree line. An alternative method would be to collect the measurements using LIDAR.

In Google Earth, all evidence of streambank erosion and mass wasting were noted for both banks within the reaches of interest (CSI metric 5). The total reach length effected by mass wasting was marked with a line parallel to the reach length in Google Earth, in order to calculate the percentage of reach length affected by instability (CSI Metric 6). A similar method was used for measuring the percentage of the bank affected by woody vegetative cover (CSI Metric 7) and the percentage of the bank affected by accretion (CSI Metric 8).

Evidence of fluvial erosion included historical widening or migration evidenced in the historical imagery, focusing on the imagery within a year at most. Other pieces of evidence included scouring around any permanent structures, lack of depositional features in places you would expect them, scouring evidenced by sudden lack of vegetation or change in bank material, or clear signs of cutting into channel bars. Degradation, the process of the fluvial erosion acting on the channel bed, was evidenced by the apparent loss of mid-channel bars. Care was taken to ensure that it was an apparent loss of the bar not simply that the bar was invisible due to high flows. In some cases, degradation was assumed to occur where it was not definitively evidenced visually. For example, where there was no evidence for channel widening, but there were several gullies formed. This indicated that there was enough energy for erosion to be occurring, but since it was not being used to widen the channel, it was assumed that it was being used to erode sediment on the channel bed.

Evidence of mass wasting included channel widening, evidence of bank slumping, trees that leaned or had fallen into the channel, fracture lines in the top of the bank, and jagged edges at the top of the bank. The procedure counted channel widening as both fluvial and mass wasting, since it was not always clear from Google Earth which mechanism was predominantly responsible for the channel widening and they are linked processes. Evidence that the channel has widened is sometimes obvious, as in Figure 4. To determine channel widening, only photos from the same source were compared. Other examples of what was counted as mass wasting are illustrated in Figure 5.

Next, the percentage of the reach-length supported by woody vegetation (CSI metric 7) was measured using the Google Earth measuring tool. If the woody vegetative canopy reached the edge of the bank, then it was assumed to provide support (Heeren et al., 2012). If there was evidence of mass wasting, that portion of the bank was considered to not be supported by the woody cover. This same measurement was used to assess bank protection (part of CSI metric 2). If a bank had greater than or equal to 50% woody cover it was classified as protected.

Evidence of accretion were also noted in Google Earth (CSI Metric 8). Evidence of accretion included the formation of any kind of depositional bar, including mid-channel, lateral, and point bars. Deposition around permanent structures, if present, were also included. Accretion was assessed for each bank separately, with it possible for one bank to be made up entirely of a point bar, while the opposite bank could manifest accretion as a mid-channel bar.

Figure 6 provides a good example of an analyzed reach. The blue line represented the reach length, the green line represented the percentage of the right bank supported by woody vegetation, the red line represented bank affected by mass wasting (evidenced by a fallen tree which was visible in another photo from the same year), and the brown line represented the percentage of the left bank experiencing accretion. Note how lines were not drawn for metrics that were deemed to make up the entire reach length. For example, lines were not

drawn for woody protection that provided for 100% of the left bank, or the sand bar making up 100% of the right bank.

By their very nature, analyzing a reach for evidence of degradation, channel widening, and accretion provided the necessary information to determine the stage of channel evolution (CSI metric 9). Each stage was associated with these three different processes. Stage 1 was a stable and unmodified channel. Stage 2 was a constructed channel. Stage 3 was degradation alone while stage 4 was both degradation and widening. Stage 5 was associated with both aggradation and widening, and stage 6 was associated with a restored equilibrium after a disturbance. To determine the stage of channel evolution, the following questions were answered:

- (1.) Is there evidence of degradation (see evidence for fluvial erosion, besides channel widening)?
- (2.) Is there evidence of historical widening (see evidence for fluvial/mass wasting)?
- (3.) Is there evidence of aggradation (see evidence for accretion)?

If all three questions were answered as 'No', then the reach was determined to fall into stage 1 of the channel evolution. If only question 1 was answered as 'Yes', then it was considered stage 3. If questions 1 and 2 were answered as 'Yes', then it was considered stage 4. If questions 2 and 3 were answered as 'Yes', then it was considered stage 5. If only question 3 was answered 'Yes', then it was considered stage 6. It was deemed not applicable to place any of the

streams in this study into stage 2, which indicates a constructed channel. If all three questions were answered 'Yes', it was scored as a stage 4, since all three processes are occurring (degradation, widening, accretion), it makes sense to have a higher score indicating instability.

### **Channel Bed/Bank Characterization**

Several metrics fall under the generic heading of bed or bank characterization. These include primary bed material (CSI Metric 1), bed protection (CSI Metric 2), root depth (BEHI Metric 2), root density (BEHI Metric 3), surface protection (BEHI Metric 4), primary bank material (BEHI Adjustment #1), and stratification (BEHI Adjustment #2). These characteristics are usually estimated in the field based on visual observations. This study focused on attempting to estimate these characteristics using the USDA (2017) Web Soil Survey.

#### Determining Primary Bank Material & Stratification

While Web Soil Survey only has information as deep as approximately 2 m, it was assumed that this was enough information to make determinations about the streambanks. In order to use Web Soil Survey, it was first helpful to export shapefiles of the Area of Interest (AOI) that contained the cross sections for each site. It was noted that while the imagery displayed in Web Soil Survey appeared to be up to date when compared to Google Earth, the placement of the stream (denoted by a W in the soil map) was off, as can be seen in Figure 7. Professional judgement was used to determine the most appropriate soil type

based on the position of the stream in the relevant year determined using the historical imagery in Google Earth. There were also few instances where the stream noted in the soil map overlapped with the stream bank, and the representative soil type was selected from the surrounding soil types. This was done by noting how the soil types are related to slope. As can be seen in Figure 8, some soil types are clearly linked to the hillslope formations while some are more closely related to the valley floor. In this case, in deciding between using the Sm or CIF soil types, the Sm soil type was selected based on its closer topographic proximity to the selected bank, where it is clear that the CIF soil type is related to the beginning of significant hillslopes.

The BEHI has two RGA score adjustments that are directly related to soil types and horizons: one for the primary bank material and one for the presence and number of stratified layers. For this study, it was decided to utilize the representative values of percent sand-silt-clay and the percent fragments reported for each soil horizon in the “Particle Size and Course Fragments” report under the Soil Physical Properties tab.

In order to use the Web Soil Survey to assess bank material, it was decided to use the soil’s  $d_{50}$  using the percent sand-silt-clay and the percent fragments provided by Web Soil Survey soil reports. The percent fragments is reported on a volumetric basis of the whole soil, while the percent sand-silt-clay is reported on a weight basis for the soil sample excluding anything larger than sand (2 mm). The percent sand-silt-clay first was converted into a whole-sample



percentage by using the percent fragments to determine the percentage of the whole soil consisting of fines (sand-silt-clay). Since there is a difference in how the percent fragments and fines are reported, the expected error from using this method increases. Once all of the percentages represent whole soil sample ratios, the soil class that contains 50% or more of the sample can be determined. This method determines the  $d_{50}$  soil class for each soil layer. Finally, the soil class that made up the highest percentage of the vertical bank, based on the reported soil horizons, was used to represent the primary bank material.

In order to determine the presence of stratification, the primary bank material for each soil horizon is used along with the erodibility associated with different soil sizes. First, the median soil size for each soil class (USDA classification system) was used to assign a soil size to each layer. The size was then used to determine the critical shear stress,  $\tau_c$ , and the erodibility coefficient,  $k_d$ , using the bank material worksheet in BSTEM version 5.4. Then Figure 9 from Hanson and Simon (2001) was used to determine the erodibility class associated with that soil class. Since the true  $d_{50}$  was not known, each soil class had a range of erodibility classes. Given that there was some overlap between erodibility classes and soil classes (Table 4), the certainty of stratification being present would increase if there were a difference of more than one erodibility class. But for this study, a stratified layer was identified if there was any change in erodibility class combined with an order of magnitude of difference in the  $k_d$ . The points assigned to each primary bank material and stratification scenario are summarized in Table 2.

It should also be noted that Web Soil Survey only reports up to 2 m below the surface. If the streambanks are taller than this, then you would expect less accuracy in both the methods for determining primary bank material and stratification. In particular, if the stratification that is described in the Web Soil Survey is on part of a bank that is never going to be exposed to water, then the expected risk of erosion is diminished.

### Bank/Bed Protection

The main indicator for bank protection was the percentage of the bank supported by woody cover as described in the reach length methods. Additional factors related to the bank material was also considered. Web Soil Survey provides information in its soil reports on both the presence of rock fragments greater than or equal to 2 mm. If there was a significant (more than 50% coverage) of soil fragments, or if the primary bank material was bedrock/boulder/cobbles, then these factors were also considered in the bank protection determination (CSI Metric 2).

The main indicator of bed protection used in this study was the primary bed material obtained from the field reports available from the closest USGS Stream Gages. If the bed material size was bigger than gravel, the bed was counted as protected. Additional factors considered was the depth to a restrictive layer and percent of fragments on the surface. It was assumed that a restrictive layer, if present, would provide bed protection and that a high percentage of fragments on the surface (greater than or equal to 50%) would correlate to

streambed armoring and/or bank protection. The estimated depth to a restrictive layer is reported in several different places in Web Soil Survey. For this study, the soil report “Map Unit Description” under AOI Inventory in the Soil Data Explorer tab was used to find the depth to a restrictive layer. The percent of the surface covered with rock fragments greater than or equal to 2 mm is reported in “Fragments on the Soil Surface” under the Soil Physical Properties tab. These two criteria were considered in addition to the primary bed material in determining bed protection.

#### Root Depth and Root Density

Web Soil Survey also provides information on what kind of vegetation you might expect to find on that particular soil type. Typically, these were determined using the “AOI Component Description (Nontechnical)” soil report under the AOI inventory tab. A few soil types did not provide any vegetative information except for an Ecological Site, Plant Association, or a Habitat Type (reported under the same name in the “Rangeland and Forest Vegetation Classification, Productivity, and Plant Composition” soil report under the Vegetative Productivity tab). In those cases, the Ecological Site Description was used to determine the typical plant species. The Ecological Site Description can be found using the database provided by USDA (2018a).

Only species in the historic climax vegetation, woody species, and cool-season grasses were included. The grassy and woody species were the categories focused on since these two categories appear to be what is deemed

important in bank stabilization modeling (Pollen and Simon, 2005). There were some instances where only generic species were listed on Web Soil Survey, such as “oak” or “willow, and in those cases, the OSU Extension (1998) *Riparian Area: Management Handbook* was used to provide names of species based on the ecoregion.

Once the list of species was acquired, the USDA (2018c) PLANTS database was used to determine a minimum root depth for each species in the woody species and grass species categories, which was then used to get an average root depth for the critical bank. If the soil consisted of a complex, or multiple soil types with different plant species associated with it, then the soil type that made up the majority of the matrix was used.

Once the average root depth was determined, the BEHI Metric 2 score was calculated, using the bank height measured in LIDAR. Since roots are counted as a form of surface protection (Heeren et al., 2012; Rosgen, 2014), the surface protection percentage (BEHI Metric 4) was set equal to the percentage of vertical bank protected by roots (BEHI Metric 2). This provided a percentage that most likely overestimated surface protection, since the root density is not taken into account. But it may also average out, since it also does not take into account other forms of protection, such as bank or bed material.

Since the literature on root structure did not provide a wide range of options, historical root density measurements were used to come up with a correlation to the percentage ratios used in BEHI. Professional judgement was

used to correlate the vegetation type and assemblages to the root density stability rankings provided by the BEHI. Since the root density metric is one of the least sensitive metrics in the BEHI, it was not deemed critical to obtain a vegetative matrix that could predict the complete range of values. The vegetation class (none, vegetated-grass, vegetated-woody) of the critical bank was evaluated using Google Earth, where the class was determined by the vegetation type that appeared to make up the majority of the reach in question. For an example, see Figure 10. For reaches identified as being predominantly grass, the 10 to 14% root density class was selected. For reaches identified as being predominantly woody, the 30 to 54% root density class was selected. If a reach was predominantly bare, then the <5% root density class was used.

## **Stream/Channel Geometry Methods**

### Methodology for Bankfull Depth Measurement

Given the nature of the bankfull stage and the difficulties in identifying it, several potential alternative methods were tested in this study. Since the identification of bankfull stage is important, not just for the BEHI, it was deemed worthwhile to find a method that was more precise. These methods relied on the use of the bankfull indicators and the return interval flows, which are often associated with return periods of approximately 1.5 to 2 years (Leopold, 1995).

Past studies of stream morphology have developed regional equations relating bankfull metrics to other stream characteristics, drainage area for example. Bankfull depth measurements derived from regional equations could

potentially improve the RGA, since the equations typically rely on some other more easily measured stream characteristic. For example, this study tested equations that used things like meander length which can be measured in Google Earth, and drainage area which can be obtained from USGS (2018c) StreamStats. All of the regional equations tested in this study are summarized in Table 5.

The selected regional equations tested in this study include Dutnell (2000) and Bieger et al. (2015) relationships between mean bankfull depth and drainage area, Williams (1986) relationship between bankfull depth and stream meander features. While Dutnell (2000) equations were developed in Oklahoma, Williams (1986) equations were developed using data from all over the world. The applicability of empirical equations is usually determined by the circumstances and location of development. Both factors can be assessed as to how similar the current study area is to the cases in which the equations were developed. The more similar, the more likely the equations will be applicable and accurate. Using empirical equations that were developed using data outside of the study area may prove to be inaccurate. Williams (1986) equations were included in this study since they are being used regardless of the development area, as can be seen by their inclusion in Wildland Hydrology's field notebook (Leopold et al., 1998).

Williams (1986) bankfull depth equations listed below, are dependent on meander features. Meander features were measured using Google Earth's measuring tool:

$$D = 0.027L_m^{0.66} \quad (1)$$

$$D = 0.036L_b^{0.66} \quad (2)$$

$$D = 0.037B^{0.66} \quad (3)$$

$$D = 0.085R_c^{0.66} \quad (4)$$

$$D = 0.12W^{0.69} \quad (5)$$

$$D = 0.12W^{0.69}K^{1.46} \quad (6)$$

where  $D$  represents bankfull mean depth,  $L_m$  represents meander wavelength,  $L_b$  along-channel bend length,  $B$  represents the meander belt width,  $R_c$  represents the radius of curvature,  $W$  bankfull width, and  $K$  represents sinuosity. Figure 11 from Williams (1986) helps visually show what features are being identified and how to measure them. The current study attempted to replicate meander identification methods used by Williams (1986), which included assigning a single wavelength to each meander. When calculating sinuosity, at least two meander wavelengths were included, to be consistent with historical methods as recorded in the unpublished final reports (Saenz et al., 2016; Storm et al., 2010).

One method Williams (1986) provided was not replicated in the current study. Williams recommends that circular arcs of known radius be superimposed over the image to find the radius that best matches the main channel. Google Earth, however does not have such capabilities, so it was left to the best

judgment of the user what radius best matched each scenario. This was often done by drawing two potential radii from the outside edge of the meander to the approximate center of the curve and then comparing their lengths to ensure that they were similar. The bankfull width was estimated in Google Earth as well. The same method was used as was described for the digital method for measuring the degree of constriction.

One caveat to using the Williams equations is that stream shape limitations applied in the development stage of this study. While the majority of streams exhibited a distinct meander pattern, some of the smaller streams lacked a measureable meander. For example, see Figure 12 which compares a second order and fourth order stream used in this study. The first four Williams equations were not applied to streams that did not have an identifiable meander pattern.

Dutnell (2000) developed equations predicting mean bankfull depth, bankfull width, and bankfull cross sectional area using drainage area. These equations were developed using data from all over Oklahoma and divided using several factors including stream type, mean annual precipitation, or ecoregion. Dutnell recommended using the equations with the highest  $R^2$  values, which were the ones grouped by precipitation, or ecoregion. Drainage area was determined using the USGS (2018c) StreamStats. This study used the same maps as Dutnell to determine which equations were applicable to the study sites, which included equations for the Central Great Plains ecoregion and the 23 through 33 in mean annual precipitation group. There were several ecoregions



and precipitation groups which did not have enough data to calculate an equation, and in those cases, the equations Dutnell (2000) developed using all the available data was used:

$$\text{Precipitation Group (23-33 in)} \quad D = 2.21 * DA^{0.082} \quad (7)$$

$$\text{Precipitation Group (All):} \quad D = 2.81 * DA^{0.074} \quad (8)$$

$$\text{Ecoregion (Central Great Plains):} \quad D = 2.13 * DA^{0.090} \quad (9)$$

$$\text{Ecoregion (All):} \quad D = 2.81 * DA^{0.073} \quad (10)$$

where  $D$  stands for bankfull depth and  $DA$  stands for drainage area. It should be noted that while Dutnell (2000) found that the equations based on ecoregion performed the best overall in terms of  $R^2$  values, the equations predicting mean bankfull depth had the lowest  $R^2$  values compared to the other predictive equations.

The last set of regional equations tested in this study were the equations developed by physiographic regions of the United States by Bieger et al. (2015). Bieger et al. (2015) used data from across the United States and developed equations for the entire US as well as for both a coarse and fine division of physiographic regions. It was noted that an equation developed for a fine physiographic region would be expected to perform better than an equation developed nationally. It should be noted that the equations developed by Bieger et al. (2015) included the same data Dutnell (2000) used in the development of his equations. The same map as Bieger et al. (2015) was used to determine the coarse physiographic regions for each site, which included the region called the

Interior Highlands. Similar to the situation in Dutnell (2000), there was not enough data available for some regions to develop an equation, especially for some of the finer scale regions. Therefore, this study focused on testing the USA and the course physiographic equations:

$$\text{Physiographic Division (Interior Highlands):} \quad D = 2.27 * DA^{0.267} \quad (11)$$

$$\text{Physiographic Division (Interior Plains):} \quad D = 0.38 * DA^{0.191} \quad (12)$$

$$\text{Physiographic Division (USA):} \quad D = 0.30 * DA^{0.213} \quad (13)$$

where  $D$  stands for bankfull depth and  $DA$  stands for drainage area.

An alternative method for determining bankfull depth was tested, which relied on the Manning's equation and the two year return interval flow. This alternative method was referred to as the  $Q_2$  method.

The Manning's equation (14) was rearranged to solve for the depth of flow. Using the 2-year return interval flow, the depth was assumed to be bankfull depth:

$$Q = \frac{1}{n} AR^{2/3} S^{1/2} \quad (14)$$

where  $Q$  is the discharge,  $n$  is a roughness coefficient known as Manning's  $n$ ,  $A$  is the channel's cross sectional area,  $R$  is the hydraulic radius, and  $S$  is the channel slope. The slope and the discharge are obtained using the USGS (2018c) StreamStats, and the cross sectional area and the hydraulic radius are dependent on the assumed channel shape. The shape of the channel was

assumed to be triangular. The side slopes must also be assumed; in this case 2:1 side slopes were used.

Since the Manning's  $n$  was unknown, the Monte Carlo Method was used to determine the most likely value of flow depth given a random Manning's  $n$ . 100 random Manning's  $n$  values were used to calculate the flow depth for each cross section. The Manning's  $n$  values were randomly selected from a range of  $N$ -values provided in tables 5 and 6 of Chow (1995). The  $n$  ranged from 0.025 to 0.15 for natural channels less than 30.5 m, and 0.025 to 0.1 for channels wider than 30.5 m. The 100 different depths generated were then run in Minitab to determine the most likely value, represented as the mean or median, depending on if the values were normally distributed at 90% confidence intervals.

There are two tables provided by Chow (1995): one for channels less than 30.5 m across the other for channels wider than 30.5 m. Given the number of values provided by each table, the one for channels less than 30.5 m wide could be represented as a triangular distribution, while the other table only had enough values to be represented as a uniform distribution. There was some concern about which table of Manning's  $n$  values to use, especially for the higher order streams, since they had the greater chance of having channels greater than 30.5 m across. Using a simple percent difference analysis there was only an average 6 percent difference between the mean predicted bankfull depths. Even though there did not appear to be a significant difference between using the two distributions, it was decided that it would be best to use the appropriate

distribution for each cross section, as determined by the calculated top-widths. If the calculated top-width was greater than 30.5 m for a majority of the cross sections, then the uniform distribution was used. Otherwise, the triangular distribution was used. It was usually fairly easy to tell which points would need the uniform distribution, given the width of the channel at baseflow. Given the need to calculate the depth a minimum of 100 times with different Manning's n, it was decided that Bentley (2009) FlowMaster was not an appropriate tool for this study. It could potentially be used in future usage of this method if more is known about the channel's shape or roughness. However, given the number of unknowns and the need to perform a minimum of 100 repetitions for each cross section, it was decided best to use Microsoft Excel to solve for bankfull depth. Flowmaster was still used to verify that the excel equations worked.

The PeakFQ method is the same as the  $Q_2$  method, the only difference being in the source used to get the flow rate. PeakFQ refers to the free tool available through USGS that performs flood frequency analysis using stream gage data (USGS, 2014). The software uses peak flow data and calculates the flow for different exceedance probabilities. For this project, the stream gages with the largest record years closest to the study reaches were selected. Once the stream gages were selected, the peak flow data was downloaded from USGS as a watstore file, which was then used in the default settings of PeakFQ to get the Bulletin 17B flow estimates for different exceedance probabilities. Data available up to the year the RGA was collected was used in the PeakFQ calculation.

Equation 15 was used to determine what exceedance probability to use in the PeakFQ analysis results:

$$P = \frac{1}{T} \quad (15)$$

where  $P$  is the exceedance probability and  $T$  is the recurrence interval in years.

For a recurrence interval of 1.5 years, the exceedance probability is equal to 0.667. The PeakFQ software automatically calculates this flow as well as several others, including the exceedance probability for two-year recurrence interval.

Once the flow was obtained from the PeakFQ results, that flow can be used to estimate the flow at the cross section using unit area loading. Once the estimated flow at each cross section was obtained, the same Monte Carlo process as was used in the  $Q_2$  method was used to calculate the flow depth using the Manning's equation (14) and using the appropriate distribution for Manning's  $n$ . Similar to the method for  $Q_2$ , the mean or median flow depth was reported depending on if the calculated depths were normally distributed or not.

The first step of the LIDAR method is to access and download the LIDAR data at the highest resolution possible. LIDAR availability can be checked on the United States' Interagency Elevation inventory (NOAA, 2018), which provides helpful information such as data set names, the month/year collection date, quality level, vertical accuracy, and point spacing. LIDAR data is available from USGS (2018a) Earth Explorer, USGS (2018b) National Map viewer, as well as USDA (2018b) Geospatial Data Gateway. Depending on Esri (2013) ArcGIS and LIDAR processing capabilities, it may be more appropriate to consider using

LIDAR data that has been fully processed into a Digital Elevation Model (DEM). There are resources on how to develop a DEM if only raw raster data is available; e.g. Fagan and Maidment (2012) or Sumerling (2011).

Once a DEM for the study sites was downloaded into ESRI ArcGIS, NAIP imagery was downloaded and added to ArcMap as well. NAIP imagery combined with LIDAR can help confirm the shape of the channel, as can be seen in Figure 13. Overlaying the NAIP imagery with a transparency of 50% over the LIDAR shows how well the channels match up and can help identify features. The NAIP imagery should be from the same year as the LIDAR, if possible. Using the NAIP imagery alongside the LIDAR data helped utilize the change in sediment and vegetation bankfull indicators.

Once the cross section was drawn perpendicular to the stream flow using the 3-D analyst toolbar in ArcGIS, the cross section was analyzed. The first thing identified was a flat section in the cross section, if present, which was assumed to be the stream surface (Faux et al., 2009). Depending on the size of the stream at the time of the LIDAR collection and the resolution of the data, the length of the flat surface will vary. For example, Figure 14 and Figure 15 illustrates how some streams are small enough that, depending on the LIDAR resolution, there may be little to no obvious water surface. For Figure 15, note the distinct difference between the left and right banks. Typical banks observed for fourth order streams included similar bank structures, with a critical bank and extensive point bar. If the flat surface at the bottom of the valley is assumed to represent

the width of the stream at the point in time that the LIDAR was taken, represented as  $W_f$ , the date the LIDAR was collected can be used to determine the flow associated with  $W_f$ . The surface water of secondary channels were not included in the measurement of  $W_f$ . If there were midchannel bars, then the surface water was counted as the entire distance across, including the midchannel bar. Secondary channels and midchannel bars were distinguished using aerial imagery, both NAIP and Google Earth.

Next, the LIDAR cross section was examined again to identify bankfull stage. The LIDAR method depends on identifying a depositional surface as the primary indicator of bankfull (Leopold, 1995). Following the examples from the training videos (Leopold, 1995), the tops of point bars were considered the primary indicator. If there was no obvious point bar in Google Earth or the NAIP imagery, then the top of any other depositional surface, including mid-channel bars, were used as bankfull indicators. If there were multiple surfaces that appeared to be depositional in the LIDAR cross section, NAIP and Google Earth imagery was used to help make the best determination. For example, in Figure 16, NAIP and Google Earth imagery revealed that there was woody vegetation covering surface 1, which was taken to indicate less frequent flow. Therefore, surface 2 was considered bankfull. If there were no depositional features in the LIDAR cross section, which was often the case in the smaller order streams included in this study, then the primary indicator of bankfull was a change in slope (for example, Figure 14).

Once the bankfull indicator was identified, which was sometimes only apparent on the non-critical bank, the bankfull width ( $W_{Bf}$ ) was measured. NAIP imagery and Google Earth was used to assess whether or not the proposed bankfull width was reasonable, based on any obvious changes in soil type or vegetation (for example Figure 10). Once the bankfull width was identified, the depth of the channel from the bankfull indicator to the bottom of the LIDAR-captured channel can be measured ( $H_{Bf}$ ), which represents the bankfull height from the surface of the water. Finally, bankfull depth ( $D_{Bf}$ ) can be determined by simply adding  $d_L$  to  $D_f$ . To summarize, Figure 17 illustrates how LIDAR was assumed to interact with the water surface, and the different relevant measurements for this study. The bankfull depth and height measurements using LIDAR were both assessed.

Braided channels provided a unique challenge in identifying bankfull, as the primary channel could change significantly within a short amount of time. It therefore becomes unclear in the LIDAR which channel is the primary one and what to include in bankfull. For this study, the main channel was determined based on how wide and deep it was. The main channel was selected such that the deepest point in the cross section was included. Bankfull was then identified as the elevation at which water would begin to flood the main channel's banks.

For more examples of how aerial imagery was used to help identify bankfull, see Figure 18 and Figure 19. For Figure 18, the most active point bar was selected to represent bankfull (the green line). Notice how the green line is



approximately the same length as the approximate bankfull width measured in Google Earth. For Figure 19, the depositional surface chosen to represent the bankfull stage was the one that most closely matched the estimated bankfull in Google Earth.

#### Methodology for Measuring “Baseflow” Depth

Three different sources for the base flow ( $Q_b$ ) were tested. The first method utilized both LIDAR and stream gage data (LIDAR+StreamGage). The top width of the channel was measured using LIDAR, and a similar method to  $Q_2$  and  $Q_{1.5}$  was used, assuming a trapezoidal channel shape with 2:1 side slopes. Rearranging the Manning’s equation (14), the depth of the water was calculated and assumed to represent the baseflow depth ( $D_f$  in Figure 17). The appropriate Manning’s  $n$  table and distribution from Chow (1995) was used, depending on the measured top width. For the streams where a top width was undetectable (Figure 14), a triangular channel shape was assumed. The baseflow depth was then calculated using the flow data from the date the LIDAR was collected.

The second method, referred to as the StreamGage method, relied solely on USGS stream gage data. For this study, the average daily flows were collected from the appropriate gage from time periods as close as possible to the on-site RGA collection dates. A triangular channel shape with 2:1 side slopes was assumed. The Manning’s  $n$  distribution used in the Monte Carlo simulations depended on the calculated channel width and on the provided tables by Chow (1959).

The final alternative source for the base flow was the average daily flow provided by USGS (2018c) StreamStats. This method was referred to as the StreamStats method. The average daily flow is linked to the USGS stream gages and regression equations for ungagged streams. A triangular channel shape with 2:1 side slopes was assumed. The Manning's n distribution used in the Monte Carlo simulations depended on whether or not the calculated channel width was greater than or less than 30.5 m.

#### Methodology for Bank Measurements

The other necessary channel measurements, such as bank height and face length, were obtained using the same LIDAR cross section used to identify bankfull height. The top of the bank was typically identified as the point where valley floor ended and the slope down to the channel began. In some cases, the channel was adjacent to terraces and secondary channels. In those cases, bank height was identified as the top of the surface immediately adjacent to the main channel, not the secondary channel or the terrace (example: Figure 20). Once the top of both the left and right banks were identified, the bank height was obtained by getting the distance between the top of the bank and the lowest point in the LIDAR cross section. It should also be noted that only the measurements taken for the critical bank were used in any of the calculations required.

After the top of the banks have been identified, the distance formula was used to calculate the face length. It was calculated using two points, one being

the top of the bank, the second being the point where the surface water of the main channel ended and the bank in question began.

Once both the bank height and face length was measured, the bank angle was calculated by dividing the bank height by the face length. Given the nature of LIDAR, the ability to detect if the bank angle is greater than 90° was not possible. It was therefore assumed that the bank angle was less than or equal to 90°. This is significant since the BEHI scores the ratios differently if the angle is greater than 90° or not.

## **Development Stage**

### Study Area Description

Two different ecoregions were covered in the developmental data's study region, with two streams located in west-central Oklahoma in the Central Great Plains ecoregion, and the other streams in northeastern Oklahoma in the Ozark Highlands ecoregion (Figure 21). These sites were selected because historical RGA data were available. These sites were used in class projects at Oklahoma State University in the Biosystems & Agricultural Engineering Department course BAE6520 *Geomorphic Stream Assessment*. The class projects involved the implementation of both the CSI and BEHI to assess these two ecoregions. The final report for the Great Plains ecoregion was completed in 2016 (Saenz et al., 2016). The stream size was defined using Strahler (1964) stream order classification. The Great Plains streams included Fivemile Creek and the Willow creek of the Fort Cobb Watershed, second order streams (Figure 22). The Ozark

streams included the Barren Fork of the Illinois River, and the Spavinaw Creek, fourth order streams (Figure 23). The final report for the Ozark ecoregion was submitted to the Oklahoma Conservation Commission in 2010 (Storm et al., 2010). The selected stream gages are reported in Table 6, and the locations of the selected stream gages can be seen in Figure 24 through Figure 27.

### Reach Determination

The historical reaches were clearly reported for the Barren Fork and Spavinaw sites. The same reaches were used for the digital assessments. For the Fort Cobb sites, where reaches were not explicitly recorded, the banks running approximately 30.5 m both up and down stream of the historical cross section were analyzed taking care to avoid any bridges or streambank affected by bridges.

### Historical Data Set

Three teams of two collected RGAs for Barren Fork and Spavinaw on July 13 and 14, 2010. One team of three and one team of four students collected RGAs for Fivemile and Willow on August 10 and 11, 2016. The final RGA scores were determined through group consensus based on site photos, RGA measurements and feedback from instructors.

For this study, the final RGA scores were based on an average of the team measurements. Some teams recorded data for both banks and indicated which one was the actively eroding bank, other teams only recorded data on the actively eroding bank, and some teams recorded data on both with no indication

of which was the critical bank. Given the lack of consistency between teams, all data were used, including the critical and noncritical banks. Averaging all of the data provided measurements that were then used in the comparison of the on-site and digital methods.

The logistics of averaging all the measurements was problematic. Both the BEHI and the CSI contained metrics that were scored based on a percentage that was not tied to a direct measurement. The teams subsequently recorded metric ranges, not a single value. In order to average these scores between the teams, the average percent range was selected for each team. A similar method was used in the root depth metric, which typically recorded as a percentage. Next, the bank height was multiplied by the root depth percentage to obtain the metric. For metrics requiring a score for left and right banks, the measurements for the left and right banks were averaged separately.

For the bank angle metric, the scoring was based on the ratio of bank height and face length. There were two different ranges, one for banks less than or equal to a 90 degree angle, and the second range for banks with an angle greater than 90 degrees. Since choosing the proper range was dependent on a visual assessment, the range was chosen based on the selection by the majority of teams.

Another issue with the historical data was the bed and bank protection in CSI metric 2. There were discrepancies in the scoring method between the field data sheets and the final reports. In order for this metric to be comparable across

different classes, the field data sheet scoring was used. According to the field data sheets, a channel with both bed and bank protection received a score of zero, thus indicating the bank was the most stable. If a channel has no bed protection, then one point was added to the final score. If only one bank was protected, then two points were added, and if neither bank was, three points were added. Finally, if there was no bed or bank protection, the metric score was four.

Using the described methods to average the teams' scores, the aggregated scores were compared to the historical rankings, given in Figure 28 and Figure 29. It should be noted that the final report for the 2016 RGAs (FM1 to WC2) did not include a final score, just a final stability ranking. So in order to compare the team averaged scores and the team adjusted scores, stream cross-sections FM1 to WC2 were assigned representative scores within the reported stability ranking. In general, averaging the teams' scores produced similar stability rankings to the team's adjusted score. There were a few points where the team decided to either raise or lower the stability ranking based on professional judgement. The development data for this study were compared to the team averaged scores, hereafter referred to as the historical scores. Any digital method that obtained the same stability ranking as the historical score was considered a success.

## Notes on Methods

The score and ranking system for BEHI used in this study is summarized in Table 1 and Table 2. It should be noted that this study used a slightly modified version of the adjustment factors in order to match the historical methods. It should also be noted that the teams assessing the Barren Fork and Spavinaw streams did not record the BEHI adjustments, which could impact the comparisons.

For the current study, since there was historical RGAs being used and comparisons with measurements made with digital resources, Google Earth historical imagery was utilized. The imagery that most closely matched the RGA collection date was used to assess the digital RGAs for the development data. One exception was when analyzing the structure of the stream at the time the LIDAR was collected. Then the LIDAR collection date was used.

For the most part, the flight dates were provided by NRCS (correspondence with Lori Hatfield). For the Fort Cobb streams, the original flight maps/contract were obtained from the National Geospatial Center of Excellence (correspondence with Stephen Nechero). The LIDAR data resolution and flight dates are recorded in Table 7.

The determination of the root density method used in the digital assessment was determined using the development dataset. Arranging the averaged historical densities from least to greatest and correlating it to the identified vegetation class (from Google Earth) resulted in the following

relationship assumed and used on the validation sites. Densities reported in the 0 to 14% class were predominantly identified as grass (five out of six) while the densities reported in the 15 to 100% were identified as woody (17 out of 23). Averaging the root densities in the 0 to 14% class range, the mean was 10% and the median was 12%. Therefore, for reaches identified as being predominantly grass, then the 10 to 14% root density class was selected. Averaging the 15 to 100% root densities, the mean was 48% and the median was 50%. Therefore, for reaches identified as being predominantly woody, the 30 to 54% root density class was selected.

### **Validation Stage**

In order to validate the methods described, sites were selected where the proposed methods were done off-site, then RGAs were performed on-site. The final category rankings were then compared. The digital RGAs were collected by the author using the methods described before the site visits. Sites were selected using Blue Thumb's interactive site map (Blue Thumb, 2018) and using the following description of qualifications. The goal was to select at least two sites that were similar to the development sites and two that were contrasting. Validation streams had to be minimally urbanized and within second to fourth order. In order to show the method applicability, several different ecoregions (EPA level IV) were selected including two sites in the same ecoregions as the ones used to develop the methods.



The stream orders were reported by Blue Thumb, for the most part. For the streams which were not reported, the EPA watershed calculator tool was used to determine the stream order. Each of the selected streams, the stream order, and the number of reaches assessed are recorded in Table 8. The USGS stream gages used are recorded in Table 8, and their locations in relation to the actual sites can be seen in Figure 30 to Figure 34. Bankfull depth was calculated using the different methods described, using the relevant regional equations, which are summarized in Table 5. In addition, the LIDAR data resolutions used are noted in Table 7, which also includes the LIDAR information for the development stage as well. Table 7 also records the flight date, if known, and the s\_date, which was obtained using the advanced data viewer for the national map (USGS, 2018b). The s\_date was assumed to represent the flight date, if more data that is detailed was unavailable. It should be noted that since the validation sites were a lot more spread out, the variability in the LIDAR resolution is a little higher than it was for the development stage. A team of one to two students who had taken the class and collected some of the historical RGAs performed the on-site RGAs for the validation stage. The author of the current project was also present, but only to provide physical assistance and help identify the reaches to be assessed. In order to reduce bias from the author's previous knowledge of the sites, the author did not provide any input to the on-site assessments. The time required to complete the RGAs for both the on and off-site methods were noted.

## Fully Digital Scores

In order to determine sensitivity of the RGA to remotely assessed metrics, aggregate scores were generated using combinations of the on-site and the digitally assessed metrics. The resultant scores were then compared to the on-site score, and if the stability ranking was the same, it was counted as a success. The success rates were calculated for both the individual methods as well as for the fully digital methods. It should be noted that the success rate is not equivalent to method accuracy. What is being measured is the RGA metric sensitivity, not the ability of the digital method to get the same measurement as the on-site method.

The coefficient of success ( $S^2$ ) was created in order to describe the weighted success rate, and is similar to the coefficient of determination. It is supposed to describe the points that failed and how far or close they were to being considered a success.  $S^2$  was calculated for each stability ranking. The first step was to divide the historical scores into each stability ranking. Then all scores that fell outside of the correct (on-site) stability ranking were analyzed. Each digital score was subtracted by the mean digital score. Then those values were squared and summed. This value was referred to as the  $S^2$  Total Sum of Squares (TSS), the equivalent of the TSS used in the  $R^2$  determination. Next, the digital scores that failed were subtracted from the closest score that would have counted as a success. Those values are then squared and summed. This provides the Explained Sum of Squares (ESS). The final  $S^2$  value was calculated by dividing the ESS by the TSS, subtracting that value from 1, then multiplying by

100%. The  $S^2$  value ranged from 0 to 100%, with 0 representing significant differences in scores, while 100% represented scores that fell within the same stability ranking. In summary, the different digital resources used for each metric are summarized in Table 9 and the known data limitations are in Table 10.

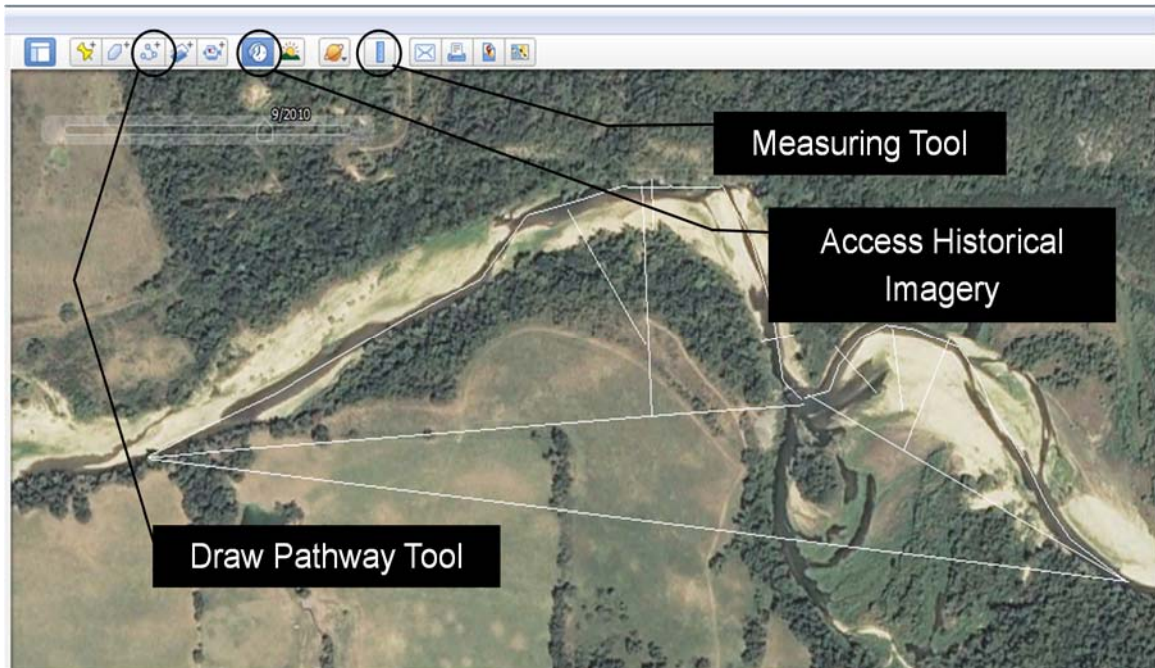


Figure 3: An example of how a stream meander feature is analyzed using the measuring and drawing tool as well as the historical imagery in Google Earth. Google Earth cited the image as coming from the U. S. Department of Agriculture, Farm Service Agency.



Figure 4: The Google Earth image on the top was taken in 2008, while the picture on the bottom was taken in 2010. The red line indicates the top of the bank in 2010 in both pictures. The blue arrow indicates the direction the channel is going to migrate towards. Google Earth cited the top image from the U. S. Department of Agriculture, Farm Service Agency, and the bottom image as DigitalGlobe.



Figure 5: Examples of obvious mass wasting as evidenced by large cracks in the top bank. Google Earth cited both images as coming from DigitalGlobe.



Figure 6: The stream is flowing from the bottom to the top of the image, so that the left bank is on the left side of the image. The blue line represents the reach length, the green line represents woody vegetation that does not make up 100% of the reach. The red line represents bank affected by mass wasting, which is evidenced by a fallen tree visible in a different image. The brown line represents deposition that does not make up 100% of the reach. Google Earth cited the image as coming from the U. S. Department of Agriculture, Farm Service Agency.



Figure 7: Example of Web Soil Survey map. Note how the stream, denoted by a W in the soil map, does not line up with the course of the stream in the background imagery.



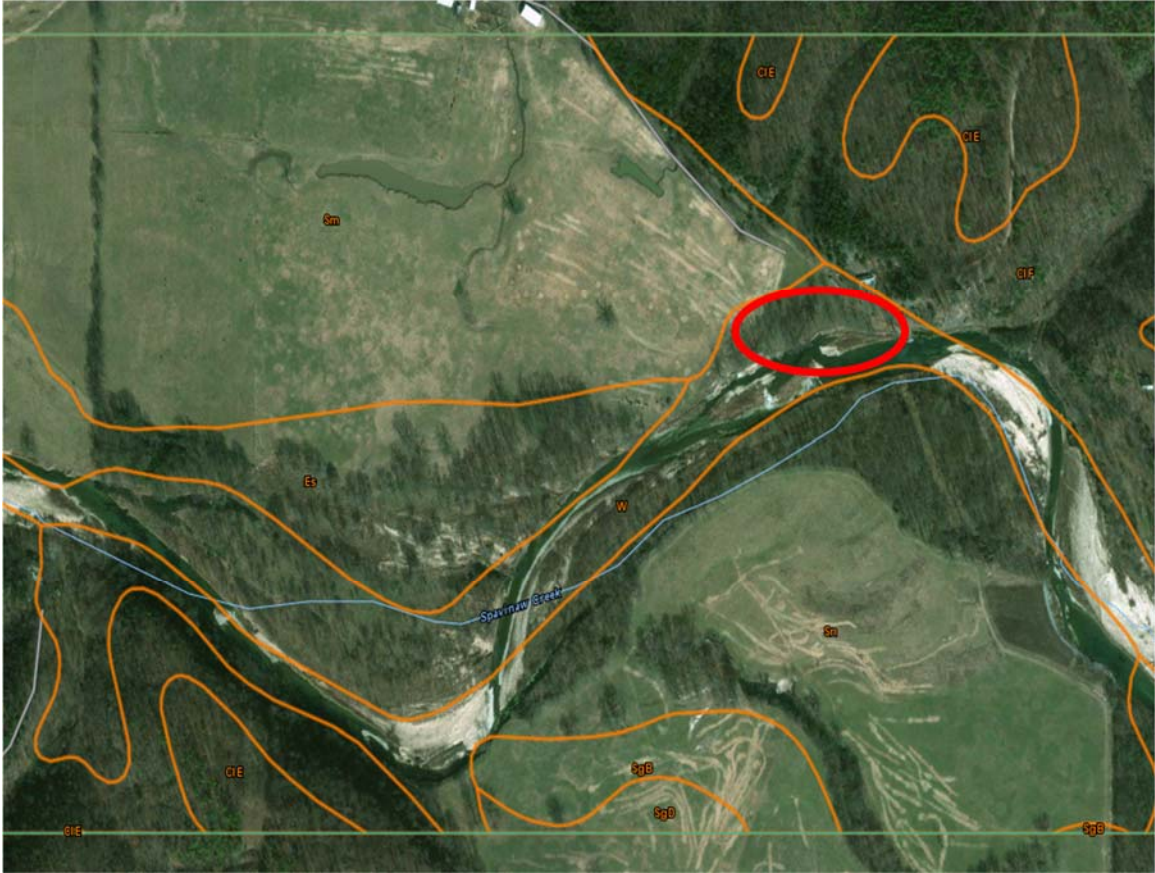


Figure 8: Note the selected streambank that is denoted as water (W) in the soil map. In this case, in deciding between using the Sm or CIF soil types, the Sm soil type was selected based on its closer topographic proximity to the selected bank.

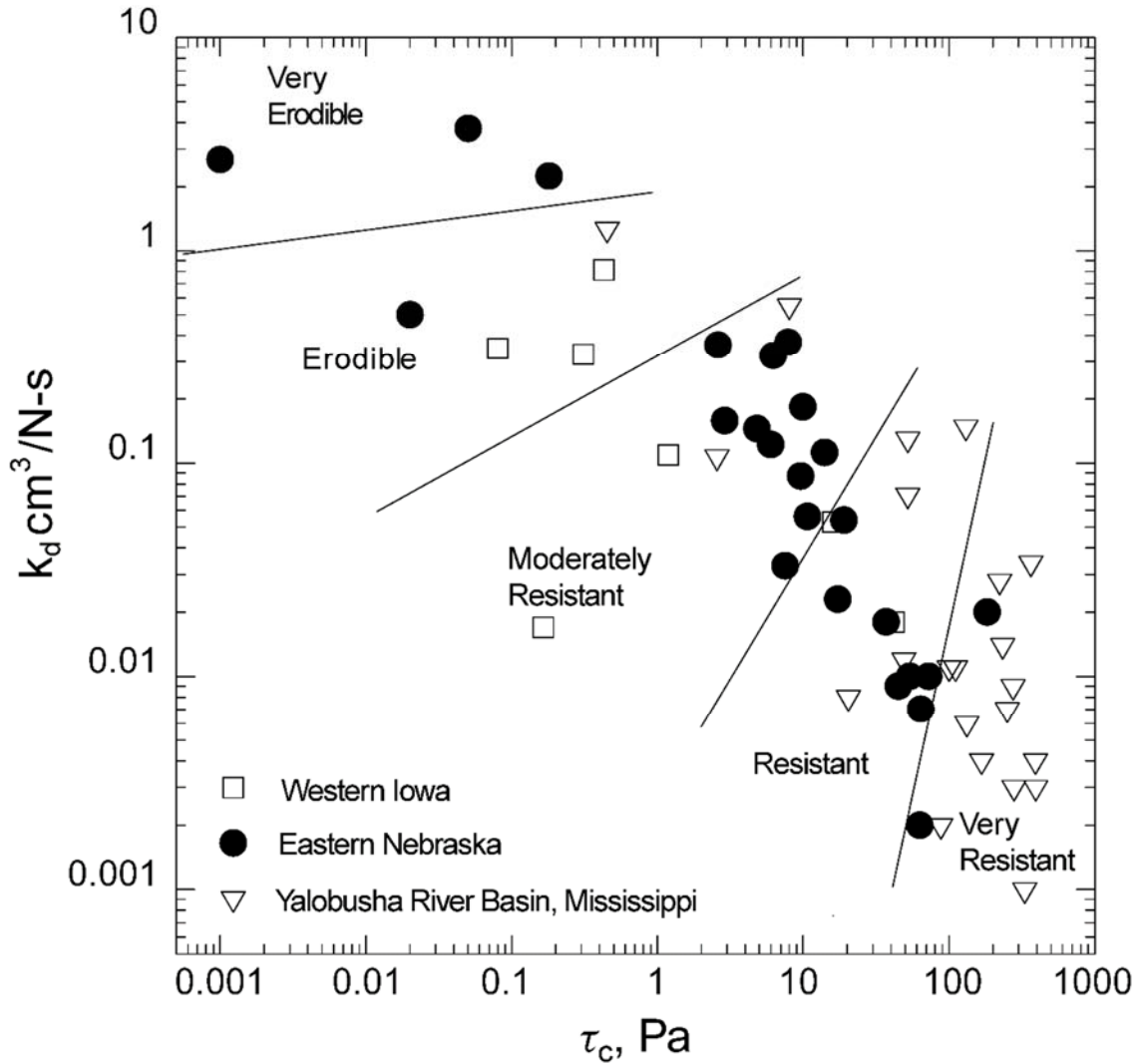


Figure 9: Figure 8 from Hanson and Simon (2001), describing the erodibility classes as defined by the critical shear stress ( $\tau_c$ ) and the erodibility coefficient ( $k_d$ ). Developed for cohesive soils.

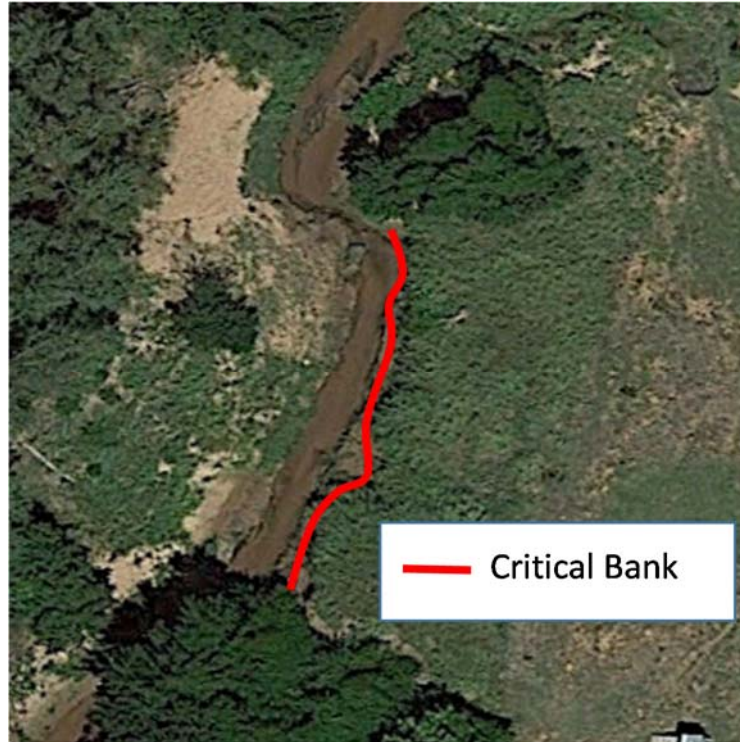


Figure 10: Example of Google Earth vegetation type identified as Vegetated-Grass. Location: WC3. Obtained using Google Earth. Imagery date: 7/26/2015.

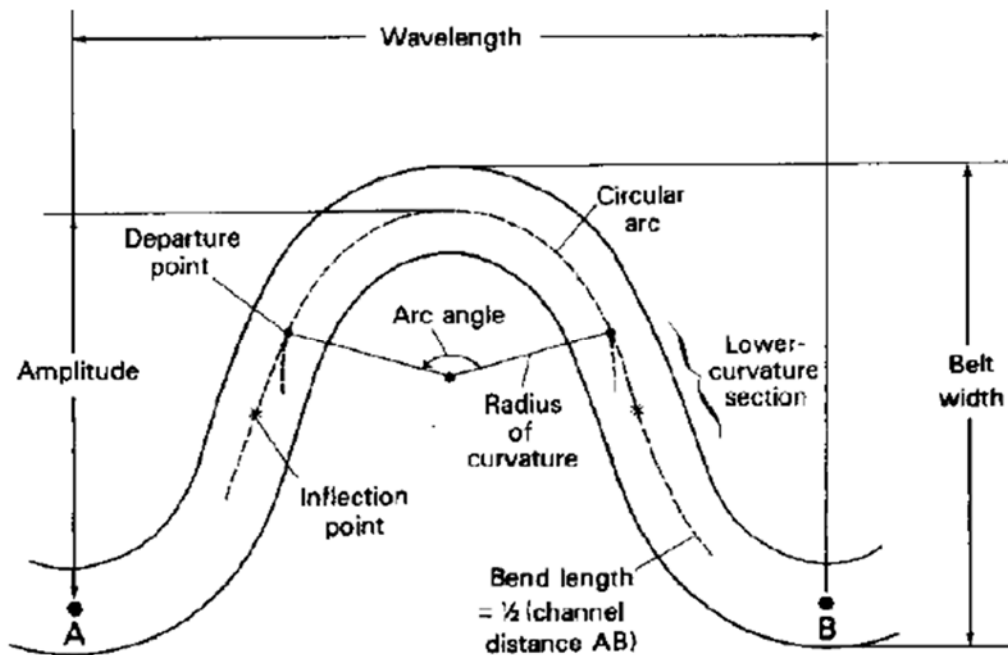


Figure 11: Figure 1 from Williams (1986). Describes meander features and how to measure them.



Figure 12: Meander measurements for a site in the Fort Cobb reservoir (left) and from Barren Fork (right). Notice that at a similar eye altitude (in bottom right corner of each picture) there is a significant difference in meandering. Google Earth cited the image on the right as coming from the U. S. Department of Agriculture, Farm Service Agency.

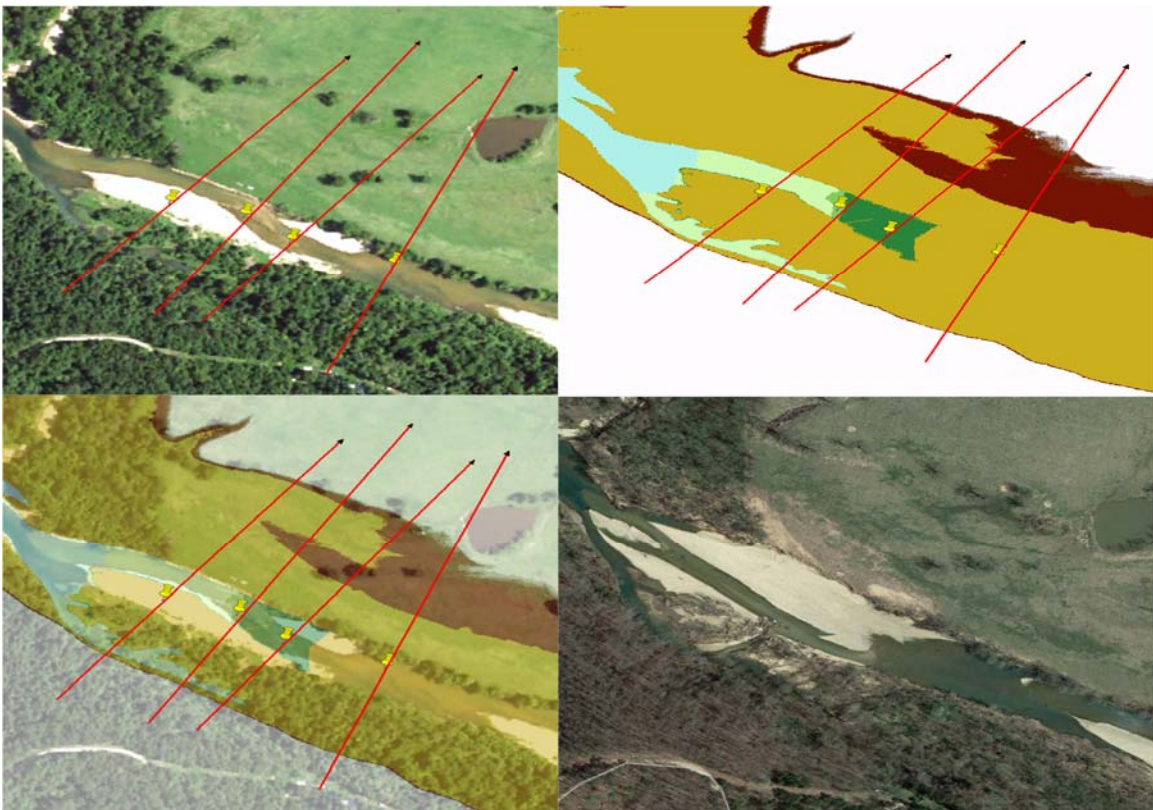


Figure 13: Clockwise from the top left corner: 1) NAIP imagery and the cross sections for Station D. 2) DEM. 3) DEM with NAIP overlaid at 50% transparency. 4) Google Earth image for comparison.

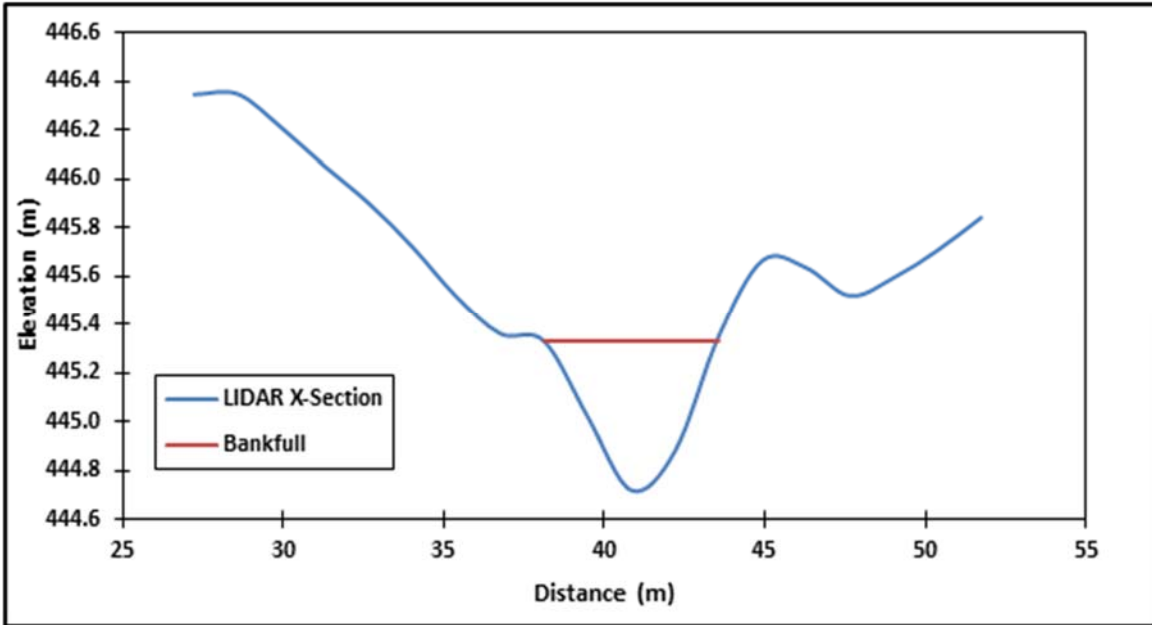


Figure 14: LIDAR cross section from Fivemile, a second order stream, with estimated Bankfull height indicated at the first major change in slope. Cross section taken from the left bank to the right.

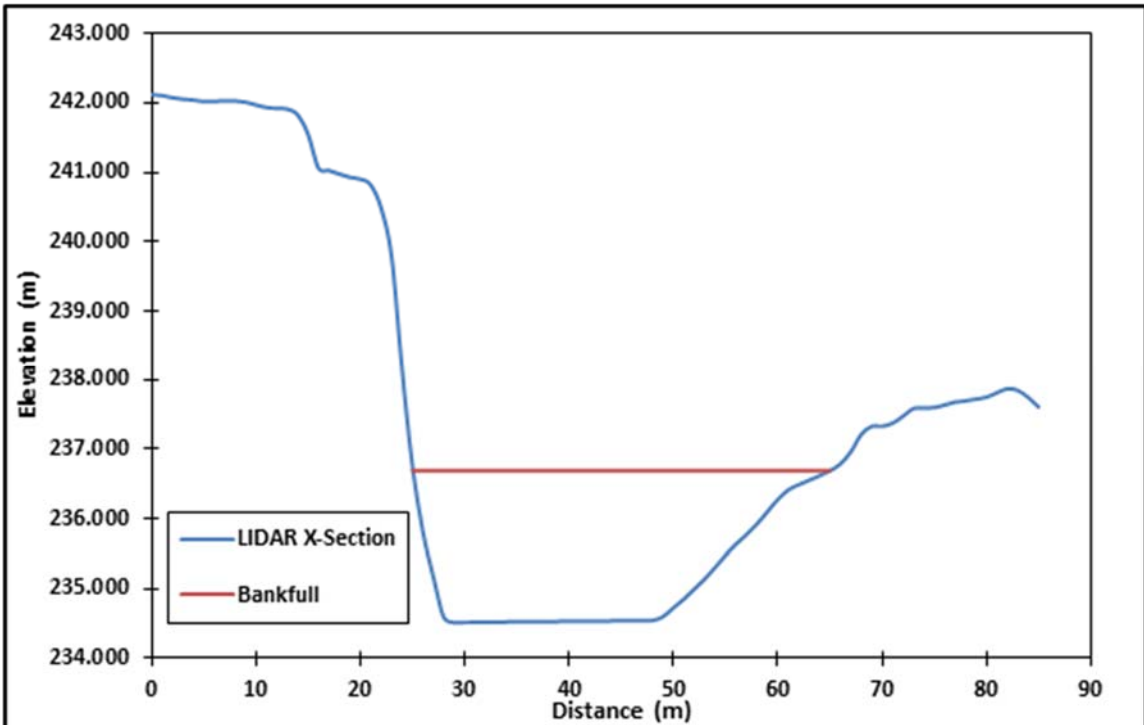


Figure 15: LIDAR cross section from Barren Fork, a fourth order stream, with estimated bankfull depth indicated at the first major change in slope. Cross section taken from the left bank to the right.

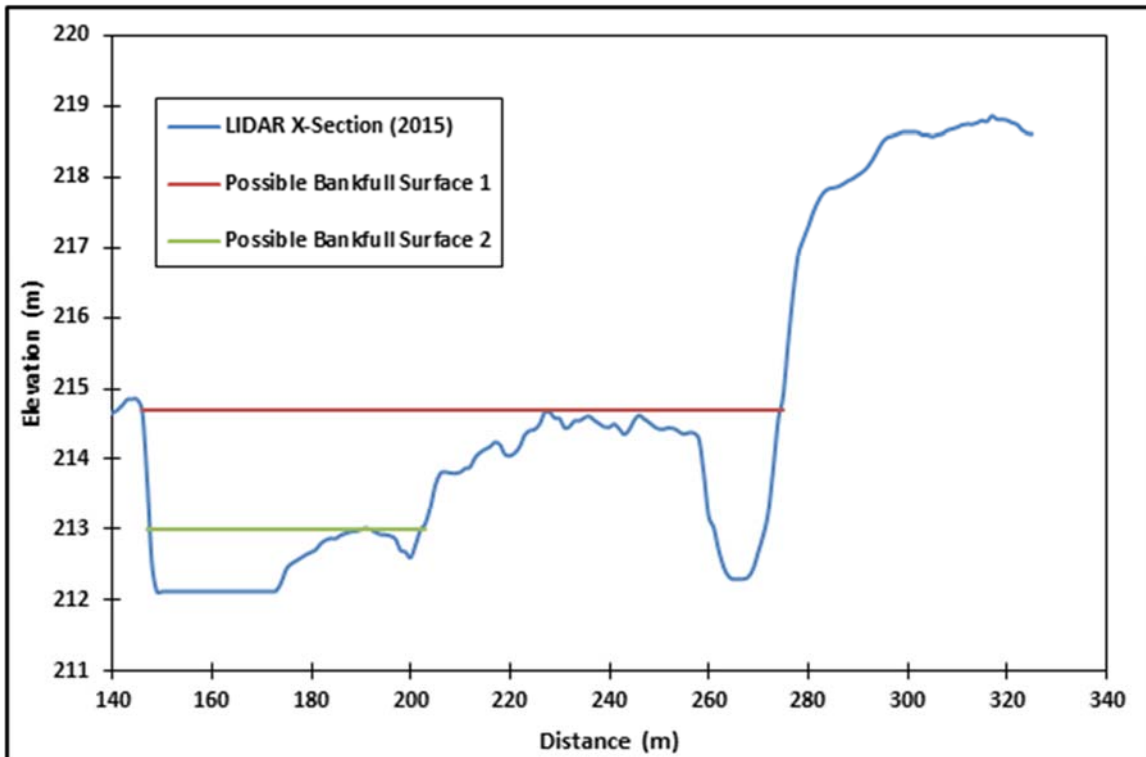
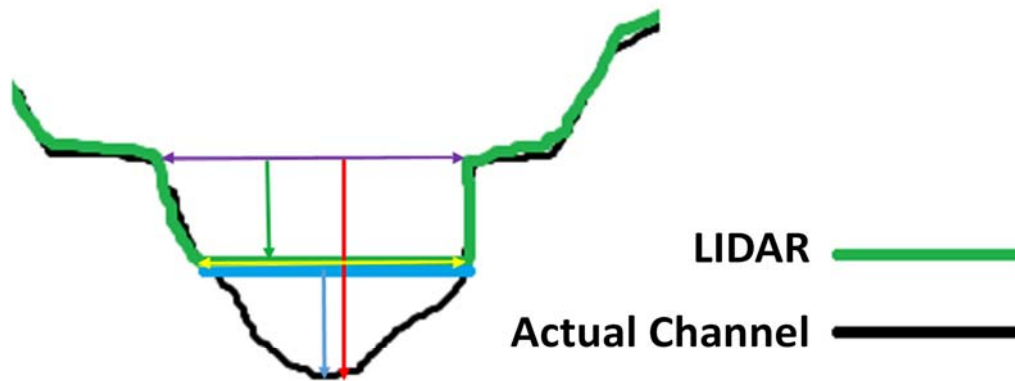


Figure 16: LIDAR cross section with two possible bankfull surfaces. Cross section taken from the left bank to the right.



Bankfull Depth:  $D_{Bf} = H_{Bf} + D_f$   
 Bankfull Width:  $W_{Bf}$   
 Baseflow Depth:  $D_f$   
 Bankfull Height:  $H_{Bf}$   
 Base Flow Width:  $W_f$

Figure 17: An Example of how it was assumed LIDAR interacts with an actual channel. The different relevant measurements are identified.

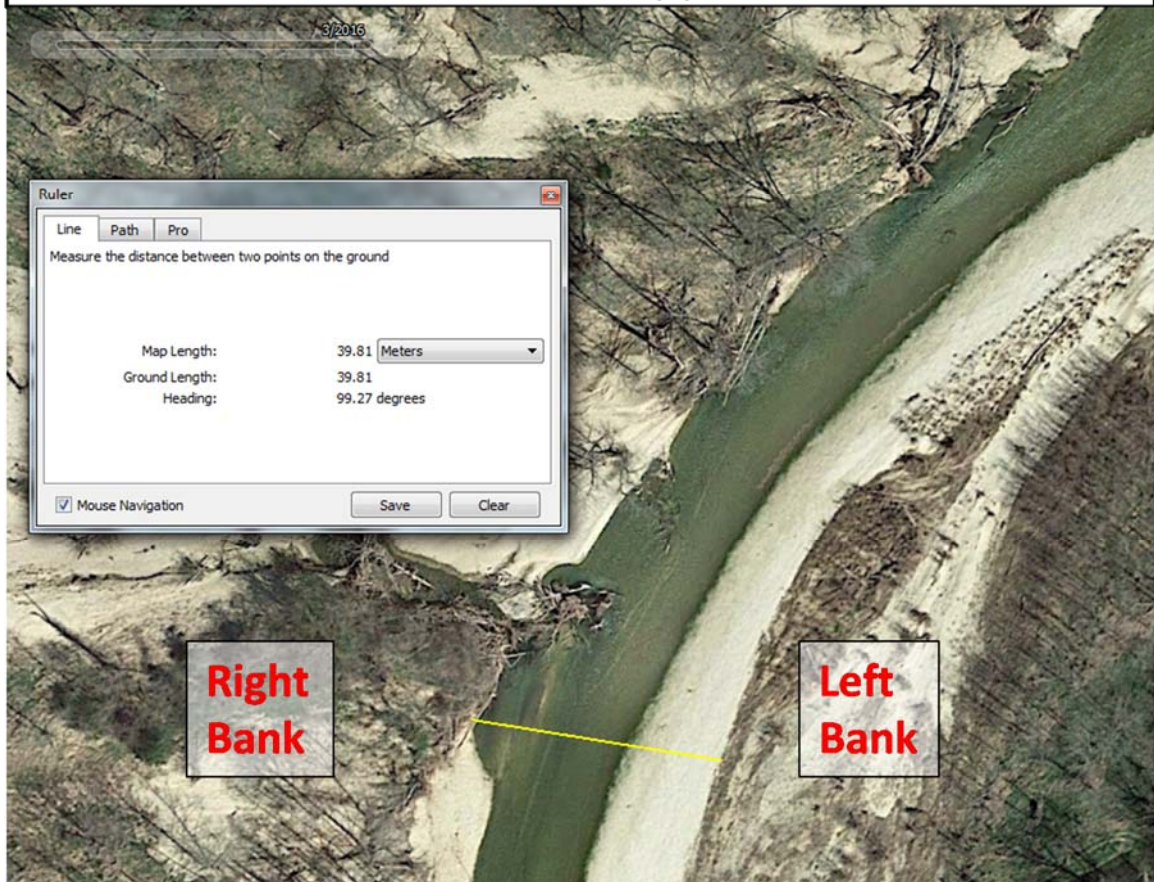
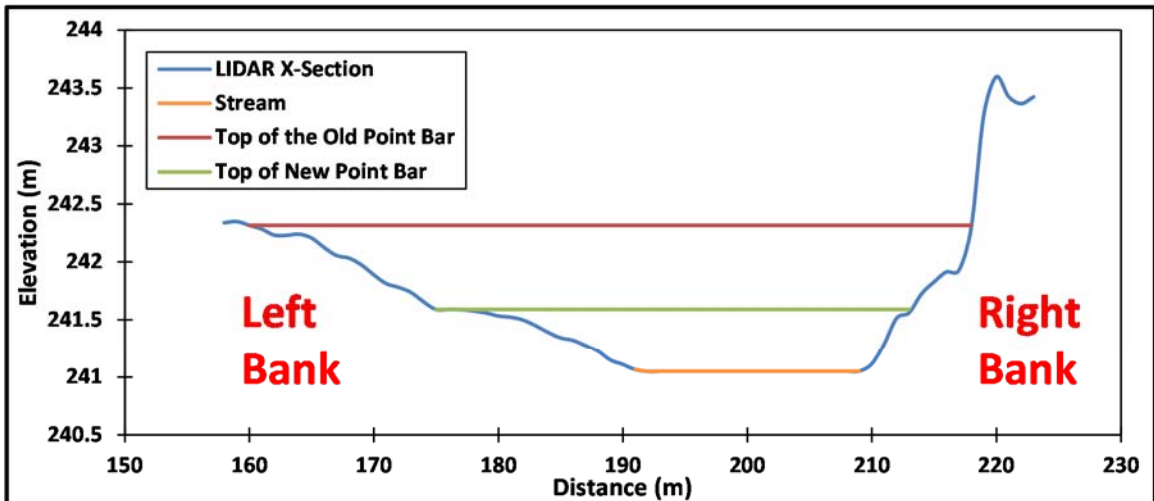


Figure 18: Notice how there is a distinct line in the point bar in the Google Earth Image (taken in 3/20/2016), while the LIDAR cross section captured both this point bar (green line) as well as what appears to be an old, less active point bar (red line). Note the stream is flowing from the top right down, with the left and right banks noted on the image.

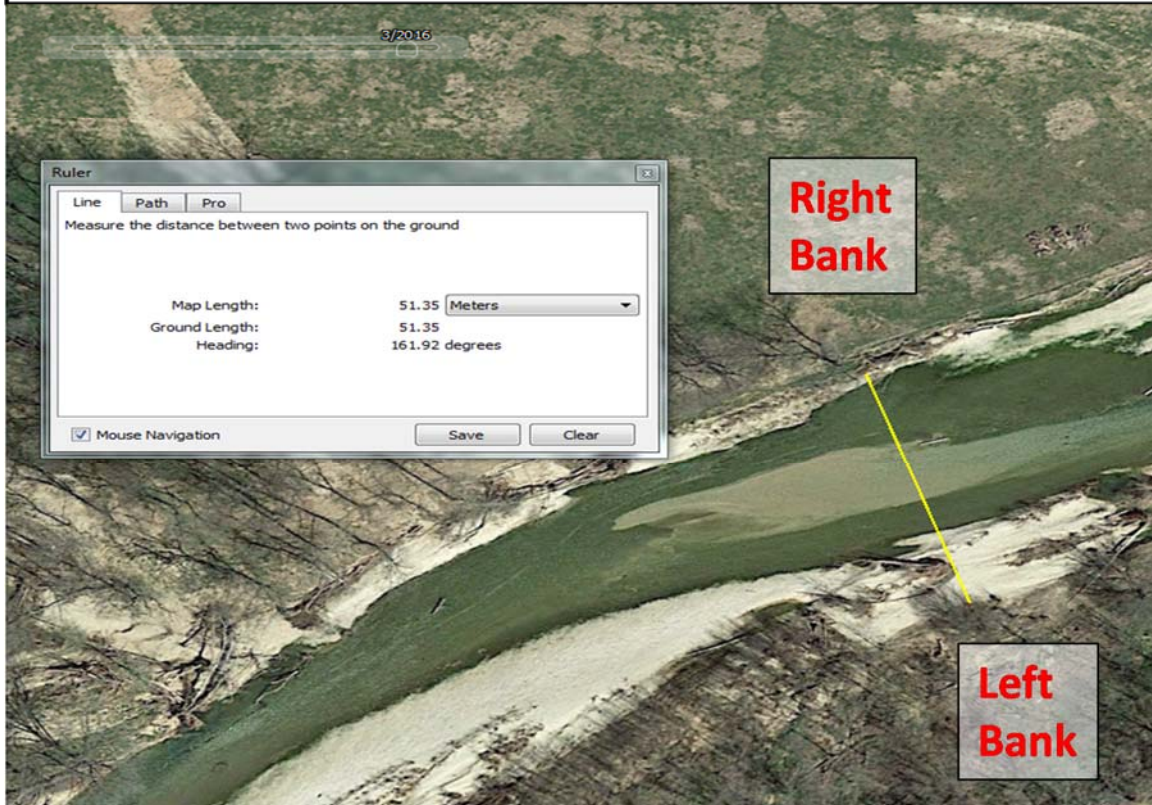
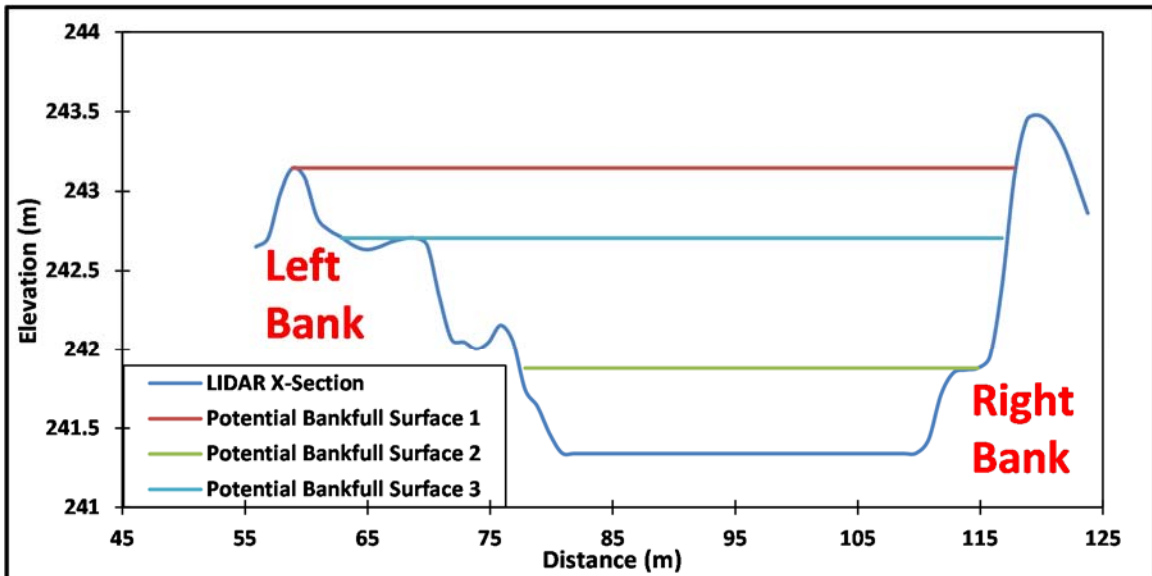


Figure 19: In this example, there were several depositional surfaces and no clear indication of where the top of the apparent point bar was. The light blue line was chosen to represent the bankfull stage as it most closely matched the estimated bankfull in Google Earth.



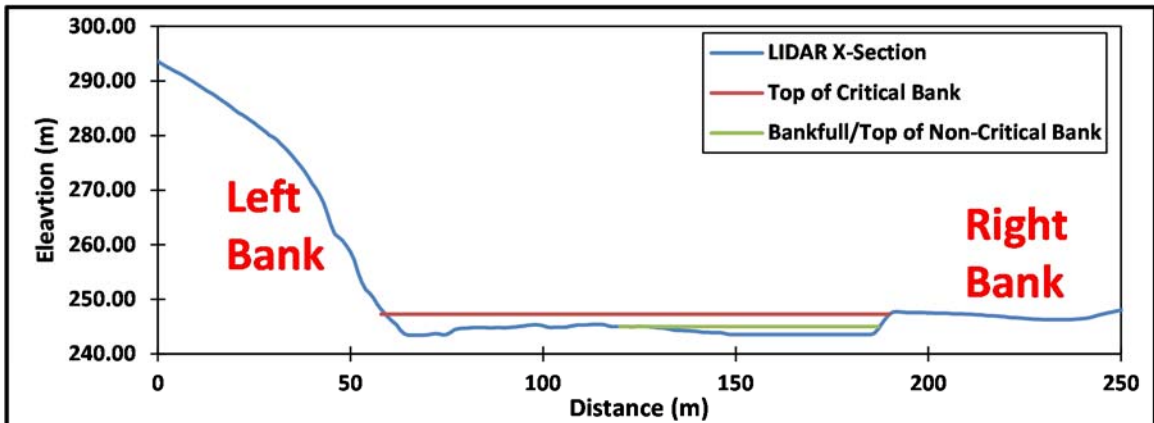


Figure 20: Note the terrace and secondary channel on the left, which can be confirmed in the Google Earth Image. The green line represents the bankfull depth, which also corresponded to the top of the left bank, and the red line indicates the top of the right bank.

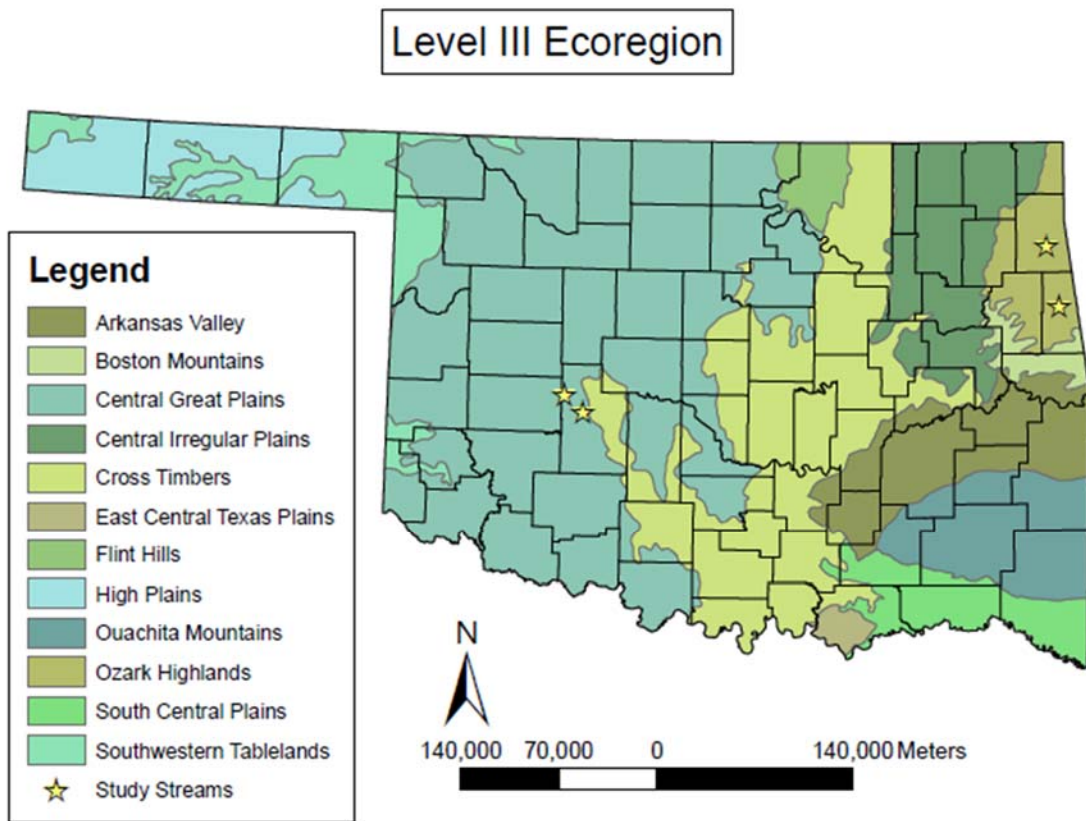


Figure 21: US Environmental Protection Agency Level III Ecoregions for Oklahoma (Woods et al., 2005).

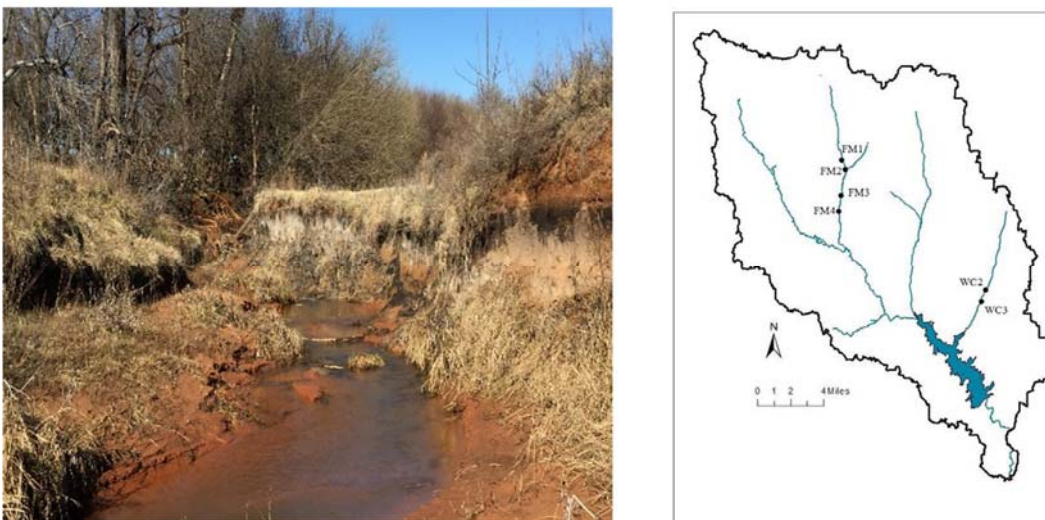


Figure 22: Fivemile Creek in western Oklahoma (left) and the Fort Cobb Watershed (right) with site locations (Saenz et al., 2016).

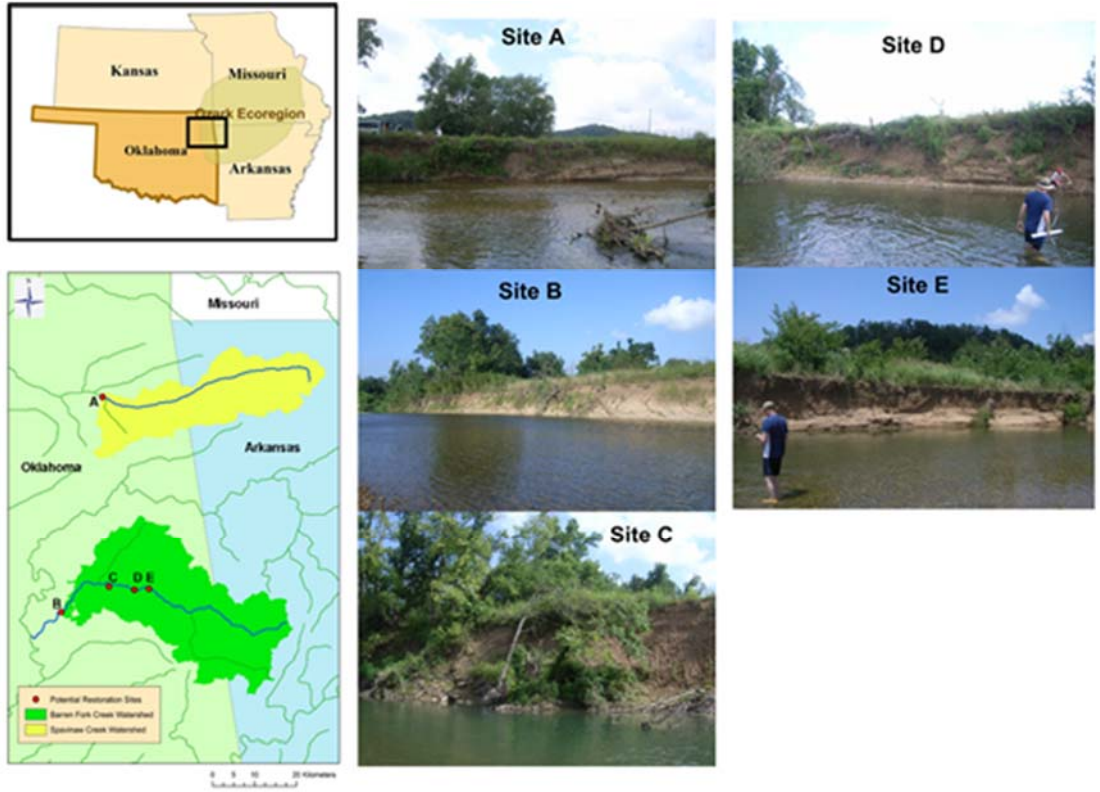


Figure 23: Figure 1 from Heeren et al. (2012). Location of Ozark streams used in the study. Site A was on Spavinaw, and sites B-E were on Barren Fork.

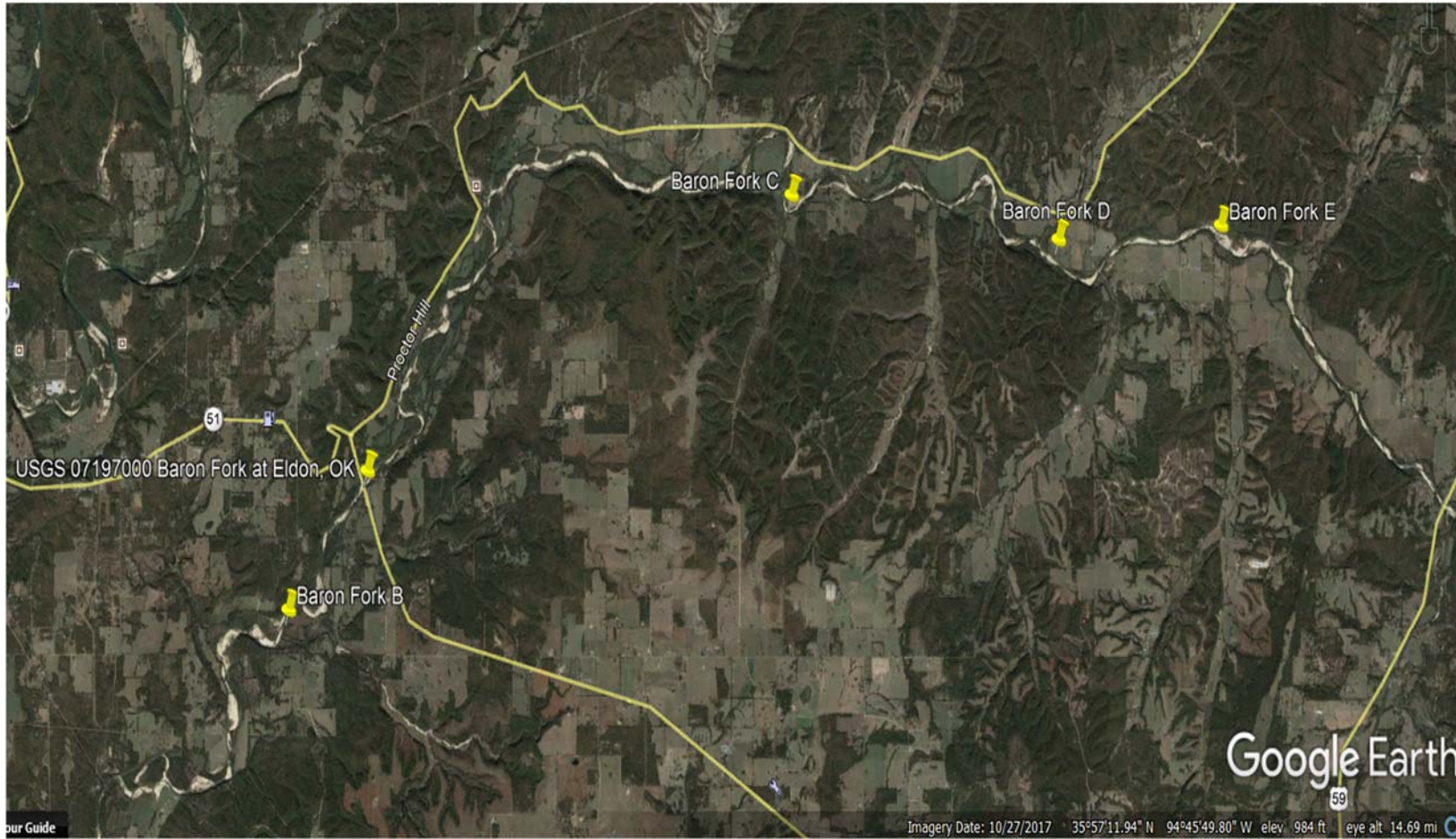


Figure 24: Locations of the historical Stations and the USGS Stream gage used in this study. Image obtained from Google Earth, imagery date: 10/27/2017.

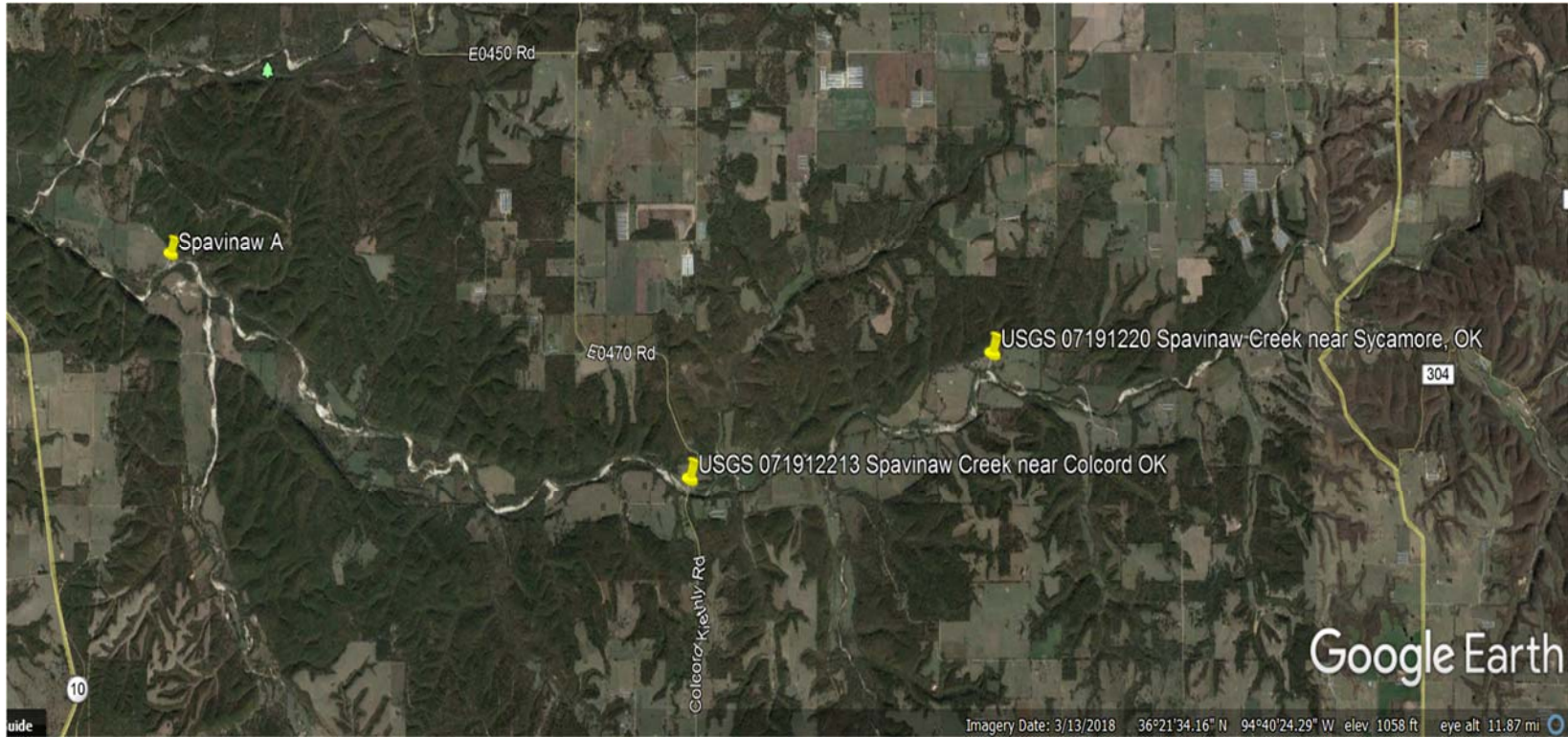


Figure 25: Locations of the historical Stations and the USGS Stream gages used in this study. Image obtained from Google Earth, imagery date: 3/13/2018.

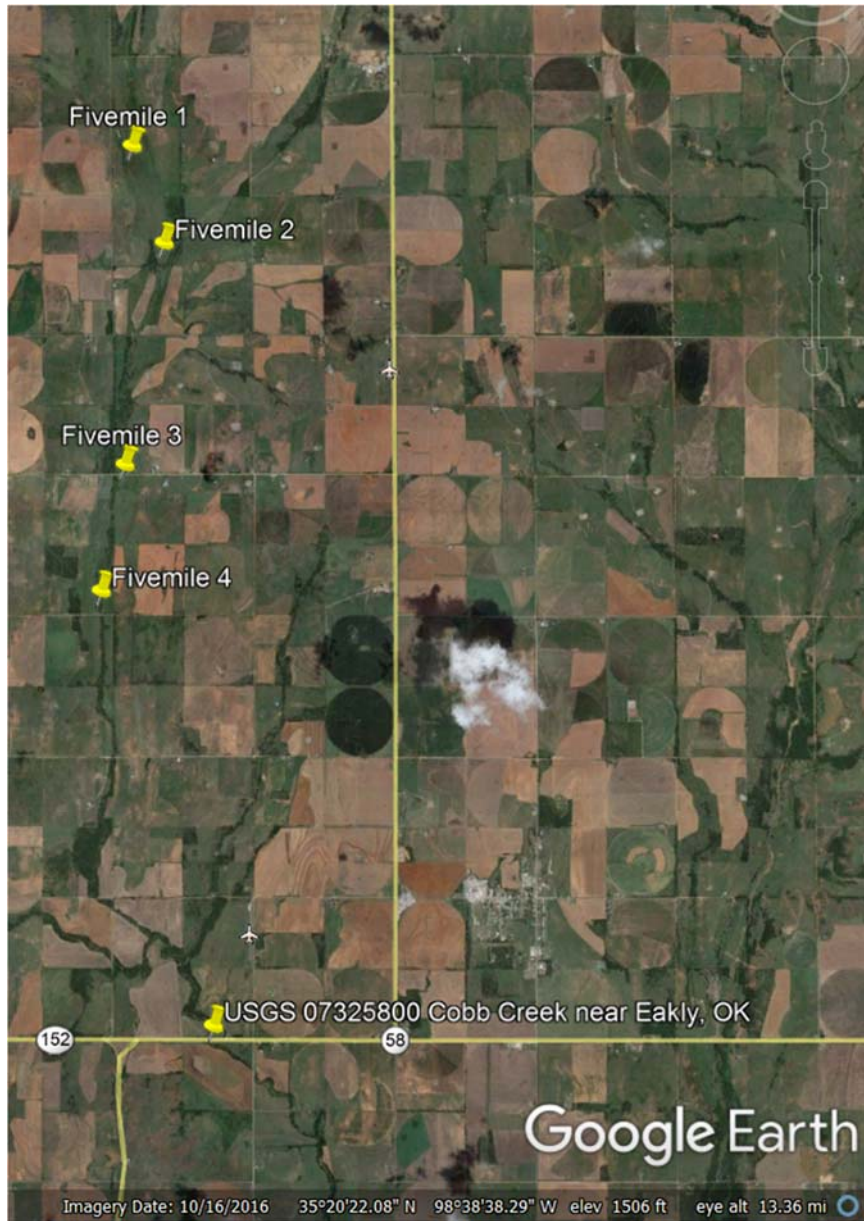


Figure 26: Locations of the historical Stations and the USGS Stream gages used in this study. Image obtained from Google Earth, imagery date: 10/16/2016.

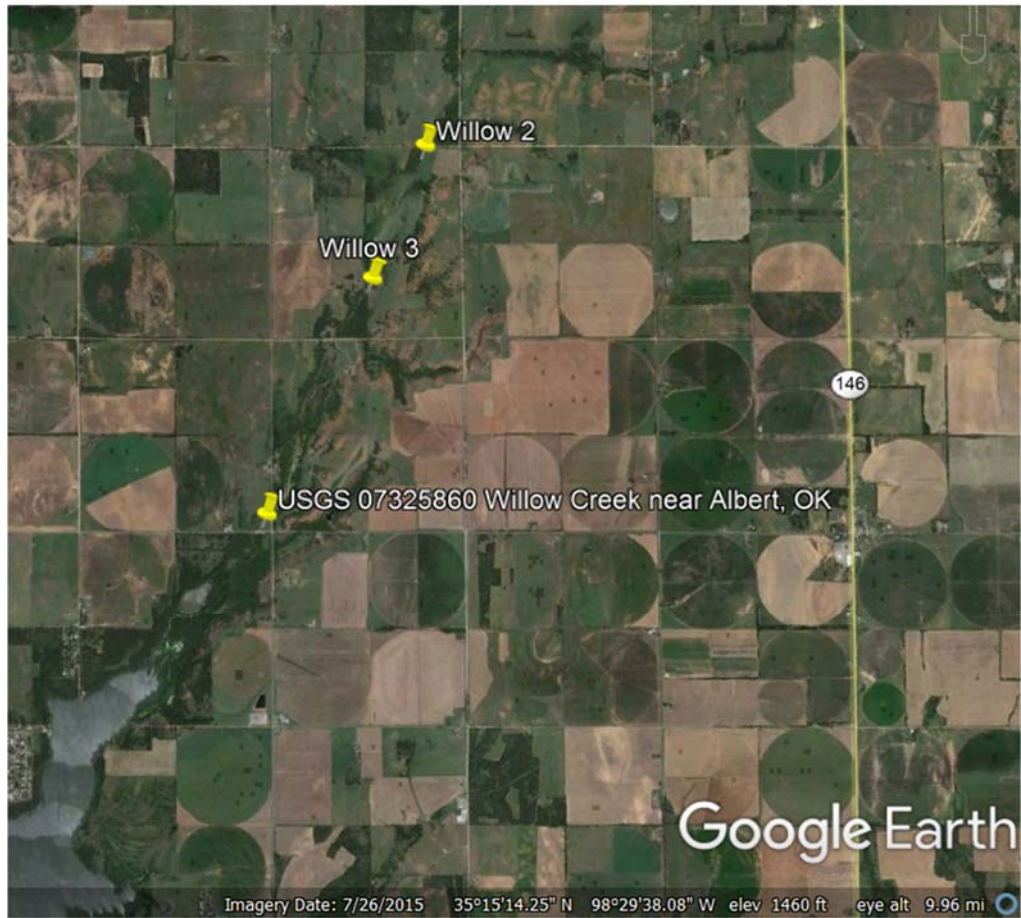


Figure 27: Locations of the historical Stations and the USGS Stream gages used in this study. Image obtained from Google Earth, imagery date: 7/26/2015.

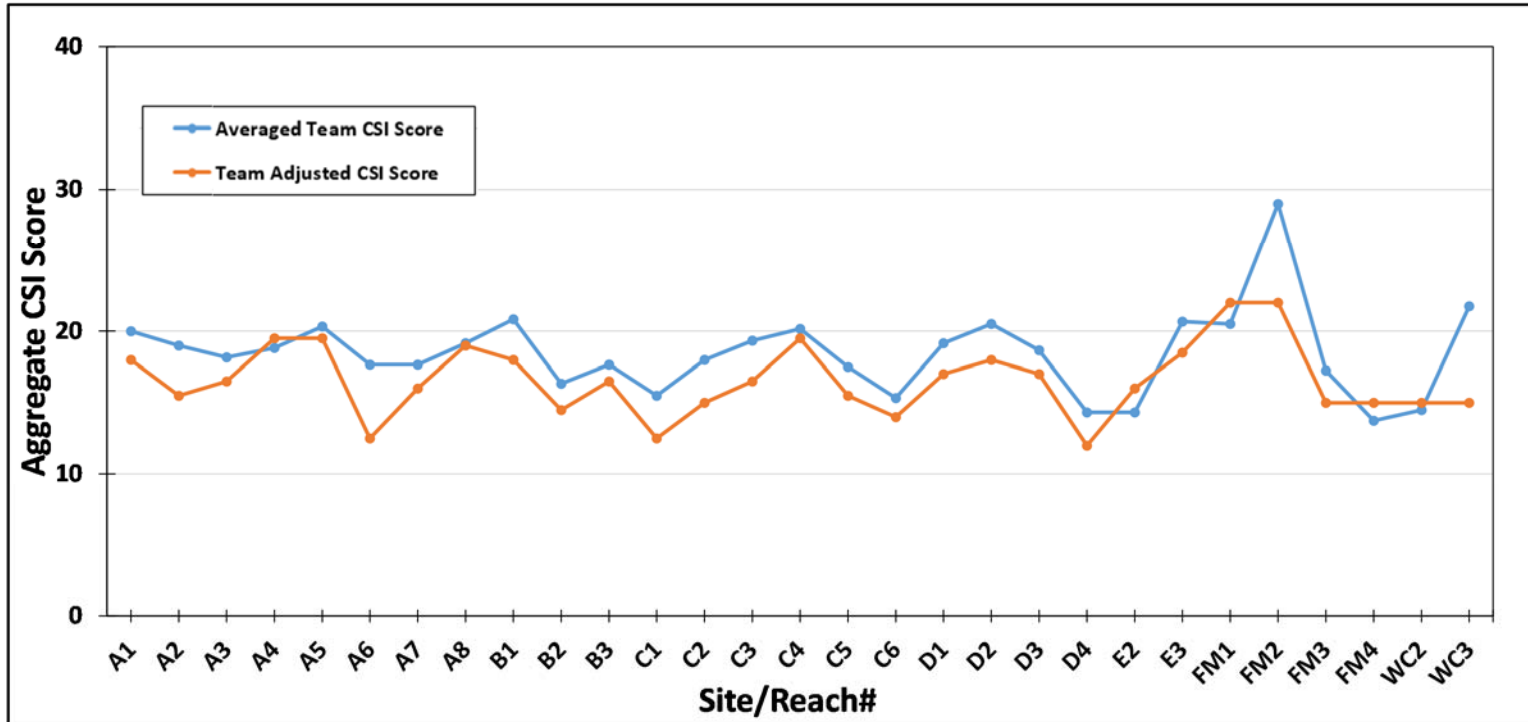


Figure 28: Comparison between the original team adjusted scores and the averaged team score using the development data set (which later are referred to as the historical aggregate score). Note that the final reports for FM1-WC3 sites only reported the final team adjusted stability rank, so an appropriate score was assigned to these points.



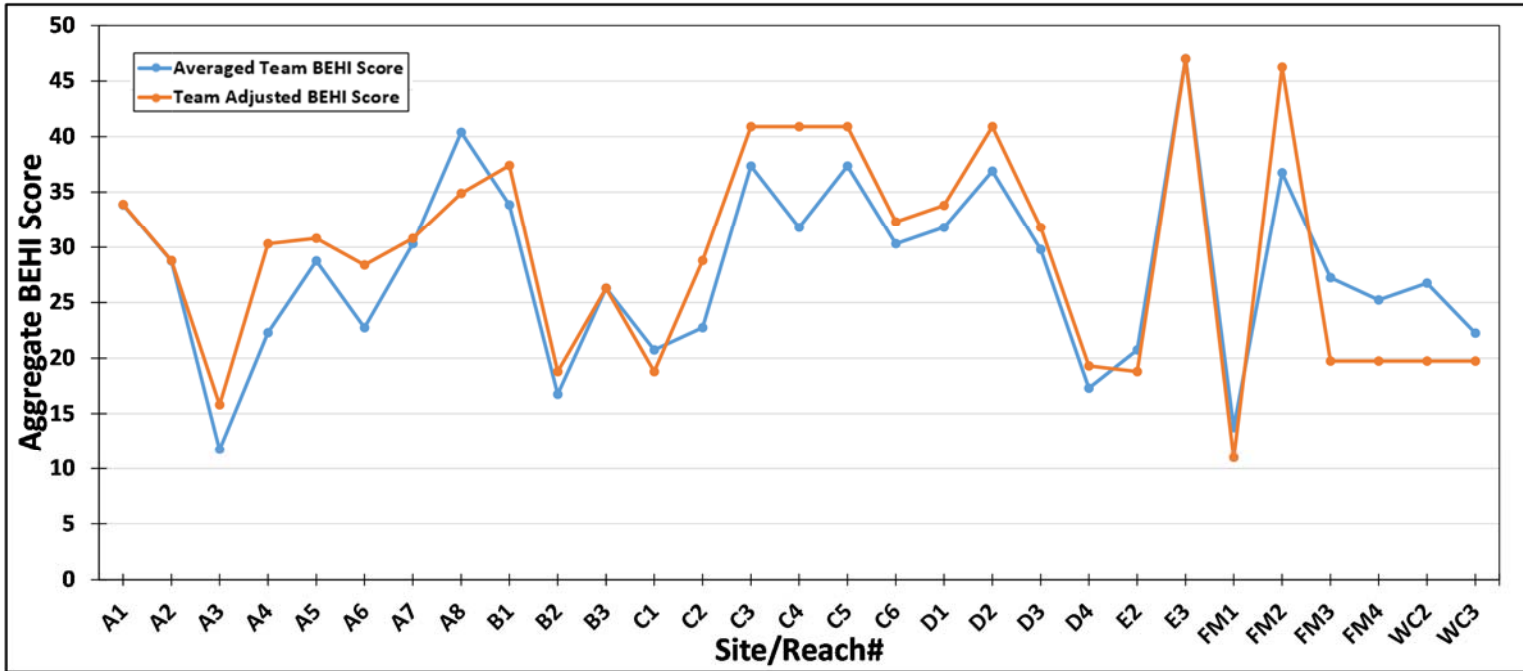


Figure 29: Comparison between the original team adjusted scores and the averaged team score using the development data set (which later are referred to as the historical aggregate score). Note that the final reports for FM1-WC3 sites only reported the final team adjust

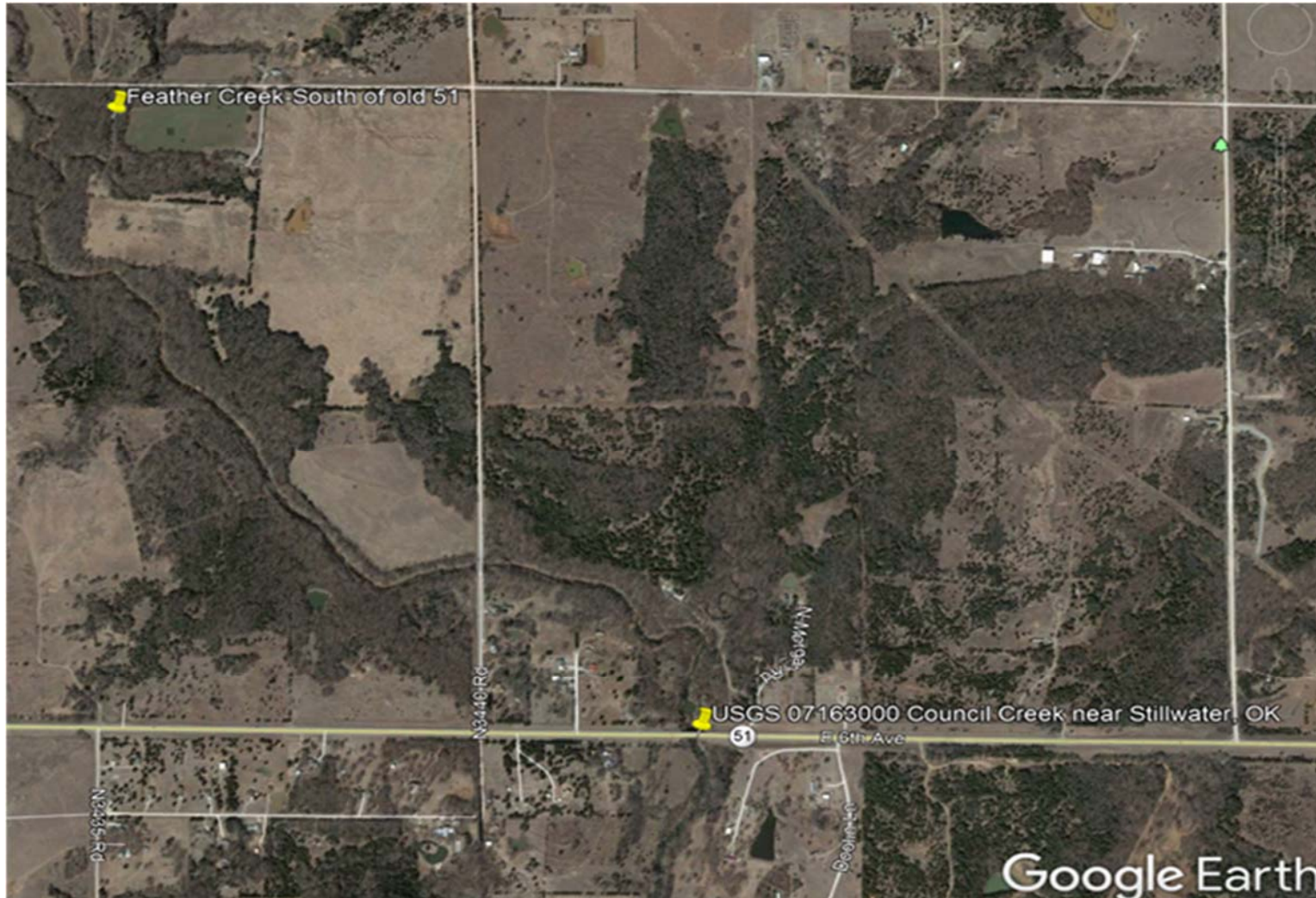


Figure 30: Validation sites and stream gage used for Feather Creek in the Central Great Plains Ecoregion. Imagery was obtained using Google Earth, eye altitude at 396 m, imagery date of 2/25/2014.

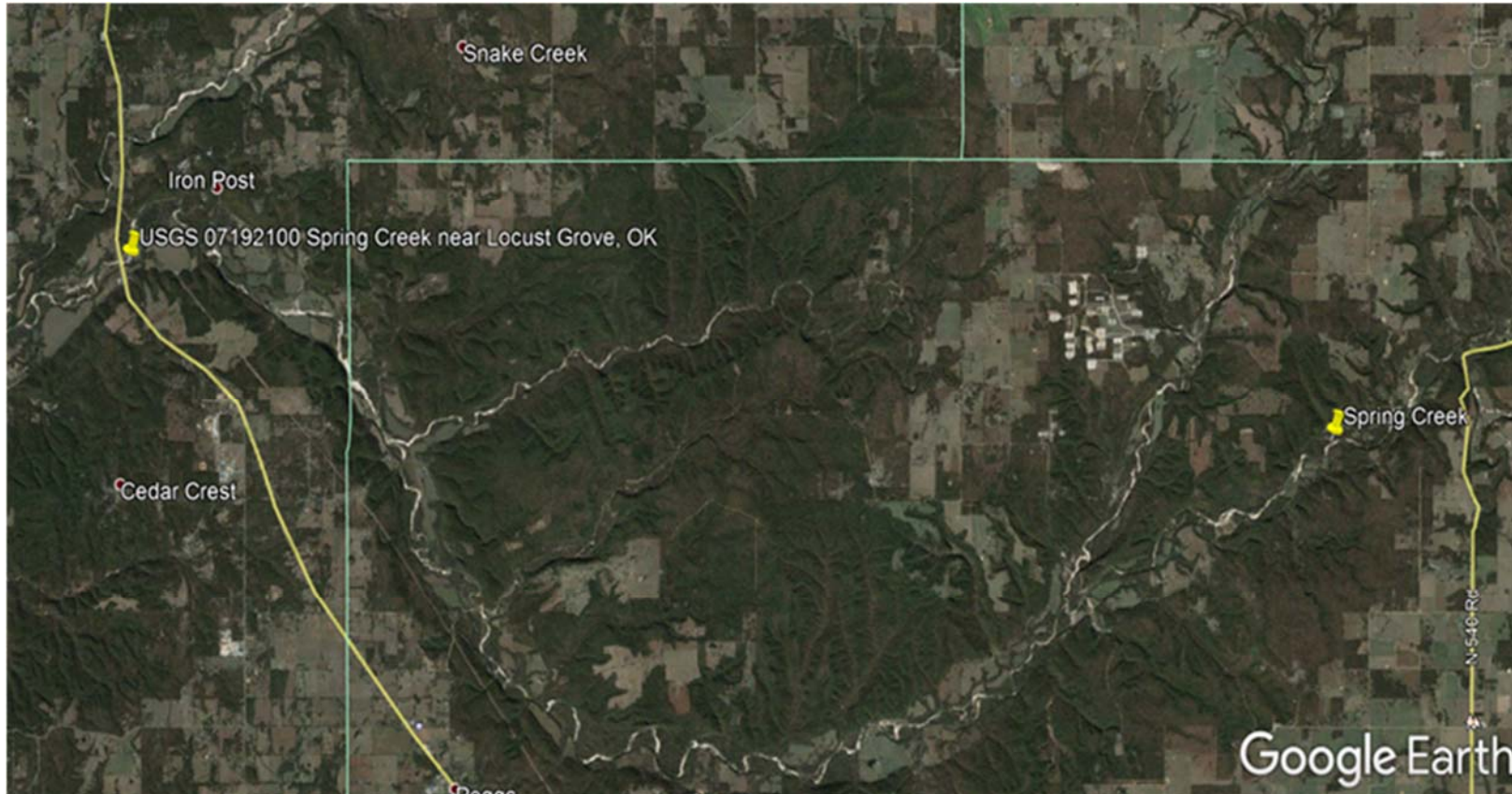


Figure 31: Validation site and stream gage used for Spring Creek in the Ozarks Ecoregion. The imagery was obtained using Google Earth, eye altitude at 24 km, imagery date of 10/27/2017.

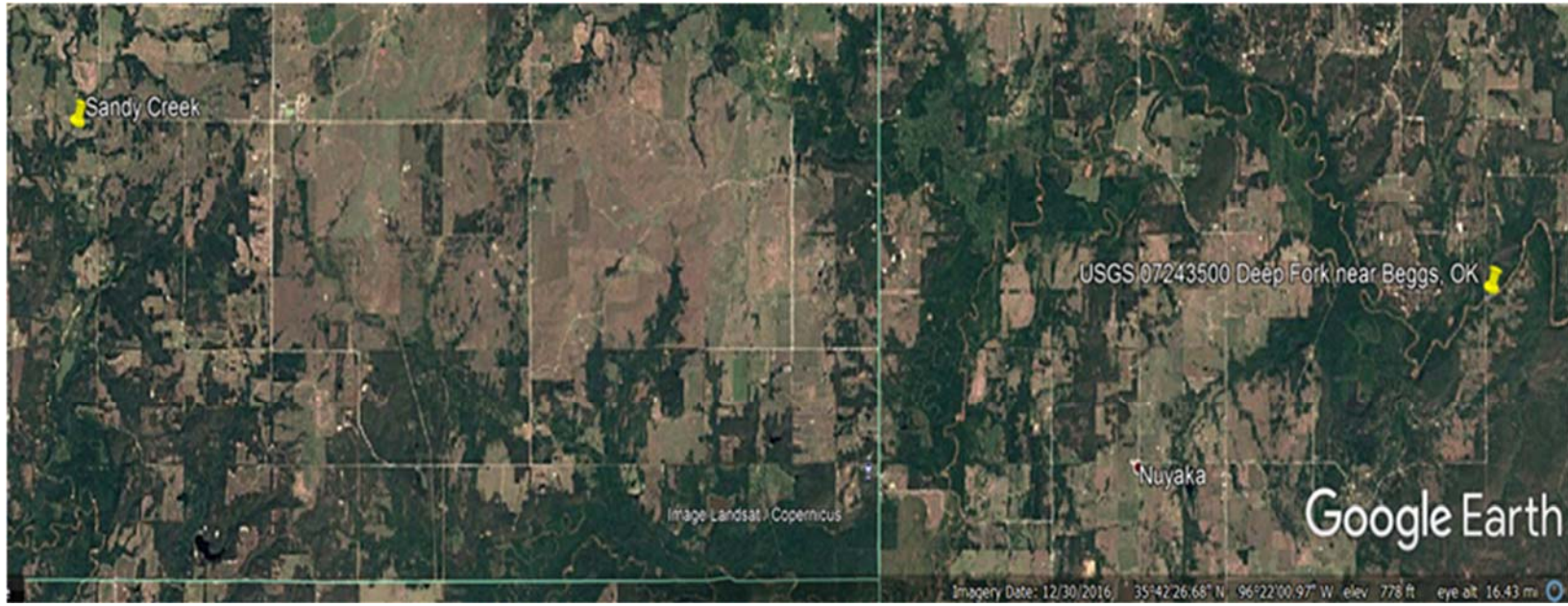


Figure 32: Validation site and stream gage used for Sandy Creek in the Cross Timbers Ecoregion. Imagery was obtained using Google Earth, eye altitude at 27 km, and imagery date of 12/30/2016.



Figure 33: Validation site and stream gage for Black Fork. Imagery was obtained using Google Earth, with eye elevation at 19 km, and imagery date of 3/20/2016.



Figure 34: Validation site and stream gage for Fourche Maline. Imagery was obtained using Google Earth, with eye elevation at 189 m, and imagery date of 1/17/2018.

Table 4: Soil classes used and associated ranges of size,  $\tau_c$ ,  $k_d$ , and erodibility class. For this study, the representative diameters were used to determine erodibility class.

| <b>Soil Class</b>                   | <b>Boulders:<br/>&gt;= 600<br/>mm</b> | <b>Stones:<br/>250-599 mm</b> | <b>Cobbles:<br/>75-249 mm</b> | <b>Gravel:<br/>2-74 mm</b>       | <b>Sand:<br/>0.05-2 mm</b>      | <b>Silt:<br/>0.002-0.05 mm</b> | <b>Clay:<br/>&lt;0.002 mm</b> |
|-------------------------------------|---------------------------------------|-------------------------------|-------------------------------|----------------------------------|---------------------------------|--------------------------------|-------------------------------|
| <b>Representative Diameter (mm)</b> | 600                                   | 424.5                         | 162                           | 38                               | 1.025                           | 0.026                          | 0.001                         |
| <b>Range of <math>\tau_c</math></b> | > 582.23                              | 582.23-243                    | 242.03-72.90                  | 71.93-1.43                       | 1.43-0.04                       | 0.04-0.00                      | 0                             |
| <b>Range of <math>k_d</math></b>    | 0.004                                 | 0.004-0.006                   | 0.006-0.012                   | 0.012-0.084                      | 0.084-0.530                     | 0.530-2.649                    | 2.649                         |
| <b>Range of Erodibility Class</b>   | Very Resistant                        | Very Resistant                | Very Resistant - Resistant    | Resistant - Moderately Resistant | Moderately Resistant - Erodible | Erodible - Very Erodible       | Very Erodible                 |

Table 5: Regional equations used to calculate bankfull depth, for both the development and validation stages of the project. D = bankfull depth, L<sub>m</sub> = Meander Wavelength, L<sub>b</sub> = Along-Channel Bed Length, B = Meander Belt Width, R<sub>c</sub> = Radius of Curvature, W = Bankfull Width, K = Sinuosity, and DA = Drainage Area.

| Source               | Input                          | Diagnostic (e.g. Ecoregion)                | Equation                   |
|----------------------|--------------------------------|--|----------------------------|
| Williams (1986)      | Meander Wavelength (m)         | N/A  | $D = 0.027L_m^{0.66}$      |
| Williams (1986)      | Channel Bed Length (m)         | N/A  | $D = 0.036L_b^{0.66}$      |
| Williams (1986)      | Belt Width (m)                 | N/A  | $D = 0.037B^{0.66}$        |
| Williams (1986)      | Radius of Curvature (m)        | N/A  | $D = 0.085R_c^{0.66}$      |
| Williams (1986)      | Bankfull Width (m)             | N/A  | $D = 0.12W^{0.69}$         |
| Williams (1986)      | Bankfull Width (m) + Sinuosity | N/A  | $D = 0.12W^{0.69}K^{1.46}$ |
| Dutnell (2000)       | Drainage Area (sq. mi)         | Precipitation - 23-33 in                   | $D = 2.21 * DA^{0.082}$    |
| Dutnell (2000)       | Drainage Area (sq. mi)         | Precipitation - 34-43 in                   | $D = 5.51 * DA^{0.029}$    |
| Dutnell (2000)       | Drainage Area (sq. mi)         | Precipitation – All                        | $D = 2.81 * DA^{0.074}$    |
| Dutnell (2000)       | Drainage Area (sq. mi)         | Ecoregion - Central Great Plains           | $D = 2.13 * DA^{0.090}$    |
| Dutnell (2000)       | Drainage Area (sq. mi)         | Ecoregion - Central OK/Tx Plains           | $D = 2.13 * DA^{0.090}$    |
| Dutnell (2000)       | Drainage Area (sq. mi)         | Ecoregion - All                            | $D = 2.81 * DA^{0.073}$    |
| Bieger et al. (2015) | Drainage Area (sq. km)         | Physiographic Division -Interior Highlands | $D = 2.27 * DA^{0.267}$    |
| Bieger et al. (2015) | Drainage Area (sq. km)         | Physiographic Division -Interior Plains    | $D = 0.38 * DA^{0.191}$    |
| Bieger et al. (2015) | Drainage Area (sq. km)         | Physiographic Division - USA               | $D = 0.30 * DA^{0.213}$    |



Table 6: USGS Stream gages and station ID for the development stage of the project. Note that all stations consist of several cross sections from only one land owner except for, FM1-2, FM3-4, and WC2-3, which represent single cross sections per station and land owners that span several stations.

| Stream      | Station | No. of Cross Sections | USGS Gage   | No. of Years of Record |
|-------------|---------|-----------------------|---|------------------------|
| Spavinaw    | A       | 8                     | USGS 07191220 Spavinaw Creek near Sycamore, OK & USGS 071912213 Spavinaw Creek near Colcord, OK | 55                     |
| Barren Fork | B       | 3                     | USGS 07197000 Barren Fork at Eldon, OK  | 68                     |
|             | C       | 6                     |   |                        |
|             | D       | 4                     |   |                        |
|             | E       | 2                     |   |                        |
| Fivemile    | FM1     | 1                     | USGS 07325800 Cobb Creek near Eakly, OK   | 49                     |
|             | FM2     | 1                     |   |                        |
|             | FM3     | 1                     |   |                        |
|             | FM4     | 1                     |   |                        |
| Willow      | WC2     | 1                     | USGS 07325860 Willow Creek near Albert, OK  | 21                     |
|             | WC3     | 1                     |   |                        |

Table 7: Details on LIDAR data used in both the development and validation stages of the project. The stream orders for the Fourche Maline and Spring Creek were determined using USEPA (2017b) WATERS GeoViewer tool.

| Stream of Interest         | Data Set Name   | Stream Order | Resolution         | Date               |
|----------------------------|---|--------------|--------------------|--------------------|
| <b>Development Stage</b>   |   |              |                    | <b>Flight Date</b> |
| Fivemile                   | 2010 NRCS Washita River Plus, OK                      | 2            | 2 m                | 12/13/2009         |
| Willow                     |   | 2            | 2 m                | 12/13/2009         |
| Barren Fork                | 2016 NRCS - Adair, Delaware, Cherokee, Sequoyah LIDAR | 4            | 1 m                | 12/3/2015          |
| Spavinaw                   |   | 4            | 1 m                | 1/24/2016          |
| <b>Validation Stage</b>    |   |              |                    | <b>s_date</b>      |
| Feather Creek              | NRCS Project (OK_Area1-1A_2011)                       | 2            | 2 m                | 12/6/2011          |
| Fourche Maline             | 2012 OK LIDAR - NRCS Priority Project                 | 2            | 2 m                | 1/4/2012           |
| Sandy Creek                | 2012 OK LIDAR - NRCS Priority Project (NRCS-Area1C)   | 3            | 2 m                | 12/15/2011         |
| Spring Creek               | 2016 NRCS - Adair, Delaware, Cherokee, Sequoyah LIDAR | 3            | 1 m                | 12/1/2015          |
| Black Fork of Poteau River | OK_NRCS-Area1E_2012                                   | 4            | 1/3 arc second NED | 7/4/1905           |

Table 8: USGS Stream gages and station ID used in the validation stage of the project. Note the time frame of monitoring, which had an impact on the methods used.

| <b>Station</b>             | <b>No. of Cross Sections</b> | <b>USGS Gage</b>                                     | <b>Period of Active Stream Gage Monitoring (Daily Data)</b> | <b>Method Restrictions</b>                       |
|----------------------------|------------------------------|--|---|--|
| Feather                    | 1                            | USGS 07163000 Council Creek near Stillwater, OK      | From 1934 to 1993   | Baseflow Depth (No current gage data)            |
| Sandy                      | 2                            | USGS 07243500 Deep Fork near Beggs, OK               | From 1938 to Current  | None   |
| Spring                     | 2                            | USGS 07192100 Spring Creek near Locust Grove, OK     | From 2017 to Current  | PeakFQ (too little data to calculate statistics) |
| Black Fork of Poteau River | 1                            | USGS 07247250 Black Fork below Big Creek nr Page, OK | From 1992 to Current  | None   |
| Fourche Maline             | 2                            | USGS 07247500 Fourche Maline near Red Oak, OK        | From 1938 to Current  | None   |

Table 9: Summary of all required measurements/observations, the corresponding RGA metrics, and the sources used in this study.

| Measurement/<br>Observation                                 | RGA         | Metric         | Google<br>Earth | LIDAR | USDA<br>Web<br>Soil<br>Survey | USGS<br>Stream<br>Gages | USGS<br>Stream<br>Stats |
|---|-------------|----------------|-----------------|-------|-------------------------------|-------------------------|-------------------------|
| Bank Height (BH)  | BEHI<br>CSI | 1-2, 4-5<br>3b |                 | •     |                               |                         |                         |
| Bankfull Height (BFH)                                       | BEHI        | 1              |                 | •     |                               |                         |                         |
| Plan-form Channel<br>Geometry                               | BEHI        | 1              | •               |       |                               |                         |                         |
| Bankfull Flow (Q <sub>2</sub> )                             | BEHI        | 1              |                 |       |                               |                         | •                       |
| Bankfull Flow (Q <sub>1.5</sub> )                           | BEHI        | 1              |                 |       |                               | •                       |                         |
| Channel Slope   | BEHI<br>CSI | 1<br>3         |                 |       |                               |                         | •                       |
| Root Depth (RD)   | BEHI        | 2, 4           |                 |       | •                             |                         |                         |
| Root Density  | BEHI        | 3              | •               |       |                               |                         |                         |
| Face Length (FL)  | BEHI        | 5              |                 | •     |                               |                         |                         |
| Primary Bank Material                                       | BEHI        | Adj. 1         |                 |       | •                             |                         |                         |
| Stratification  | BEHI        | Adj.2          |                 |       | •                             |                         |                         |
| Primary Bed Material  | CSI         | 1-2            |                 |       |                               | •                       |                         |
| Restrictive Layer Depth                                     | CSI         | 2              |                 |       | •                             |                         |                         |
| Base Flow Depth-<br>StreamStats (D)                         | CSI         | 3              |                 |       |                               |                         | •                       |
| Base Flow Depth-<br>StreamGage (D)                          | CSI         | 3              |                 |       |                               | •                       |                         |
| Base Flow Depth-<br>LIDAR+StreamGage (D)                    | CSI         | 3              |                 | •     |                               | •                       |                         |
| Channel Width at Cross<br>Section (W)                       | CSI         | 4              | •               |       |                               |                         |                         |
| Channel Width Upstream<br>(W <sub>u</sub> )                 | CSI         | 4              | •               |       |                               |                         |                         |
| Erosion Presence/Type                                       | CSI         | 5, 9           | •               |       |                               |                         |                         |
| Reach Length  | CSI         | 6-8            | •               |       |                               |                         |                         |
| Length Parallel to Reach<br>Affected by Mass Wasting        | CSI         | 2, 6           | •               |       |                               |                         |                         |
| Length Parallel to Reach<br>Affected by Woody<br>Vegetation | CSI         | 7              | •               |       |                               |                         |                         |
| Length Parallel to Reach<br>Affected by Accretion           | CSI         | 8, 9           | •               |       |                               |                         |                         |
| Degradation   | CSI         | 5, 9           | •               |       |                               |                         |                         |
| Channel Widening  | CSI         | 5, 6, 9        | •               |       |                               |                         |                         |

Table 10: Impacts of data limitations in the digital RGAs.

| Data Source     | RGA Impacted | Percent of RGA Impacted (%) | RGA Metric #               | Data Resolution - Impact         | Data Gap - Impact  |
|-----------------|--------------|-----------------------------|----------------------------|----------------------------------|--|
| Google Earth    | BEHI         | 50                          | 1<br>2, 4                  | Can reduce accuracy              | Limits Bankfull Method Options Cannot Identify Vegetation Type                                   |
|                 | CSI          | 67                          | 4<br>5-9                   | Can result in compounding errors | Limits Constriction Method Options Impossible to Assess  |
| LIDAR           | BEHI         | 80                          | 1-2, 4-5                   | Can reduce accuracy              | Impossible to Assess   |
|                 | CSI          | 22                          | 3<br>3<br>4                | Can reduce accuracy              | Impossible to Assess<br>Limits Normal Depth Method Options<br>Limits Constriction Method Options |
| Stream Gage     | BEHI         | 20                          | 1                          | Can reduce accuracy              | Limits Bankfull Method Options   |
|                 | CSI          | 11                          | 1                          | Can reduce accuracy              | Impossible to Assess   |
| Web Soil Survey | BEHI         |                             | 2<br>4<br>Both Adjustments | Can reduce accuracy              | N/A  |
|                 | CSI          |                             | 2                          | Can reduce accuracy              | N/A  |

## CHAPTER III

### RESULTS & DISCUSSION

#### Reach Length Methods

Using the techniques described in the **Error! Reference source not found.**, CSI metrics 4 through 9 and part of metric 2 were scored (see Table 3 for metric numbers and names). The success rate of the methods was assessed for individual metrics as well as combinations of metrics. Since bank protection was determined based on percentage of woody cover, it was the only reach length metric to not be assessed alone. The results for all of the metrics measured in Google Earth are summarized in Table 11. Google Earth data replaced the historical measurements with an average success rate of 94%. In other words, on average for this study, 94% of the time, replacing a score measured on site with one measured in Google Earth generated the same RGA stability ranking as the on-site historical assessment. The metrics with the highest success rates for the development data set were the degree of constriction, the percentage of the bank supported by woody species, the percentage of the reach affected by accretion, and identifying streambank erosion/type. The remaining metrics still performed well at a 90% success rate. Using Google Earth to assess all 6.5 metrics had an overall success rate of 79%. The risk was underestimated for four of the six cross sections that failed.

It was unexpected for the CSI metrics 6, 7 and 8 to do so well in the development stage, given the differences in how these metrics are measured digitally versus on-site. In the field, an estimate was made based on what the observer could see from the representative cross section. On the other hand, in Google Earth an actual measurement of the reach length affected was made. Besides the difficulty in identifying mass wasting from aerial photos, Google Earth estimates may be arguably better measurements, while adding minimal time for a digital RGA method. Part of the reason the CSI metrics 5 and 9 did so well could be because they identified evidence of different processes and were not the actual measurement or estimation of how much of the reach was affected by those processes. However, the digital RGA method could become more accurate as satellite imagery quality increases. Another reason that percent bank affected by mass wasting was less successful was because channel widening was assumed to be a function of both mass wasting and fluvial erosion processes, when it was possible to be one or the other.

There was the risk of a biased assessments of the development data set since the historical scores were known a priori, which could also explain, in part, the high success rates. The historical assessments, however, were not intentionally reviewed prior to the digital RGA assessment. During the method development, the Google Earth methods were reasonably repeatable and the conclusions reasonable for someone who had never seen the sites before.

Another issue to consider was temporal differences in data. The RGAs for the fourth order streams were collected on July 13 and 14 of 2010, the Google Earth imagery was taken in April 2010, and the LIDAR flight dates were December 3, 2015 for Barren Fork and January 24, 2016 for Spavinaw (Table 7). When comparing the LIDAR data from late 2015 and early 2016 to the Google Earth imagery from April 2010, the critical bank was not always constant, especially when only evaluating it as the outside edge of a meander. This change in critical bank could explain some of the error.

Even though there was difficulty identifying the stage of channel evolution noted by the historical RGA reports, the Google Earth estimates had a relatively high success rate (90%) identifying the same risk category. The rate at which these methods identified the same historical stage of channel evolution, on the other hand, was 24%. This was counting the number of times that the Google Earth assessment identified the same stage as at least one of the teams from the historical assessments. Part of the reason this rate was so low could be explained by the difficulty to discern any evidence of degradation in Google Earth. It was difficult to detect downgrading, since 3-D images in Google Earth tend to be built using low resolution DEMs causing image warping (Fisher et al., 2012). Since the success rate was still high, it may be possible to properly identify sites that are the most unstable, even if the stage is not properly identified. Another possible reason the Google Earth assessments did not match the historically identified stages was because of the questions used. In Heeren et al. (2012), it was noted that the erosional processes were not the sole



determination of the stage, but also the vegetation. The questions proposed in the methods could potentially be improved by adding in some questions about the vegetation.

For the validation sites, there were similar results (Table 11), with an average success rate for individual metrics being 89%. The metrics that did the best were the degree of constriction, percentage of bank affected by mass wasting, and the percentage of the bank affected by accretion, with success rates of 100%. The metrics that did the worst were the identification of erosion presence/type and the combination of percent woody cover and bank protection, with a success rate of 75%. However, the combination of all 6.5 digital metrics performed worse in the validation, with a success rate of 38%, compared to the development at 79%. It should be noted that there were only eight validation RGAs, so the validation success rates are calculated with a smaller sample size than the development success rates.

## **Channel Bed/Bank Characterization Methods**

### Primary Bank Material & Stratification

The results for the characterization methods are summarized in Table 12. The method to obtain the primary bank material and stratification appeared to do well in comparison to the historical adjustments made for the second order streams. Both methods only failed once out of the six RGAs performed on second order streams. However, as mentioned before, the historical RGAs for the fourth order streams did not use these two adjustments. This could explain

why the success rates are low, since the adjustments were applied to all of the historical sites, while only the second order streams historically used them. The success rates were 52% for the primary bank material and 62% for stratification.

For the validation stage of the project, the adjustment factors were applied to both the digital and the on-site scores. The success rates were higher for the validation sites, with 75% for primary bank material, and 88% for stratification. The stratification adjustment factor could potentially be improved by adding additional scenarios which take into account the likely effects difference changes in soil layers would cause. For example, a denser layer above a layer of sand would be more likely to cause the bank to be undercut, than a layer of sand above a denser layer.

It should also be noted that while Web Soil Survey reports up to approximately a 2 m depth, the bank heights may be greater than that. In the case of the development stage, 79% of the stations had bank heights greater than 2 m reported. On average, the banks were taller than 2 m by 62%. For the validation sites, all eight of the sites had bank heights taller than 2 m, greater by 78% on average. It is important to recognize that the difference in actual bank height and the depth of soils reported could significantly affect the accuracy of the digital RGA. For example, consider how Web Soil Survey is used to identify primary bank material. The depth of each horizon is critical in determining which soil type is predominant when considering the vertical bank. If the entire bank is

not represented, then it is more likely that the primary bank material will be misidentified.

### Bank/Bed Protection

The results for the bank/bed protection metrics are summarized in Table 11. Using Google Earth to identify bank protection, defined as greater than or equal to 50% woody coverage, had a fairly high success rate in the development stage at 90%. On the other hand, the validation success rate was lower, at 75%. Bank protection also had a low rate of accuracy. Only 21% of the Google Earth assessments matched at least one of the team's historical assessments of bank protection. The validation's accuracy increased slightly, from 21% to 38%. The discrepancy could be in part because of differences in method. While historically, the bank protection was assessed visually, the digital RGA measured the reach scale presence of woody vegetation and provided a threshold level that defined bank protection. This method was more methodical, and possibly less subjective, though Google Earth estimates could have overestimated the influence of woody vegetation due to the simplified method for determining supportive woody cover. The digital method relied on a simple decision matrix. If the crown of the tree reached the channel, then it was counted as supportive. This was true for all cases except where it was clear that the bank was experiencing mass failures.

It was originally assumed that a restrictive layer, if present, would provide bed protection and that a high percentage of fragments on the surface would correlate to streambed armoring and/or bank protection. This may not be a valid

assumption, and further consideration should be made of these reports from Web Soil Survey before they are used further in RGAs. For the development stage, Web Soil Survey reported no restrictive layer within 2 m of the top of the soils, and minimal surface protection provided by fragments. The main indicator of bed protection used in this study ended up being the primary bed material obtained from the USGS Stream Gages. If the bed material size was bigger than gravel, the bed was counted as protected. None of the development sites had any indicators of bed protection. Therefore, none of the sites received a score for bed protection (CSI metric 2b). This resulted in a 90% success rate for the CSI when evaluated in combination with the methods described to find the percent of woody cover and the bank protection. Evaluated on its own, there was a 100% success rate when using the Web Soil Survey to determine bed protection.

Even though this method appeared to be successful, some teams historically reported the presence of bed protection. The question is whether these proposed methods has the capability of identifying the presence of bed protection. The validation results illustrate the need for a more refined method, as the success rate decreased from 100% to 75%. The accuracy also dramatically decreased in the validation stage from 97% to 0% for bed protection. Since bed protection was determined based primarily on bed material type, it is not surprising that the validation success rate and accuracy decreased for them as well. Caution is recommended before saying these proposed methods to determine bed protection should be recommended for every situation.

## Root Depth and Root Density

The results for the vegetation metrics are summarized in Table 12. The method developed to get an average root depth appeared to perform well with a success rate of 93% when evaluated by itself. When evaluated with bank height (obtained using LIDAR), the success rate dropped to 55%. When both the bank height and the average root depth were used to get the minimum surface protection values, the success rate was 24%. Using the average root depth by vegetation type was also attempted, but performed worse than when using the average (success rate of 86%).

This reduction in success rate appears to be due more to the compounded error of using bank height from LIDAR than necessarily error in the vegetation and surface protection estimates. This is illustrated by the increase in success rate when just considering the root depth and the resulting surface protection estimates, which had a success rate of 72%. Since the bank height influences four out of five of the BEHI metrics, it makes sense that the error would be compounded when replacing the historical with the LIDAR measurement. Not to mention the error that could be a result from the LIDAR being from a different year than the RGAs were collected. However, another point to consider is the digital methodology. The resulting root depth used for the development sites did not vary as much across the different sites, especially in comparison to the on-site measurements (Figure 35). The fact that the digital method did not vary across the different sites could indicate limitations in the method's ability to differentiate between sites.

The root density method using just two vegetation classes (woody and grass) appeared to perform adequately, with a success rate of 90%. Setting the surface protection equal to root density was also tested and resulted in a success rate of 62%, which is lower than using the root depth metric. The success rate was calculated for the combination of the following digital data: the root depth, root density and surface protection metrics. When using the root depth values for surface protection, the success rate was 48%, while when using the root density, the success rate was 45%. Based on these calculations using the development data, it appears that the root depth ratio method was better at representing the surface protection.

The vegetative metrics performed similarly in the validation stage. Both the root depth and the root depth ratio dropped in their success rates from 93 to 75% and 55 to 50%, respectively. Using the root depth ratio to estimate surface protection had a slight increase in success rate, from 24 to 38%. Part of the reason the root depth ratio methods did poorly could be their reliance on minimum root depths provided by NRCS PLANTS database, and while both trees and woody species were included in the average root depth, this ended up resulting in a number which did not vary greatly across the different soil types. Another reason the root depth ratio methods performed poorly could be because the species used are just expected representatives reported by Web Soil Survey. The species reported by Web Soil Survey may not accurately represent what is actually growing on site. Given that the root density method was derived using the historical values, it is slightly surprising that this method did not perform

worse than a success rate of 75%. Especially when considering the wide range of ecoregions used. Caution should still be used, and method revision may still be necessary to be more accurate, especially when considering bank protection, which is more than just the presence of roots.

## **Stream/Channel Geometry Methods**

### Methodology for Bankfull Depth Measurement

Bankfull height is the measurement from the surface of the water to the top of the bankfull indicators. That is the value that is used in the BEHI metric 1. However, for this study and comparison, we were interested in finding a method that could predict bankfull depth (the measurement from the bottom of the channel to top of the bankfull indicators). In addition, most ecoregional equations are developed to find the average bankfull depth, not height, so it was easier to compare everything to bankfull depth. Therefore, the statistics are comparing the predicted values to the historical bankfull depth (measured baseflow depth plus the measured bankfull height). The LIDAR derived bankfull height was also included in the statistical assessments. Since it would be easier to use the bankfull height instead of the bankfull height plus the calculated baseflow depth, it made sense to include it on its own in the comparisons. It should be noted that the statistics calculated for each method were chosen based on the work done by Harmel and Smith (2007) on assessing hydrologic modeling.

Another point to keep in mind when interpreting the results is that the success rate is measuring how much each method affects the overall RGA

score. The bankfull metric is complicated by the fact that it is not the bankfull alone but it is the ratio of the bankfull and bank height. The success rates for each bankfull method were calculated for the development stage and recorded in Table 13 and Table 14. The success rates for the validation stage were recorded in Table 15. It should be noted that the validation streams were not assessed separately based on stream order. This was because there were fewer sites and a wider range of stream orders than there was in the development stage, including a second, third, and fourth order stream, based on the Blue Thumb reports. In addition, while there were no measurable meander features in the second order streams used in the development stage, there was no such problem in the validation stage. Therefore, all bankfull methods were applied to all stream orders in the validation stage.

This study focused on Bieger et al. (2015) coarser resolution equations rather than the equations developed for the finer resolution regions, due to the lack of data points to develop the equations as was discussed in the methodology section. The Bieger et al. (2015) equations based on physiographic regions did fairly well in the development stage with a success rate of 86%. Analyzing the assessments that failed, the equation developed for the coarse physiographic region underestimated the risk for fourth order streams, but overestimated the risk for second order streams. In terms of how well the Bieger et al. (2015) equation was able to replicate the historical measurements, the statistics are reported in Table 16. The equation did not perform well in terms of  $R^2$  (only 9%), meaning that it did not explain the variabilities well.



It should be noted that both the equation grouped by ecoregion and the equation grouped by precipitation developed by Dutnell (2000) were used initially, but there were no significant differences between the two in terms of performance. This may be due to the lack of information available for the study sites, especially data in the Ozark Highlands ecoregion.

Dutnell (2000) equations developed for the state of Oklahoma (excluding the panhandle) and developed by ecoregion had similar results in terms of success rate (both at 90%). The fact that they were equal could be because the Great Plains ecoregion is one of the largest ecoregions while the Ozark Highlands is one of the smaller ecoregions. This meant that a large proportion of the data contributing to the statewide equation was from the Great Plains. On the other hand, there was not a lot of data used to develop the equation for the Ozark Highlands. This could explain why there is not a big difference between any of the Dutnell (2000) equations used (Table 16).

The equations developed by Williams (1986) had a wide range of success (Table 13 and Table 14). Some of the methods proposed were not applicable to the second order streams, given the need to measure clear stream plan-form features. The equations that could be applied to both the second and fourth order streams was the one dependent on knowing the stream's sinuosity and bankfull width, and the equation dependent on bankfull width alone. The equation dependent on bankfull width alone had a success rate of 72% while adding in the sinuosity raised the success rate to 83%. The success rates for the equations

that only were applicable to fourth order streams are reported in Table 14. These included the equations developed for meander geometry, one using the belt width, the bed length, the radius of curvature, and one using the meander wavelength. Out of all of these equations, the one using the belt width performed the best with a success rate of 78%, while the bed length equation performed the worst with a success rate of 43%. The equation using belt width also appeared to do well in terms of the other statistics (Table 16), with an  $R^2$  of 41%. Given the difficulty in measuring the radius of curvature in Google Earth, it was surprising the equation performed fairly well at 65%. One possible reason the equations dependent on the estimated bankfull width did better than the equations dependent on meander geometry could indicate that the features identified as bankfull from Google Earth matched well with the indicators used by the historical evaluators.

Interestingly, all of the ecoregional equations overestimated the risk associated with second order streams, but underestimated the risk for fourth order streams. This could be related to the sites used in the development stage and not indicative of the relationship between ecoregional equations and stream order in general.

Using the two-year return period provides a method that is consistent and is not reliant on the opinion of the observer(s) on the location of the ambiguous and at times misleading bankfull indicators. The  $Q_2$  method also has potential in the determination of bankfull depth where no bankfull indicators are present,

which is a possibility in steep streams (Leopold, 1995). There are assumptions that have to be made with the  $Q_2$  method, such as the channel shape and the side slopes, which may have impacted the accuracy.

The  $Q_2$  method had one of the worst bankfull method success rates at 45%, underestimating the risk assessment. Comparing the second order streams, the  $R^2$  is relatively high at 67%, with two out of the six failing to match the historical BEHI risk assessments. Comparing the fourth order streams, the  $R^2$  is at 39%, failing fourteen out of twenty-three. The fully digital RGA still underestimated the risk category when applied to both stream orders, with a success rate of 31%.

The PeakFQ method of obtaining bankfull depth could be more applicable than the  $Q_2$  method, since it has the ability to provide a wide range of return interval flows, including 1.05, 1.5, and 2-year return intervals. This is helpful, since not all sites will have the same bankfull return interval.

The 1.5-year peak flows obtained using PeakFQ did not appear to match the historically identified bankfull much better than the 2-year flows. The success rate was a little higher at 52%. The success rate increased because the two RGAs that failed from the second order streams using the  $Q_2$  method were successful using the  $Q_{1.5}$  method. Besides those two cross sections, the same cross sections that failed using  $Q_2$  failed using the  $Q_{1.5}$  method. Both methods underestimated the RGA risk assessment score.

It is worth noting that the 1.5 bankfull depth method did have a 100% success rate for the second order streams while the  $Q_2$  method successfully matched RGA categories for four out of six. This could imply that the flows associated with the bankfull indicators identified in the field are closer to 1.5-year peak flows than 2-year peak flows for second order streams. These results could imply that the bankfull indicators are associated with flows that are more frequent than a 2-year return interval, which is backed up by the increase in the success rate when using the  $Q_{1.5}$  method.

The goal of the LIDAR method was to get the most accurate picture of the cross section as possible with the available data. The strength of the LIDAR method lies in the real world, real-time data that it is based on. It relies on the key indicator, the change in slope (Leopold, 1995), and reduces the reliance on judgements made in the field.

While the LIDAR method provides the most accurate image of the stream, it also is limited by need for high-resolution data. This method is reliant on LIDAR data that is not always available for the area of interest, and even if available is not guaranteed to be data with a high enough resolution to detect topographic bankfull indicators. Another limitation may be the time, especially in this study, since we are interested in comparing these measurements generated from LIDAR to historical measurements. Working with LIDAR data also requires some knowledge about how to work with ESRI ArcGIS. Finally, LIDAR data is not

always available in a fully processed form such as a DEM, and some processing of the raw raster data may be necessary in order to use this method.

The LIDAR bankfull height measurements appeared to do well in comparison to the historical averages of the team measurements (Figure 36). The grouping of the points around the on-to-one line illustrates this. The LIDAR methods for measuring bankfull height appears to underestimate for second order streams. Success rates were calculated for both the bankfull height by itself and the bankfull height plus baseflow depth calculated using the LIDAR geometry. The bankfull height performed better than the bankfull depth (bankfull height plus baseflow depth). Using just the bankfull height had a success rate of 83% while the bankfull depth had a success rate of 59%.

Using just the bankfull height appeared to work well, though it appears to not be the most appropriate method for second order streams, since it failed three out of six of them when evaluated alone. Part of the reason that it did poorly on second order streams could be just the combination of the smaller stream size and the lower LIDAR resolution. It could be that the results could be improved if 1-m resolution LIDAR was used on second order streams. Two cross sections which failed using the bankfull height method were close to the downstream end of a meander. One in particular appeared to be part of a transitioning floodplain, which could have confused some of the bankfull indicators.

If the channel is actively changing, this could introduce conflicting information in the analysis. For example, the LIDAR data for the Barren Fork and Spavinaw streams were collected in December 2015 and January 2016, respectively. But the original RGAs were collected in 2010. The Fort Cobb sites were evaluated in 2016, but LIDAR was not available for it more recently than 2010. The Google Earth assessments of the development data were done using aerial imagery from the same years as the historical collection dates.

A two-way Analysis of Variance (ANOVA) was performed on the development data set of historical bankfull depth and bankfull depth obtained using methods applicable to both second and fourth order streams. No validation data were considered in this test. Method and Stream Order acted as the treatment variables with the response variable being Bankfull Depth. The only methods that produced statistically similar results to the historical bankfull depth was the LIDAR bankfull height and depth (LIDARHeight and LIDARDepth). The interaction plot (Figure 37) appears to indicate that the regional equations are underestimating the bankfull depth. Note how in the figure, the  $Q_{1.5}$  and  $Q_2$  methods overestimate bankfull depth for fourth order streams, but provide a good estimate for second order streams, which was also reflected in the success rates (Table 13 and Table 15). This was confirmed using a one-way ANOVA using just the second order streams with Method as the treatment variable and Bankfull Depth as the response variable. The results showed that the LIDAR bankfull height and depth were still significantly similar, but the  $Q_{1.5}$  and  $Q_2$  methods also produced significantly similar results. Caution should be used when considering

these results, since development data only included six representatives of second order streams, so the power of this relationship should be confirmed with future work.

It should also be noted that while there was a clear distinction between what methods were statistically more accurate, once inserted into the fully digital RGA, the influence this single measurement had appears to decrease. For example, while Dutnell (2000) equations had the best success rates when bankfull depth was the only thing measured digitally at 90%, in the fully digital BEHI the success rate dropped to 38% for the State-wide equation and 31% for the ecoregion-specific equation. Comparing all of the bankfull methods in terms of their success rate for the fully digital BEHI, the success rates ranged from 28 to 38, with slightly higher success rates for methods applied to fourth order streams. All success rates using the development data for the fully digitized BEHI and changing bankfull method are summarized in Table 13 and Table 14.

The different bankfull methods were also applied to the validation sites, and the resulting success rates analyzing just the digital bankfull value as well as the fully digital BEHI are included in Table 15. It should be noted that in the development stage there were some Williams (1986) equations that could not be applied to the second order streams due to the lack of a clear meander pattern. In the validation stage of the project there was no problem identifying the meander patterns for all of the different stream sizes. The results are similar, though the fully digital methods appeared to benefit from the different ecoregional

equations, with the Williams (1986) equation using the radius of curvature getting one of the highest fully digital success rate of 63%. The PeakFQ method also performed better for the validation stage (Table 15). On its own, the PeakFQ results had a success rate of 88%, and in the fully digital assessment, it had 63%. The increase in performance could be because the majority of the streams were smaller than fourth order, while in the development stage, the majority were fourth order. The validation results support the hypothesis that the PeakFQ method works well for lower order streams (Figure 37). The LIDAR bankfull height method did not perform as well as the PeakFQ method, with a success rate of 38% compared to 34% in the development stage. The LIDAR bankfull depth method on the other hand, performed better at 50%. This could indicate that the LIDAR bankfull height method works better on fourth order streams, given the higher number of fourth order streams assessed in the development stage versus the validation stage. It should be remembered though, that this equation is not always applicable, if the stream does not exhibit measureable meander patterns. It should also be noted that there were only eight validation sites.

#### Methodology for Measuring “Baseflow” Depth

Unsurprisingly, the most precise method (LIDAR+StreamGage) provided the estimate that most closely matched the historical measurements, despite the fact that the LIDAR was obtained at a different time than the original RGAs. The other methods overestimated, with values obtained using StreamStats providing the highest estimates (Figure 38). In terms of statistics, none of the methods



were significantly similar to the historical values, using a Tukey's analysis with an alpha of 0.1. However, the StreamGage and LIDAR+StreamGage method did produce similar methods. The StreamGage mean was 3.8 and the LIDAR+StreamGage mean was 3.3. The results were similar when stream order was added into the analysis. This implies that adding in the top width from LIDAR does not necessarily increase the accuracy.

The results for the validation stage were similar, with the highest success rate being associated with the LIDAR+StreamGage method (100%). There were only eight validation sites, and given the lack of current gages, there were three sites where this method could not be used. However, supplementing using StreamStats for those sites did not adversely affect the results. Using the average daily flow from StreamStats resulted in a success rate of 88%. It is interesting that the LIDAR+StreamGage method performed the best, considering the fact that the LIDAR was collected at significantly different times than the historical RGAs. This could simply relate to a long-term hydraulic regime that is being reflected in constant baseflow depths.

Analyzing the development data in terms of how well each method did in the digital CSI, the StreamStats method had a 79%, the StreamGage method had an 86%, and the LIDAR+StreamGage method had a 93% success rate. The success rate increased for the fully digital CSI as well, with a success rate of 72% for the StreamStats method, 76% for the StreamGage method, and 83% for the LIDAR+StreamGage method. The success rate for the fully digital validation

CSI did not increase, but the scores did appear to become closer to the correct score.

Either way, it appears that the LIDAR+StreamGage method is the most accurate out of the three options. The limiting factor to this method is the fact that it relies on knowing the precise day the LIDAR was collected. This information is not always readily available. More recent LIDAR data sets appear to be better at reporting this piece of information. The USGS National Map, advanced viewer, was fairly consistent with its reporting of metadata, including the s\_date and e\_date, which define the start and end date of the project collection (Archuleta et al., 2017; USGS, 2016). This may be only as precise as years.

Besides lacking easily accessible LIDAR flight date information, there are other limitations to using the LIDAR+StreamGage method. Another potential limitation is the absence of gages on the stream of interest. Not every stream is gaged, which could limit the use of both the LIDAR+StreamGage method, but also the StreamGage method. In those instances, the StreamStats method may be the only option.

All of the Monte Carlo calculated depths for both the bankfull and baseflow depth flows are recorded in Table A - 1.

### Methodology for Bank Measurements

The results for all bank measurements is summarized in Table 17. Using LIDAR to get bank height did better in the CSI than in the BEHI, with a success rate of 97% in comparison to 66%. In general, it appears that LIDAR had a higher

success rate when used in CSI than when used in BEHI. This makes sense, since the CSI is less reliant on actual bank feature measurements, while the BEHI is heavily reliant on such measurements. Part of the reason the LIDAR bank height performed poorly in the BEHI is because three of the five metrics are dependent on bank height. Therefore, changes in the bank height affect almost every score. There are also more stability rankings than in the CSI. Both of these combined just means that there is more room for error in the CSI than in the BEHI and the chances of being pushed into the wrong category is higher.

The LIDAR-derived bank height was further analyzed by only using the LIDAR bank height in one metric at a time. In other words, using the LIDAR bank height for all four metrics resulted in a success rate of 66%, while using it just in the individual metrics had success rates as follows. Using the LIDAR bank height in just the bank height to bankfull height ratio (BEHI metric1) had a success rate of 90%. In the root depth metric (BEHI metric 2) the success rate was 83%. In the bank angle metric (BEHI metric 5) the success rate was 90%.

The validation stage performed similarly (Table 17), though the LIDAR bank height performed better, at 88%. This could indicate a learning curve for the author in the identification of banks between the development and validation stage. Another possibility could be a difference between the bank measurements caused by averaging all of the team measurements, which sometimes included both banks, while only the critical bank was measured with LIDAR. This could

have led to larger errors in the development stage, while in the validation stage, only the critical banks were used in both the digital and on-site assessments.

## **Validation**

As described in the methodology, the validation sites were chosen, then the digital assessments were performed before the site visit. Extraneous reaches were digitally assessed in order to provide several options during the site visit. This allowed for some flexibility in case of reaches that ended up being inaccessible. Flexibility was possible, since the point of the site-assessments was not necessarily to rank different parts of the same stream, but to provide comparisons of performance between the digital and on-site assessments.

There may have been some bias in the digital assessments of the Fourche Maline sites. In particular, the visual assessments. Since several of the previous validation sites had been unstable, a more stable site would have been good to evaluate using the digital methods. Since more stable results were hoped for, the risk could have been underestimated. However, because there was no obvious signs of mass wasting or channel widening, the digital CSI ranking of stable was obtained. The majority of the site evaluations for the validation sites fell into at least moderately unstable rankings. This could present some bias to the results of the validation, since no stable reaches were assessed. One reason for the high number of unstable sites could be the method used to select sites. One of the factors considered was ease of access to the stream. This meant that several of the locations were either up or downstream

from a bridge. While efforts were made to go far enough up or downstream to be outside of the range of influence, the presence of the bridge could still have affected the state of channel stability.

Two of the site evaluations were done at flows that were barely wadeable, making some of the measurements more difficult to perform, in particular the channel width at the cross section and upstream. The Fourche Maline and Black Fork Streams had base flow depths averaging 1.4 m. The difficulty in measurement led to the channel widths being visually estimated. The difficulty experienced in accessing the sites could have biased the on-site scores. This highlights a benefit to using Google Earth, as the measurement of the channel width is not hindered by the current state of the stream.

It should be noted that the reach classified as reach 1 for Fourche Maline (Figure 39), had appeared homogenous from the aerial imagery, while the site visit revealed more variation, especially in terms of woody debris and mass wasting. The upper part of the reach was experiencing severe slumping and a high percentage of woody debris in the water, but on-site assessment was performed further downstream, where the banks were more stable and accessible, though the highly unstable on-site CSI score still reflected the overall instability of the reach.

Initially, Black Fork reach 1 was going to be the only reach assessed on-site. Reach 1 was preferable, since reach 2 had a secondary channel, and reach 3 was heavily braided with permanent vegetation, making the critical bank

difficult to determine. However, due to the high base flow, reach 2 was the only reach assessed on-site. The secondary channel was not included in the on-site assessment, so the banks associated with the main channel were the only ones used in the assessments and measurements.

The validation results provided some valuable insights. While the CSI appeared to do well in the development stage, the success rate for the fully digital score for the validation stage was 38%. The problem encountered during the validation process was especially true for the Feather Creek site. The most recent imagery available from Google Earth was taken in 2014 while the assessment was performed in 2018. The reach was heavily wooded, which implied protection and the resultant digital score was Moderately Unstable (11 points). However, the site-visit revealed several pieces of erosion evidence that the aerial imagery did not capture. There was evidence of erosion and possible streambank instability that were not visible from the aerial imagery. The channel was also incised, which meant that the woody cover provided less significant support than was assumed from the imagery. Finally, because the view of the reach was obstructed, the stage was not correctly identified. Since the digital methods are interconnected, the problems are compounded. If the channel is small, the view can more easily become obstructed. If you cannot see the channel, then you cannot identify the evidence of erosion, which means you cannot properly identify the stage of channel evolution. This could explain the resulting increase in the difference in scores between the development and validation stages.

It was also noted that all of the reaches that failed in the validation stage tended to be on straighter reaches (Figure 40 and Figure 41). This could be highlighting a limitation in the digital methods. It does make sense for the digital assessment of straighter reaches to be less accurate. Straighter reaches were more difficult to determine the critical bank, and tended to be more easily obscured by trees than reaches that had a clear meander and point bar.

Because of the difference in performance between the development stage and the validation stage in the results for the CSI, different combinations of the digital and on-site data were tested to identify any combination that yielded better success rates, assuming that the on-site assessments were correct. Using the information provided by Table 18 to Table 22, the first combinations tested used the onsite data for the percent woody cover/bank protection, as well as the percent of bank accretion. None of these combinations appeared to have a positive effect on the success rate. The best combination that this study found was obtained by taking the on-site assessments and adding the digital assessments one metric at a time until there was a dramatic drop in success rate, and any additional digital data decreased the success rate significantly. The best combo only failed one out of the eight validation sites (success rate = 88%), and used the digital methods for the degree of incision, the degree of constriction, identification of streambank erosion, percent of accretion, and the stage of channel evolution. This combination is may not be significant, given there are only eight validation sites, and neglects the consideration that some of

the CSI metrics may be improved by the digital methods. However, the same combination used for the development stage did have a success rate of 86%.

While the reach-length assessments done from Google Earth can be severely hampered by visual obstructions as demonstrated with the evaluation of Feather Creek, there is still a lot of potential for this tool. As long as there is no major misidentification of the reaches, Google Earth has the potential to be more accurate than on-site estimation of reach-length properties. For example, visual estimations of the reach-length accretion and instability could be biased by what is more predominantly visible at the assessed cross section, while the Google Earth measurements consider the whole reach-length. As mentioned above, future users do need to be aware of the limitations. There is not always high-resolution imagery that is also recent. There is also the chance of evidence of erosion and mass wasting being invisible from Google Earth, either because of heavy vegetation, or because the bank is undergoing processes not visible from above. For example, undercutting of the bank may not be detectable from Google Earth until it has caused more drastic mass wasting events. It is also difficult to ascertain whether the trees on the bank are actually providing support, also demonstrated in the Feather Creek validation site. To address the limitations, it may be advisable to add some kind of decision matrix to the digital methods, which reduces the amount of assumed support depending on the degree of incision and/or the height of the bank.



The source of the largest amount of error for the digital BEHI was from the primary bank material score adjustment. This caused as much as a twenty point difference between the digital score and the on-site score. Using the information provided by Table 18 to Table 22, the digital BEHI was adjusted to test if adding site information for the primary bank material, stratification, the root depth ratio/surface protection combo, and the bank angle had any affect on the success rates. Assessing just the primary bank material increased the success rate for the validation sites from 38% to 63%. Using the on-site measurement of root depth and bank height, as well as the surface protection also increased the success rate to 63%. Using the on-site assessments for surface protection and primary bank material increased the success rate to 75%. Adding the on-site root depth and bank height did not improve the success rate, though it did affect which stations failed. Using the on-site assessment for stratification did not improve the success rate. To summarize, at least with the validation sites, it appears that the accuracy of the digital BEHI can be improved by assessing the percent of surface protection and identifying the primary bank material on-site.

A final consideration that should be made in this study is that the methods are affected by subjectivity and uncertainty. In terms of the methods, the weighting of the BEHI metrics is subjective (Sass and Keane, 2012), and were developed using limited ecoregions (Rosgen, 2001). As was discussed in the previous chapter, the methods are affected by the individuals performing the assessment (Bigham, 2016). And while the on-site assessments are assumed to be correct, they may not actually reflect the condition of the study reach. In the

development stage of the study, the RGAs were collected in teams, which should have reduced some of the uncertainty. With the validation stage, the data was collected by one team of about two people. Because there was only one team, the uncertainty about the on-site assessments increased.

### **Fully Digital Scores**

The success rates were calculated for both the individual metrics but also for the fully digital score and the results are summarized in Figure 42 through Figure 45. The fully digital CSI appeared to perform extremely well with a success rate of 83%. This was using the LIDAR critical bank height and the LIDAR derived baseflow depth. The BEHI on the other hand did not perform as well, with a success rate of 34%. This was using the LIDAR derived bankfull height and all other methods as described above. Part of the reason the fully digital BEHI performed so poorly is just the compounding of errors when combining all of the methods. Another thing to keep in mind is that the comparisons are not perfect, as the historical second order RGAs used the BEHI adjustment factors while the fourth order streams did not. Another point of consideration is that the digital score used the critical bank measurements, while the historical score was derived from an average that often included both banks. Add to that the large point difference which can be introduced when the primary bank material is misidentified, which happened 72% of the time, on average between the development and validation stages.

In order to identify the metrics causing the greatest difference between on-site and digital assessments, the average difference between each metric was determined for both the development and validation stage of the project. The results are summarized in Table 18. For the BEHI, the average difference in final score (aggregate) between the development and validation stage are similar, with -10.2 and -11.7 points respectively. The sources of difference appear to be the same as well, with the primary bank material (adj1) causing as much as a negative 8.8 point difference in the validation stage. This makes sense, as the primary bank material can adjust the final score by as much as -20 points. Stratification (adj2) had a larger impact on the development stage than the validation stage, going from a difference of -2.2 points to only 0.6. On the other hand, the root density (metric 3) performed fairly well in the development stage with only a difference of -0.8 points, while the validation stage had a difference of 1.4. This makes sense, given that the root density method used was derived from the historical values.

For the CSI, there is not as clear of a pattern. While the development stage performed extremely well, with only an average 0.8 difference between the on-site and digital assessments, the validation stage increased to an average 8.8 difference. Each metric contributes the same amount of points, except for the bed/bank protection metric, which has the potential to add an extra two points. Because of this even point distribution, there is not a clear implication of one metric influencing the score more than the others, such as the primary bank material does in the BEHI. It appears that each metric contributed a little error,

which was reflected in the total score differences. The increase between the score differences between the development and validation stage could indicate that there was some bias, but some of it could relate to the types of sites used in the two different stages.

Another aspect considered was the effect time had on the results. The CSI is dependent on Google Earth imagery, but often there was a difference between when the RGA was collected and when available Google Earth imagery was taken. Available LIDAR data was not collected at the same time as the collection date, which influences both the digital CSI and BEHI, since both have physical channel measurements that rely on LIDAR. Given the heavy dependency of the BEHI on LIDAR, the relationship between the overall score and the difference in time between the LIDAR and the on-site assessment was focused on. Using the LIDAR bankfull height for the digital BEHI and the LIDAR+StreamGage method to get the baseflow depth for the CSI, the resulting digital scores were compared to the on-site scores. The percent difference between the scores were plotted against the time difference, using the LIDAR time difference for the BEHI and the Google Earth time difference for the CSI. The results are reported in Figure 46 and Figure 47.

As can be seen in Figure 46, the CSI does appear to do better when the imagery used is more recent. This makes sense, since a stream can be actively changing even between the time the Google Earth photo is taken and the site visit is performed. This is not always true as illustrated by the two points

representing the biggest difference in time. The point that succeeded represents the validation assessment done at Black Fork. As Black Fork is a larger stream, it makes some sense that a larger time difference had little effect, as the larger stream may change more slowly. The point that failed is the validation assessment done at Feather creek, which has already discussed at length.

For the LIDAR data, the digital CSI does not seem particularly affected by the time it was collected (Figure 48). The CSI was able to sustain between -40 and 40 percent differences in score before failing. For the BEHI, time does not appear to have as clear a relationship (Figure 47). This is illustrated by the fact that there are several points that failed and points that succeeded that have the same difference in time. Figure 47 does illustrate how sensitive the BEHI is overall, with the majority of the success falling within the -20 to 20 percent difference range. In comparison, the CSI is not as sensitive to the overall difference in scores, with a range of approximately -30 to 40 percent difference while still correctly identifying the stability ranking (assuming that the on-site assessments are correct). This lack of a clear coincidence between the time difference in the LIDAR and the coinciding difference in aggregate score is interesting. A clear improvement in performance as the time difference got smaller was expected. A possible explanation could be that some of these metrics could be more constant over time while some are changing. This could mask the effect that time has when looking at the overall change in score. However, graphing the percent difference between the LIDAR and on-site

measurements did not reveal any obvious patterns either (Figure A - 5 through Figure A - 7 in the appendix).

There are similar results if LIDAR resolution is considered, as can be seen in Figure 49 and Figure 50. The LIDAR resolution does appear to affect the sensitivity of the CSI (Figure 49). While there is some overlap between the points that failed, at the 1-m resolution LIDAR there is a large allowance in the percent difference, ranging from -40 to 40%. As the resolution decreases in quality, the allowance also appears to decrease. The BEHI exhibits a similar pattern (Figure 50), though the percent difference allowance is smaller, ranging from around -10 to 10% at 1-m resolution. The difference in time was also considered, using the collection date as the datum, and the results are reflected in Figure A - 8 and Figure A - 9.

Finally, each station/reach was tabulated along with each metric or metric combination it had failed. The complete list is included in Table A - 2 and Table A - 3 in the appendix. The points that failed the fully digital method were analyzed to determine if there were any other individual metrics/metric combos that had also failed. The percentage of individual metrics/metric combos that failed out of all of the fully digital failures are listed in Table 19 and Table 20, and could indicate metrics that if measured on-site, may improve the accuracy of the digital assessment. The stations that failed the fully digital RGAs were recorded, along with the other metrics that failed in Table 21 and Table 22.

For the CSI, Table 21 shows slight differences between the development and validation stages. Given that the majority of the digital CSI is evaluated in Google Earth, it makes sense that station/reaches which failed using all Google Earth Methods also failed the fully digital RGA. For the development stage, there appears to have been more trouble with the combination of the identification of erosion and the percent mass wasting. While the validation stage appeared to have more trouble with any metric that included the percent of bank supported by woody cover. As can be seen from Table 22, there is a consistent trend between the development and validation stages for the BEHI. The root depth ratio appears to be significant, as well as the primary bank material, which has been noted before for its large point influence on the overall score (Table 18).

The difference in reach determination is another point of discussion concerning the difference in digital CSI performance between the development and validation stage. Since the historical reaches were pre-determined for the Barren Fork and Spavinaw streams in the development stage, there was little concern about whether or not the features considered in the digital assessment were within the study reach. The Fivemile and Willow reaches were not reported, so the digital reaches were estimated by assessing approximately 30.5 m above and below the cross section. This assumed reach length could have been an overestimate of the reach actually considered in the on-site assessments. This could explain why the Fivemile and Willow RGAs performed poorly in the fully digital RGA, with five out of six failing (Table 19). The longer digital reach could have included features and evidence that was not originally considered. A similar

phenomenon could have happened between the validation digital and on-site assessment, and would explain the decreased overall success rate.

The validation process highlighted some of the limitations of Google Earth. For example, the Feather Creek site was limited by the fact that high-resolution imagery had not been collected for that site since 2014 while the site visit was conducted in 2018. It was also noted that the amount of woody cover visible from Google Earth implied a highly stable channel, but the site visit revealed that the channel was incised and experiencing erosion. The error was compounded by the fact that the channel was not very wide, which made it difficult to assess with Google Earth. Since the woody cover obscured the imagery of the channel, other assessments were affected, including identifying evidence of erosion or mass wasting, which in turn was needed to correctly identify the stage of channel evolution. Caution should therefore be taken when using the digital CSI. When the channel was small and the overhead canopy appeared to be dense, the digital methods proposed would more likely predict a stable reach. It should also be noted that since Google Earth imagery was only updated periodically, there was the chance that pertinent information could be missed, or even impossible to identify due to obstructions such as cloud cover.

Another possible explanation for the decreased performance in the digital CSI is the size of the streams assessed in the validation stage. As was noted previously, five out of the six second-order streams failed the fully digital CSI in the development stage (Table 19). Despite the poor performance of the second



order streams, since the majority of the development sites were fourth order streams, the development stage digital CSI performed well overall (83%). This could explain why the validation stage results were so much lower (38%), as the majority of the sites were from stream orders between second and third. Based on these comments, the digital CSI methods may not be as accurate on smaller order streams. This would make sense, as smaller streams were harder than larger streams to analyze visually on the same scale and resolution image.

### The Coefficient of Success

The results for the fully digital scores can be understood better through the resulting  $S^2$  values. The  $S^2$  values for each RGA category are summarized in Table 23 and Table 24. Some idea of how successful the digital methods were gained by considering Figure 42 through Figure 45. All points that fall inside the shaded boxes are counted as successful. The  $S^2$  values help quantify how successful the methods were by describing the distance between the points that failed are from a score that would have been counted as a success. The figures can also illustrate how the different methods affect the final scores. For example, Figure 43 shows how the use of the LIDAR+StreamGage method may not have increased the success rate (more points inside the shaded boxes), but the points are closer to the correct ranking. It is possible to more accurately describe which stability categories the digital RGA is having trouble identifying. For example, in Figure 44, the points that fell inside the “High” stability ranking box, had a success rate of 46% (Table 24). In other words, 46% of the points were correctly identified as “High” out of all of the points that should have been counted as

“High”. The points that failed are a mixture of being overestimated by one and two stability rankings, with an  $S^2$  of 24%.

The Coefficient of Success was calculated for both the development and validation stage. For the BEHI, it appears that the results are similar for the development and validation stage, with the higher stability rankings tending to be more successful. The CSI, however, performed worse during the validation stage, severely underestimating the risk category compared to the on-site assessment. The LIDAR+StreamGage method was not applicable to all of the validation sites, due to a lack of appropriate gage data, or the lack of any gage connected to the stream of interest.

#### Time: Digital vs. On-Site

The amount of time it took to perform the digital and the on-site assessments were approximated and then the average time it took for each reach was estimated. The results are summarized in Table 25 and Figure 51. In terms of the amount of time required to perform digital RGAs, on average each validation site took about seven hours to assess digitally, while the on-site assessments took on average about 10 hours per trip. The average time spent assessing each reach was two hours for the digital assessment, while it was twice that for the on-site assessment, taking about four hours per reach. This included travel time to each site. Streams assessed on the same trip were combined for the time estimate.

It should also be noted that the time it took to perform the digital RGAs included some extraneous steps, in particular when calculating the bankfull depth and the baseflow depth. These extraneous methods were typically only applied to the reaches that were actually assessed on-site. While not all of the methods were applied to all of the reaches, this still added steps to the digital assessment that you would not necessarily apply in actual practice. One step which was not included in the time it took to perform the digital methods was the time it took to set up the worksheets to calculate bankfull and baseflow depth using a random Manning's  $n$  value, relying on the Monte Carlo method. In future work, the use of the Monte Carlo method to calculate bankfull and base flow depth is possible, though it could take more time. Another option to be considered in future work would be to rely on tables and images from Chow (1995), or relying on other methods for estimating  $n$  (e.g. USDA (2012) or Arcement and Schneider (1989)).

It does appear that the digital assessments are not very time-efficient when only evaluating a few reaches, since the amount of time was fairly constant, taking about seven hours to assess either two reaches or four reaches. However, the time it takes to digitally assess reaches could decrease as the digital methods become more accurate and less extraneous information is gathered. The possibility to automate the methods should also be considered for future work. Automating the methods would further decrease the amount of time required to perform the digital assessments.

## **Digital Method Accuracy**

While the focus of this study was to illustrate how digital data could be used in RGAs and get the same stability ranking, the individual method accuracy should also be considered. The method accuracy was measured by calculating the percentage of reaches where the digital method obtained the same result as the on-site method. The same result was defined as the same RGA metric score.

For the development data, if at least one team had the same categorical result, for example, the same erosion types identified, then the method was given half a point. A full point was assigned to reaches if the averaged team assessment had the same result as the digital method. For methods which involved measurements, the average team measurements were used to compare to the digital method. A full point was assigned to any reach where the same metric score was obtained. For the validation data, the digital results were directly compared to the on-site data, since there was only one set of measurements for each reach.

The results are summarized in Table 26. The digital methods with the highest accuracy averaged across both the development and validation stages included the degree of constriction, degree of incision identifying streambank erosion types for CSI and stratification for BEHI. Several CSI accuracies decreased for the validation stage, which could indicate bias in the development stage. Another possibility could be the digital methods worked well for the development sites, but did not have the capabilities to detect the broad range of

variability tested in the validation stage. For example, the primary bed material and the bed protection had high success rates and accuracy in the development stage, but decreased drastically in the validation stage. But the development data predominantly was made up of gravel for the fourth order streams (twenty-two out of twenty-three) and the second order streams all fell between the sand and silt/clay as designated by the data collection sheet. On the other hand, the validation reaches ranged from silt/clay to boulder/cobble and had a variety of gage data available. The gage placement, and the date when the bed material was assessed could have had an impact on the validation results. Even though the accuracy decreased for several of the CSI metrics, the digital CSI methods appeared to be more accurate overall in comparison to the digital BEHI methods.

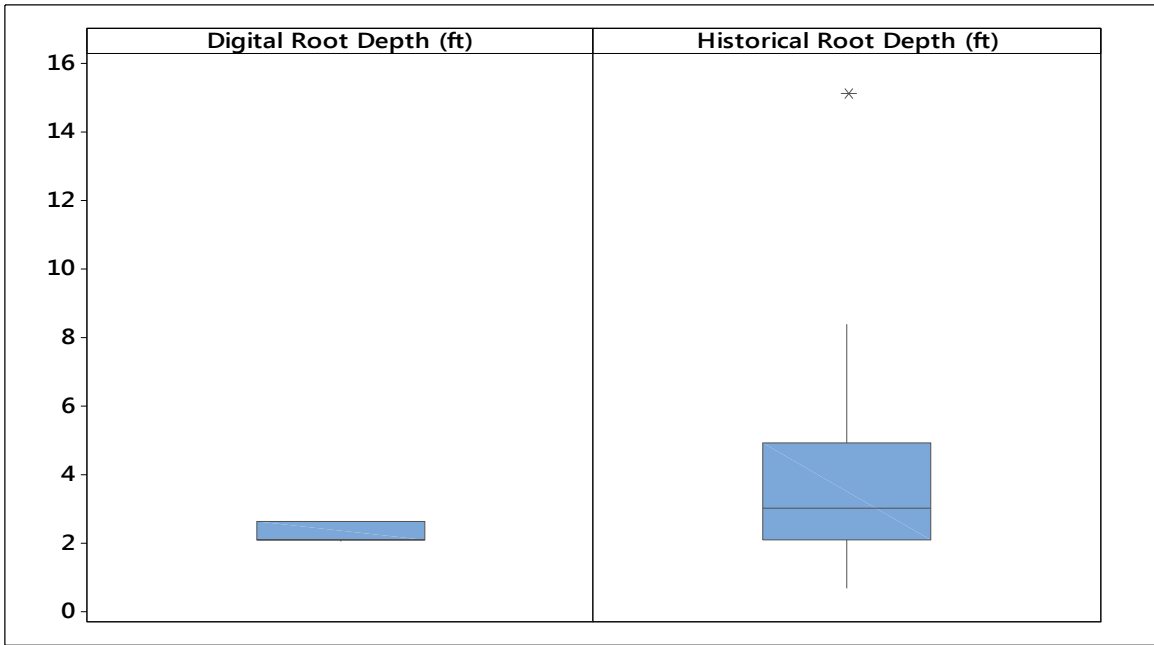


Figure 35: Boxplots of the root depth obtained digitally and the root depth obtained on-site using the development data set.

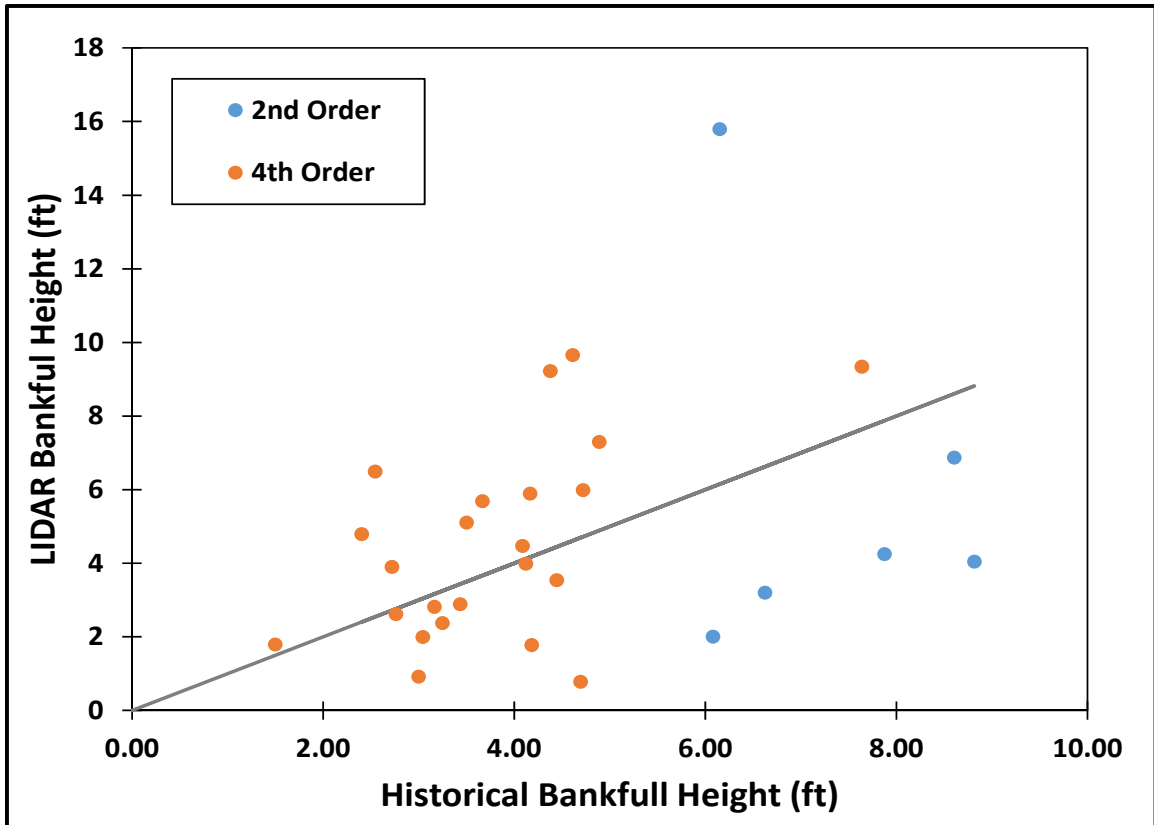


Figure 36: Comparison of bankfull height measured in LIDAR and on-site using the development data set.

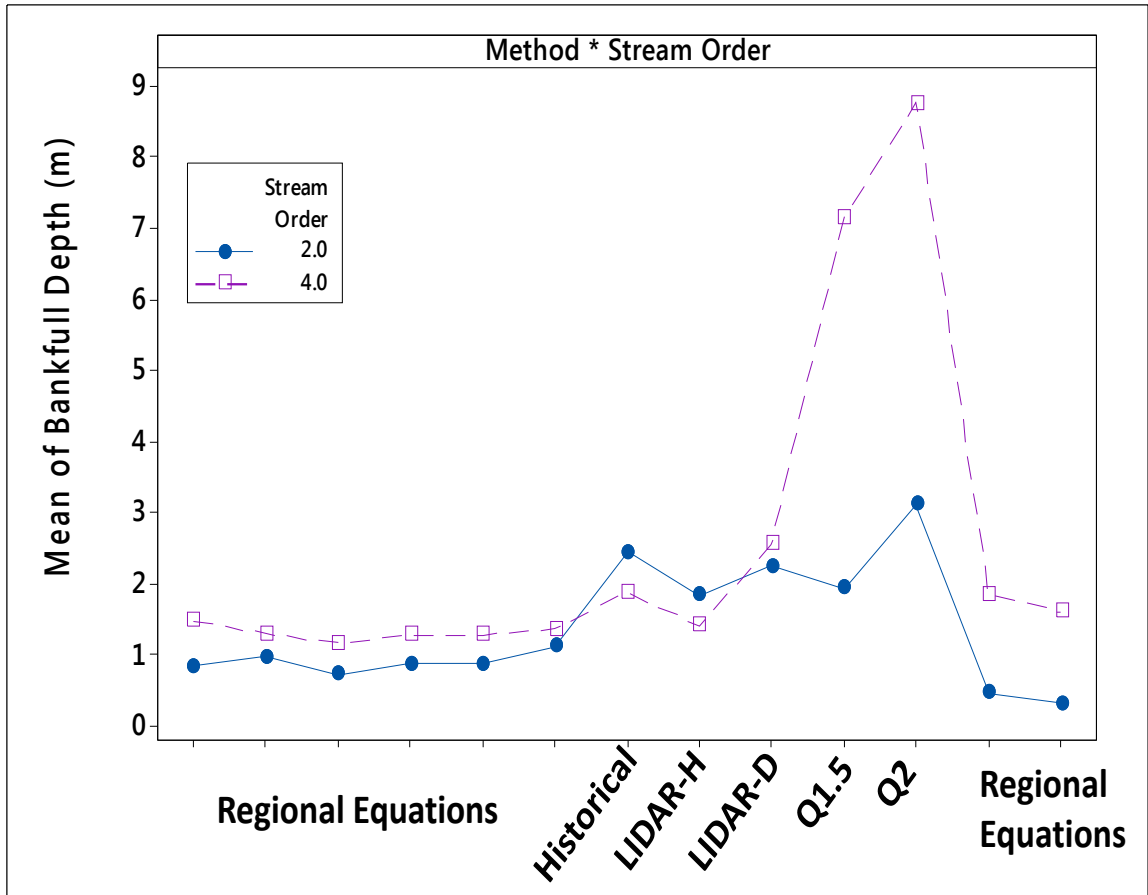


Figure 37: Interaction plot for the Two-Way Analysis of Variance (ANOVA) with Bankfull Depth as the response variable and Method and Stream Order as the treatment variables LIDAR-H refers to the bankfull height measured in LIDAR, LIDAR-D represents the bankfull height measured in LIDAR plus the baseflow depth measured using the LIDAR+StreamGage method.

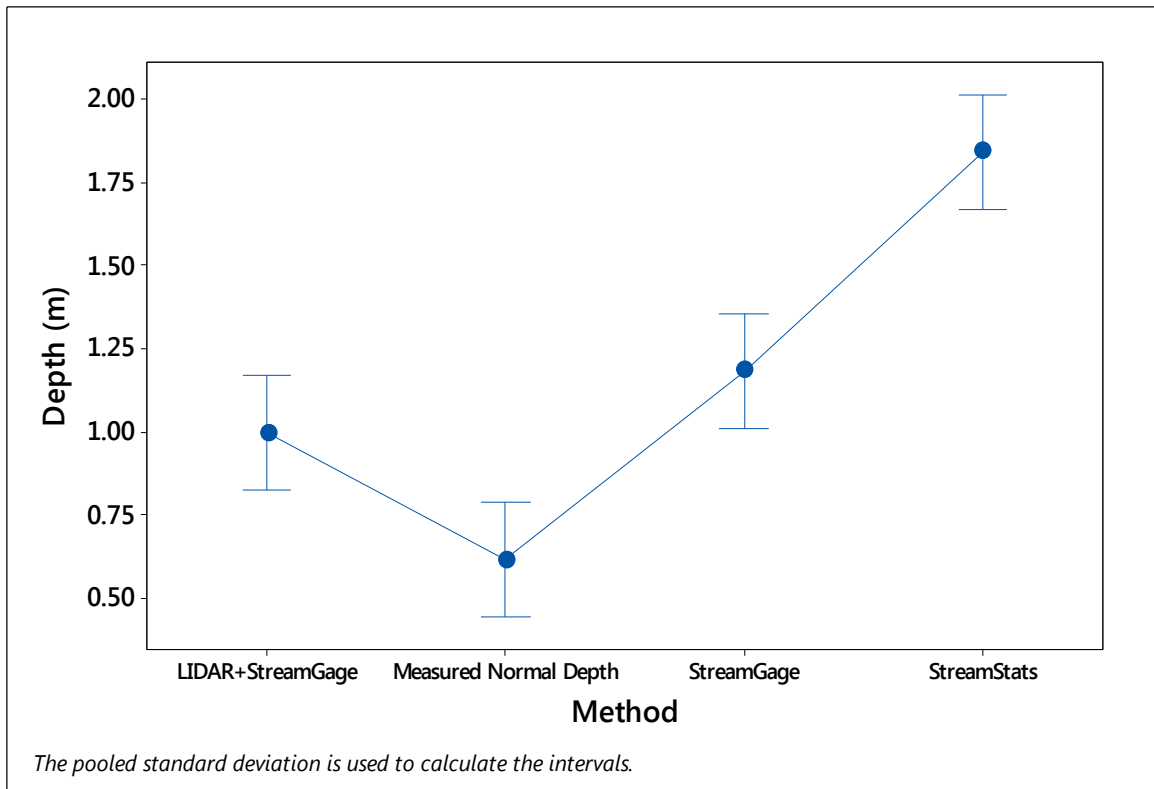


Figure 38: Interval plot comparison between baseflow depth measured on-site (historical), vs. various digital methods using the development data.



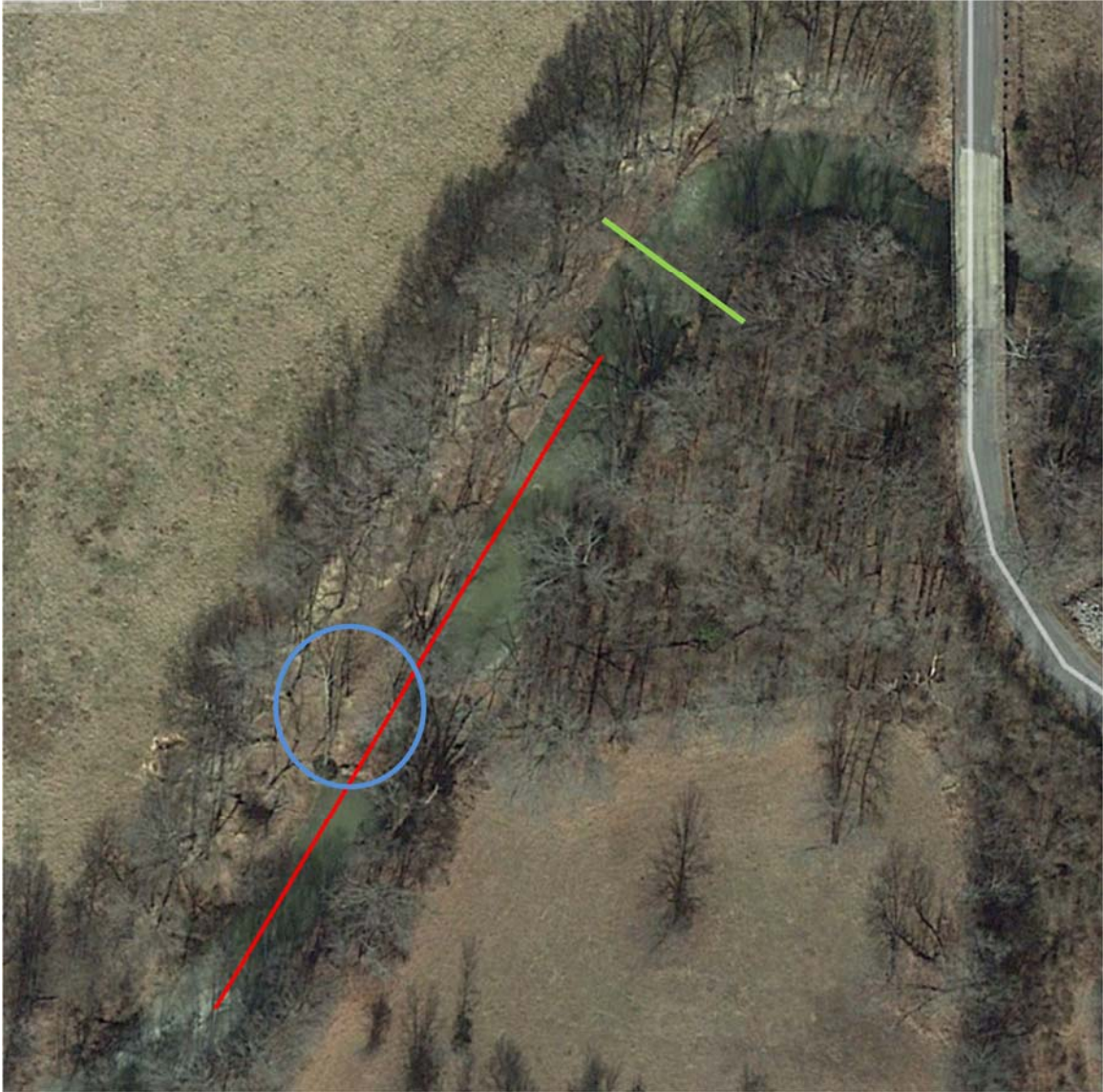


Figure 39: Validation Site\_Fourche Maline - Reach 1. Google Earth image taken 1/17/2018. The red line represents the original reach used in the digital assessment. The circle is highlighting where major slumping was apparent on-site. The green line represents where the on-site assessment was performed.



Figure 40: Google Earth images (various imagery dates) of all the validation reaches that failed the digital Channel Stability Index (CSI). Going clockwise starting in the top left corner: Fourche Maline, reach 1 & 2; Feather; Spring, reach 4; Sandy, reach 1. Note how these reaches are relatively straight.



Figure 41: Google Earth images (various imagery dates) of the validation reaches which had a successful digital Channel Stability Index (CSI). Going clockwise and starting from the top: Spring reach 2, Black Fork reach 2, and Sandy reach 5. Note the clear meander present.

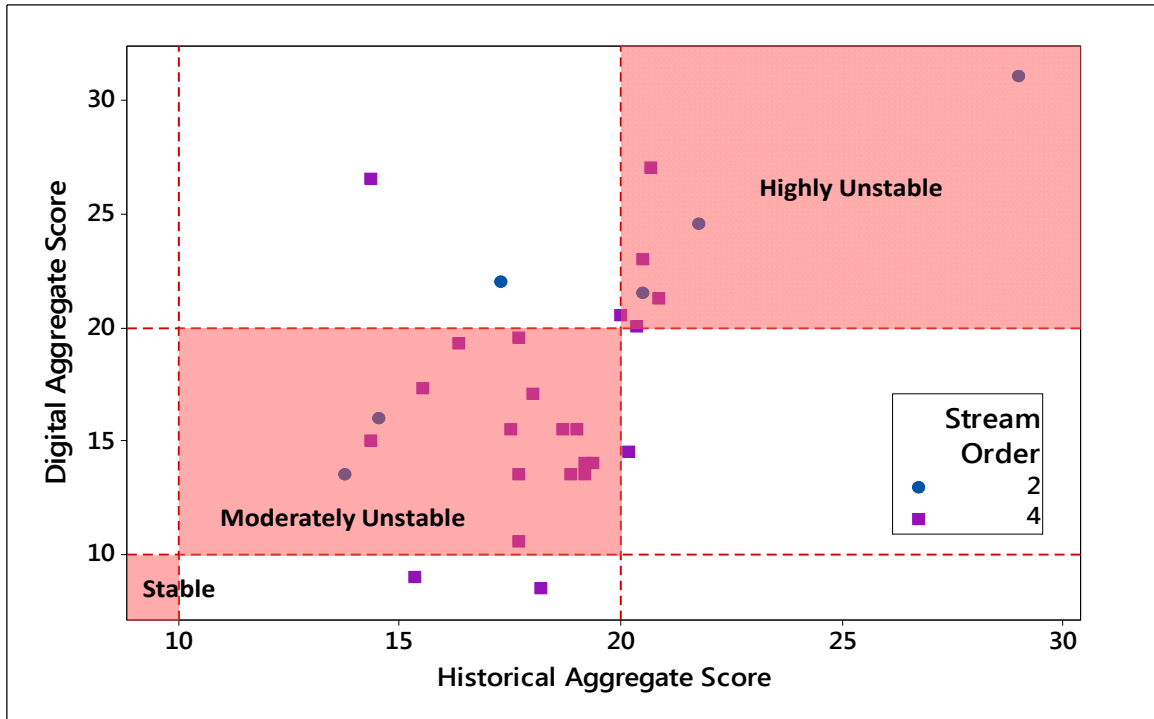


Figure 42: Development Channel Stability Index (CSI) comparing the historical vs the fully digital scores, separated by stream order. Any points that fall inside the shaded box are counted as successful.

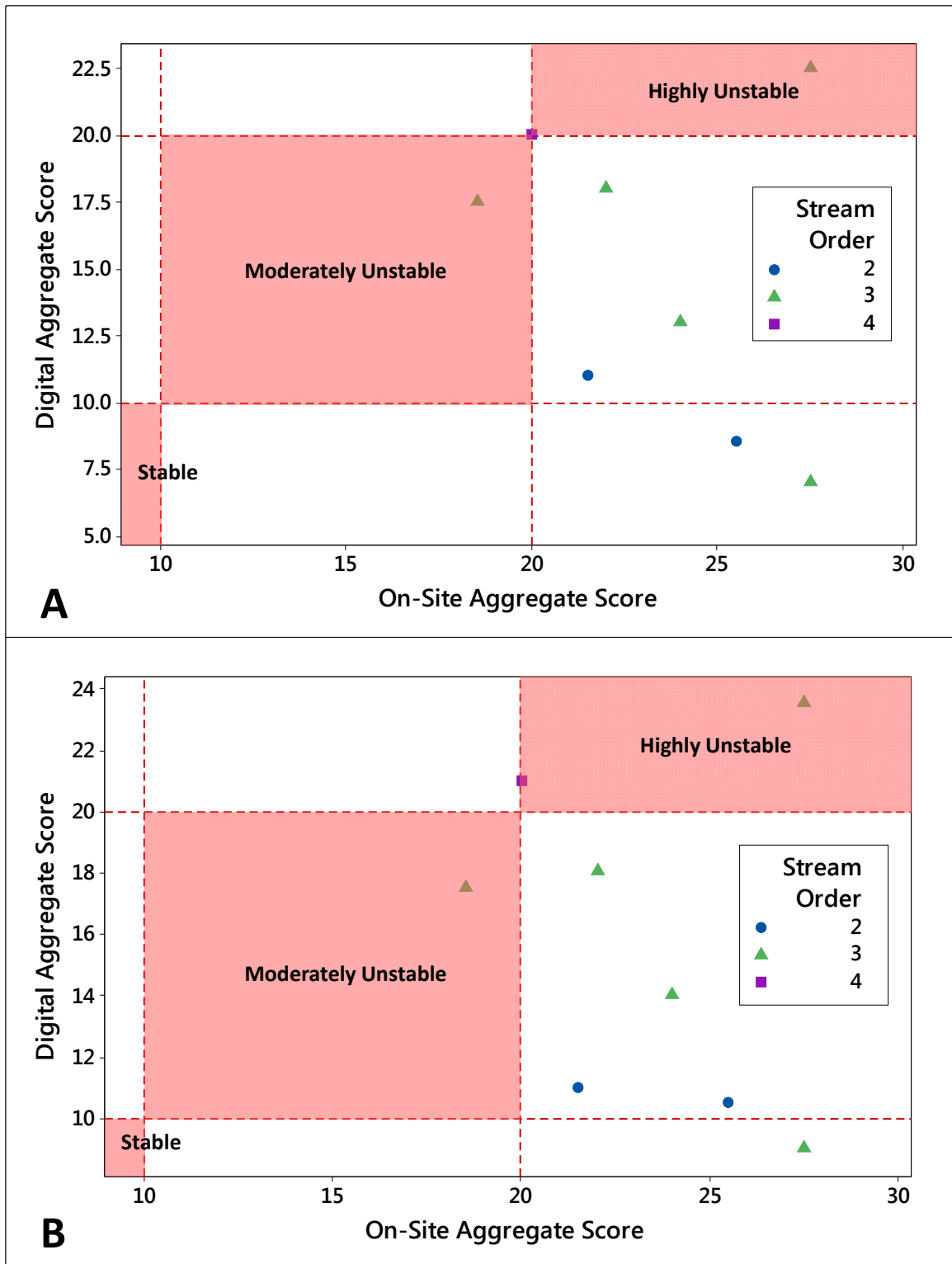


Figure 43: Validation Channel Stability Index (CSI) comparing the on-site vs the fully digital scores, separated by stream order. Any points that fall inside the shaded box are counted as successful. A. Using only the StreamStats method for baseflow depth. B. Using the LIDAR+StreamGage method where data allowed.

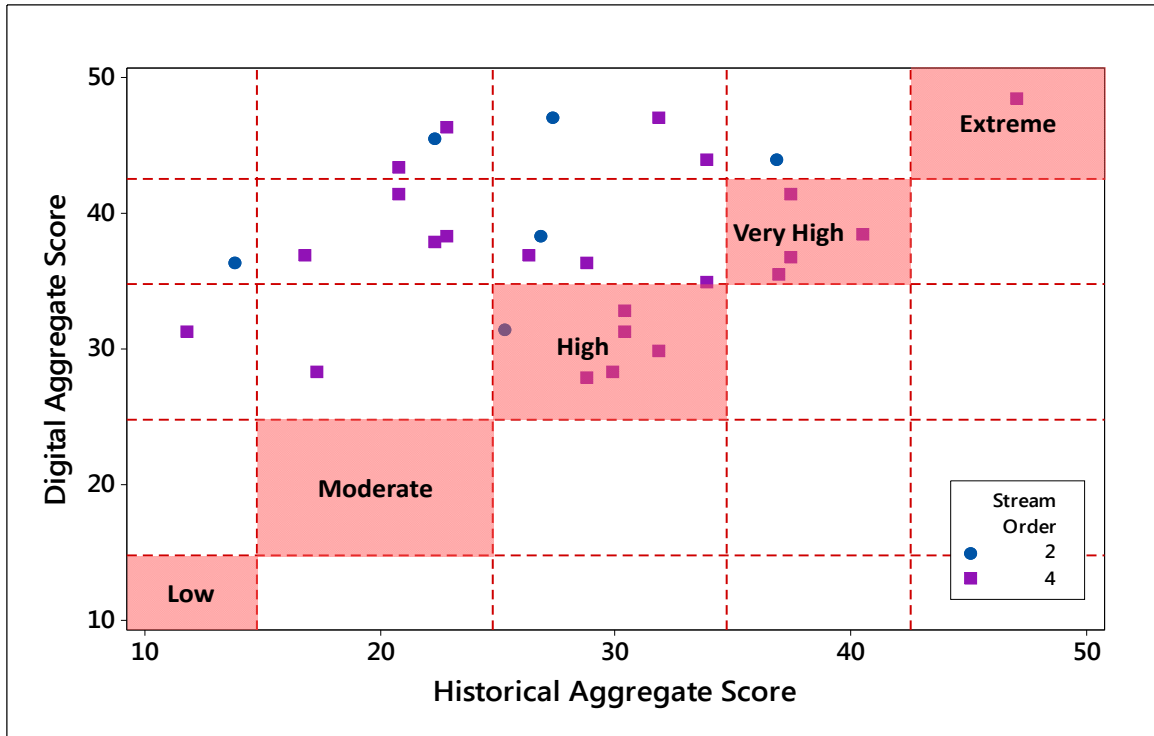


Figure 44: Validation Bank Erosion Hazard Index (BEHI) comparing the on-site vs the fully digital scores, separated by stream order. Any points that fall inside the shaded box are counted as successful.

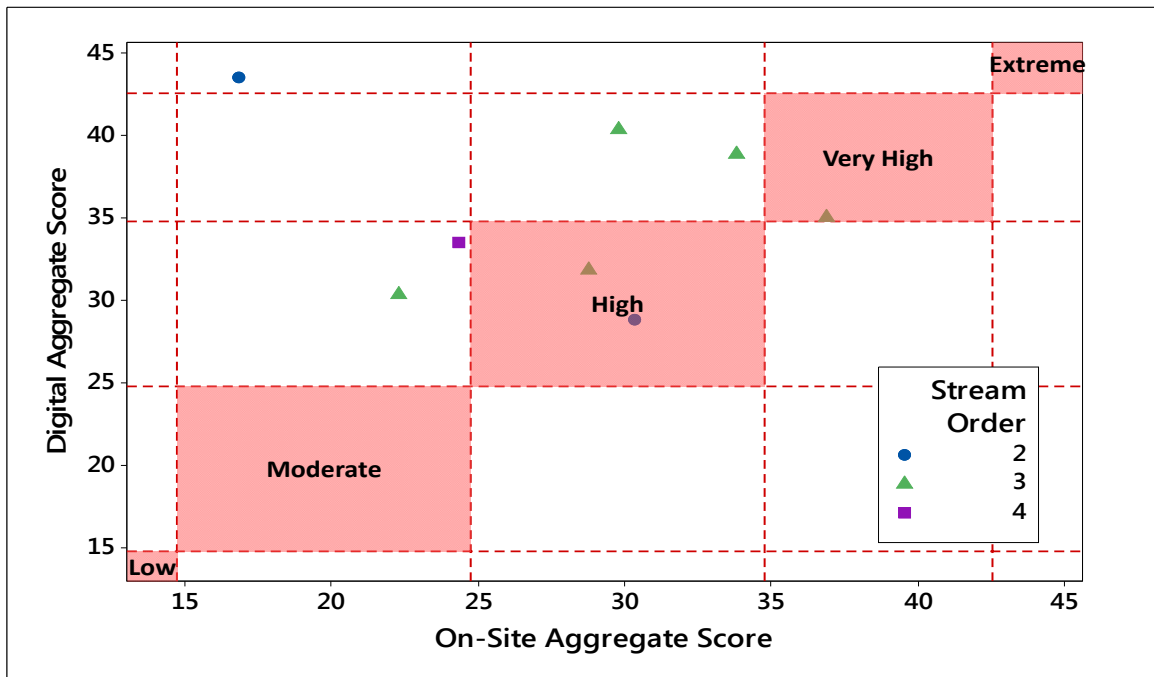


Figure 45: Validation Bank Erosion Hazard Index (BEHI) comparing the on-site vs the fully digital scores, separated by stream order. Any points that fall inside the shaded box are counted as successful.

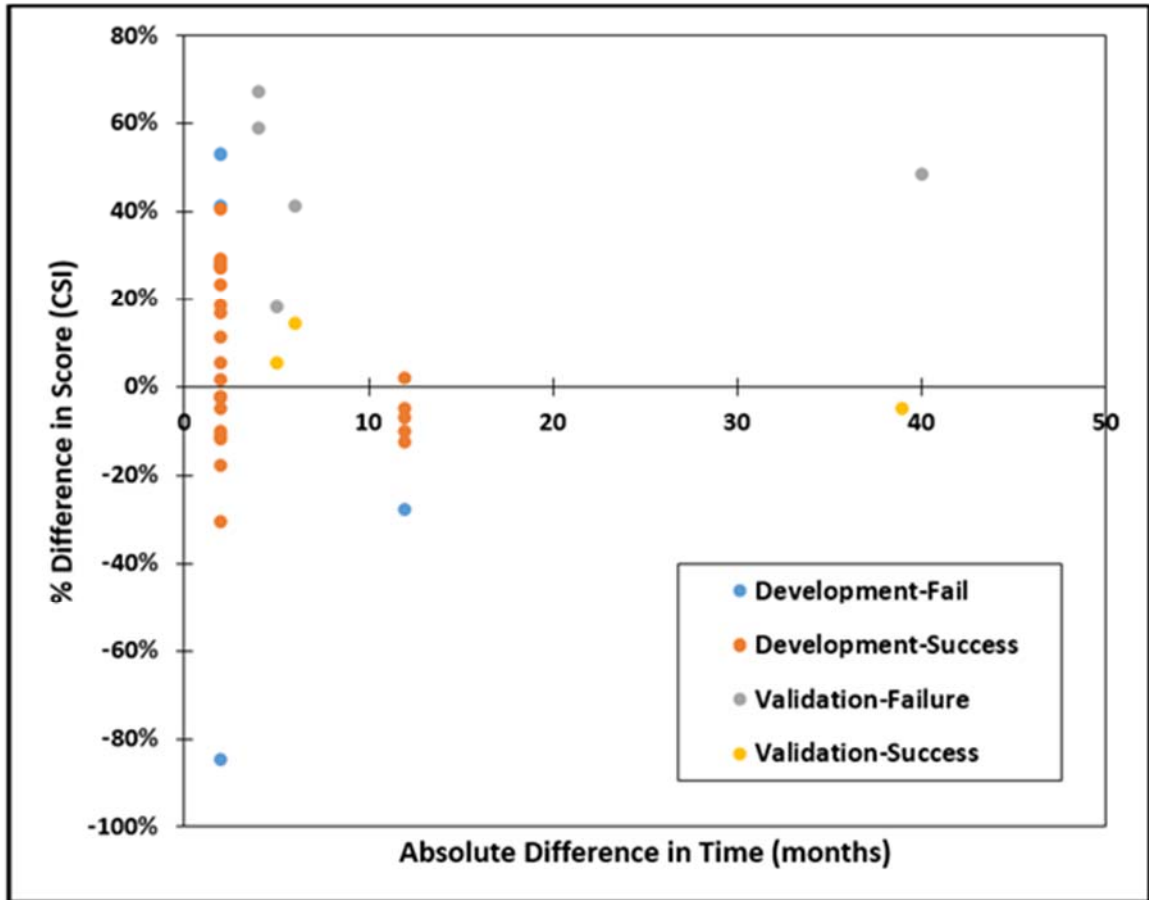


Figure 46: The absolute difference in time between the Google Earth imagery used and the on-site assessment, plotted against the resulting percent difference between the digital Channel Stability Index (CSI) and on-site score. Both development and validation stage data was used.

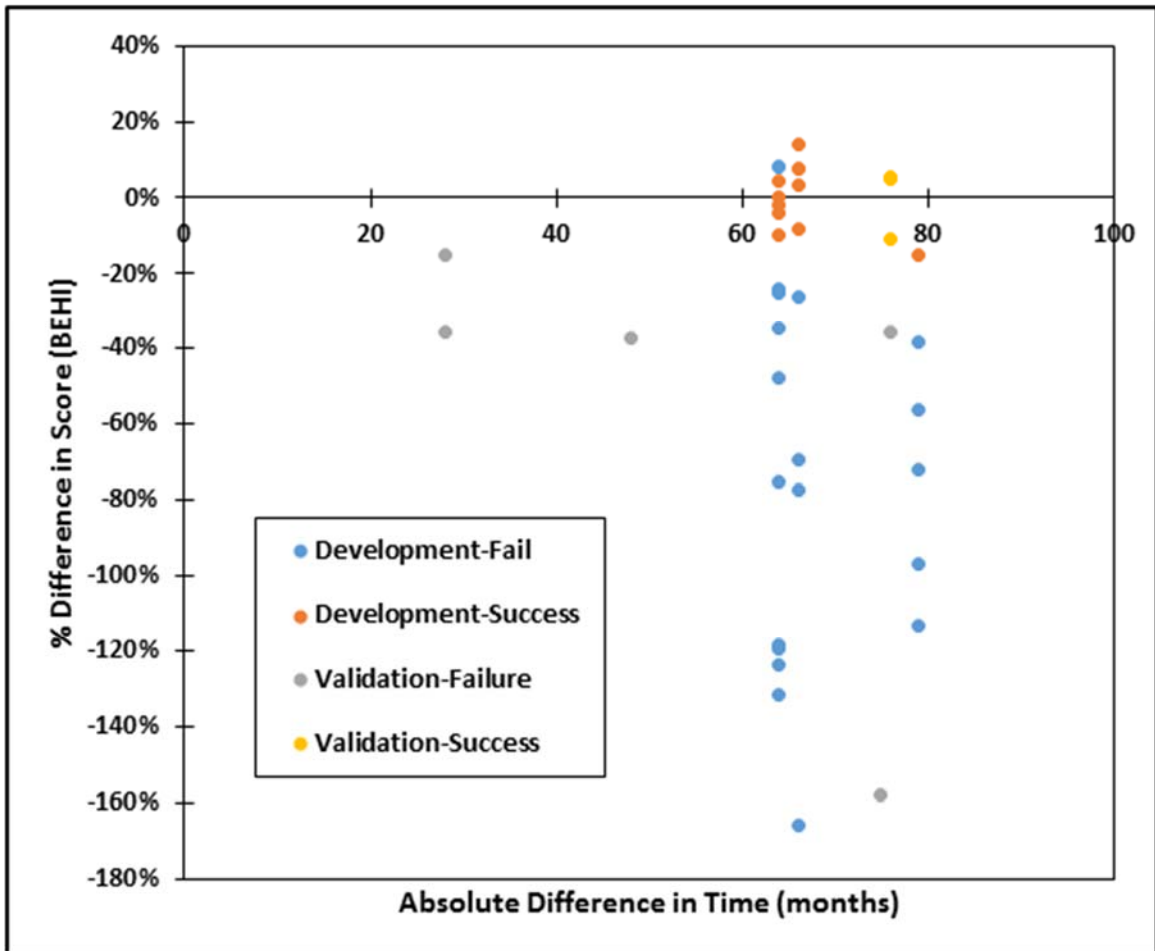


Figure 47: The absolute difference in time between the LIDAR collection date used and the on-site assessment, plotted against the resulting percentage difference between the digital Bank Erosion Hazard Index (BEHI) and on-site score. Both development and validation stage data was used.



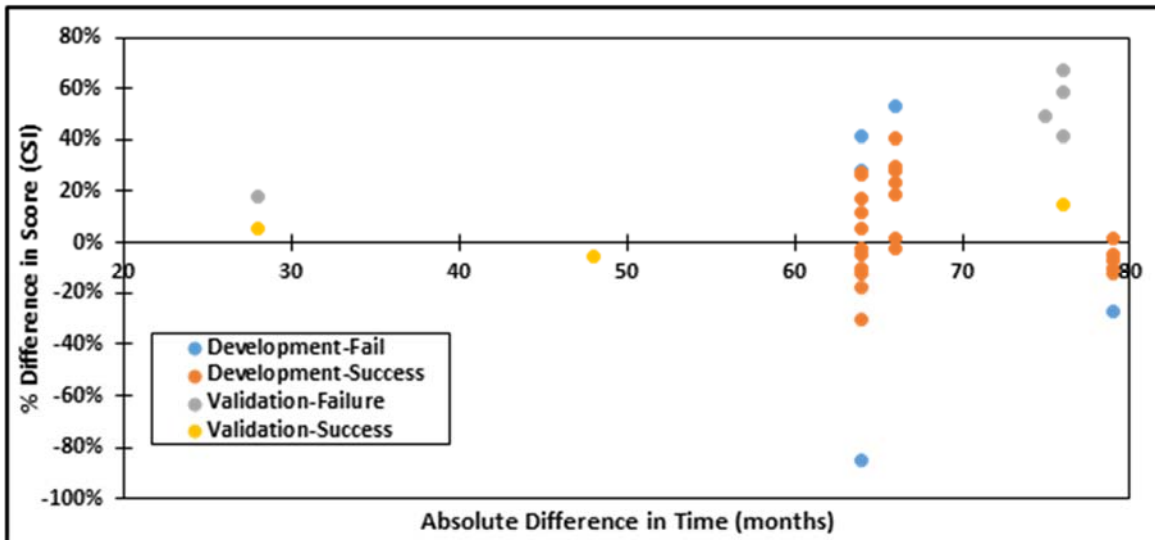


Figure 48: The absolute difference in time between the LIDAR collection date used and the on-site assessment, plotted against the resulting percent difference between the digital Channel Stability Index (CSI) and on-site score. Both development and validation stage data was used.

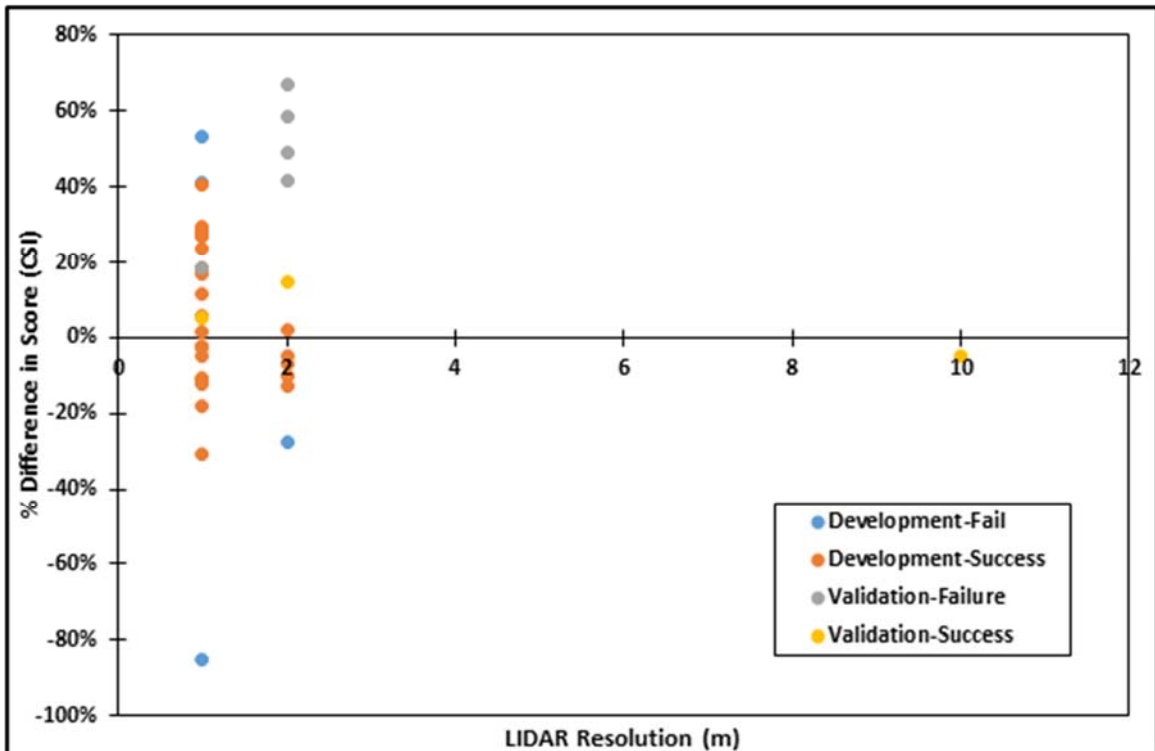


Figure 49: LIDAR resolution used vs. the resulting percent difference between the digital and on-site Channel Stability Index (CSI) on-site score. Both development and validation stage data was used.

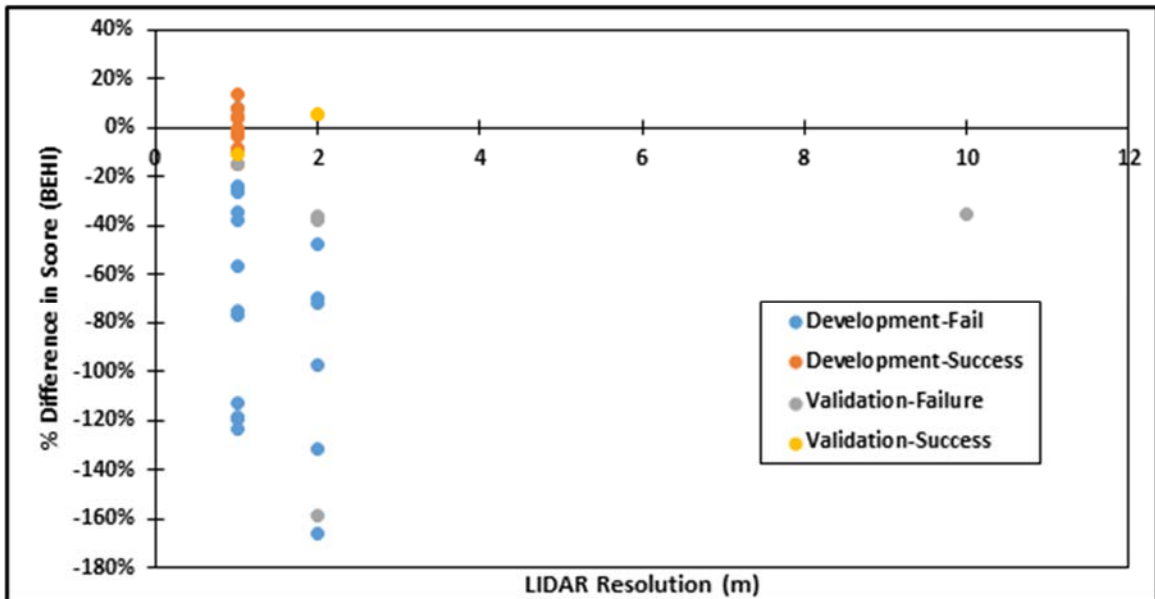


Figure 50: LIDAR resolution used vs. the resulting percent difference between the digital and on-site Bank Erosion Hazard Index score. Both development and validation stage data was used.

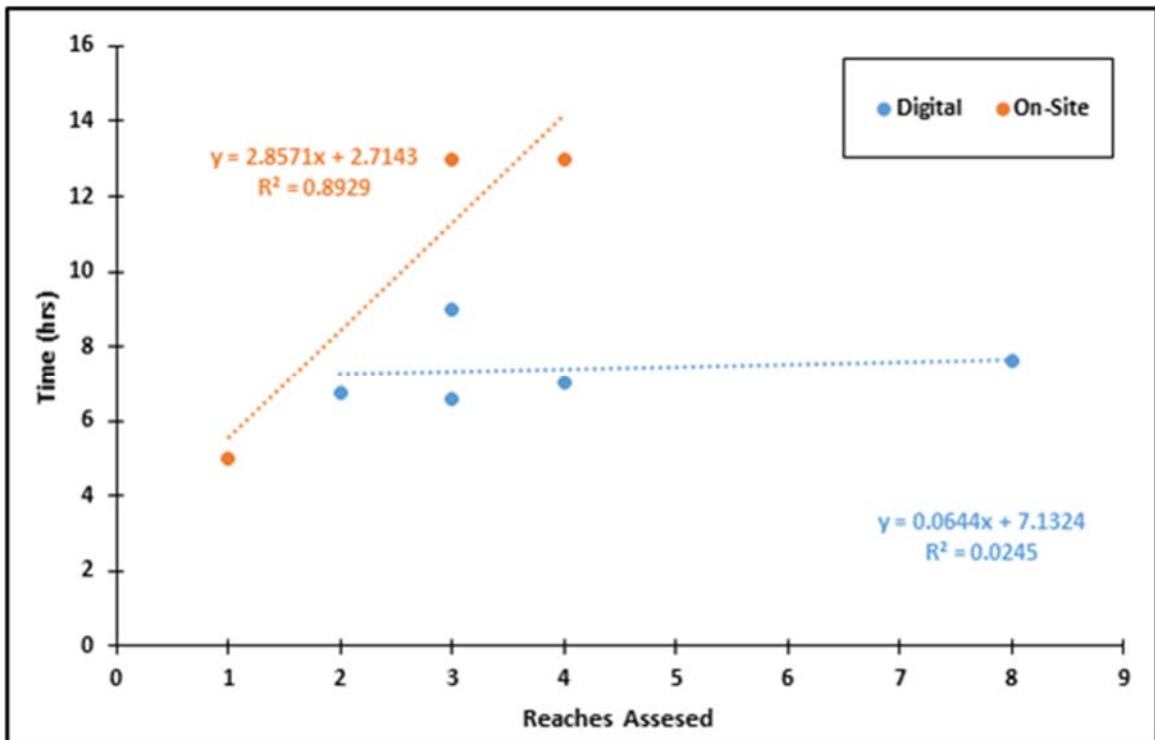


Figure 51: Comparison between the amount of time needed vs the number of validation reaches assessed for the on-site and digital methods.

Table 11: Digital RGA success rates using Google Earth compared to historical RGAs for all Channel Stability Index (CSI) metrics. The methods tested are described in the Reach Length section of the methods.

| Channel Stability Index Metric | Metric-Reach Length  | Development      |                              | Validation       |                              |
|--------------------------------|--|------------------|------------------------------|------------------|------------------------------|
|                                |  | Success Rate (%) | Over or Under Estimate Risk? | Success Rate (%) | Over or Under Estimate Risk? |
| 4                              | Degree of Constriction                                     | 97               | Over                         | 100              | N/A                          |
| 5                              | Identifying Streambank Erosion (None-Fluvial-Mass Wasting) | 97               | Under                        | 75               | Both (1 each)                |
| 6                              | Percentage of Bank Affected by Mass Wasting                | 90               | Under                        | 100              | N/A                          |
| 7                              | Percentage of Bank Supported by Woody Vegetation           | 97               | Over                         | 88               | Under                        |
| 2b & 7                         | Percent Woody Cover + Bank Protection                      | 90               | Under                        | 75               | Under                        |
| 8                              | Percentage of Bank with Accretion                          | 97               | Under                        | 100              | N/A                          |
| 9                              | Stage of Channel Evolution                                 | 90               | Both (2 out of 3 Over)       | 88               | Under                        |
| All-of-the-Above               |  | 79               | Both (4 out of 6 Under)      | 38               | 38                           |
| Average Success Rate           |  | 94               |                              | 89               |                              |

Table 12: Digital RGA success rates for the Bed/Bank Characterization methods from Bank Erosion Hazard Index (BEHI) and the Channel Stability Index (CSI), for both the development and validation data.

| Bed/Bank Characterization Metrics           | Data Source(s)  | RGA  | Development      |  | Validation       |                              |
|---|---|------|------------------|--|------------------|------------------------------|
|   |   |      | Success Rate (%) | Over or Under Estimate Risk?                           | Success Rate (%) | Over or Under Estimate Risk? |
| Primary Bank Material                       | Web Soil Survey   | BEHI | 52               | Over   | 75               | Under                        |
| Stratification                              | Web Soil Survey   |      | 62               | Both (only 1 was under)                                | 88               | Over                         |
| Root Depth                                  | Web Soil Survey + NRCS PLANTS Database  |      | 93               | Over   | 75               | Over                         |
| Root Depth Ratio (Root Depth + Bank Height) | Web Soil Survey, LIDAR  |      | 55               | Both (2 out of 13 under)                               | 50               | Over                         |
| Root Depth Ratio + Surface Protection       | Web Soil Survey, LIDAR  |      | 24               | Both (4 out of 22 under)                               | 38               | Over                         |
| Root Density                                | 3 Categories Using Assumed Root Depths and Bank Height (Grass/Bare, Grass, woody) |      | 90               | Both (Over for the 2nd Order, Under for the 4th Order) | 75               | Both (one each)              |
| Primary Bed Material                        | USGS Stream Gages   |      | CSI              | 100  | N/A              | 75                           |
| Bed Protection                              | Web Soil Survey   | 100  |                  | N/A  | 88               | Under                        |
| Percent Woody Cover + Bank/Bed Protection   | Web Soil Survey, Google Earth   | 90   |                  | Under  | 75               | Under                        |

Table 13: Development success rates for Bank Erosion Hazard Index (BEHI) using digital Bankfull methods as well as the fully digital BEHI applied to second and fourth order streams as well as the fully digital success rate.

| <b>Metric-Bankfull</b>  | <b>Data Source(s)</b>         | <b>Success Rate (%)</b> | <b>Overestimate or Underestimate Risk?</b> | <b>Digital Success Rate (%)</b> |
|---|-------------------------------|-------------------------|--|---------------------------------|
| Bankfull Depth – Bieger et al. (2015)                         | Physiographic Region (Course) | 86                      | 2nd Order - Over<br>4th Order - Under      | Both - 34<br>4th - 43           |
| Bankfull Depth – Dutnell (2000)                               | Ecoregional                   | 90                      | 2nd Order - Over<br>4th Order - Under      | Both - 38<br>4th - 43           |
| Bankfull Depth – (Bankfull Width) Williams (1986)             | Google Earth                  | 72                      | 2nd Order - Over<br>4th Order - Under      | Both - 31<br>4th - 39           |
| Bankfull Depth – (Bankfull Width + Sinuosity) Williams (1986) | Google Earth                  | 83                      | 2nd Order - Over<br>4th Order - Under      | Both - 28<br>4th - 35           |
| Bankfull Depth - Q <sub>2</sub>                               | USGS Stream Stats             | 45                      | Under                                      | Both - 31<br>4th - 39           |
| Bankfull Depth - Q <sub>1.5</sub>                             | USGS Stream Gages + PeakFQ    | 52                      | Under                                      | Both - 31<br>4th - 35           |
| Bankfull Depth - LIDAR  | LIDAR + USGS Stream Gages     | 59                      | 2nd Order - Both<br>4th Order - Under      | Both - 28<br>4th - 30           |
| Bankfull Height - LIDAR                                       | LIDAR                         | 83                      | 2nd Order - Both<br>4th Order - Both       | Both - 34<br>4th - 39           |

Table 14: Development stage success rates for Bank Erosion Hazard Index (BEHI) using digital Bankfull methods from Williams (1986) applied to fourth order streams as well as the fully digital BEHI.

| <b>Metric-Bankfull</b> | <b>Measured Planform Feature</b> | <b>Data Source</b> | <b>Success Rate (%)</b> | <b>Overestimate or Underestimate Risk?</b> | <b>Digital Success Rate (%)</b> |
|------------------------|----------------------------------|--------------------|-------------------------|--|---------------------------------|
| Bankfull Depth         | Belt Width                       | Google Earth       | 78                      | Both (4 out of 5 Under)                    | 39                              |
| Bankfull Depth         | Bed Length                       | Google Earth       | 43                      | Under                                      | 39                              |
| Bankfull Depth         | Radius                           | Google Earth       | 65                      | Under                                      | 35                              |
| Bankfull Depth         | Wavelength                       | Google Earth       | 52                      | Under                                      | 35                              |

Table 15: Validation stage success rates for Bank Erosion Hazard Index (BEHI) using digital Bankfull methods that applied to all validation streams.

| <b>Metric-Bankfull</b>                                      | <b>Data Source(s)</b>         | <b>Success Rate (%)</b> | <b>Overestimate or Underestimate Risk?</b> | <b>Digital Success Rate (%)</b> |
|---|-------------------------------|-------------------------|--|---------------------------------|
| Bankfull Depth - Bieger et al. 2015                         | Physiographic Region (Course) | 88                      | Over                                       | 38                              |
| Bankfull Depth - Dutnell 2000                               | Ecoregional                   | 88                      | Over                                       | 38                              |
| Bankfull Depth - Williams 1986 (Bankfull Width)             | Google Earth                  | 100                     | N/A  | 38                              |
| Bankfull Depth - Williams 1986 (Bankfull Width + Sinuosity) | Google Earth                  | 88                      | Over                                       | 38                              |
| Bankfull Depth - Williams 1986 (Belt Width)                 | Google Earth                  | 88                      | Over                                       | 38                              |
| Bankfull Depth - Williams 1986 (Bed Length)                 | Google Earth                  | 100                     | N/A  | 50                              |
| Bankfull Depth - Williams 1986 (Radius)                     | Google Earth                  | 100                     | N/A  | 63                              |
| Bankfull Depth - Williams 1986 (Wavelength)                 | Google Earth                  | 100                     | N/A  | 50                              |
| Bankfull Depth - Q <sub>2</sub>                             | USGS Stream Stats             | 63                      | Under                                      | 38                              |
| Bankfull Depth - Q <sub>1.5</sub> *                         | USGS Stream Gages + PeakFQ    | 88                      | Under                                      | 63                              |
| Bankfull Depth - LIDAR                                      | LIDAR + USGS Stream Gages     | 100                     | N/A  | 50                              |
| Bankfull Height - LIDAR                                     | LIDAR                         | 75                      | Over                                       | 38                              |

\*There was not enough data from the Spring gages to perform the PeakFQ method, so the Q<sub>2</sub> values were used instead for the Spring RGAs.

Table 16: All statistics for how well each bankfull method was able to match the historical measurement of bankfull depth using the development data set. (S2, Coefficient of Success; RMSE, Root Mean Square Error).

| <b>Method</b>                    | <b>Stream Order</b> | <b>Nash Sutcliff Coefficient</b> | <b>S<sup>2</sup></b> | <b>RMSE (m)</b> | <b>R<sup>2</sup></b> | <b>Average Relative Error (m)</b> |
|----------------------------------|---------------------|----------------------------------|----------------------|-----------------|----------------------|-----------------------------------|
| <i>BiegerPhysiographicCourse</i> | 2 & 4               | -1.78                            | 0.35                 | 0.95            | 0.09                 | 0.26                              |
| <i>BiegerPhysiographicFine</i>   |                     | -1.92                            | 0.42                 | 0.97            | 0.00                 | 0.33                              |
| <i>BiegerUSA</i>                 |                     | -2.89                            | 0.37                 | 1.12            | 0.10                 | 0.41                              |
| <i>DutnellEcoregion</i>          |                     | -2.29                            | 0.38                 | 1.03            | 0.14                 | 0.35                              |
| <i>DutnellPrecip</i>             |                     | -2.25                            | 0.38                 | 1.03            | 0.14                 | 0.34                              |
| <i>DutnellState</i>              |                     | -1.57                            | 0.41                 | 0.91            | 0.10                 | 0.28                              |
| <i>LIDARHeight</i>               |                     | -2.30                            | 0.52                 | 1.03            | 0.12                 | 0.24                              |
| <i>LIDARDepth</i>                |                     | -3.62                            | 0.47                 | 1.22            | 0.14                 | -0.29                             |
| <i>Q<sub>1.5</sub> Both</i>      |                     | -74.9                            | 0.12                 | 4.96            | 0.01                 | -2.36                             |
| <i>Q<sub>2</sub> Both</i>        |                     | -124.                            | 0.09                 | 6.37            | 0.09                 | -3.32                             |
| <i>WilliamsBankfullWidth</i>     |                     | -2.68                            | 0.12                 | 1.09            | 0.21                 | 0.11                              |
| <i>WilliamsSinWidth</i>          |                     | -2.72                            | 0.25                 | 1.10            | 0.05                 | 0.25                              |
| <i>BiegerPhysiographicCourse</i> |                     | 4                                | -0.38                | 0.45            | 0.66                 | 0.22                              |
| <i>BiegerPhysiographicFine</i>   | -0.91               |                                  | 0.47                 | 0.78            | 0.21                 | 0.26                              |
| <i>BiegerUSA</i>                 | -1.51               |                                  | 0.43                 | 0.89            | 0.22                 | 0.33                              |
| <i>DutnellEcoregion</i>          | -1.12               |                                  | 0.43                 | 0.82            | 0.23                 | 0.27                              |
| <i>DutnellPrecip</i>             | -1.09               |                                  | 0.43                 | 0.81            | 0.23                 | 0.27                              |
| <i>DutnellState</i>              | -0.79               |                                  | 0.43                 | 0.75            | 0.23                 | 0.22                              |
| <i>LIDAR Height</i>              | -1.17               |                                  | 0.62                 | 0.83            | 0.23                 | 0.24                              |
| <i>LIDARDepth</i>                | -3.04               |                                  | 0.57                 | 1.13            | 0.36                 | -0.38                             |
| <i>Q<sub>1.5</sub> Both</i>      | -93.43              |                                  | 0.15                 | 5.46            | 0.15                 | -3.02                             |
| <i>Q<sub>2</sub> Uniform</i>     | -149.82             |                                  | 0.11                 | 6.89            | 0.18                 | -3.98                             |
| <i>WilliamsBankfullWidth</i>     | -0.43               |                                  | 0.20                 | 0.67            | 0.06                 | -0.07                             |
| <i>WilliamsBedLength</i>         | -3.29               |                                  | 0.52                 | 1.16            | 0.24                 | -0.53                             |
| <i>WilliamsBeltWidth</i>         | -0.42               |                                  | 0.75                 | 0.67            | 0.41                 | -0.04                             |
| <i>WilliamsRadius</i>            | -0.48               |                                  | 0.36                 | 0.68            | 0.00                 | -0.25                             |
| <i>WilliamsSinWidth</i>          | -0.03               |                                  | 0.47                 | 0.57            | 0.21                 | 0.09                              |
| <i>WilliamsWavelength</i>        | -2.47               |                                  | 0.43                 | 1.05            | 0.02                 | -0.46                             |

Table 16 continued: All statistics for how well each bankfull method was able to match the historical measurement of bankfull depth using the development data set. (S2, Coefficient of Success; RMSE, Root Mean Square Error).

| <i>Method</i>                     | <i>Stream Order</i> | <i>Nash Sutcliff Coefficient</i> | <i>S<sup>2</sup></i> | <i>RMSE (m)</i> | <i>R<sup>2</sup></i> | <i>Average Relative Error (m)</i> |
|-----------------------------------|---------------------|----------------------------------|----------------------|-----------------|----------------------|-----------------------------------|
| <i>BiegerPhysiographicCourse</i>  | 2                   | -25.5                            | 0.84                 | 1.64            | 0.01                 | 0.65                              |
| <i>BiegerPhysiographicFine</i>    |                     | -21.5                            | 0.85                 | 1.51            | 0.01                 | 0.60                              |
| <i>BiegerUSA</i>                  |                     | -29.3                            | 0.82                 | 1.75            | 0.01                 | 0.70                              |
| <i>DutnellEcoregion</i>           |                     | -24.7                            | 0.84                 | 1.61            | 0.01                 | 0.64                              |
| <i>DutnellPrecip</i>              |                     | -24.4                            | 0.84                 | 1.60            | 0.01                 | 0.64                              |
| <i>DutnellState</i>               |                     | -17.4                            | 0.87                 | 1.37            | 0.01                 | 0.54                              |
| <i>LIDARHeight</i>                |                     | -24.2                            | 0.83                 | 1.60            | 0.01                 | 0.23                              |
| <i>LIDARDepth</i>                 |                     | -22.3                            | 0.83                 | 1.54            | 0.02                 | 0.06                              |
| <i>Q<sub>1.5</sub> Triangular</i> |                     | -3.19                            | 0.95                 | 0.65            | 0.01                 | 0.20                              |
| <i>Q<sub>2</sub> Triangular</i>   |                     | -4.19                            | 0.95                 | 0.73            | 0.29                 | -0.28                             |
| <i>WilliamsBankfullWidth</i>      |                     | -39.0                            | 0.80                 | 2.01            | 0.06                 | 0.81                              |
| <i>WilliamsSinWidth</i>           |                     | -44.4                            | 0.78                 | 2.14            | 0.14                 | 0.87                              |



Table 17: Success rate for all channel geometry measurements. Used the average measurement from both banks (bank height, face lengths, etc.), not critical banks. Also used over-all success rates. Only put methods from Williams that applied to both second and fourth order streams. Channel Stability Index (CSI), Bank Erosion Hazard Index (BEHI).

| Metric-Channel Geometry                          | Data Source(s)            | RGA  | Development      |                              | Validation       |                              |
|--|---------------------------|------|------------------|------------------------------|------------------|------------------------------|
|  |                           |      | Success Rate (%) | Over or Under Estimate Risk? | Success Rate (%) | Over or Under Estimate Risk? |
| Constriction                                     | Google Earth              | CSI  | 97               | Over                         | 100              | N/A                          |
| Bank Height                                      | LIDAR                     | CSI  | 93               | Under                        | 100              | CSI- N/A                     |
| Face Length                                      | LIDAR                     | BEHI | 55               | Both (6 over, 7 under)       | 88               | over                         |
| Face Length                                      | LIDAR                     | BEHI | 86               | Under                        | 100              | N/A                          |
| Baseflow depth                                   | LIDAR + USGS Stream Gages | CSI  | 93               | Under                        | 100*             | Under                        |
| Baseflow depth                                   | USGS Stream Gages         | CSI  | 86               | Under                        | 88*              | Under                        |
| Baseflow depth                                   | USGS StreamStats          | CSI  | 79               | Under                        | 88               | Under                        |
| Degree of Incision (Bank height, Baseflow depth) | LIDAR + USGS Stream Gages | CSI  | 86               | Under                        | 88*              | Under                        |

\*Complete gage data not available for all locations; StreamStats used to fill gaps.

Table 18: Average point difference between the individual metrics obtained on-site vs. digital. The aggregate category is referring to the average difference in overall score.

| RGA  | Metric                           | Average Difference (On Site - Digital) |            |
|------|----------------------------------|--|------------|
|      |                                  | Development                            | Validation |
| BEHI | Bank/Bankfull Height Ratio       | -0.4                                   | -1.6       |
|      | Root Depth Ratio                 | -1.8                                   | -2.1       |
|      | Root Density                     | -0.8                                   | 1.4        |
|      | Surface Protection               | -2.2                                   | -2.3       |
|      | Bank Angle                       | 1.3                                    | 1.1        |
|      | Adj1-Bank Material               | -4.1                                   | -8.8       |
|      | Adj2-Stratification              | -2.2                                   | 0.6        |
|      | Aggregate                        | -10.2                                  | -11.7      |
| CSI  | Primary Bed Material             | 0.0                                    | 1.1        |
|      | Bed/Bank Protection              | 1.0                                    | 1.4        |
|      | Degree of Incision               | 0.1                                    | 0.8        |
|      | Degree of Constriction           | -0.2                                   | 0.3        |
|      | Streambank Erosion               | 0.3                                    | 1.0        |
|      | Streambank Instability           | -0.1                                   | 1.5        |
|      | Established Riparian Woody Cover | 0.0                                    | 1.1        |
|      | Bank Accretion                   | -0.1                                   | -0.3       |
|      | Stage of Channel Evolution       | -0.2                                   | 1.9        |
|      | Aggregate                        | 0.8                                    | 8.8        |

Table 19: All metric/metric combinations that failed in the development stage. LIDAR was used to obtain the bankfull depth, and the LIDAR+StreamGage method was used to obtain the baseflow depth.

| Site/Reach# | Failed Metrics |  |     |   |
|-------------|----------------|--|-----|---|
|             | #              | Bank Erosion Hazard Index  | #   | Channel Stability Index   |
| A3          | 8              | Bank Height, Primary Bank Material, Stratification, Root Depth Ratio, Root Depth Ratio + Surface Protection, Bank Angle, Bank/Bankfull Height Ratio, <b>Fully Digital</b>                  | 2   | Combo-All GE Methods, <b>Fully Digital</b>  |
| A4          | 2              | Primary Bank Material, <b>Fully Digital</b>  | N/A | N/A   |
| A5          | 1              | <b>Fully Digital</b>   | N/A | N/A   |
| A6          | 9              | Bank Height, Primary Bank Material, Stratification, Root Depth Ratio, Root Depth Ratio + Surface Protection, Bankfull Height, Bank Angle, Bank/Bankfull Height Ratio, <b>Fully Digital</b> | N/A | N/A   |
| B1          | 3              | Primary Bank Material, Stratification, <b>Fully Digital</b>  | N/A | N/A   |
| B2          | 2              | Root Depth Ratio + Surface Protection, <b>Fully Digital</b>  | N/A | N/A   |
| B3          | 3              | Face length, Bank Angle, <b>Fully Digital</b>  | N/A | N/A   |
| C1          | 8              | Bank Height, Primary Bank Material, Stratification, Root Depth Ratio, Root Depth Ratio + Surface Protection, Bank Angle, Bank/Bankfull Height Ratio, <b>Fully Digital</b>                  | N/A | N/A   |
| C2          | 8              | Bank Height, Primary Bank Material, Stratification, Root Depth Ratio, Root Depth Ratio + Surface Protection, Bank Angle, Bank/Bankfull Height Ratio, <b>Fully Digital</b>                  | N/A | N/A   |
| C4          | 8              | Bank Height, Primary Bank Material, Stratification, Root Depth Ratio, Root Depth Ratio + Surface Protection, Bank/Bankfull Height Ratio, <b>Fully Digital</b>                              | 9   | Baseflow Depth, Identifying Erosion, Percent Mass Wasting, Identifying Erosion+Percent Mass Wasting, Stage of Channel Evolution, Percent Woody Cover+Bank Protection, Percent Woody Cover+Bed/Bank Protection, Combo-All GE Methods, <b>Fully Digital</b> |
| C5          | 4              | Face length, Root Depth Ratio + Surface Protection, Root Density, <b>Fully Digital</b>   | N/A | N/A   |
| C6          | N/A            | N/A  | 2   | Combo-All GE Methods, <b>Fully Digital</b>  |

Table 19 continued: All metric/metric combinations that failed in the development stage. LIDAR was used to obtain the bankfull depth, and the LIDAR+StreamGage method was used to obtain the baseflow depth.

| Site/Reach#                 | Failed Metrics |   |     |  |
|-----------------------------|----------------|---|-----|--|
|                             | #              | Bank Erosion Hazard Index   | #   | Channel Stability Index  |
| D2                          | 1              | <b>Fully Digital</b>  | N/A | N/A  |
| D4                          | 3              | Root Depth Ratio, Root Depth Ratio + Surface Protection, <b>Fully Digital</b>   | N/A | N/A  |
| E2                          | 7              | Bank Height, Primary Bank Material, Stratification, Root Depth Ratio, Root Depth Ratio + Surface Protection, Bank/Bankfull Height Ratio, <b>Fully Digital</b>               | 3   | Identifying Erosion+Percent Mass Wasting, Combo-All GE Methods, <b>Fully Digital</b> |
| FM1                         | 8              | Primary Bank Material, Root Depth, Root Depth Ratio, Root Depth Ratio + Surface Protection, Root Density, Bankfull Height, Bank/Bankfull Height Ratio, <b>Fully Digital</b> | N/A | N/A  |
| FM3                         | 2              | Root Depth Ratio + Surface Protection, <b>Fully Digital</b>   | 2   | Combo-All GE Methods, <b>Fully Digital</b>   |
| FM4                         | 4              | Root Depth Ratio, Root Depth Ratio + Surface Protection, Bankfull Height, <b>Fully Digital</b>  | N/A | N/A  |
| WC2                         | 2              | Root Depth Ratio + Surface Protection, <b>Fully Digital</b>   | N/A | N/A  |
| WC3                         | 8              | Bank Height, Root Depth, Root Depth Ratio, Root Depth Ratio + Surface Protection, Root Density, Bankfull Height, Bank/Bankfull Height Ratio, <b>Fully Digital</b>           | N/A | N/A  |
| # of Fully Digital Failures |                | 19  |     | 5  |

Table 20: All metric/metric combinations that failed in the validation stage. The LIDAR method was used to obtain the bankfull depth, and the LIDAR+StreamGage method, where possible, was used to obtain the baseflow depth. If the LIDAR+StreamGage method was not possible, the StreamStats method was used.

| Site/Reach#                 | Failed Metrics |   |     |  |
|-----------------------------|----------------|---|-----|--|
|                             | #              | Bank Erosion Hazard Index   | #   | Channel Stability Index  |
| F1                          | 3              | Primary Bank Material, Root Depth Ratio + Surface Protection, <b>Fully Digital</b>  | 7   | Identifying Erosion, Percent Woody Cover, Woody Cover+Bank Protection, Percent Woody Cover+Bed/Bank Protection, Stage of Channel Evolution, Combo-All GE Methods, <b>Fully Digital</b> |
| Sp2                         | 6              | Primary Bank Material, Root Depth, Root Depth Ratio, Root Depth Ratio + Surface Protection, Bank height, <b>Fully Digital</b> | N/A | N/A  |
| Sp4                         | 3              | Root Depth Ratio, Root Depth Ratio + Surface Protection, <b>Fully Digital</b>   | 3   | Percent Woody Cover+Bank Protection, Combo-All GE Methods, <b>Fully Digital</b>  |
| Sy1                         | N/A            | N/A   | 2   | Combo-All GE Methods, <b>Fully Digital</b>   |
| B2                          | 4              | Root Depth Ratio, Root Depth Ratio + Surface Protection, Root Density, <b>Fully Digital</b>                                   | N/A | N/A  |
| FRM1                        | N/A            | N/A   | 3   | Percent Woody Cover+Bed/Bank Protection, Combo-All GE Methods, <b>Fully Digital</b>  |
| FRM2                        | 3              | Root Depth Ratio, Root Depth Ratio + Surface Protection, <b>Fully Digital</b>   | 2   | Combo-All GE Methods, <b>Fully Digital</b>   |
| # of Fully Digital Failures | 5              |   | 5   |  |

Table 21: Percentage of Channel Stability Index (CSI) metrics that failed when assessed individually for a specific reach/station which also failed the fully digital RGA. Both the development and validation stage was included. For the digital scores, the LIDAR+StreamGage method was used where applicable, and the StreamStats method otherwise.

| Metric                                   | Development                |     | Validation |     |
|--|----------------------------|-----|------------|-----|
|  | Individual Metric Failures |     |            |     |
|  | Number                     | (%) | Number     | (%) |
| Primary Bed Material                     | 0                          | 0   | 0          | 0   |
| Bank Height                              | 0                          | 0   | 0          | 0   |
| Baseflow Depth                           | 1                          | 20  | 0          | 0   |
| Degree of Constriction                   | 0                          | 0   | 0          | 0   |
| Identifying Erosion                      | 1                          | 20  | 1          | 20  |
| Percent Mass Wasting                     | 1                          | 20  | 0          | 0   |
| Identifying Erosion+Percent Mass Wasting | 2                          | 40  | 0          | 0   |
| Percent Woody Cover                      | 0                          | 0   | 1          | 20  |
| Percent Woody Cover+Bank Protection      | 1                          | 20  | 2          | 40  |
| Percent Woody Cover+Bed/Bank Protection  | 1                          | 20  | 2          | 40  |
| Percent Accretion                        | 0                          | 0   | 0          | 0   |
| Stage of Channel Evolution               | 1                          | 20  | 1          | 20  |
| All GE Methods                           | 5                          | 100 | 5          | 100 |
| Fully Digital Fails                      |                            | 5   |            | 5   |

Table 22: Percentage of Bank Erosion Hazard Index (BEHI) metrics that failed when assessed individually for a specific reach/station which also failed the fully digital RGA. Both the development and validation stage was included. The LIDAR bankfull height method was used for the digital methods.

| Metric                                | Development                |     | Validation |     |
|---------------------------------------|----------------------------|-----|------------|-----|
|                                       | Individual Metric Failures |     |            |     |
|                                       | Number                     | (%) | Number     | (%) |
| Bank Height                           | 7                          | 37  | 1          | 20  |
| Bankfull Height                       | 4                          | 21  | 0          | 0   |
| Bank/Bankfull Height Ratio            | 8                          | 42  | 0          | 0   |
| Root Depth                            | 2                          | 11  | 1          | 20  |
| Root Depth Ratio                      | 10                         | 53  | 4          | 80  |
| Root Depth Ratio + Surface Protection | 14                         | 74  | 5          | 100 |
| Root Density                          | 3                          | 16  | 1          | 20  |
| Face length                           | 2                          | 11  | 0          | 0   |
| Bank Angle                            | 5                          | 26  | 0          | 0   |
| Primary Bank Material                 | 9                          | 47  | 2          | 40  |
| Stratification                        | 7                          | 37  | 0          | 0   |
| Fully Digital Fails                   |                            | 19  |            | 5   |

Table 23: Coefficient of Success for the Channel Stability Index (CSI). The LIDAR+StreamGage method was used to obtain the baseflow depth for the development stage. For the validation stage, both the LIDAR+StreamGage and the StreamStats method were used and tested.

| Score               | Success Rate (%) | Coefficient of Success - S <sup>2</sup> (%) | Success Rate (%)         | Coefficient of Success - S <sup>2</sup> (%) | Success Rate (%)               | Coefficient of Success - S <sup>2</sup> (%) |
|---------------------|------------------|---|--------------------------|---|--------------------------------|---|
|                     | Development      |   | Validation - StreamStats |   | Validation – LIDAR+StreamGage* |   |
| Moderately Unstable | 80               | 85  | 100                      | N/A   | 100                            | N/A   |
| Highly Unstable     | 89               | 83  | 29                       | 0   | 29                             | 0   |
| Over all            | 83               | 96  | 38                       | 0   | 38                             | 0   |

\*There was not enough data to perform the LIDAR+StreamGage data on all of the points. StreamStats was used to fill the gaps.

Table 24: Coefficient of Success for the Bank Erosion Hazard Index. The LIDAR Bankfull Height was the bankfull method used.

| Score     | Success Rate (%) | Coefficient of Success - S <sup>2</sup> (%) | Success Rate (%) | Coefficient of Success - S <sup>2</sup> (%) |
|-----------|------------------|---|------------------|---|
|           | Development      |   | Validation       |   |
| Low       | 0                | 0   | N/A              | N/A   |
| Moderate  | 0                | 0   | 0                | 0   |
| High      | 46               | 24  | 67               | 70  |
| Very High | 80               | 96  | 100              | N/A   |
| Extreme   | 100              | N/A   | N/A              | N/A   |
| Over all  | 38               | 0   | 38               | 0   |



Table 25: Approximate time it took to perform the digital and On-Site Rapid Geomorphic Assessments for the validation stage.

| Validation Stream | Digital      |            |            | On-Site      |            |            |
|-------------------|--------------|------------|------------|--------------|------------|------------|
|                   | # of Reaches | Time (hrs) | Time/Reach | # of Reaches | Time (hrs) | Time/Reach |
| Feather Creek     | 2            | 7          | 3          | 1            | 5          | 5          |
| Sandy Creek       | 3            | 9          | 2          | 2            | 13         | 3          |
| Spring Creek      | 8            | 8          | 1          | 2            |            |            |
| Black Fork        | 3            | 7          | 2          | 1            | 13         | 4          |
| Fourche Maline    | 4            | 7          | 2          | 2            |            |            |
| Average:          | 5            | 7          | 2          | 2            | 10         | 4          |

Table 26: Individual metric accuracy for both the development and validation data. Methods were evaluated similar to success rate, with a full point being assigned to reaches where the same score was obtained using the digital and on-site method. If at least one team got the same categorical assessment, then half a point was given.

| RGA  | Metric                     | Method Accuracy |            |         |
|------|----------------------------|-----------------|------------|---------|
|      |                            | Development     | Validation | Average |
| BEHI | Bank/Bankfull Height       | 3%              | 25%        | 14%     |
| BEHI | Root Depth (%)             | 10%             | 13%        | 12%     |
| BEHI | Root Density (%)           | 10%             | 13%        | 12%     |
| BEHI | Surface Protection (%)     | 21%             | 38%        | 30%     |
| BEHI | Bank Angle                 | 17%             | 50%        | 34%     |
| BEHI | Primary Bank Material      | 17%             | 38%        | 28%     |
| BEHI | Stratification             | 28%             | 88%        | 58%     |
| CSI  | Primary Bed Material       | 93%             | 0%         | 47%     |
| CSI  | Bed Protection             | 97%             | 0%         | 49%     |
| CSI  | Bank Protection            | 21%             | 25%        | 23%     |
| CSI  | Degree of Incision (%)     | 66%             | 38%        | 52%     |
| CSI  | Degree of Constriction (%) | 62%             | 88%        | 75%     |
| CSI  | Streambank Erosion (LB)    | 79%             | 50%        | 65%     |
| CSI  | Streambank Erosion (RB)    | 76%             | 25%        | 51%     |
| CSI  | Streambank Instability (%) | 28%             | 0%         | 14%     |
| CSI  | Percent Woody Cover (%)    | 24%             | 0%         | 12%     |
| CSI  | Percent Accretion (%)      | 38%             | 38%        | 38%     |
| CSI  | Stage of Channel Evolution | 24%             | 25%        | 25%     |

## **CHAPTER IV**

### **SUMMARY, CONCLUSIONS, AND RECOMMENDATIONS**

The goal of this project has been to demonstrate the possibility of improving RGAs by incorporating digital data. Methods paralleling the on-site assessments were developed using several different readily available resources, including Web Soil Survey and the USGS (2018c) StreamStats. While the digital RGAs do not always reflect the same stability ranking as the on-site methods, this project has shown that a fully digital RGA is possible.

#### **Digital RGA Limitations**

Relying on these digital methods to perform RGAs has several limitations. First, these methods were developed and tested in various locations in Oklahoma. Caution should be used when attempting to apply these methods in other locations, and continued testing will be needed in order to quantify more fully their applicability and effectiveness in Oklahoma.

## Data Gaps

Digital methods rely on the availability of data. If there is not information available, then these methods are not feasible. For example, several stream did not have ideal stream gage data available (Table 8). Some had gages that were not close and had not been updated since the 1990s, and some streams did not have a gage on it at all. This is especially important when considering that gage data is needed to identify the bed material (CSI metric 1). If there is no gage on the stream, then the likelihood of correctly identifying the bed material is lowered. It is also worth noting that even if there is a gage on the stream of interest, it may not be close enough to the reach being evaluated to accurately identify the bed material.

Lack of gage data also affects the calculation of the base flow depth that is needed for the CSI (metric 3). Though the addition of LIDAR top width did not appear to statistically increase the accuracy, the LIDAR+StreamGage method was the most successful. If there is no stream gage data, then the USGS (2018c) StreamStats average daily flow can be used, but the results will be less accurate. As was seen from Figure 38, the more accurate and detailed information available, the more successful the method.

Lack of gage data also affects the ability to calculate  $Q_{1.5}$  bankfull depth. If there is old gage data available, the  $Q_{1.5}$  bankfull depth can still be calculated, but it probably will not be an accurate reflection of the current hydrologic conditions of the site. In addition, if there is no gage data available, or not

enough, then the PeakFQ program will not be able to calculate the  $Q_{1.5}$  bankfull flow at all. This could be significant, especially for smaller streams, which appeared to do well using the  $Q_{1.5}$  method (Table 15 and Figure 37), and are more likely to be ungagged. For small-ungagged streams, the recommended solution would be to rely on  $Q_2$  calculations from the USGS (2018c) StreamStats, with the understanding that the reliability of the digital assessment will most likely go down.

Another area where important data may be lacking is LIDAR. LIDAR is not always going to be available, and is not always going to be relatively recent. Even a year can drastically change the stream reach in question. It should be remembered that the LIDAR has been collected at a point in time, which may or may not reflect the current hydrological and morphological state of the stream. The digital BEHI is especially affected by the lack of LIDAR, with three out of the five metrics directly dependent on bank measurements.

While the digital RGAs are only dependent on the stream gages for a few things (alternative bankfull method, calculating normal depth alternative, and the streambed material), in the future a site of interest may lack more significant data such as LIDAR (Table 10). In those cases, it may be necessary to collect on-site data, or perform a modified digital RGA that only relies on the data that is available.

## Data Resolution

As described in the discussion of the validation results, there were cases of the Google Earth imagery being limited by channel visibility, which is determined by the channel size, presence and density of woody vegetation, and the quality and timing of the imagery. In those cases where channel visibility is compromised due to either physical obstructions or poor image resolution, the digital RGA can still be performed, but the results will most likely be impacted.

It should also be noted that while many of the digital RGAs were performed at the reach scale, the digital data used to perform them were most likely not performed at that fine of scale. For example, the soil maps provided by Web Soil Survey are usually collected at a scale of 1 X 24,000. Using the maps at smaller scales than they were made increase the error in the determination of the soil type. This could affect the digital BEHI especially, since its score can be significantly be altered based on the soil type.

Both the CSI and the BEHI appear to be affected by the LIDAR resolution, with decreasing allowances of measurement accuracy (Figure 49 and Figure 50). For the CSI, 1-m resolution has about a -40 to 40 percent difference allowance. For the BEHI, the allowance is much smaller, ranging from about a -15 to 15 percent difference allowance for 2-m resolution, which is one of the more standard resolutions.

## **Digital RGA Recommendations**

### General Recommendations

As has been shown, there does appear to be a correlation with the time of collection used in the digital RGAs (Figure 46 through Figure 47). The CSI appears to be more sensitive to the time the data was collected, especially for Google Earth imagery used. Staying within 12 months for Google Earth imagery could help the results of future digital CSIs. In other words, when available, use as recent as possible imagery and LIDAR.

For calculating the baseflow depth, the more information the better. When available, using the LIDAR top width and stream gage flow from the date the LIDAR was collected does appear to get the most accurate and successful results (Figure 38 and Table 12). So where available, those resources should be used. But in the cases where those resources are not available, alternative methods exist. For example, the USGS (2018c) StreamStats method for measuring normal depth, which does not rely on the presence of stream gages or the availability of LIDAR. Another consideration is the LIDAR flight dates, which are not always readily available, so using some other date to get the stream gage flow would be recommended. For example, the s\_date could be used, which may impair the accuracy, but does appear to work comparatively well (Table 17).

For bed protection, the main indicator used was the primary bed material obtained from the USGS Stream Gages. The depth to restrictive layers and the percentage of fragments on the surface were considered as well. But given the

uncertainty of obtaining accurate bed material from stream gages, either due to distance or complete lack of stream gages, this metric may have to be assessed on-site. Also, the assumptions regarding the use of a restrictive layer or reported surface fragments from Web Soil Survey in the determination of bed protection was questionable. If there is gage data at an appropriate distance from the study reach, it may be advisable to supplement the bed/bank protection determination using Google Earth to identify woody debris or larger boulders.

Due to the lack of a known on-site Manning's  $n$  values, the best recommendation that could be made is to continue to use the Monte Carlo method when using the  $Q_2$  or  $Q_{1.5}$  methods to get bankfull depth and for the baseflow depth calculations (all methods). Another option would be to assume a Manning's  $n$  based on the aerial imagery of the site and the tables provided by Chow (1995). Or other similar methods for estimating  $n$  (e.g. USDA (2012) or Arcement and Schneider (1989)).

For both the development and validation stage, the Google Earth metrics performed very well individually. Caution should be used when applying all of the Google Earth metrics at once, as this appears to affect the overall success, with only a 38% success rate when used on the validation sites (Table 11). One of the biggest limitations to the digital CSI is the potential for missing key visual clues due to lack of available Google Earth imagery. If current (no older than a year, based on Figure 46) Google Earth imagery is not available, then this study would recommend using available NAIP imagery.



While limitations to the digital RGAs exist, it may be possible to improve the accuracy by measuring certain metrics on site. For example, in the BEHI, the primary bank material can change the score by as much as twenty points, which can significantly affect the stability ranking. This is illustrated in the Feather Creek validation site, where the bank material was incorrectly identified in the digital method as sand while the on-site observations identified it as cobbles. This led to a total difference in score of twenty points, a three-step change in stability ranking. If just the primary bank material is identified on site, then the same error could be avoided in the future. Another option would be to discard the BEHI adjustment factors entirely; a practice that was employed in the historical RGAs performed on the Barren Fork and Spavinaw streams.

Based on the comparisons between the digital and on-site assessments performed for validation, it appears that measuring the following metrics on site may improve the overall accuracy of the digital score. These are based on the metrics that had the highest point impact, as seen in Table 18, and correlate well with the average individual metric accuracy as recorded in Table 26. For the BEHI, assessing the primary bank material, surface protection, and or root depth. For the CSI, the best digital and on-site combination found thus far is to measure the primary bed material, bed/bank protection, percent streambank instability, and percent woody cover on-site. Given the high uncertainty of on-site estimates of reach-length features (percent instability and percent woody cover), there may be grounds to say the Google Earth estimates are more accurate. This is of course assuming that no major change in channel has occurred since the time

the Google Earth imagery was taken and the on-site assessment. There is also not taking into account the uncertainty in the determination of supportive woody cover in the Google Earth measurements.

### Bankfull Recommendations

It appears that the method used to obtain the bankfull depth does not have a significant impact on the overall success of the digital BEHI, especially for higher order streams. This is based on the overall differences in scores calculated in Table 18 as well as the success rates calculated for the fully digital scores in Table 13 and Table 14, which did not vary significantly for the different methods. On the other hand, for lower order streams similar to the ones used in the validation stage of the project, the bankfull method does significantly impact the fully digital score (Table 15). Statistically, the LIDAR bankfull height method and the LIDAR bankfull depth method produced significantly similar results to the historical measurements (Figure 37). In terms of success rate, Williams (1986) equation using the radius of curvature and the  $Q_{1.5}$  method produced the highest fully digital success rate of 63% for the validation data. It should be remembered though, that Williams (1986) equation is not always applicable, if the stream does not exhibit measurable meander patterns. It does appear that the  $Q_{1.5}$  method would be a reasonable option for smaller order streams (Table 15 and Figure 37). The Dutnell (2000) ecoregional equation also performed relatively well for the development sites and is not hindered by the need for measurable meander features. The LIDAR bankfull height method also performed well in the fully

digital method at 38% success for the validation sites and 34% at the development sites.

Combining the statistics performed on the development data and the success rates from both the development and validation stage, the following recommendations can be made. Where available, the LIDAR bankfull height method should be used. And if not available, or of low resolution, the Williams (1986) radius of curvature equation should be used. And if the study stream has no measurable meanders, then the Dutnell (2000) ecoregional equation should be used. The size of the stream should also be considered, as the  $Q_{1.5}$  method does appear to work well for lower order streams.

### **Digital RGA Benefits**

There are several benefits to using the proposed digital RGA methods. These include the fact that they are not dependent on land access, provide alternative bankfull identification methods, and are still relatively easy to perform. Time is another factor to consider. While the BEHI and the CSI can typically be completed within an hour for a reach, the digital assessments can take up to approximately two hours per reach. While the digital RGAs may require a little more time, depending on the available data and individual skills in ArcGIS, time and cost-benefits can still be gained from not having to travel on-site, as well as only having to pay one person instead of a whole team of people. Additionally, there is not a linear relationship between the number of reaches assessed and assessment time (Figure 51). It appears that there is a steeper increase for time

required to perform on-site assessments, while the amount of time to perform the digital assessments was relatively uniform. This implies that the digital assessments are better suited for assessing multiple reaches. This relationship is dependent on the amount of travel required, and therefore should not be assumed to be always true.

### **Answering the Research Questions:**

In summary, the following questions have been answered by this study.

1. How sensitive are RGAs to the use of data measured off-site?

Some digital metrics performed better than others did. Referring back to Table 18, the digital metrics that contributed most to the overall difference in scores was the primary bank material, the root depth ratio, and the surface protection in the BEHI. It should be noted that the digital method for determining the surface protection is the same as the method for determining the root depth ratio. The CSI metrics were not as sensitive to the use of digital data, illustrated by the even distribution of points to each metric. Compounding errors, however, can reduce the digital CSI's accuracy.

2. Are there metrics that have to be measured on site, i.e. there is no digital data?

None of the RGA metrics lacked digital options. However, there is the chance that a study stream is not gaged, which could lead to the necessity of either modifying the digital RGA, or measuring the metrics on-site. In particular, if there is no gage data available, then the primary bed material could not be determined.

The baseflow depth calculation would also be affected, though there is a digital alternative in the USGS (2018c) StreamStats. If there is no available LIDAR data, then several metrics would be affected. In particular, the bank height would be hard to otherwise obtain, which would affect both the digital CSI and BEHI. In particular, the digital BEHI would be impossible to perform, as all five metrics are dependent on bank measurements. The digital CSI would not be as drastically affected, as only one metric, the degree of incision, would be impossible to calculate.

3. Is there an applicable stream size for these integrated methods?

The stream order does appear to have an impact on several of the digital metrics, but in terms of applicability, the methods have been tested on stream sizes from second to fourth order. The digital CSI methods in particular appear to perform better on fourth order streams. Applying the methods on streams smaller than second order would not be recommended, unless higher resolution data was available.

4. How sensitive are digital RGAs to data resolution?

Data resolution affects the data by changing the allowances for error. The digital BEHI is more sensitive to error, and appears to need higher resolution data to perform better. However, even with 1-m resolution data, the BEHI only allowed from -10 to 10% error in overall score. The digital CSI, on the other hand, was not as sensitive to resolution, still performing well at 2-m resolution data. At 1-m resolution, the digital CSI had an error allowance from -40 to 40%.

In terms of image resolution, this does not affect the digital BEHI. The digital CSI, on the other hand is highly dependent on the ability to see and distinguish erosion features. However, the digital CSI did perform well using Google Earth imagery as old as from 2010.

5. Are digital RGAs affected by different data collection dates being used in the same assessment?

Time appears to have an impact on the data used in the digital RGAs. It should be expected for this impact to increase as the number of significant flow events, or land use changes increase. For this study, it appears that imagery within a year tended to perform well. For the LIDAR data, there was less of a clear pattern. Again, this all depends on the stream in question and the number of channel changing events that have occurred between the times that the LIDAR was collected and the time of the RGA.

### **Future Work**

This study has demonstrated the usefulness and applicability of digital methods incorporated into RGAs. There is still room for improvement. For example, several ArcGIS tools were not tested in this study. Potentially, use of one of these tools could reduce subjectivity still present in the LIDAR bankfull method. There were also several digital methods that could be improved.

### **Stage of Chanel Evolution**

Using the digital method could potentially have a large impact on the final score, based on the validation (Table 18), though the success rates were high for

the method assessed individually (Table 11). However, the number of times that the digital method identified the stage of channel evolution correctly (assuming on-site assessments were correct) was only 24% for the development sites. This implies that further improvement to the method would be useful. To improve this method, it may be advisable to add other steps into the method. For example, some kind of measurement of degradation, such as the incision ratio (VTDEC, 2003). Another option could be the identification of secondary floodplain formation in LIDAR or Google Earth, which is an indicator of stage 6. Another option would be to add some questions about the vegetation (Heeren et al., 2012) to help identify the stage more precisely.

Another potential tool which could increase the accuracy of the digital method would be to use LIDAR and aerial imagery to identify the formation of secondary floodplains. The stream channel would need to be large enough and the LIDAR resolution would need to be high enough to detect the change in slope. The use of aerial imagery, either NAIP or Google Earth could help verify the LIDAR assessment. If a secondary floodplain is formed, then the reach may be in stage 6 of the channel evolution model.

#### Bank Protection and Woody Cover

While the methods developed were more methodical than on-site estimates, caution should be used when using the digital methods for determining woody cover and bank protection or both. As was highlighted in the validation results, if the imagery is older by more than a year, than the chances

are greater that the channel has changed. Also, given the difficulty in visually determining whether the woody vegetation is adding or subtracting to stability in Google Earth, this method is likely to underestimate the stability ranking. Caution should especially be used when applying these methods to smaller channels where the view is obstructed by the woody vegetation. It may be beneficial to add into the digital assessment some kind of adjustment factor for bank height, reducing the initial estimate of the percent of supportive woody cover. The correction factor could be used to reduce the percentage of woody cover for banks that are taller than the average root depth of the trees. This would possibly reduce error in the amount of assumed protection in the digital CSI.

It should also be noted that the method for determining bank protection only considers percentage of the reach supported by woody cover. For future use, it may be beneficial to add in other metrics of bank protection, such as bank/bed material, or visible woody debris.

#### Bankfull Depth Determination

The LIDAR methods could potentially be improved by creating some kind of toolbox to determine the bankfull height automatically. An ArcGIS toolbox could potentially be made which identifies the bankfull height using the DEM and decision matrices. This would reduce the subjectivity of the LIDAR method, which relies on user bias. User bias includes the user's knowledge and understanding of bankfull and elevation interpretation experience.



The described methods have only been tested on streams within Oklahoma and on streams ranging in different sizes, from second order up to fourth order. Therefore, the findings do not necessarily apply to any stream outside of the study. Further validation is needed to determine the digital methods efficacy in other states and for other stream sizes. An easy follow up would be to use the digital methods described, apply them to other streams with published RGA data, and perform a comparison similar to the one done on the development sites in this study. For example, published CSIs for a stream in Georgia exist (Mukundan et al., 2011).

#### Other BEHI Metrics

The fully digital BEHI has room for improvement, as evidenced by a low success rate at 38% for both the development and validation stages, and with lower metric accuracies. Depending on the level of accuracy needed for future studies, considerations should be made to the improvement of the digital methods.

Caution should be taken in relying on the method used for root density. Only 29 historical root densities reported for two different ecoregions in Oklahoma were used to develop the method used in the validation. In future work, if they are available, other databases or studies which provide specific information on root densities would be useful. However, the lack of root density information was not considered an absolute obstacle to the digital BEHI, since it is one of the least sensitive metrics (Bigham, 2016). It also did not appear to

affect the final score significantly, in either the development or the validation stage results. However, the lack of a larger data set and wider range of sampling ecoregions does make the use of this method in other areas more likely to be erroneous.

The root depth ratio did not perform as well as hoped, with a low average accuracy of approximately 11%. Potential for improvement of this method could lie in gaining more information on the average root depths of typical species, relying on other studies. Or potentially separating the average minimum root depth by vegetation type identified in Google Earth. This was attempted with the development data set, but had poor results. Though the poor results could potentially be explained by the averaged historical bank heights used.

The surface protection ratio could potentially be improved by considering other factors besides root depth, for example, combining root depth and root density by multiplying the two ratios. Other considerations could be to include other factors, like the bank/bed material. Or adding a visual assessment of other forms of protection, like woody debris. This would possibly help increase the accuracy of the digital assessment of surface protection by including more of the other factors which are usually considered in the on-site assessment.

The stratification adjustment factor could potentially be improved by adding additional scenarios which take into account the likely effects difference changes in soil layers would cause. For example, a denser layer above a layer of sand would be more likely to cause the bank to be undercut, than a layer of sand

above a denser layer. On the other hand, the method described in this study performed fairly well as it is, with a high success rate evaluated on its own (62% for development, 88% for validation), and had a good average accuracy (58%).

### Automating Digital Rapid Geomorphic Assessments

Considering the future of RGAs, it is important to consider its affective application to large watersheds. If possible, the digital RGA could more easily and efficiently be applied to larger study areas. Automating the digital BEHI would probably be simple, given the availability of ArcGIS toolboxes that already exist which identify bank features. The next step would be to incorporate those toolboxes into one ArcGIS toolbox which identified bank and bankfull height, face length, and calculated the corresponding ratios. It would also need to have access to Web Soil Survey and some kind of root depth database in order to determine the BEHI adjustment factors and the root depth/bank protection metrics.

On the other hand, the CSI would most likely require some kind of classified imagery and decision matrices to “visually” assess the different RGA metrics. There are a few metrics which are dependent on bank measurements, which could probably be done using ArcGIS toolboxes. Despite the difficulty in automating the digital CSI, it is still a valid consideration given the criticisms of the BEHI in general, as well as the overall better performance in comparison to the BEHI demonstrated in this study.

## **Conclusion**

The goal of this project was to demonstrate the potential of incorporating digital data into RGAs. While the digital RGAs do not always reflect the same stability ranking as the on-site methods, this project has shown that a fully digital RGA is possible with room for improvement. Future applications of the digital methods should consider both the sensitivity of the RGA metric to digital data, availability and quality of digital data in the area of interest, as well as the accuracy of the digital methods. Even with low digital accuracy, it may be that these proposed methods provide an adequate first step in streambank stability analysis.

## REFERENCES

- Atha, J. B. 2014. Identification of Fluvial Wood Using Google Earth. *River Research and Applications* 30(7).
- Arcement, G.J and V. R. Schneider. 1989. PAPER 2339 Guide for Selecting Manning's Roughness Coefficients for Natural Channels and Flood Plains. USGS, ed.
- Archuleta, C. M., E. W. Constance, S. T. Arundel, A. J. Lowe, K. S. Mantey, and L. A. Phillips. 2017. The National Map seamless digital elevation model specifications: U.S. Geological Survey Techniques and Methods, book 11, chap. B9. Available at: <https://doi.org/10.3133/tm11B9>
- Bentley. 2009. *FlowMaster*.
- Bieger, K., H. Rathjens, P. M. Allen, and J. F. Arnold. 2015. Development and Evaluation of Bankfull Hydraulic Geometry Relationships for the Physiographic Regions of the United States. *JOURNAL OF THE AMERICAN WATER RESOURCES ASSOCIATION* 51(3):842-858.
- Bigham, K. A. 2016. Evaluation and Application of the Bank Assessment for Non-Point Source Consequences of Sediment (BANCS) Model Developed to Predict Annual Streambank Erosion Rates KANSAS STATE UNIVERSITY, Department of Biological and Agricultural Engineering, Manhattan, Kansas
- Blue Thumb, Oklahoma. 2018. Interactive Site Map. Available at: <http://www.bluethumbok.com/volunteer-written-data-interpretations.html>.
- Boardman, J. 2016. The value of Google Earth™ for erosion mapping. *Catena* 143.
- Chow, V. T. 1995. *Open Channel Hydraulics*. McGraw-Hill Book Company, New York Toronto London.
- CIRIA. 1990. *Use of Vegetation in Civil Engineering*. Butterworths. London.
- Dutnell, R. C. 2000. Development of Bankfull Discharge and Channel Geometry Relationships for Natural Channel Design in Oklahoma Using a Fluvial Geomorphic Approach. University Of Oklahoma, Civil Engineering, Norman, Oklahoma
- Esri. 2013. ArcGIS. Ver. 10.2.

Fagan, C., and D. R. Maidment. 2012. Converting a LAS Data to a DEM and Performing a Watershed Delineation. University of Texas.

Faux, R. N., J. M. Buffington, M. G. Whitley, S. H. Lanigan, and B. B. Roper. 2009. Chapter 6.—Use of Airborne Near-Infrared LiDAR for Determining Channel Cross-Section Characteristics and Monitoring Aquatic Habitat in Pacific Northwest Rivers: A Preliminary Analysis. In *PNAMP Special Publication: Remote Sensing Applications for Aquatic Resource Monitoring*.

Fisher, G. B., C. B. Amos, B. Bookhagen, D. W. Burbank, and V. Godard. 2012. Channel Widths, Landslides, Faults, and Beyond: The New World Order of High-Spatial Resolution Google Earth Imagery in the Study of Earth Surface Processes. *Special Paper of the Geological Society of America* 492.

Google. 2018. Google Earth Pro.

Habberfield, M. W., S. S. Blersch, S. J. Bennett, and J. F. Atkinson. 2014. Rapid Geomorphic and Habitat Stream Assessment Techniques Inform Restoration Differently Based on Levels of Stream Disturbance. *JOURNAL OF THE AMERICAN WATER RESOURCES ASSOCIATION* 50(4).

Hanson, G. J., and A. Simon. 2001. Erodibility of Cohesive Streambeds in the Loess Area of the Midwestern USA. *Hydrological Processes* 15.

Harmel, R. D., C. T. Hann, and R. C. Dutnell. 1999. Evaluation of Rosgen's Streambank Erosion Potential Assessment in Northeast Oklahoma. *JOURNAL OF THE AMERICAN WATER RESOURCES ASSOCIATION* 35(1).

Harmel, R. D., and P. K. Smith. 2007. Consideration of Measurement Uncertainty in the Evaluation of Goodness-of-Fit in Hydrologic and Water Quality Modeling. *Journal of Hydrology* 337.

He, L., and G. V. Wilkerson. 2011. Improved Bankfull Channel Geometry Prediction Using Two-Year Return-Period Discharge. *JOURNAL OF THE AMERICAN WATER RESOURCES ASSOCIATION* 47(6).

Heeren, D. M., A. R. Mittlestet, G. A. Fox, D. E. Storm, A. T. Al-Madhhachi, T. L. Midgley, A. F. Stringer, K. B. Stunkel, and R. D. Tejral. 2012. Using Rapid Geomorphic Assessments to Assess Streambank Stability in Oklahoma Ozark Streams. *Transactions of the ASABE* 55(3):957-968.

Johnson, P. A., G. L. Gleason, and R. D. Hey. 1999. Rapid Assessment of Channel Stability in Vicinity of Road Crossing. *JOURNAL OF HYDRAULIC ENGINEERING* 125(6).

Keeton, W. S., E. M. Copeland, S. M. z. P. Sullivan, and M. C. Watzin. 2017. Riparian forest structure and stream geomorphic condition: implications for flood resilience. *Canadian Journal of Forest Resarch* 47(4).

Kelley, J. 2017. *DEM analysis and Detection of Riparian areas*. Oregon State University.

Krymer, V. 2012. Stream Restoration and Cribwall Performance,

Leopold, L. 1995. A Guide for Field Identification of Bankfull Stage in the Western United States. USDA Forest Service, Rocky Mountain Forest and Range Experiment Station, Stream Systems Technology Center, eds: Youtube.

Leopold, L., D. Rosgen, and H. L. Silvey. 1998. *The Reference Reach Field Book*. Wildland Hydrology.

Lewis, J. M. 2010. Methods for Estimating the Magnitude and Frequency of Peak Streamflows for Unregulated Streams in Oklahoma. U.S. Department of the Interior; U.S. Geological Survey 2010–5137.

McKean, J., D. Nagel, D. Tonina, P. Bailey, C. W. Wright, C. Bohn, and A. Nayegandhi. 2009. Remote Sensing of Channels and Riparian Zones with a Narrow-Beam Aquatic-Terrestrial LIDAR. *Remote Sensing* 1(4).

Mckinley, R., D. Radcliffe, and R. Mukundan. 2013. A Streamlined Approach for Sediment Source Fingerprinting in a Southern Piedmont Watershed, USA. *Journal of Soils and Sediments* 13(10).

Merwade, V., A. Cook, and J. Coonrod. 2008. GIS techniques for creating river terrain models for hydrodynamic modeling and flood inundation mapping. *Environmental Modelling & Software* 23.

MOE. 2003. Stormwater Management Planning and Design Manual. O. M. o. t. Environment, ed. Ontario. Canada: Queen's Printer for Ontario.

Mukundan, R., D. E. Radcliffe, and J. C. Ritchie. 2011. Channel Stability and Sediment Source Assessment in Streams Draining a Piedmont Watershed in Georgia, USA. . *Hydrological Processes* 25(8).

Newton, S. E., and D. M. Drenten. 2015. Modifying the Bank Erosion Hazard Index (BEHI) Protocol for Rapid Assessment of Streambank Erosion in Northeastern Ohio. *Journal of Visualized Experiments* 96.

NOAA. 2018. United States Interagency Elevation Inventory. National Oceanic and Atmospheric Administration. U.S. Geological Survey, Federal Emergency Management Agency, U.S. Department of Agriculture, U.S. Forest Service, National Park Service, and U.S. Army Corps of Engineers. Available at: <https://coast.noaa.gov/inventory/>

OSU-Oklahoma Cooperative Extension Service, Division of Agricultural Sciences and Natural Resources, and the Oklahoma Conservation Commission. 1998. Riparian Area. E-952. Management Handbook.

Pollen, N., and A. Simon. 2005. Estimating the Mechanical Effects of Riparian Vegetation on Stream Bank Stability Using a Fiber Bundel Model. *Water Resources Research* 41.

Pollen, N., A. Simon, and A. J. C. Collison. 2004. *Advances in Assessing the Mechanical and Hydrologic effects of Riparian Vegetation on Streambank Stability*. Riparian Vegetation and Fluvial Geomorphology, Water Science and Application, AGU. Washington, D.C.

Rinaldi, M., N. Surian, F. Comiti, and M. Bussetini. 2015. A methodological framework for hydromorphological assessment, analysis and monitoring (IDRAIM) aimed at promoting integrated river management. *Geomorphology* 251.

Rosgen, D. L. 1996. *Applied River Morphology*. Wildland Hydrology.

Rosgen, D. L. 2001. A Practical Method of Computing Streambank Erosion Rate.

Rosgen, D. 2014. *River Stability Field Guide*. Second ed. Wildland Hydrology, Fort Collins.

Roux, C., A. Alber, M. Bertrand, L. Vaudor, and H. Piégay. 2015. "FluvialCorridor": A new ArcGIS toolbox package for multiscale riverscape exploration. *Geomorphology* 242.

Royo, M. L., R. Ranasinghe, and J. A. Jiménez. 2016. A Rapid, Low-Cost Approach to Coastal Vulnerability Assessment at a National Level. *Journal of Coastal Research* 32(4):932-945.

Saenz, A., B. Masasi, H. Enlow, K. Khand, J. Stivers, S. Nazari, and S. Rasoulzadeh. 2016. Rapid Geomorphic Assessment of Fivemile and Willow Creek – Final Report. Oklahoma State University. (Unpublished).

Sass, C. K., and T. D. Keane. 2012. Application of Rosgen's Bancs Model for NE Kansas And the Development of Predictive Streambank Erosion Curves. *JOURNAL OF THE AMERICAN WATER RESOURCES ASSOCIATION* 48(4).

Simon, A., and A. J. C. Collison. 2002. Quantifying the Mechanical and Hydrologic Effects of Riparian Vegetation on Streambank Stability. *Earth Surface Processes and Landforms* 27.

Simon, A., and P. W. Downs. 1995. An Interdisciplinary Approach to Evaluation of Potential Instability in Alluvial Channels. *Geomorphology* 12:215-232.



- Simon, A., M. Doyle, M. Kondolf, F. D. S. Jr., B. Rhoads, and M. McPhillips. 2007. Critical Evaluation of How the Rosgen Classification and Associated “Natural Channel Design” Methods Fail to Integrate and Quantify Fluvial Processes and Channel Response. *JOURNAL OF THE AMERICAN WATER RESOURCES ASSOCIATION* 43(5):1117-1131.
- Simon, A., and C. R. Hupp. 1986. Channel Evolution in Modified Tennessee Channels. In *4th Federal Interagency Sedimentation Conference*.
- Simon, A., and L. Klimetz. 2008. Magnitude, Frequency, and Duration Relations for Suspended Sediment in Stable (“Reference”) Southeastern Streams. *JOURNAL OF THE AMERICAN WATER RESOURCES ASSOCIATION* 44(5):1270-1283.
- Soar, P. J., N. P. Wallerstein, and C. R. Thorne. 2017. Quantifying River Channel Stability at the Basin Scale. *Water* 9.
- Storm, D. E., G. A. Fox, A. T. Al-Madhhachi, D. M. Heeren, T. L. Midgley, A. R. Mittelstet, A. F. Stringer, K. B. Stunkel, and R. D. Tejral. 2010. Rapid Geomorphic Assessment in the Ozark Ecoregion of Oklahoma for the Barren Fork of the Illinois River and Spavinaw Creek. Oklahoma State University. (Unpublished).
- Strahler, A. N. 1964. Quantitative geomorphology of drainage basins and channel networks. In *Handbook of Applied Hydrology*, Section 4-2. Ven te Chow, ed. New York, N.Y.: McGraw Hill.
- Sumerling, G. 2011. Lidar Analysis in ArcGIS 10 for Forestry Applications. 49. United States of America.
- USDA, NRCS. 2012. Part 630 Hydrology, Chapter 14 Stage Discharge Relations. In *National Engineering Handbook*.
- USDA, NRCS. 2017. Web Soil Survey. Available at: <https://websoilsurvey.sc.egov.usda.gov/App/HomePage.htm>
- USDA, NRCS. 2018a. Ecological Site Information System. Available at: <https://esis.sc.egov.usda.gov/Default.aspx>
- USDA, NRCS. 2018b. Geospatial Data Gateway. Available at: <https://datagateway.nrcs.usda.gov/GDGHome.aspx>
- USDA, NRCS. 2018c. The PLANTS Database. Greensboro, NC 27401-4901 USA.: National Plant Data Team. Available at: <http://plants.usda.gov>
- USEPA. 2017a. National Water Quality Inventory: Report to Congress. Report number 841-R-16-011.

USEPA. 2017b. WATERS (Watershed Assessment, Tracking & Environmental Results System) GeoViewer. Available at:  
<https://www.epa.gov/waterdata/waters-geoviewer>

USGS. 2014. *PeakFQ*. Ver. 7.1.

USGS. 2016. National Elevation Dataset (NED) Data Dictionary. Available at:  
[https://nationalmap.gov/3DEP/documents/Data\\_dictionary\\_%2020160115.pdf](https://nationalmap.gov/3DEP/documents/Data_dictionary_%2020160115.pdf)

USGS. 2018a. Earth Explorer. Available at: <https://earthexplorer.usgs.gov>

USGS. 2018b. The National Map. Available at:  
<https://viewer.nationalmap.gov/advanced-viewer/>

USGS. 2018c. StreamStats. ODOT, OWRB. Available at:  
<https://streamstats.usgs.gov/ss/>

VTDEC. 2003. Stream geomorphic assessment handbook: rapid stream assessment. Vermont Department of Environmental Conservation (VTDEC), ed. Waterbury, Vt.: Vermont Agency of Natural Resources. Department of Environmental Conservation. Water Quality Division.

Williams, B. S., E. D'Amico, J. H. Kastens, J. H. Thorp, J. E. Flotemersch, and M. C. Thoms. 2013. Automated riverine landscape characterization: GIS-based tools for watershed-scale research, assessment, and management. *Environmental Monitoring and Assessment* 185.

Williams, G. P. 1986. River Meanders and Channel Size. *Journal of Hydrology* 88:147-164.

Wilson, G. V., R. K. Periketi, G. A. Fox, S. M. Dabney, F. D. Shields, and R. F. Cullum. 2006. Soil properties controlling seepage erosion contributions to streambank failure. *Earth Surface Processes and Landforms*.

WSDNR. 2011. Washington Forest Practices Rules: Identifying and Measuring the Bankfull Channel Width: Part 1 & 2. Youtube.

## APPENDIX

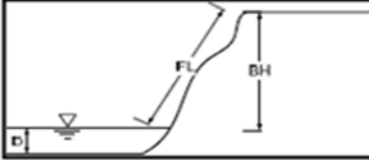
**BANK EROSION HAZARD INDEX (BEHI) 2016**

River/Creek \_\_\_\_\_ Station \_\_\_\_\_

Date \_\_\_\_\_ Crew \_\_\_\_\_

**0. Preliminary Data (Left and Right Banks Looking Downstream):**

|                                       |                 |                  |  |  |  |
|---------------------------------------|-----------------|------------------|--|--|--|
| Bank Heights (BH)                     | Left (ft) _____ | Right (ft) _____ |  |  |  |
| <i>(Floodplain/Terrace Elevation)</i> |                 |                  |  |  |  |
| Bankface Lengths (FL)                 | Left (ft) _____ | Right (ft) _____ |  |  |  |
| <i>(Bankfull Height (BFH), ft)</i>    |                 |                  |  |  |  |
| Root Depth on Bank (RD)               | Left (ft) _____ | Right (ft) _____ |  |  |  |



**1. Bank Height/Bankfull Height = BH/BFH – Circle One:**

|         |           |         |         |         |      |
|---------|-----------|---------|---------|---------|------|
| 1.0-1.1 | 1.11-1.19 | 1.2-1.5 | 1.6-2.0 | 2.1-2.8 | >2.8 |
| 1.45    | 2.95      | 4.95    | 6.95    | 8.5     | 10.0 |

Notes: \_\_\_\_\_

**2. Root Depth (% of Bank Height) = RD/BH – Circle One:**

|         |        |        |        |       |       |
|---------|--------|--------|--------|-------|-------|
| 90-100% | 50-89% | 30-49% | 15-29% | 5-14% | <5.0% |
| 1.45    | 2.95   | 4.95   | 6.95   | 8.5   | 10.0  |

Notes: \_\_\_\_\_

**3. Root Density (%) – Percentage of Streambank Surface Covered by Plant Roots – Circle One:**

|         |        |        |        |       |       |
|---------|--------|--------|--------|-------|-------|
| 80-100% | 55-79% | 30-54% | 15-29% | 5-14% | <5.0% |
| 1.45    | 2.95   | 4.95   | 6.95   | 8.5   | 10.0  |

Notes: \_\_\_\_\_

**4. Surface Protection (%) – Percentage of Streambank Covered by Plant Roots, Downed Logs and Branches, Rocks, etc.) – Circle One:**

|         |        |        |        |        |        |
|---------|--------|--------|--------|--------|--------|
| 80-100% | 55-79% | 30-54% | 15-29% | 10-14% | <10.0% |
| 1.45    | 2.95   | 4.95   | 6.95   | 8.5    | 10.0   |

Notes: \_\_\_\_\_

**5. Bank Angle (°) – Circle One:**

|                     |              |               |              |              |         |
|---------------------|--------------|---------------|--------------|--------------|---------|
| 0-20°               | 21-60°       | 61-80°        | 81-90°       | 91-119°      | >119°   |
| BH/FL (= 0.00-0.34) | (=0.35-0.86) | (=0.87-0.985) | (=0.985-1.0) | (=0.87-0.99) | (<0.87) |
| 1.45                | 2.95         | 4.95          | 6.95         | 8.5          | 10.0    |

Notes: \_\_\_\_\_

Rosgen Channel Classification (See Next Page) \_\_\_\_\_ Total Score: \_\_\_\_\_

**PRIMARY BANK MATERIAL:** (Clay: -20, Silt/Boulder/Bedrock: 0, Gravel: 5, Sand: +10, Cobble: -10)  
**STRATIFICATION:** (None: 0, Two Layers: 5, Multiple Layers, +10)

Figure A - 1: Bank Erosion Hazard Index data collection sheet 1 out of 2. Note that the primary bank material and stratification indicators were added and used for the validation sites.

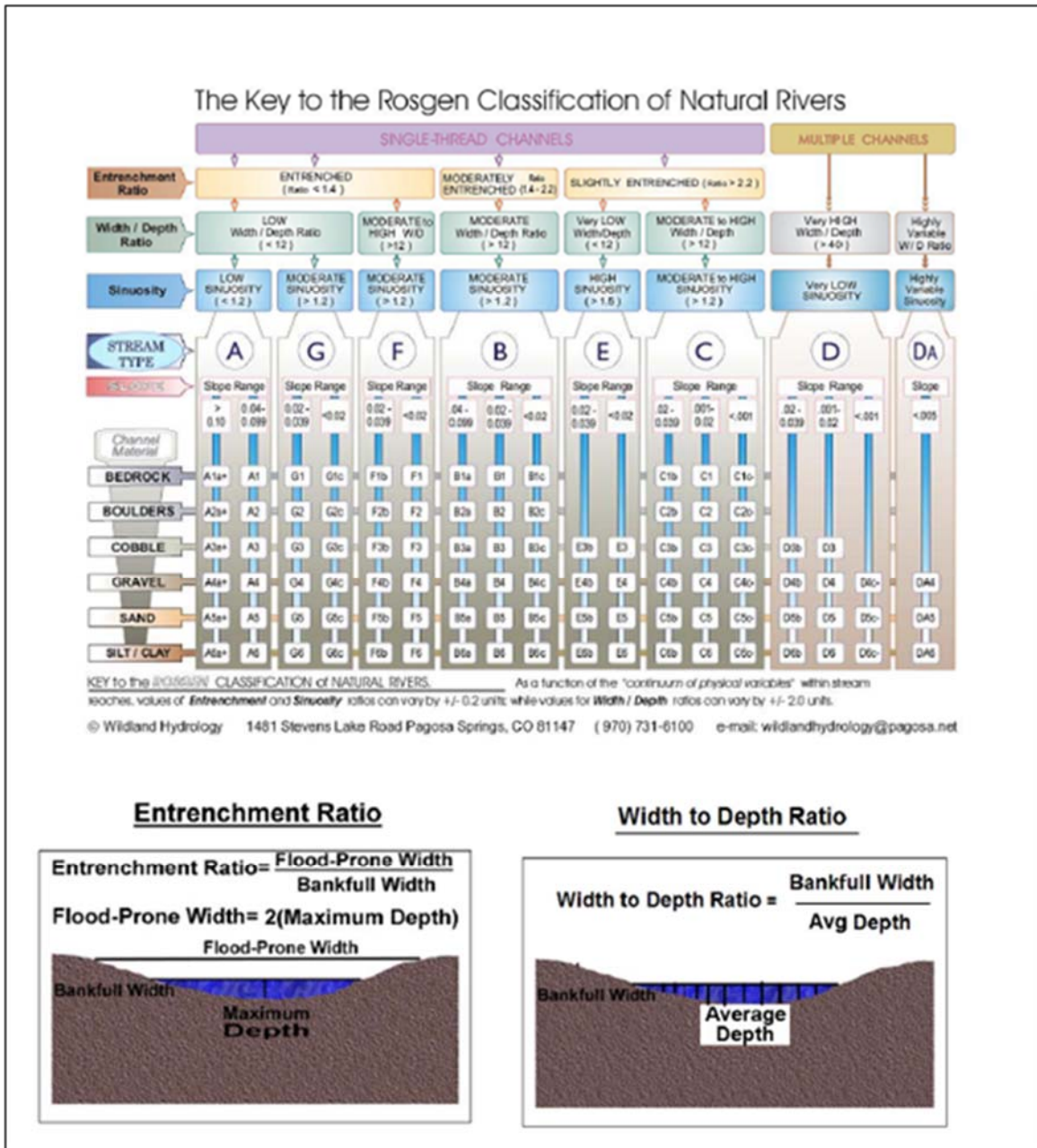


Figure A - 2: Bank Erosion Hazard Index data collection sheet 2 out of 2.

OSU MODIFIED CHANNEL-STABILITY INDEX 2010/2016

River/Creek \_\_\_\_\_ Station \_\_\_\_\_

Date \_\_\_\_\_ Crew \_\_\_\_\_

0. Preliminary Data (Left and Right Banks Looking Downstream):

Bank Heights (BH) Left (ft) \_\_\_\_\_ Right (ft) \_\_\_\_\_  
 (Floodplain/Terrace Elevation)

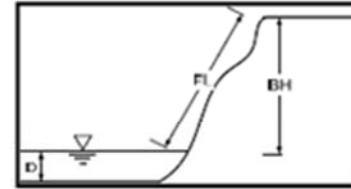
Bankface Lengths (FL) Left (ft) \_\_\_\_\_ Right (ft) \_\_\_\_\_

River Stage at "Base Flow" (D, ft) \_\_\_\_\_

Estimated Width of Channel Transect, W (ft) \_\_\_\_\_ Upstream, W<sub>u</sub> (ft) \_\_\_\_\_

Average Diameter of Streambed Sediment (in) \_\_\_\_\_

Bank Gullies None \_\_\_\_\_ Width (ft) \_\_\_\_\_ Depth (ft) \_\_\_\_\_



1. Primary Bed Material:

| Bedrock | Boulder/Cobble | Gravel | Sand | Silt/Clay | Value |
|---------|----------------|--------|------|-----------|-------|
| 0       | 1              | 2      | 3    | 4         | _____ |

Notes: \_\_\_\_\_

2. Bed/Bank Protection:

| Bed and Banks Both Protected | No Bed Protection | (Add) | Only 1 Bank Protected | No Banks Protected | Value |
|------------------------------|-------------------|-------|-----------------------|--------------------|-------|
| 0                            | 1                 |       | 2                     | 3                  | _____ |

Notes: \_\_\_\_\_

3. Degree of Incision (Relative Elevation of "Base Flow"/Floodplain Elevation) = D/(BH+D):

| 0-10% | 11-25% | 26-50% | 51-75% | 76-100% | Value |
|-------|--------|--------|--------|---------|-------|
| 4     | 3      | 2      | 1      | 0       | _____ |

Notes: \_\_\_\_\_

4. Degree of Constriction (Relative Decrease in Top-Bank Width from Upstream) = W/W<sub>u</sub>:

| 0-10% | 11-25% | 26-50% | 51-75% | 76-100% | Value |
|-------|--------|--------|--------|---------|-------|
| 4     | 3      | 2      | 1      | 0       | _____ |

Notes: \_\_\_\_\_

5. Streambank Erosion (Each Bank – Add Values for Multiple Mechanisms):

|       | None | Fluvial | Mass Wasting | Value |
|-------|------|---------|--------------|-------|
| Left  | 0    | 1       | 2            | _____ |
| Right | 0    | 1       | 2            | _____ |

Figure A - 3: Channel Stability Index data collection sheet 1 out of 2.

**6. Streambank Instability (Percent of Each Bank Failing by Mass Wasting):**

|      | 0-10% | 11-25% | 26-50% | 51-75% | 76-100% | Value |
|------|-------|--------|--------|--------|---------|-------|
| Left | 0     | 0.5    | 1      | 1.5    | 2.0     | _____ |
| Left | 0     | 0.5    | 1      | 1.5    | 2.0     | _____ |

Notes: \_\_\_\_\_

**7. Established Riparian Woody-Vegetative Cover (Each Bank):**

|      | 0-10% | 11-25% | 26-50% | 51-75% | 76-100% | Value |
|------|-------|--------|--------|--------|---------|-------|
| Left | 2     | 1.5    | 1      | 0.5    | 0       | _____ |
| Left | 2     | 1.5    | 1      | 0.5    | 0       | _____ |

Notes: \_\_\_\_\_

**8. Occurrence of Bank Accretion (Percent of Each Bank with Fluvial Deposition):**

|      | 0-10% | 11-25% | 26-50% | 51-75% | 76-100% | Value |
|------|-------|--------|--------|--------|---------|-------|
| Left | 2     | 1.5    | 1      | 0.5    | 0       | _____ |
| Left | 2     | 1.5    | 1      | 0.5    | 0       | _____ |

Notes: \_\_\_\_\_

**9. Stage of Channel Evolution Model:**

| I | II | III | IV | V | VI  | Value |
|---|----|-----|----|---|-----|-------|
| 0 | 1  | 2   | 4  | 3 | 1.5 | _____ |

Notes: \_\_\_\_\_

**Total Score:** \_\_\_\_\_

The diagram illustrates the Channel Evolution Model through six stages:

- Stage I. Sinuous, Premodified:**  $h < h_c$ . Shows a sinuous channel with trees on the banks.
- Stage II. Constructed:**  $h < h_c$ . Shows a straightened channel with a floodplain.
- Stage III. Degradation:**  $h < h_c$ . Shows a channel with a deepening plunge pool.
- Stage IV. Degradation and Widening:**  $h > h_c$ . Shows a channel with a terrace and slumped material.
- Stage V. Aggradation and Widening:**  $h > h_c$ . Shows a channel with a terrace, aggraded material, and slumped material.
- Stage VI. Quasi Equilibrium:**  $h > h_c$ . Shows a channel with a terrace, bank, bankfull, and aggraded material.

Legend:  $h_c$  = critical bank height;  $h > h_c$  = direction of bank or bed movement.

The longitudinal profile shows Stages I, II, III, IV, V, and VI along a channel reach. Key features include a precursor knickpoint, primary knickpoint, plunge pool, secondary knickpoint, top bank, aggradation zone, and oversteepened reach.

Figure A - 4: Channel Stability Index data collection sheet 2 out of 2.

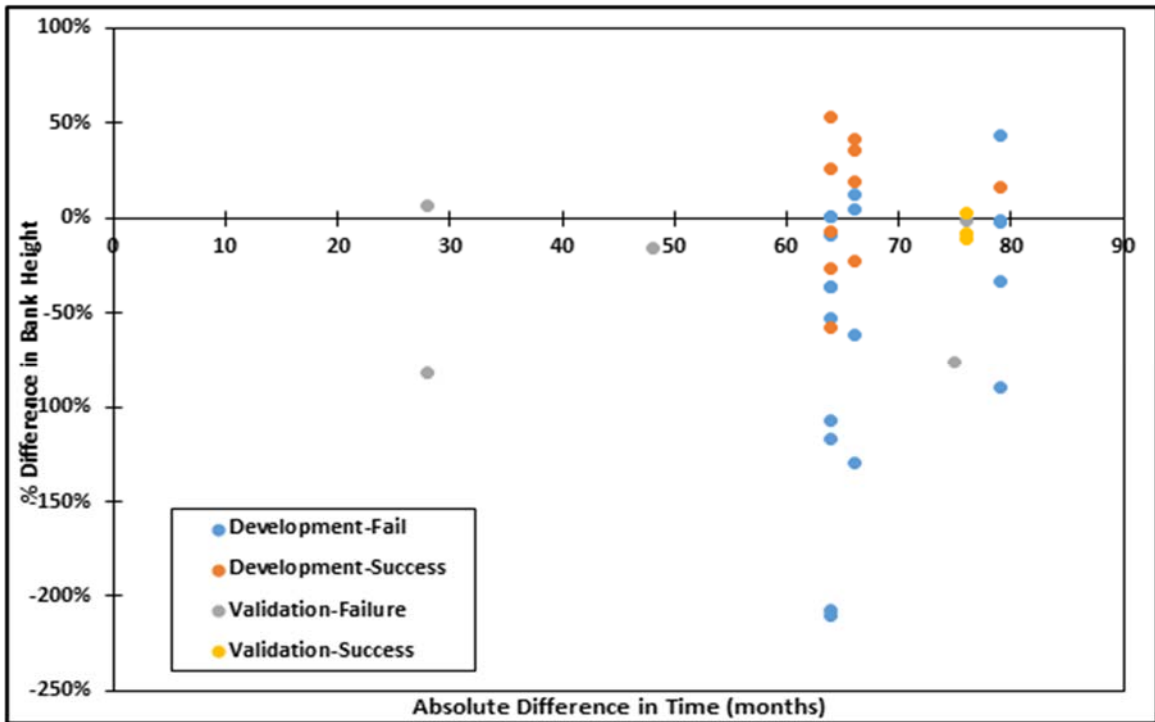


Figure A - 5: The percent difference in bank height when using digital or on-site measurements, graphed against the absolute difference between the times when each was collected.

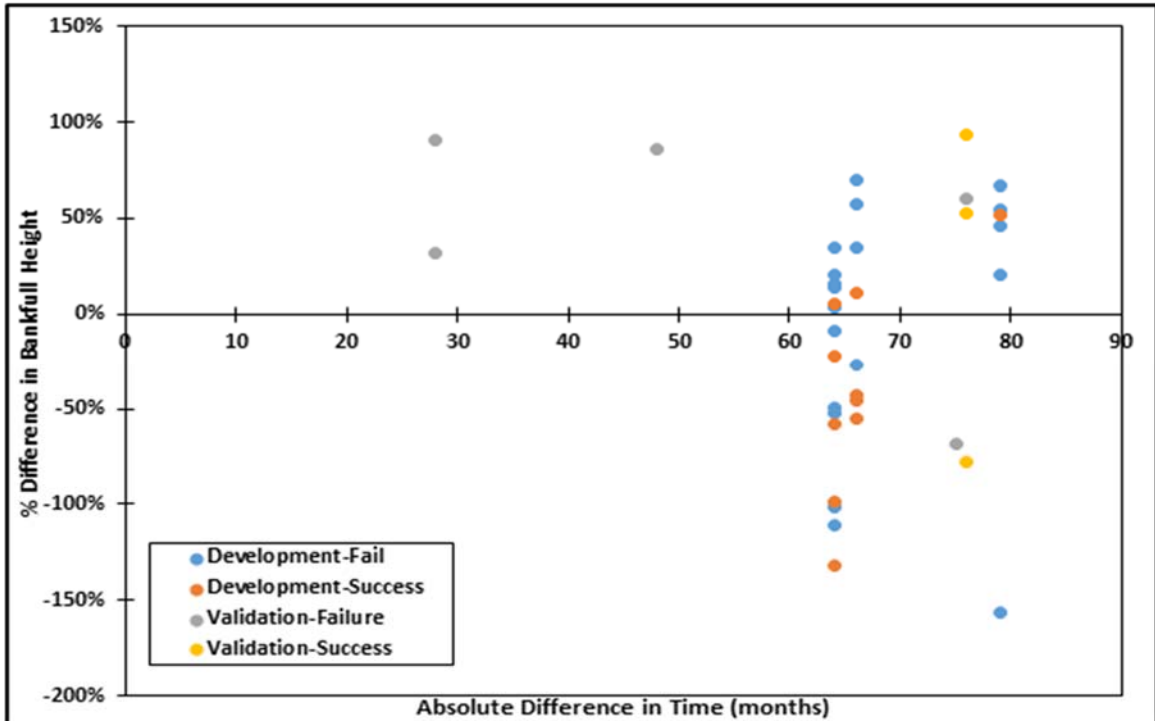


Figure A - 6: The percent difference in bankfull height when using digital or on-site measurements, graphed against the absolute difference between the times when each was collected.

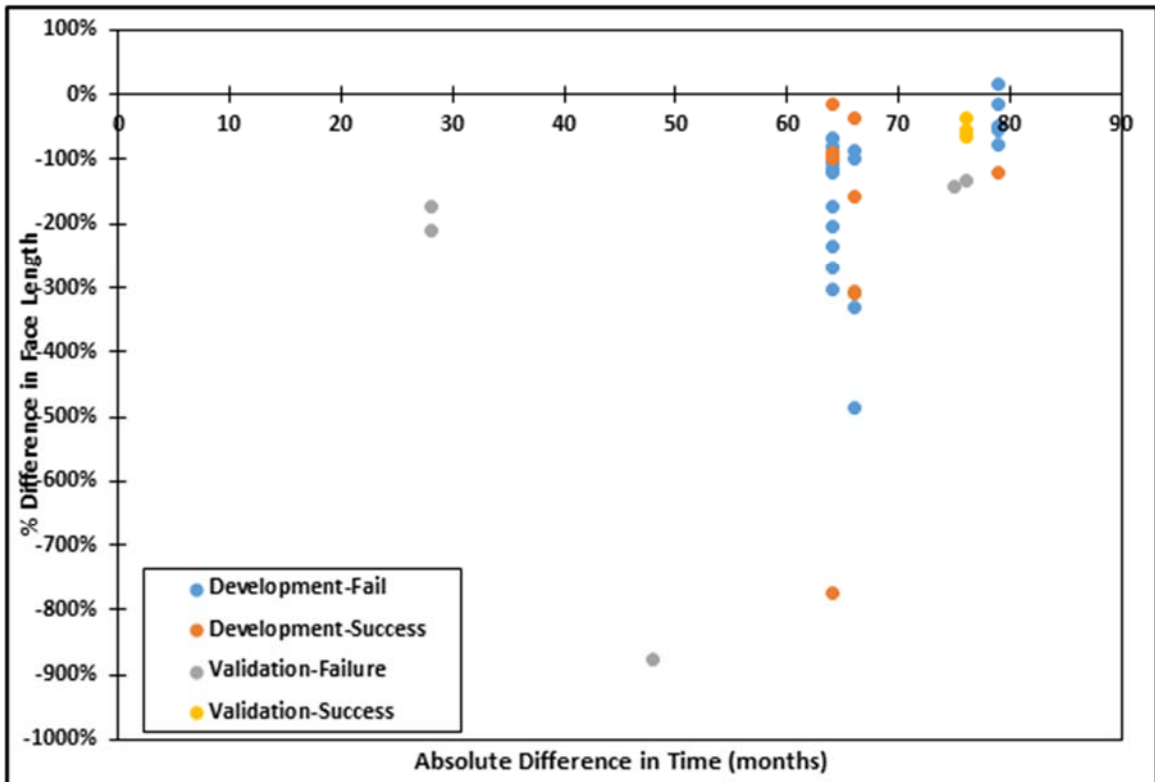


Figure A - 7: The percent difference in face length when using digital or on-site measurements, graphed against the absolute difference between the times when each was collected.



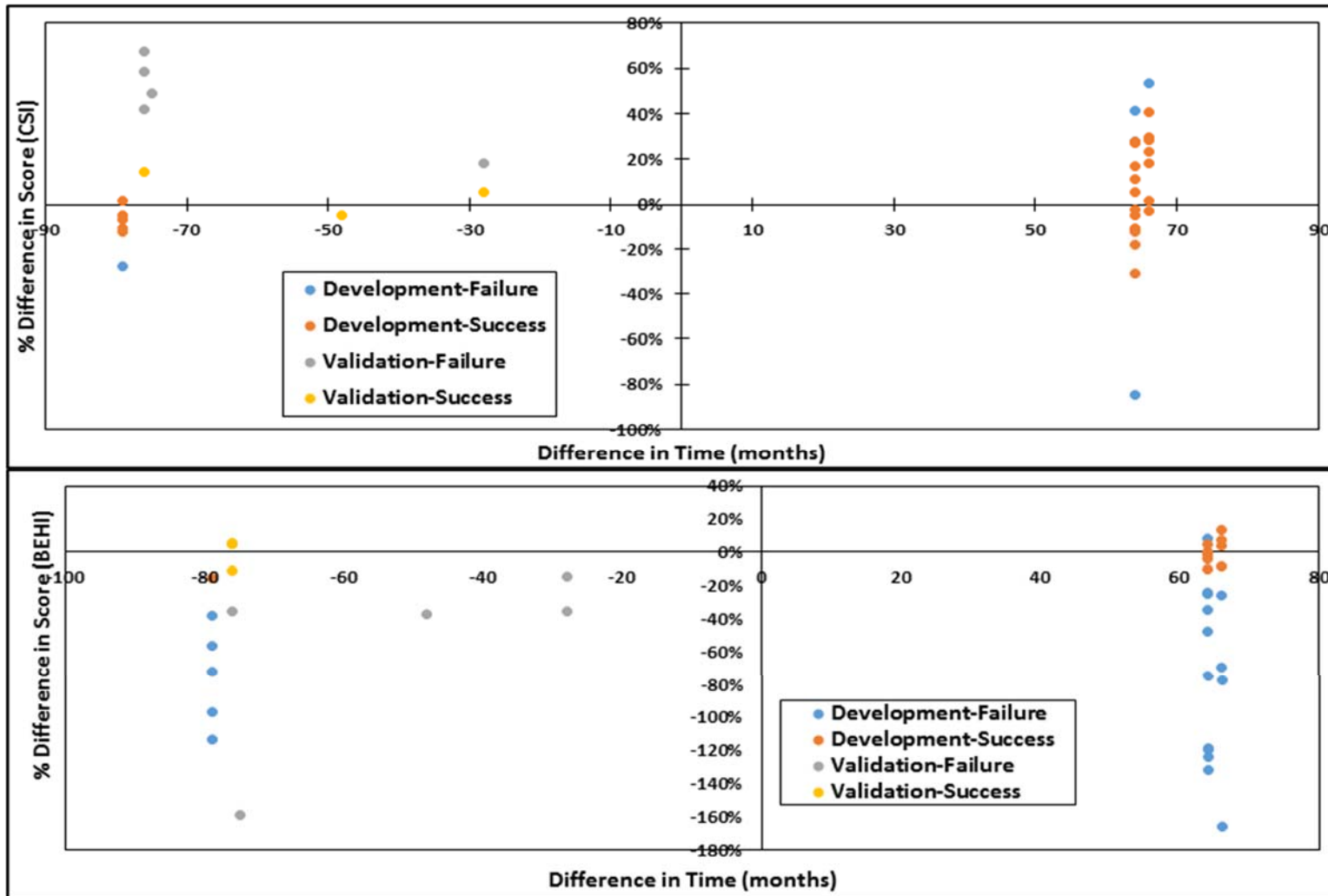


Figure A - 8: Percent difference in score versus the difference in time when the LIDAR and the on-site assessments were collected.

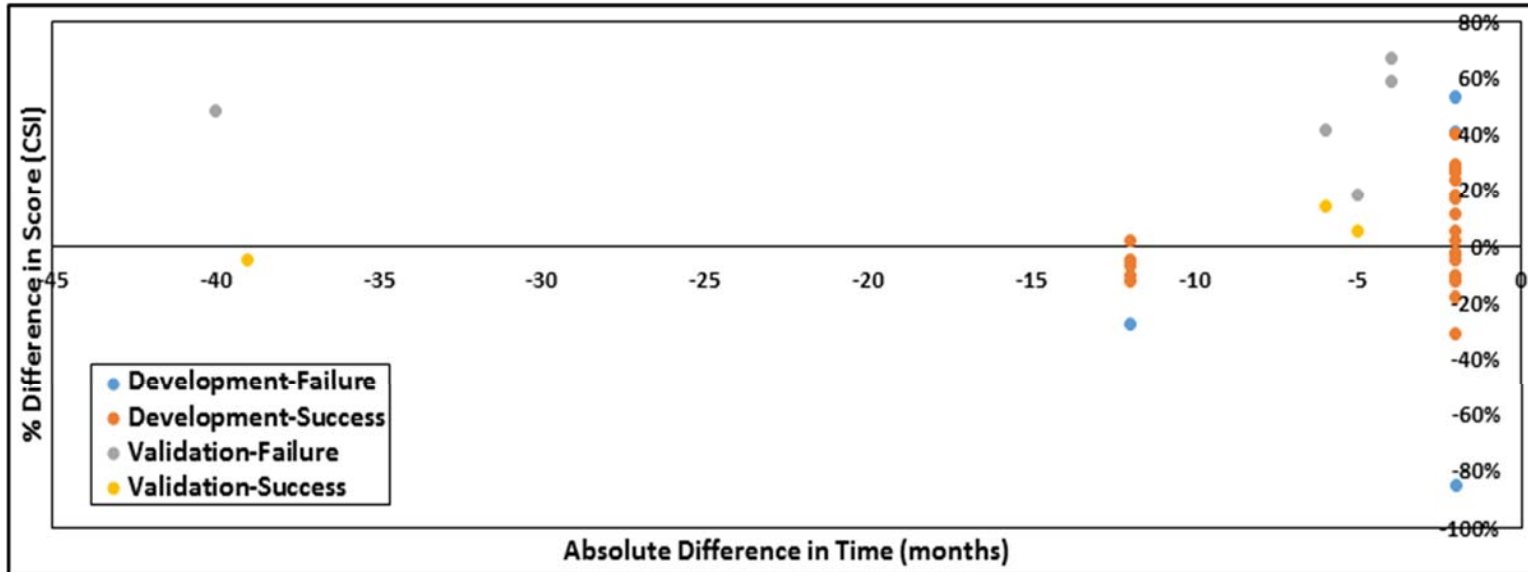


Figure A - 9: Percent difference in score versus the difference in time when the Google Earth imagery and the on-site assessments were collected.

Table A - 1: Development Monte Carlo Depth and Manning's n. The method and volumetric flow (Q) used is noted along with the corresponding shape of the channel assumed, the Manning's n distribution used. Except for the measured baseflow depth, the side slopes were assumed to be 2:1.

| Site/<br>Reach<br># | Channel<br>Shape | Manning's<br>n Dist | Stage    | Depth (m) | Manning's<br>n | Method      | Q                  |
|---------------------|------------------|---------------------|----------|-----------|----------------|-------------|--------------------|
| FM1                 | Triangular       | Triangular          | Baseflow | 0.45      | 0.002          | StreamStats | Average Daily Flow |
| FM2                 | Triangular       | Triangular          | Baseflow | 0.47      | 0.002          | StreamStats | Average Daily Flow |
| FM3                 | Triangular       | Triangular          | Baseflow | 0.58      | 0.002          | StreamStats | Average Daily Flow |
| FM4                 | Triangular       | Triangular          | Baseflow | 0.58      | 0.002          | StreamStats | Average Daily Flow |
| WC2                 | Triangular       | Triangular          | Baseflow | 0.44      | 0.002          | StreamStats | Average Daily Flow |
| WC3                 | Triangular       | Triangular          | Baseflow | 0.46      | 0.002          | StreamStats | Average Daily Flow |
| A1                  | Triangular       | Triangular          | Baseflow | 2.03      | 0.007          | StreamStats | Average Daily Flow |
| A2                  | Triangular       | Triangular          | Baseflow | 2.00      | 0.006          | StreamStats | Average Daily Flow |
| A3                  | Triangular       | Triangular          | Baseflow | 1.95      | 0.006          | StreamStats | Average Daily Flow |
| A4                  | Triangular       | Triangular          | Baseflow | 1.95      | 0.006          | StreamStats | Average Daily Flow |
| A5                  | Triangular       | Triangular          | Baseflow | 1.98      | 0.006          | StreamStats | Average Daily Flow |
| A6                  | Triangular       | Triangular          | Baseflow | 2.06      | 0.007          | StreamStats | Average Daily Flow |
| A7                  | Triangular       | Triangular          | Baseflow | 1.98      | 0.006          | StreamStats | Average Daily Flow |
| A8                  | Triangular       | Triangular          | Baseflow | 2.07      | 0.007          | StreamStats | Average Daily Flow |
| B1                  | Triangular       | Triangular          | Baseflow | 2.54      | 0.002          | StreamStats | Average Daily Flow |
| B2                  | Triangular       | Triangular          | Baseflow | 2.55      | 0.002          | StreamStats | Average Daily Flow |
| B3                  | Triangular       | Triangular          | Baseflow | 2.63      | 0.002          | StreamStats | Average Daily Flow |
| C1                  | Triangular       | Triangular          | Baseflow | 2.31      | 0.002          | StreamStats | Average Daily Flow |
| C2                  | Triangular       | Triangular          | Baseflow | 2.38      | 0.002          | StreamStats | Average Daily Flow |

Table A - 1 continued: Development Monte Carlo Depth and Manning's n. The method and volumetric flow (Q) used is noted along with the corresponding shape of the channel assumed, the Manning's n distribution used. Except for the measured baseflow depth, the side slopes were assumed to be 2:1.

| Site/<br>Reach<br># | Channel<br>Shape | Manning's<br>n Dist | Stage    | Depth (m) | Manning's<br>n | Method      | Q   |
|---------------------|------------------|---------------------|----------|-----------|----------------|-------------|---|
| C3                  | Triangular       | Triangular          | Baseflow | 2.36      | 0.002          | StreamStats | Average Daily Flow                        |
| C4                  | Triangular       | Triangular          | Baseflow | 2.28      | 0.002          | StreamStats | Average Daily Flow                        |
| C5                  | Triangular       | Triangular          | Baseflow | 2.24      | 0.002          | StreamStats | Average Daily Flow                        |
| C6                  | Triangular       | Triangular          | Baseflow | 2.25      | 0.002          | StreamStats | Average Daily Flow                        |
| D1                  | Triangular       | Triangular          | Baseflow | 2.26      | 0.002          | StreamStats | Average Daily Flow                        |
| D2                  | Triangular       | Triangular          | Baseflow | 2.20      | 0.002          | StreamStats | Average Daily Flow                        |
| D3                  | Triangular       | Triangular          | Baseflow | 2.15      | 0.002          | StreamStats | Average Daily Flow                        |
| D4                  | Triangular       | Triangular          | Baseflow | 2.15      | 0.002          | StreamStats | Average Daily Flow                        |
| E2                  | Triangular       | Triangular          | Baseflow | 2.16      | 0.002          | StreamStats | Average Daily Flow                        |
| E3                  | Triangular       | Triangular          | Baseflow | 2.00      | 0.002          | StreamStats | Average Daily Flow                        |
| FM1                 | Triangular       | Triangular          | Baseflow | 0.28      | 0.071          | StreamGage  | USGS Stream Gage:<br>Mean Daily Discharge |
| FM2                 | Triangular       | Triangular          | Baseflow | 0.28      | 0.068          | StreamGage  | USGS Stream Gage:<br>Mean Daily Discharge |
| FM3                 | Triangular       | Triangular          | Baseflow | 0.35      | 0.066          | StreamGage  | USGS Stream Gage:<br>Mean Daily Discharge |
| FM4                 | Triangular       | Triangular          | Baseflow | 0.37      | 0.070          | StreamGage  | USGS Stream Gage:<br>Mean Daily Discharge |
| WC2                 | Triangular       | Triangular          | Baseflow | 0.23      | 0.072          | StreamGage  | USGS Stream Gage:<br>Mean Daily Discharge |
| WC3                 | Triangular       | Triangular          | Baseflow | 0.27      | 0.078          | StreamGage  | USGS Stream Gage:<br>Mean Daily Discharge |
| A1                  | Triangular       | Triangular          | Baseflow | 1.47      | 0.067          | StreamGage  | USGS Stream Gage:<br>Mean Daily Discharge |

Table A - 1 continued: Development Monte Carlo Depth and Manning's n. The method and volumetric flow (Q) used is noted along with the corresponding shape of the channel assumed, the Manning's n distribution used. Except for the measured baseflow depth, the side slopes were assumed to be 2:1.

| Site/<br>Reach<br># | Channel<br>Shape | Manning'<br>s n Dist | Stage    | Depth (m) | Manning's n | Method     | Q   |
|---------------------|------------------|----------------------|----------|-----------|-------------|------------|---|
| A2                  | Triangular       | Triangular           | Baseflow | 1.49      | 0.070       | StreamGage | USGS Stream Gage:<br>Mean Daily Discharge |
| A3                  | Triangular       | Triangular           | Baseflow | 1.43      | 0.062       | StreamGage | USGS Stream Gage:<br>Mean Daily Discharge |
| A4                  | Triangular       | Triangular           | Baseflow | 1.50      | 0.070       | StreamGage | USGS Stream Gage:<br>Mean Daily Discharge |
| A5                  | Triangular       | Triangular           | Baseflow | 1.46      | 0.066       | StreamGage | USGS Stream Gage:<br>Mean Daily Discharge |
| A6                  | Triangular       | Triangular           | Baseflow | 1.49      | 0.069       | StreamGage | USGS Stream Gage:<br>Mean Daily Discharge |
| A7                  | Triangular       | Triangular           | Baseflow | 1.47      | 0.067       | StreamGage | USGS Stream Gage:<br>Mean Daily Discharge |
| A8                  | Triangular       | Triangular           | Baseflow | 1.50      | 0.069       | StreamGage | USGS Stream Gage:<br>Mean Daily Discharge |
| B1                  | Triangular       | Triangular           | Baseflow | 1.51      | 0.058       | StreamGage | USGS Stream Gage:<br>Mean Daily Discharge |
| B2                  | Triangular       | Triangular           | Baseflow | 1.54      | 0.061       | StreamGage | USGS Stream Gage:<br>Mean Daily Discharge |
| B3                  | Triangular       | Triangular           | Baseflow | 1.57      | 0.064       | StreamGage | USGS Stream Gage:<br>Mean Daily Discharge |
| C1                  | Triangular       | Triangular           | Baseflow | 1.46      | 0.075       | StreamGage | USGS Stream Gage:<br>Mean Daily Discharge |
| C2                  | Triangular       | Triangular           | Baseflow | 1.46      | 0.075       | StreamGage | USGS Stream Gage:<br>Mean Daily Discharge |
| C3                  | Triangular       | Triangular           | Baseflow | 1.43      | 0.073       | StreamGage | USGS Stream Gage:<br>Mean Daily Discharge |
| C4                  | Triangular       | Triangular           | Baseflow | 1.37      | 0.065       | StreamGage | USGS Stream Gage:<br>Mean Daily Discharge |

Table A - 1 continued: Development Monte Carlo Depth and Manning's n. The method and volumetric flow (Q) used is noted along with the corresponding shape of the channel assumed, the Manning's n distribution used. Except for the measured baseflow depth, the side slopes were assumed to be 2:1.

| Site/<br>Reach<br># | Channel<br>Shape | Manning'<br>s n Dist | Stage    | Depth<br>(m) | Manning's<br>n | Method           | Q   |
|---------------------|------------------|----------------------|----------|--------------|----------------|------------------|---|
| C5                  | Triangular       | Triangular           | Baseflow | 1.42         | 0.071          | StreamGage       | USGS Stream Gage:<br>Mean Daily Discharge |
| C6                  | Triangular       | Triangular           | Baseflow | 1.41         | 0.070          | StreamGage       | USGS Stream Gage:<br>Mean Daily Discharge |
| D1                  | Triangular       | Triangular           | Baseflow | 1.33         | 0.074          | StreamGage       | USGS Stream Gage:<br>Mean Daily Discharge |
| D2                  | Triangular       | Triangular           | Baseflow | 1.26         | 0.064          | StreamGage       | USGS Stream Gage:<br>Mean Daily Discharge |
| D3                  | Triangular       | Triangular           | Baseflow | 1.26         | 0.065          | StreamGage       | USGS Stream Gage:<br>Mean Daily Discharge |
| D4                  | Triangular       | Triangular           | Baseflow | 1.23         | 0.060          | StreamGage       | USGS Stream Gage:<br>Mean Daily Discharge |
| E2                  | Triangular       | Triangular           | Baseflow | 1.26         | 0.069          | StreamGage       | USGS Stream Gage:<br>Mean Daily Discharge |
| E3                  | Triangular       | Triangular           | Baseflow | 1.22         | 0.067          | StreamGage       | USGS Stream Gage:<br>Mean Daily Discharge |
| FM1                 | Triangular       | Triangular           | Baseflow | 0.37         | 0.063          | LIDAR+StreamGage | USGS Stream Gage:<br>Mean Daily Discharge |
| FM2                 | Triangular       | Triangular           | Baseflow | 0.39         | 0.062          | LIDAR+StreamGage | USGS Stream Gage:<br>Mean Daily Discharge |
| FM3                 | Triangular       | Triangular           | Baseflow | 0.51         | 0.065          | LIDAR+StreamGage | USGS Stream Gage:<br>Mean Daily Discharge |
| FM4                 | Triangular       | Triangular           | Baseflow | 0.53         | 0.057          | LIDAR+StreamGage | USGS Stream Gage:<br>Mean Daily Discharge |
| WC2                 | Triangular       | Triangular           | Baseflow | 0.30         | 0.068          | LIDAR+StreamGage | USGS Stream Gage:<br>Mean Daily Discharge |
| WC3                 | Triangular       | Triangular           | Baseflow | 0.34         | 0.059          | LIDAR+StreamGage | USGS Stream Gage:<br>Mean Daily Discharge |

Table A - 1 continued: Development Monte Carlo Depth and Manning's n. The method and volumetric flow (Q) used is noted along with the corresponding shape of the channel assumed, the Manning's n distribution used. Except for the measured baseflow depth, the side slopes were assumed to be 2:1.

| Site/<br>Reach<br># | Channel<br>Shape | Manning'<br>s n Dist | Stage    | Depth<br>(m) | Manning's<br>n | Method           | Q   |
|---------------------|------------------|----------------------|----------|--------------|----------------|------------------|---|
| A1                  | Trapezoidal      | Trian-<br>gular      | Baseflow | 0.55         | 0.072          | LIDAR+StreamGage | USGS Stream Gage:<br>Mean Daily Discharge |
| A2                  | Trapezoidal      | Trian-<br>gular      | Baseflow | 1.08         | 0.064          | LIDAR+StreamGage | USGS Stream Gage:<br>Mean Daily Discharge |
| A3                  | Trapezoidal      | Trian-<br>gular      | Baseflow | 0.70         | 0.068          | LIDAR+StreamGage | USGS Stream Gage:<br>Mean Daily Discharge |
| A4                  | Trapezoidal      | Trian-<br>gular      | Baseflow | 0.28         | 0.073          | LIDAR+StreamGage | USGS Stream Gage:<br>Mean Daily Discharge |
| A5                  | Trapezoidal      | Trian-<br>gular      | Baseflow | 0.48         | 0.073          | LIDAR+StreamGage | USGS Stream Gage:<br>Mean Daily Discharge |
| A6                  | Trapezoidal      | Trian-<br>gular      | Baseflow | 0.68         | 0.070          | LIDAR+StreamGage | USGS Stream Gage:<br>Mean Daily Discharge |
| A7                  | Trapezoidal      | Trian-<br>gular      | Baseflow | 0.93         | 0.072          | LIDAR+StreamGage | USGS Stream Gage:<br>Mean Daily Discharge |
| A8                  | Trapezoidal      | Trian-<br>gular      | Baseflow | 0.48         | 0.074          | LIDAR+StreamGage | USGS Stream Gage:<br>Mean Daily Discharge |
| B1                  | Trapezoidal      | Trian-<br>gular      | Baseflow | 1.46         | 0.050          | LIDAR+StreamGage | USGS Stream Gage:<br>Mean Daily Discharge |
| B2                  | Trapezoidal      | Trian-<br>gular      | Baseflow | 2.00         | 0.068          | LIDAR+StreamGage | USGS Stream Gage:<br>Mean Daily Discharge |
| B3                  | Trapezoidal      | Trian-<br>gular      | Baseflow | 2.08         | 0.067          | LIDAR+StreamGage | USGS Stream Gage:<br>Mean Daily Discharge |
| C1                  | Trapezoidal      | Trian-<br>gular      | Baseflow | 1.73         | 0.065          | LIDAR+StreamGage | USGS Stream Gage:<br>Mean Daily Discharge |
| C2                  | Trapezoidal      | Trian-<br>gular      | Baseflow | 2.07         | 0.054          | LIDAR+StreamGage | USGS Stream Gage:<br>Mean Daily Discharge |
| C3                  | Trapezoidal      | Trian-<br>gular      | Baseflow | 1.83         | 0.071          | LIDAR+StreamGage | USGS Stream Gage:<br>Mean Daily Discharge |

Table A - 1 continued: Development Monte Carlo Depth and Manning's n. The method and volumetric flow (Q) used is noted along with the corresponding shape of the channel assumed, the Manning's n distribution used. Except for the measured baseflow depth, the side slopes were assumed to be 2:1.

| Site/<br>Reach<br># | Channel<br>Shape | Manning's<br>n Dist | Stage    | Depth (m) | Manning's<br>n | Method           | Q   |
|---------------------|------------------|---------------------|----------|-----------|----------------|------------------|---|
| C4                  | Trapezoidal      | Triangular          | Baseflow | 1.89      | 0.065          | LIDAR+StreamGage | USGS Stream Gage:<br>Mean Daily Discharge |
| C5                  | Trapezoidal      | Triangular          | Baseflow | 1.72      | 0.066          | LIDAR+StreamGage | USGS Stream Gage:<br>Mean Daily Discharge |
| C6                  | Trapezoidal      | Triangular          | Baseflow | 1.06      | 0.070          | LIDAR+StreamGage | USGS Stream Gage:<br>Mean Daily Discharge |
| D1                  | Trapezoidal      | Triangular          | Baseflow | 1.33      | 0.071          | LIDAR+StreamGage | USGS Stream Gage:<br>Mean Daily Discharge |
| D2                  | Trapezoidal      | Uniform             | Baseflow | 0.94      | 0.065          | LIDAR+StreamGage | USGS Stream Gage:<br>Mean Daily Discharge |
| D3                  | Trapezoidal      | Uniform             | Baseflow | 0.80      | 0.068          | LIDAR+StreamGage | USGS Stream Gage:<br>Mean Daily Discharge |
| D4                  | Trapezoidal      | Uniform             | Baseflow | 0.72      | 0.056          | LIDAR+StreamGage | USGS Stream Gage:<br>Mean Daily Discharge |
| E2                  | Trapezoidal      | Uniform             | Baseflow | 0.63      | 0.059          | LIDAR+StreamGage | USGS Stream Gage:<br>Mean Daily Discharge |
| E3                  | Trapezoidal      | Triangular          | Baseflow | 1.05      | 0.062          | LIDAR+StreamGage | USGS Stream Gage:<br>Mean Daily Discharge |
| FM1                 | Triangular       | Triangular          | Bankfull | 2.71      | 0.069          | Q <sub>2</sub>   | Controlled 2 year<br>Flood                |
| FM2                 | Triangular       | Triangular          | Bankfull | 2.70      | 0.065          | Q <sub>2</sub>   | Controlled 2 year<br>Flood                |
| FM3                 | Triangular       | Triangular          | Bankfull | 3.34      | 0.061          | Q <sub>2</sub>   | Controlled 2 year<br>Flood                |
| FM4                 | Triangular       | Triangular          | Bankfull | 3.49      | 0.064          | Q <sub>2</sub>   | Controlled 2 year<br>Flood                |
| WC2                 | Triangular       | Triangular          | Bankfull | 3.14      | 0.073          | Q <sub>2</sub>   | Controlled 2 year<br>Flood                |



Table A - 1 continued: Development Monte Carlo Depth and Manning's n. The method and volumetric flow (Q) used is noted along with the corresponding shape of the channel assumed, the Manning's n distribution used. Except for the measured baseflow depth, the side slopes were assumed to be 2:1.

| Site/<br>Reach<br># | Channel<br>Shape | Manning's<br>n Dist | Stage    | Depth (m) | Manning's<br>n | Method         | Q                       |
|---------------------|------------------|---------------------|----------|-----------|----------------|----------------|-------------------------|
| WC3                 | Triangular       | Triangular          | Bankfull | 3.26      | 0.065          | Q <sub>2</sub> | Controlled 2 year Flood |
| A1                  | Triangular       | Uniform             | Bankfull | 8.28      | 0.061          | Q <sub>2</sub> | Controlled 2 year Flood |
| A2                  | Triangular       | Uniform             | Bankfull | 7.85      | 0.053          | Q <sub>2</sub> | Controlled 2 year Flood |
| A3                  | Triangular       | Uniform             | Bankfull | 8.13      | 0.058          | Q <sub>2</sub> | Controlled 2 year Flood |
| A4                  | Triangular       | Uniform             | Bankfull | 8.57      | 0.067          | Q <sub>2</sub> | Controlled 2 year Flood |
| A5                  | Triangular       | Uniform             | Bankfull | 8.34      | 0.062          | Q <sub>2</sub> | Controlled 2 year Flood |
| A6                  | Triangular       | Uniform             | Bankfull | 8.12      | 0.058          | Q <sub>2</sub> | Controlled 2 year Flood |
| A7                  | Triangular       | Uniform             | Bankfull | 8.48      | 0.065          | Q <sub>2</sub> | Controlled 2 year Flood |
| A8                  | Triangular       | Uniform             | Bankfull | 8.18      | 0.059          | Q <sub>2</sub> | Controlled 2 year Flood |
| B1                  | Triangular       | Uniform             | Bankfull | 9.97      | 0.064          | Q <sub>2</sub> | Controlled 2 year Flood |
| B2                  | Triangular       | Uniform             | Bankfull | 9.88      | 0.063          | Q <sub>2</sub> | Controlled 2 year Flood |
| B3                  | Triangular       | Uniform             | Bankfull | 9.73      | 0.061          | Q <sub>2</sub> | Controlled 2 year Flood |
| C1                  | Triangular       | Uniform             | Bankfull | 8.96      | 0.060          | Q <sub>2</sub> | Controlled 2 year Flood |
| C2                  | Triangular       | Uniform             | Bankfull | 9.24      | 0.065          | Q <sub>2</sub> | Controlled 2 year Flood |
| C3                  | Triangular       | Uniform             | Bankfull | 9.03      | 0.062          | Q <sub>2</sub> | Controlled 2 year Flood |
| C4                  | Triangular       | Uniform             | Bankfull | 9.13      | 0.064          | Q <sub>2</sub> | Controlled 2 year Flood |
| C5                  | Triangular       | Uniform             | Bankfull | 8.88      | 0.059          | Q <sub>2</sub> | Controlled 2 year Flood |
| C6                  | Triangular       | Uniform             | Bankfull | 9.09      | 0.063          | Q <sub>2</sub> | Controlled 2 year Flood |
| D1                  | Triangular       | Uniform             | Bankfull | 8.51      | 0.060          | Q <sub>2</sub> | Controlled 2 year Flood |
| D2                  | Triangular       | Uniform             | Bankfull | 8.66      | 0.064          | Q <sub>2</sub> | Controlled 2 year Flood |
| D3                  | Triangular       | Uniform             | Bankfull | 8.56      | 0.062          | Q <sub>2</sub> | Controlled 2 year Flood |

Table A - 1 continued: Development Monte Carlo Depth and Manning's n. The method and volumetric flow (Q) used is noted along with the corresponding shape of the channel assumed, the Manning's n distribution used. Except for the measured baseflow depth, the side slopes were assumed to be 2:1.

| Site/<br>Reach<br># | Channel<br>Shape | Manning's<br>n Dist | Stage    | Depth (m) | Manning's<br>n | Method           | Q                       |
|---------------------|------------------|---------------------|----------|-----------|----------------|------------------|-------------------------|
| D4                  | Triangular       | Uniform             | Bankfull | 8.44      | 0.060          | Q <sub>2</sub>   | Controlled 2 year Flood |
| E2                  | Triangular       | Uniform             | Bankfull | 8.62      | 0.066          | Q <sub>2</sub>   | Controlled 2 year Flood |
| E3                  | Triangular       | Uniform             | Bankfull | 8.42      | 0.064          | Q <sub>2</sub>   | Controlled 2 year Flood |
| FM1                 | Triangular       | Triangular          | Bankfull | 1.66      | 0.061          | Q <sub>1.5</sub> | PeakFQ                  |
| FM2                 | Triangular       | Triangular          | Bankfull | 1.81      | 0.073          | Q <sub>1.5</sub> | PeakFQ                  |
| FM3                 | Triangular       | Triangular          | Bankfull | 2.30      | 0.072          | Q <sub>1.5</sub> | PeakFQ                  |
| FM4                 | Triangular       | Triangular          | Bankfull | 2.27      | 0.065          | Q <sub>1.5</sub> | PeakFQ                  |
| WC2                 | Triangular       | Triangular          | Bankfull | 1.60      | 0.063          | Q <sub>1.5</sub> | PeakFQ                  |
| WC3                 | Triangular       | Triangular          | Bankfull | 1.93      | 0.075          | Q <sub>1.5</sub> | PeakFQ                  |
| A1                  | Triangular       | Triangular          | Bankfull | 5.17      | 0.081          | Q <sub>1.5</sub> | PeakFQ                  |
| A2                  | Triangular       | Triangular          | Bankfull | 5.14      | 0.080          | Q <sub>1.5</sub> | PeakFQ                  |
| A3                  | Triangular       | Triangular          | Bankfull | 5.26      | 0.084          | Q <sub>1.5</sub> | PeakFQ                  |
| A4                  | Triangular       | Triangular          | Bankfull | 5.33      | 0.087          | Q <sub>1.5</sub> | PeakFQ                  |
| A5                  | Triangular       | Triangular          | Bankfull | 5.31      | 0.086          | Q <sub>1.5</sub> | PeakFQ                  |
| A6                  | Triangular       | Triangular          | Bankfull | 5.35      | 0.087          | Q <sub>1.5</sub> | PeakFQ                  |
| A7                  | Triangular       | Triangular          | Bankfull | 5.44      | 0.092          | Q <sub>1.5</sub> | PeakFQ                  |
| A8                  | Triangular       | Triangular          | Bankfull | 5.37      | 0.088          | Q <sub>1.5</sub> | PeakFQ                  |
| B1                  | Triangular       | Uniform             | Bankfull | 9.40      | 0.061          | Q <sub>1.5</sub> | PeakFQ                  |
| B2                  | Triangular       | Uniform             | Bankfull | 9.60      | 0.065          | Q <sub>1.5</sub> | PeakFQ                  |
| B3                  | Triangular       | Uniform             | Bankfull | 9.63      | 0.066          | Q <sub>1.5</sub> | PeakFQ                  |
| C1                  | Triangular       | Uniform             | Bankfull | 8.34      | 0.063          | Q <sub>1.5</sub> | PeakFQ                  |

Table A - 1 continued: Development Monte Carlo Depth and Manning's n. The method and volumetric flow (Q) used is noted along with the corresponding shape of the channel assumed, the Manning's n distribution used. Except for the measured baseflow depth, the side slopes were assumed to be 2:1.

| Site/<br>Reach# | Channel<br>Shape | Manning's<br>n Dist | Stage    | Depth (m) | Manning's n | Method           | Q      |
|-----------------|------------------|---------------------|----------|-----------|-------------|------------------|--------|
| C2              | Triangular       | Uniform             | Bankfull | 8.29      | 0.062       | Q <sub>1.5</sub> | PeakFQ |
| C3              | Triangular       | Uniform             | Bankfull | 8.01      | 0.057       | Q <sub>1.5</sub> | PeakFQ |
| C4              | Triangular       | Uniform             | Bankfull | 8.06      | 0.058       | Q <sub>1.5</sub> | PeakFQ |
| C5              | Triangular       | Uniform             | Bankfull | 8.26      | 0.062       | Q <sub>1.5</sub> | PeakFQ |
| C6              | Triangular       | Uniform             | Bankfull | 8.11      | 0.059       | Q <sub>1.5</sub> | PeakFQ |
| D1              | Triangular       | Uniform             | Bankfull | 7.51      | 0.059       | Q <sub>1.5</sub> | PeakFQ |
| D2              | Triangular       | Uniform             | Bankfull | 7.52      | 0.060       | Q <sub>1.5</sub> | PeakFQ |
| D3              | Triangular       | Uniform             | Bankfull | 7.43      | 0.059       | Q <sub>1.5</sub> | PeakFQ |
| D4              | Triangular       | Uniform             | Bankfull | 7.64      | 0.063       | Q <sub>1.5</sub> | PeakFQ |
| E2              | Triangular       | Uniform             | Bankfull | 7.36      | 0.062       | Q <sub>1.5</sub> | PeakFQ |
| E3              | Triangular       | Uniform             | Bankfull | 6.89      | 0.054       | Q <sub>1.5</sub> | PeakFQ |

Table A - 2: All metrics that failed for each station for the development stage, both the Bank Erosion Hazard Index (BEHI), and the Channel Stability Index (CSI). Used the LIDAR bankfull height method in the BEHI, and the LIDAR+StreamGage method to get the baseflow depth in the CSI.

| Site/<br>Reach# | Metric that Failed |  |   |   |
|-----------------|--------------------|--|---|---|
|                 | #                  | BEHI   | # | CSI   |
| A1              | 2                  | Primary Bank Material, Bank/Bankfull Height Ratio  | 2 | Percent Accretion, Average Degree of Incision   |
| A2              | 1                  | Primary Bank Material  | 1 | Stage of Channel Evolution  |
| A3              | 8                  | Bank Height, Primary Bank Material, Stratification, Root Depth Ratio, Root Depth Ratio + Surface Protection, Bank Angle, Bank/Bankfull Height Ratio, <b>Fully Digital</b>                  | 2 | Combo-All GE Methods, <b>Fully Digital</b>  |
| A4              | 2                  | Primary Bank Material, <b>Fully Digital</b>  | 0 | N/A   |
| A5              | 1                  | <b>Fully Digital</b>   | 3 | Percent Mass Wasting, Percent Woody Cover+Bank Protection, Percent Woody Cover+ Bed/Bank Protection                       |
| A6              | 9                  | Bank Height, Primary Bank Material, Stratification, Root Depth Ratio, Root Depth Ratio + Surface Protection, Bankfull Height, Bank Angle, Bank/Bankfull Height Ratio, <b>Fully Digital</b> | 1 | Combo-All GE Methods  |
| A7              | 6                  | Bank/Bankfull Height Ratio, Bank Height, Stratification, Root Depth Ratio, Root Depth Ratio + Surface Protection, Bank Angle   | 0 | N/A   |
| A8              | 4                  | Primary Bank Material, Stratification, Root Depth Ratio + Surface Protection, Bank/Bankfull Height Ratio   | 0 | N/A   |
| B1              | 3                  | Primary Bank Material, Stratification, <b>Fully Digital</b>  | 4 | Baseflow Depth, Percent Woody Cover+Bank Protection, Percent Woody Cover+ Bed/Bank Protection, Average Degree of Incision |
| B2              | 2                  | Root Depth Ratio + Surface Protection, <b>Fully Digital</b>  | 1 | Identifying Erosion+Percent Mass Wasting,   |
| B3              | 3                  | Face length, Bank Angle, <b>Fully Digital</b>  | 0 | N/A   |
| C1              | 8                  | Bank Height, Primary Bank Material, Stratification, Root Depth Ratio, Root Depth Ratio + Surface Protection, Bank Angle, Bank/Bankfull Height Ratio, <b>Fully Digital</b>                  | 0 | N/A   |

Table A – 2 continued: All metrics that failed for each station for the development stage, both the Bank Erosion Hazard Index (BEHI), and the Channel Stability Index (CSI). Used the LIDAR bankfull height method in the BEHI, and the LIDAR+StreamGage method to get the baseflow depth in the CSI.

| Site/<br>Reach# | Metric that Failed |   |   |  |
|-----------------|--------------------|---|---|--|
|                 | #                  | BEHI  | # | CSI  |
| C2              | 8                  | Bank Height, Primary Bank Material, Stratification, Root Depth Ratio, Root Depth Ratio + Surface Protection, Bank Angle, Bank/Bankfull Height Ratio, <b>Fully Digital</b> | 0 | N/A  |
| C3              | 5                  | Bank Height, Root Depth Ratio, Root Depth Ratio + Surface Protection, Bank Angle, Bank/Bankfull Height Ratio  | 2 | Degree of Constriction, Stage of Channel Evolution   |
| C4              | 8                  | Bank Height, Primary Bank Material, Stratification, Root Depth Ratio, Root Depth Ratio + Surface Protection, Bank/Bankfull Height Ratio, <b>Fully Digital</b>             | 9 | Baseflow Depth, Identifying Erosion, Percent Mass Wasting, Identifying Erosion+Percent Mass Wasting, Stage of Channel Evolution, Percent Woody Cover+Bank Protection, Percent Woody Cover+ Bed/Bank Protection, Combo-All GE Methods, <b>Fully Digital</b> |
| C5              | 4                  | Face length, Root Depth Ratio + Surface Protection, Root Density, <b>Fully Digital</b>  | 0 | N/A  |
| C6              | 4                  | Primary Bank Material, Stratification, Root Depth Ratio + Surface Protection, Bankfull Height   | 2 | Combo-All GE Methods, <b>Fully Digital</b>   |
| D1              | 4                  | Bank Height, Root Depth Ratio, Root Depth Ratio + Surface Protection, Bank/Bankfull Height Ratio  | 1 | Percent Woody Cover  |
| D2              | 1                  | <b>Fully Digital</b>  | 0 | N/A  |
| D3              | 1                  | Root Depth Ratio + Surface Protection   | 0 | N/A  |
| D4              | 3                  | Root Depth Ratio, Root Depth Ratio + Surface Protection, <b>Fully Digital</b>   | 0 | N/A  |
| E2              | 7                  | Bank Height, Primary Bank Material, Stratification, Root Depth Ratio, Root Depth Ratio + Surface Protection, Bank/Bankfull Height Ratio, <b>Fully Digital</b>             | 3 | Identifying Erosion+Percent Mass Wasting, Combo-All GE Methods, <b>Fully Digital</b>   |
| E3              | 1                  | Root Depth Ratio + Surface Protection   | 2 | Bank Height, Average Degree of Incision  |

Table A – 2 continued: All metrics that failed for each station for the development stage, both the Bank Erosion Hazard Index (BEHI), and the Channel Stability Index (CSI). Used the LIDAR bankfull height method in the BEHI, and the LIDAR+StreamGage method to get the baseflow depth in the CSI.

| Site/Reach# | Metric that Failed |   |   |  |
|-------------|--------------------|---|---|--|
|             | #                  | BEHI  | # | CSI  |
| FM1         | 8                  | Primary Bank Material, Root Depth, Root Depth Ratio, Root Depth Ratio + Surface Protection, Root Density, Bankfull Height, Bank/Bankfull Height Ratio, <b>Fully Digital</b> | 3 | Percent Mass Wasting, Identifying Erosion+Percent Mass Wasting, Average Degree of Incision |
| FM2         | 2                  | Stratification, Root Depth Ratio + Surface Protection   | 0 | N/A  |
| FM3         | 2                  | Root Depth Ratio + Surface Protection, Fully Digital  | 2 | Combo-All GE Methods, <b>Fully Digital</b>   |
| FM4         | 4                  | Root Depth Ratio, Root Depth Ratio + Surface Protection, Bankfull Height, <b>Fully Digital</b>  | 0 | N/A  |
| WC2         | 2                  | Root Depth Ratio + Surface Protection, <b>Fully Digital</b>   | 0 | N/A  |
| WC3         | 8                  | Bank Height, Root Depth, Root Depth Ratio, Root Depth Ratio + Surface Protection, Root Density, Bankfull Height, Bank/Bankfull Height Ratio, <b>Fully Digital</b>           | 0 | N/A  |

Table A - 3: All metrics that failed for each station for the validation stage, both the Bank Erosion Hazard Index (BEHI), and the Channel Stability Index (CSI). Used the LIDAR bankfull height method in the BEHI, and the LIDAR+StreamGage method to get the baseflow depth in the CSI. When the LIDAR+StreamGage method was impossible, StreamStats was used.

| Stream         | Reach | Stream/Reach | Metric that Failed |   |   |   |
|----------------|-------|--------------|--------------------|---|---|---|
|                |       |              | #                  | BEHI  | # | CSI   |
| Feather        | 1     | F1           | 3                  | Primary Bank Material, Root Depth Ratio + Surface Protection, <b>Fully Digital</b>  | 7 | Identifying Erosion, Percent Woody Cover, Percent Woody Cover+Bank Protection, Percent Woody Cover+ Bed/Bank Protection, Stage of Channel Evolution, Combo-All GE Methods, <b>Fully Digital</b> |
| Spring         | 2     | Sp2          | 6                  | Primary Bank Material, Root Depth, Root Depth Ratio, Root Depth Ratio + Surface Protection, Bank height, <b>Fully Digital</b> | 2 | Identifying Erosion, Primary Bed Material   |
| Spring         | 4     | Sp4          | 3                  | Root Depth Ratio, Root Depth Ratio + Surface Protection, <b>Fully Digital</b>   | 3 | Percent Woody Cover+Bank Protection, Combo-All GE Methods, <b>Fully Digital</b>   |
| Sandy          | 1     | Sy1          | 0                  | N/A   | 2 | Combo-All GE Methods, <b>Fully Digital</b>  |
| Sandy          | 5     | Sy5          | 2                  | Stratification, Root Density  | 0 | N/A   |
| Black Fork     | 2     | B2           | 4                  | Root Depth Ratio, Root Depth Ratio + Surface Protection, Root Density, <b>Fully Digital</b>                                   | 3 | Primary Bed Material, Bed Protection, Average Degree of Incision  |
| Fourche Maline | 1     | FRM1         | 0                  | N/A   | 3 | Percent Woody Cover+ Bed/Bank Protection, Combo-All GE Methods, <b>Fully Digital</b>  |
| Fourche Maline | 2     | FRM2         | 3                  | Root Depth Ratio, Root Depth Ratio + Surface Protection, <b>Fully Digital</b>   | 2 | Combo-All GE Methods, <b>Fully Digital</b>  |

VITA

Abigail Frances Parnell

Candidate for the Degree of

Master of Science

Thesis:       INCORPORATING DIGITAL DATA INTO RAPID GEOMORPHIC  
ASSESSMENTS

Major Field: Biosystems & Agricultural Engineering

Biographical:

Education:

Completed the requirements for the Master of Science in Biosystems & Agricultural Engineering at Oklahoma State University, Stillwater, Oklahoma in December, 2018.

Completed the requirements for the Bachelor of Science in Biosystems & Agricultural Engineering at Oklahoma State University, Stillwater, Oklahoma in 2016.

Experience:

Student Trainee (Engineering) at USDA Natural Resources Conservation Services, summer 2016-2018.

Professional Memberships:

American Society of Agricultural & Biological Engineers  
OSU Chapter of Alpha Epsilon